FRIEDRICH-SCHILLER-
UNIVERSITÄT
JENA

PHYSIOLOGICAL PLASTICITY OF MARINE PHYTOPLANKTON REVEALED BY UNTARGETED METABOLOMICS

Dissertation

(kumulativ)

zur Erlangung des akademischen Grades
doctor rerum naturalium (Dr. rer. nat.)

vorgelegt dem Rat der Chemisch-Geowissenschaftlichen Fakultät
der Friedrich-Schiller-Universität Jena

von M.Sc. (Meeresbiologie) Constanze Kuhlisch
geboren am 11.08.1988 in Dresden

Gutachter:

1) Prof. Dr. Georg Pohnert, Friedrich-Schiller-Universität Jena

2) Prof. Dr. Severin Sasso, Friedrich-Schiller-Universität Jena

3) Prof. Dr. Dieter Spiteller, Universität Konstanz

Tag der öffentlichen Verteidigung: 07. November 2018

To my grandmother

„We live by our eyes and ears and tend generally to be oblivious to the chemical happenings in our surrounds. Such happenings are ubiquitous. All organisms engender chemical signals, and all, in their respective ways, respond to the chemical emissions of others. The result is a vast communicative interplay, fundamental to the fabric of life.“

Thomas Eisner & Jerrold Meinwald, 1955

Table of contents

List of abbreviations

AA	arachidonic acid
APCI	atmospheric-pressure chemical ionization
CE	capillary electrophoresis
CI	chemical ionization
DI	direct infusion
DMS	dimethylsulfide
DMSP	dimethylsulfoniopropionate
DOM	dissolved organic matter
EI	electron ionization
EPA	eicosapentaenoic acid
ESI	electrospray ionization
FAH	fatty acid hydroperoxide
FT-ICR	Fourier-transform ion cyclotron resonance
GC	gas chromatography
HPL	hydroperoxide lyase
HPLC	high performance liquid chromatography
HRMS	high resolution mass spectrometry
IAA	indole-3-acetic acid
IR	infrared
LC	liquid chromatography
LOD	limit of detection
LOQ	limit of quantification
LOX	lipoxygenase
MAA	mycosporine-like amino acid
MS	mass spectrometry

NMR	nuclear magnetic resonance
PDMS	polydimethylsiloxane
PFBHA	*O*-(2,3,4,5,6-pentafluorobenzyl) hydroxylamine
PUA	polyunsaturated aldehyde
PUFA	polyunsaturated fatty acid
RT	retention time
SIM	selected ion monitoring
SPE	solid-phase extraction
SPME	solid-phase microextraction
TLC	thin-layer chromatography
TOF	time-of-flight
UHPLC	ultra-high pressure liquid chromatography

Zusammenfassung

Mehr als 70% der Erdoberfläche sind von Wasser bedeckt, wovon ca. 97% als Meerwasser in Ozeanen und Meeren auftreten. Die lichtdurchflutete Zone dieser Fläche bildet den Lebensraum des marinen Phytoplanktons, also allen mit den Meeresströmungen treibenden, photosynthetisch aktiven Organismen. Durch die Fixierung von Kohlenstoffdioxid in organischem Material und die Bildung von Sauerstoff spielt Phytoplankton eine bedeutende Rolle für das globale Klima, biogeochemische Stoffkreisläufe, und die marine Nahrungskette. Die Dynamiken in Auftreten und Sukzession des marinen Phytoplanktons sind bis heute nur bedingt erklärbar. Dabei spielen Interaktionen mit Viren, Bakterien und Zooplankton, die über chemische Moleküle vermittelt werden, eine wichtige Rolle. Die Entschlüsselung dieser Interaktionen wurde durch die technischen Errungenschaften der letzten Jahrzehnte und datenintensive Ansätze stark voran getrieben.

In meiner Dissertation erforsche ich die Anwendungsmöglichkeiten verschiedener Metabolomics-Ansätze zur Untersuchung der Ökologie des marinen Phytoplanktons insbesondere in Feldstudien. So stellte ich den Forschungsstand von Metabolomics im Bereich der chemischen Ökologie in einem umfangreichen Übersichtsartikel zusammen, und führte ein systematisch optimiertes und standardisiertes Protokoll zur metablolomischen Analyse mariner Algen ein. Weiterhin entwickelte ich eine UHPLC-APCI-HRMS Methode zur simultanen Messung flüchtiger und nichtflüchtiger Oxylipine. Mithilfe eines GC-MS basierten, nichtselektiven Screenings intra- und extrazellulärer Metabolite beobachtete ich im Wachstumsverlauf der Mikroalge *Phaeocystis pouchetii* deren Stoffwechselveränderungen und identifizierte potentielle physiologische Marker. Um die chemische Diversität und physiologische Plastizität ganzer Phytoplankton-Gemeinschaften abzubilden, wandte ich während einer Forschungsfahrt im Nordmeer einen Meta-Metabolomics-Ansatz an.

Oxylipine spielen für marine Kieselalgen eine wichtige Rolle zur Abwehr von Fraßfeinden. Verwundungsaktiviert werden dabei Membranlipide durch eine Enzymkaskade zu polyungesättigten Aldehyden (PUAs) umgewandelt, welche einen fruchtschädigenden Effekt auf Räuber haben. Daneben werden eine Vielzahl nicht-volatiler Oxylipine mit ähnlicher Wirkung freigesetzt. Während die leichtflüchtigen PUAs direkt mittels GC-MS gemessen werden können, benötigen die polareren nichtflüchtigen Oxylipine eine LC-MS-Analytik. Die entwickelte LC-APCI-HRMS

Methode bietet zum ersten Mal die Möglichkeit, beide Substanzklassen in einer Messung zu erfassen. Durch eine sensitive Analytik von PUAs basierend auf der selektiven Aufzeichnung ausgewählter Ionen (selected ion monitoring; SIM) konnte ich erstmals Hexadienal in einer marinen Mikroalge nachweisen. Ergänzendes nichtselektives Screening von nichtflüchtigen Oxylipinen im Full Scan-Modus ermöglichte die simultane Messung von Decatrienal und 10-hydroxydeca-5*Z*,8*Z*-diensäure als zugehörigem enzymatischen Produkt. Biochemische Untersuchungen zur Freisetzung von Oxylipinen in marinen Mikroalgen werden somit erleichtert. Die kurze Probenaufarbeitungs- und Messzeit, sowie das geringe Probenvolumen, ermöglichen einen hohen Probendurchsatz sowohl in Labor- als auch Freilanduntersuchungen.

Fraß durch Ruderfußkrebse und andere biotische Interaktionen können durch die Physiologie von Algen beeinflusst werden, wie mehrfach in der Vergangenheit diskutiert wurde. Physiologische Plastizität ermöglicht es Mikroalgen außerdem, sich an veränderte Umweltbedingungen anzupassen, und erhöht somit deren Fitness und Überlebensrate. Unser Verständnis für die Stoffwechselplastizität der taxonomisch heterogenen Gruppe des marine Phytoplanktons ist allerdings noch begrenzt. Wachstumsabhängige Veränderungen intra- und extrazellulärer Metabolite der Kaltwasserart *Phaeocystis pouchetii* konnte ich durch ein nichtselektives Metabolit-Screening darstellen. Das Wachstum in Batch-Kulturen löste limitierende Veränderungen in abiotischen Parametern wie Lichtintensität und Nährstoffkonzentrationen aus. Stoffwechselveränderungen traten im Hinblick auf freie Aminosäuren auf, welche im exponentiellen Wachstum parallel zur Stickstoffaufnahme zunehmen. Wachstumslimitationen in den stationären Phasen führen u.a. in Konsequenz fortlaufender Photosynthese bei gleichzeitig reduziertem Wachstum zu einer Akkumulation von Kohlenhydraten. Die Zunahme von Produkten des Lipid-Stoffwechsels, wie zum Beispiel von α-tocopherol, mehrfach ungesättigten Fettsäuren, und Sterolen in der späten stationären Wachstumsphase, deutet auf die Notwendigkeit hin, die Stabilität der Zellmembranen aufrecht zu erhalten. Zusätzlich zu diesen allgemeinen Stoffwechselantworten existieren auch Artspezifische Stoffwechselveränderungen, z.B. im Mannitolgehalt von Haptophyten, welche daher als Taxon-spezifische physiologische und ökologische Biomarker für Umweltstudien geeignet sein könnten. Die Wachstumsphysiologie von Mikroalgen spiegelt sich auch in extrazellulären Metaboliten wider. Dabei zeigt sich im Exometabolom von

P. pouchetii eine diverse chemische Zusammensetzung aus Stoffwechsel-assoziierten Metaboliten sowie Metaboliten, welche der Regulation biotischer Interaktionen dienen. Letzteres zeigt sich in Molekülen, welche eine hohe Ähnlichkeit mit den als Infochemikalien bekannten Metaboliten Lumichrom und Indole-3-essigsäure aufweisen. Die Physiologie von Mikroalgen kann somit auch durch extrazelluläre Biomarker beschrieben werden.

Auch in natürlichen Phytoplankton-Gemeinschaften ist eine solche physiologische Plastizität zu erwarten. In einem Meta-Metabolomics-Ansatz nutzte ich nichtselektive Metabolit-Screenings, um die Stoffwechselplastizität in marinen Feldexperimenten sichtbar zu machen. Gängige Freilandexperimente zur Untersuchung von Räuber-Beute-Beziehungen stellen Verdünnungsexperimente dar. Deren Störung durch polyungesättigte Aldehyde, welche bei vorangegangener Filtration durch einige Algenarten wie *P. pouchetii* oder bestimmte Algenblütestadien freigesetzt werden können, ist in der Vergangenheit mehrfach postuliert worden. Dies konnte jedoch nicht eindeutig gezeigt werden. Durch ein nichtselektives Screening der im Filtrat gelösten Metabolite konnte ich den generellen Einfluss der Filtrationsmethode auf die chemische Zusammensetzung des Filtrats sichtbar machen. Eine Möglichkeit, auf diesen Effekt hin zu prüfen, ist die Bestimmung spezifischer Wachstumsraten. Auch die Zellphysiologie und somit intrazelluläre Metabolite stehen im Verdacht, Räuber-Beute-Beziehungen zu beeinflussen. So wurde für *P. pouchetii* mehrfach postuliert, dass die Zellphysiologie für verminderten Fraß durch Ruderfußkrebse verantwortlich sei. Während einer Ausfahrt im Nordmeer zur Untersuchung von *P. pouchetii* dominierten Phytoplankton-Gemeinschaften, konnte ich durch einen Meta-Metabolomics-Ansatz erstmals die Stoffwechselplastizität ganzer Phytoplankton-Gemeinschaften abbilden. Metabolite, wie z.B. Eicosapentaensäure, bilden als taxonomische Marker die Verteilung von Algenarten ab. Die Verbreitungsmuster von physiologischen Markern aus *P. pouchetii* Laborkulturen zeigen hingegen den Einfluss abiotischer Umweltfaktoren auf den Stoffwechsel des Phytoplanktons und die abgebildete chemische Landschaft.

Die Forschung im Bereich der Ökologie wird zu einem gewissen Grad taxonomisch definiert und ausgerichtet. Auf der Ebene von Metaboliten spielt Phylogenie hingegen weniger eine Rolle. Dies zeigt sich am Beispiel der gut untersuchten Substanzklasse der Oxylipine, deren Verbreitung und Zusammensetzung in den verschiedenen marinen Phytoplankton-Taxa keinen direkten Zusammenhang mit der globalen

Biomasse oder der ökologischen Relevanz aufweist. Dies zeigt sich auch in den Meta-Metabolomen von Phytoplankton-Gemeinschaften, deren taxonomische Signaturen durch Methodeneffekte und Nährstofflimitationen überlagert werden. Metabolomics erlaubt es, diese funktionelle Diversität und Plastizität des marinen Phytoplanktons abzubilden. Ergänzend zu den Analysen gut untersuchter Moleküle, können nichtselektive Metabolit-Screenings dabei helfen, die chemische Diversität im marinen Plankton besser zu erfassen.

Summary

More than 70% of the earth's surface is covered with water, of which about 97% is saltwater in oceans and seas. The photic zone of this area forms the habitat of the marine phytoplankton that is all drifting photosynthetic organisms. By fixing carbon dioxide in form of organic material and releasing oxygen, they play an important role for the global climate, global biogeochemical cycling, and the marine food web. However, the succession and dynamics of marine phytoplankton blooms are still not fully understood and far from being predictable. It, nevertheless, becomes evident that chemically-mediated interactions with viruses, bacteria and zooplankton are of importance. The elucidation of these interactions has been strongly driven and improved by the technical and computational achievements of the last decades.

I explored in my thesis the capabilities of different metabolomics approaches for the investigation of marine phytoplankton ecology especially in environmental studies. I conducted a comprehensive review of metabolomics in the field of chemical ecology, and introduced a systematically optimized and standardized protocol for the metabolic analysis of marine algae. Furthermore, I developed a UHPLC-APCI-HRMS method for the simultaneous profiling of volatile and non-volatile oxylipins. By performing GC-MS-based untargeted metabolite profiling of algal endo- and exometabolites, I monitored throughout growth of *Phaeocystis pouchetii* its metabolic alterations and identified potential physiological markers. During a research cruise in the Norwegian Sea, I applied a meta-metabolomics approach to map the chemical diversity and physiological plasticity of phytoplankton communities.

Oxylipins play an important role as grazer defence metabolites for marine diatoms. Cellular wounding activates the enzymatic transformation of membrane lipids to polyunsaturated aldehydes (PUAs) that have a teratogenic effect in the grazer offspring. In addition, non-volatile oxylipins are released, which show similar effects. While PUAs are typically measured by GC-MS, more polar non-volatile oxylipins are analysed by LC-MS. The developed LC-APCI-HRMS method allows for the first time to study both compound classes on one analytical platform within one run. The sensitive analysis of PUAs in selected ion monitoring (SIM) mode revealed for the first time hexadienal in a marine microalgae. Complementary untargeted profiling of non-volatile oxylipins enabled the simultaneous analysis of decatrienal and 10-hydroxydeca-5*Z*,8*Z*-dienoic acid as corresponding enzymatic product. This will

facilitate the biochemical investigation of oxylipin production in marine microalgae. The short sample processing and analysis time, as well as the low sample volume, allow a high sample throughput in both laboratory and field experiments.

Grazing and other biotic interactions may be influenced by algal physiology, as has been repeatedly discussed in the past. Physiological plasticity further allows microalgae to adapt to environmental changes, which increases their fitness and survival. However, our understanding of physiological plasticity is still limited for the taxonomically heterogeneous group of marine phytoplankton. Growth-related changes in intra- and extracellular metabolites of the cold water species *Phaeocystis pouchetii* were monitored using untargeted metabolite profiling. Batch-cultures introduced changes in growth-limiting parameters, for example, in light intensity and nutrient concentrations. Metabolic alterations occur with regard to free amino acids that increase during exponential growth in parallel to nitrogen incorporation. Growth limitation in stationary growth phases leads for example to an accumulation of carbohydrates based on a mismatch of continuing photosynthesis and limited growth. The increase in lipid-derived structures during late stationary growth including α-tocopherol, polyunsaturated fatty acids, and sterols, points to the need to sustain membrane stability. In addition to these common algal metabolism responses, also species-specific alterations exist, e.g. for haptophytes in mannitol levels, which may be used as taxon-specific physiological markers in environmental studies. Microalgal growth physiology is also reflected in extracellular metabolites. Exometabolomes of *P. pouchetii* represent diverse chemical mixtures that reflect not just growth physiology but also biotic interactions, as metabolites with high similarity to known infochemicals were present, including a lumichrome-like and indole-3-acetic acid-like compound.

The same physiological plasticity can be expected in natural phytoplankton communities. In a meta-metabolomics approach, I applied untargeted metabolite profiling to visualise metabolic plasticity in marine field experiments. A common approach to investigate predator-prey-relationships in the environment are dilution experiments. Their disturbance by PUAs, which may be released during filtration from certain phytoplankton species like *P. pouchetii* or certain bloom phases, has been postulated in the past. However, this could not be proven by targeted PUA analysis. Untargeted metabolite profiling of the extracellular metabolites in the filtrate uncovered a general treatment effect on the chemical composition of the filtrate. One possibility to control for this effect are measurements of specific growth rates. Similarly, it has

been proposed several times in the past, that cell physiology may be responsible for the reduced grazing of copepod on *P. pouchetii*. In an extensive research cruise in the Norwegian Sea investigating different phytoplankton blooms that were dominated by *P. pouchetii*, I could for the first time map the metabolic plasticity of whole phytoplankton communities using a meta-metabolomics approach. Metabolites like eicosapentaenoic acid reflected algal taxonomy and thus species distribution. The occurrence patterns of the physiological markers that were derived from *P. pouchetii* cultures visualised the strong imprint of abiotic environmental factor responses on the metabolic landscape.

Research in ecology is to a certain extent defined and driven by taxonomy. On the metabolite level, however, phylogeny is not the main driving force. This is visible for the well-investigated class of oxylipins, whose occurrence and composition throughout marine phytoplankton taxa is not directly related to global biomass and ecological significance. This is also visible for meta-metabolomes of whole phytoplankton communities, whose taxonomic signature is imprinted by treatment effects and nutrient limitation effects. Metabolomics is able to visualize the functional diversity and plasticity of the marine phytoplankton. Complementary to targeted analysis of well-known molecules, untargeted metabolite profiling will thereby help to expand the coverage of the chemical diversity in plankton ecology.

1 Introduction

1.1 The chemical ecology of marine phytoplankton

1.1.1 Chemically mediated interactions in phytoplankton ecology

Within the field of chemical ecology, interactions of organisms with their biotic and abiotic environment that are mediated by chemical molecules are investigated. Besides the identification of chemical signals also their biosynthesis, reception, signal transduction, and effects on the receiving organism and the ecosystem are studied. Originating from terrestrial ecology (see Hartmann (2008) and references therein), marine chemical ecology research is still in its advent, especially with regard to plankton communities (Poulson et al. 2009) (Fig. 1).

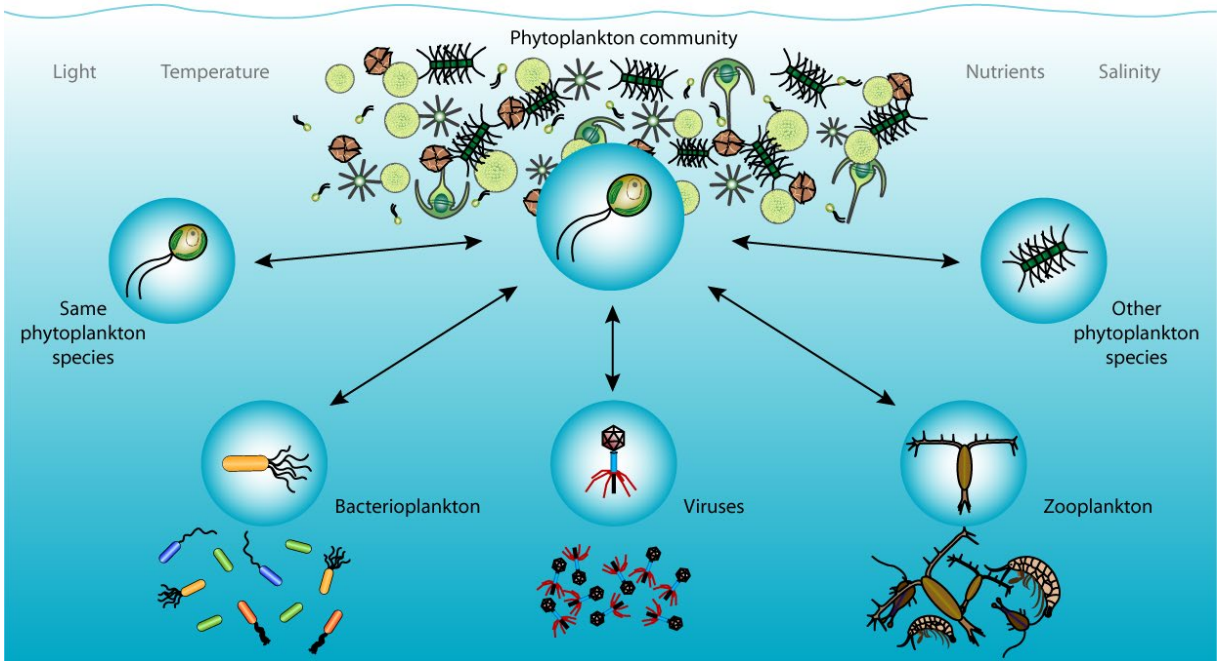

Fig. 1 Marine phytoplankton species undergo chemically mediated interactions, both within the species as well as with other phytoplankton species, zooplankton, fungi, bacteria, or viruses. Further, abiotic factors including irradiance, temperature, or nutrient availability influence their ecology.

Plankton (Greek *planktos* "errant") encompasses all aquatic organisms drifting with the ocean currents due to no or low motility. This includes viruses, bacteria, archaea, fungi, protozoa, algae and animals, spanning a size range from $<2\times10^{-7}$ m (viruses) to several meters (jellyfish). Depending on their ecological function, these taxa are classified into photoautotrophic phytoplankton (Greek *phyton* "plant") as primary producer, heterotrophic zooplankton (Greek *zoon* "animal") as consumer, and heterotrophic bacterio- and mycoplankton (Greek *mykes* "fungus") as decomposer.

The photoautotrophic phytoplankton communities play an important role on a global scale. While fixing >10^{14} g CO_2 day^{-1} phytoplankton is responsible for about 46% of the annual global net primary production and dominating the marine primary production (Field et al. 1998). Phytoplankton thus forms the base of the marine food web and influences global climate and biogeochemical cycling. Another interesting aspect of marine phytoplankton communities compared to terrestrial plants is their taxonomic diversity with representatives in prokaryotes and eukaryotes (Fig. 2). The permanent endosymbiosis of a cyanobacterium in a eukaryotic host cell led to the basal clades of rhodophytes (red algae), chlorophytes (green algae) and glaucophytes (Falkowski et al. 2004).

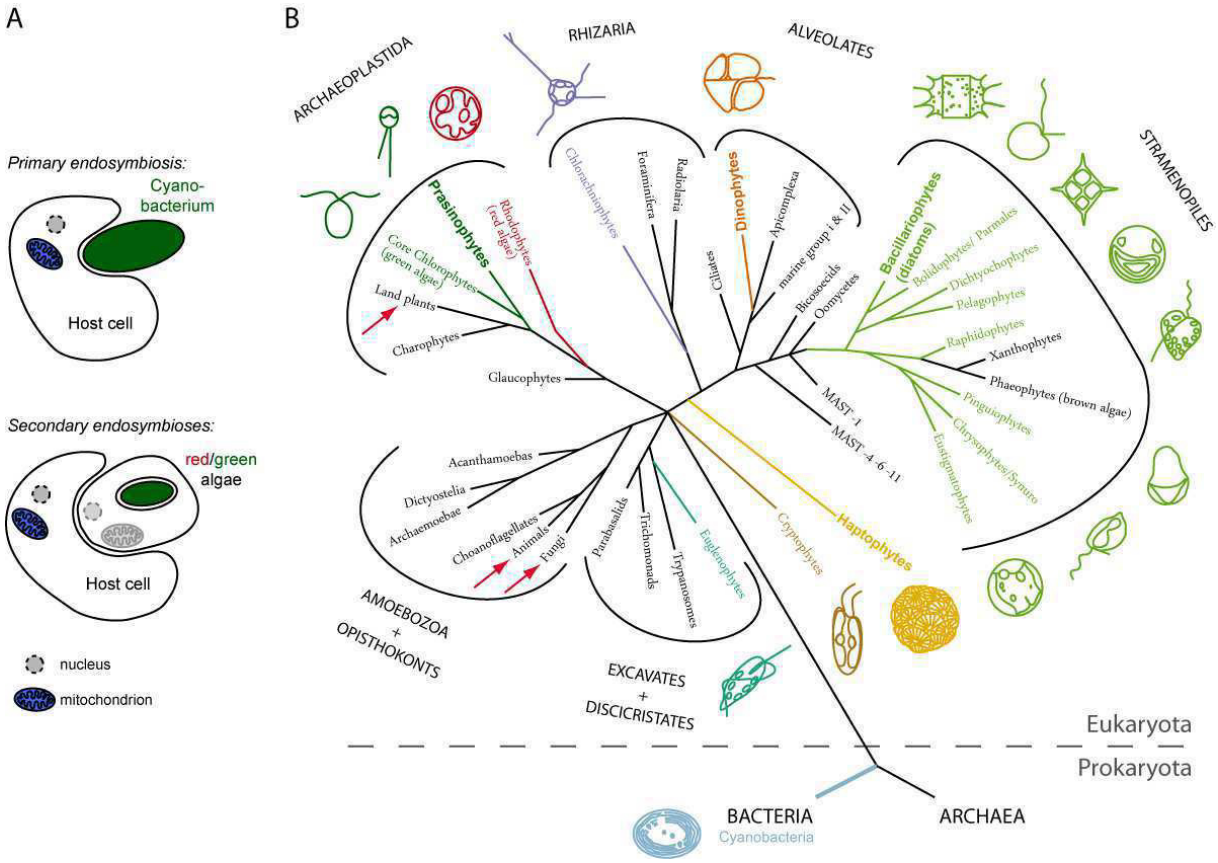

Fig. 2 Phytoplankton biodiversity as source for chemical diversity: scheme of endosymbiotic events (A) and phylogeny (B) showing the distribution of phytoplankton taxa across the eukaryotic and prokaryotic lineages. Engulfment of a prokaryotic cyanobacterium by an eukaryotic host (primary endosymbiosis) led to the clade of Archaeoplastida (marked with star). Representatives of subsequent sequential endosymbioses of red and/or green algal cells by different eukaryotic host cells (secondary endosymbioses) are found in the clade of SAR (Stramenopiles, Alveolates, Rhizaria) and Excavates and Discicristates. The red arrows point to the plant, animal and fungal kingdom. The most diverse and ecologically important phytoplankton taxa are indicated by bold letters. Figure is adapted from Not et al. (2012), copyright license no. 4284020697673.

Further diversification took place by multiple secondary endosymbioses of red and/or green algal cells leading to cryptophytes, haptophytes, stramenopiles (e.g. diatoms),

dinoflagellates, chlorarachniophytes and euglenophytes. The most dominant marine phytoplankton taxa showing also highest species diversity are diatoms, haptophytes, and dinoflagellates. Each endosymbiotic event was accompanied by a gene transfer from endosymbionts to host nuclei increasing the genetic pool (Tirichine and Bowler 2011). Together with the effect of horizontal gene transfer from bacteria and viruses (Bowler et al. 2008), phytoplankton taxa gained a large genetic diversity resulting, for example, in unusual metabolic pathways (Allen et al. 2011; Fabris et al. 2012). Also novel infochemicals may be expected in the chemical ecology of phytoplankton compared to what is known from plants. In the following, the term 'microalgae' will be used synonymously for phytoplankton, even though it includes species that are associated with the ocean floor (benthic).

As plants in the terrestrial realm, marine phytoplankton species can undergo multiple types of interactions. Phytoplankton interactions are mediated neither by visual nor auditory cues, but solely through infochemicals inducing e.g. developmental, morphological, physiological, and behavioural changes. Such infochemicals are defined as naturally occurring chemicals that mediate the interaction between two individuals inducing an adaptive response in the receiver (Dicke and Sabelis 1988). Interactions within the same species are mediated by pheromones, whereas allelochemicals occur in interactions between different species with profit for the sender (allomone), receiver (kairomone), or both (synomone). In the following, the different interactions as known for the marine phytoplankton are introduced.

Phytoplankton pheromones

Only little is known so far about intraspecific interactions covering ecologically important processes such as sexual reproduction or programmed cell death and thereby bloom succession. The first identified diatom pheromone, the diketopiperazine diproline (**1**), attracts mates in the benthic diatom *Seminavis robusta* (Gillard et al. 2013). No pheromones have yet been identified in pelagic marine microalgae. Indole-3-acetic acid (IAA, **2**) is a well-known growth regulating hormone (*'signalling molecule within multicellular organisms*') in plants. Also the marine microalgae *Emiliania huxleyi* can biosynthesize IAA (Labeeuw et al. 2016). Interestingly, only coccolith-bearing cells seem to produce IAA, whereas naked cells are more sensitive in their physiological response indicating an intraspecific signalling function (Labeeuw et al. 2016). The same molecule is mediating algae-bacteria interactions (Amin et al. 2015).

Polyunsaturated aldehydes (PUAs, e.g. **3**-**5**) - originally investigated as activated grazing defence metabolites (see 1.1.3) - can induce programmed cell death in diatom blooms thereby regulating bloom decline (Vardi et al. 2008; Vidoudez and Pohnert 2008). Similar autoinhibitory and autotoxic effects also occur in other microalgae (Olli and Trunov 2007; Yamasaki et al. 2011), however, the responsible infochemicals have not yet been identified.

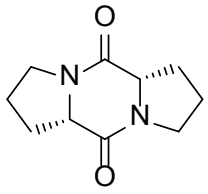

1

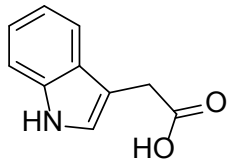

2

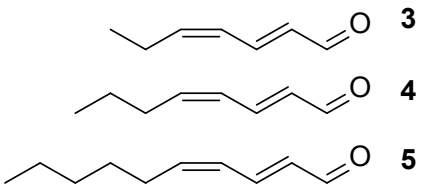

Phytoplankton allelochemicals

Interspecific interactions were investigated more intensively with the majority of allelopathic studies being conducted on allomones and grazing defence metabolites. Most of the involved infochemicals are, however, still unknown. The known neurotoxin domoic acid (**6**) is released by the diatom *Pseudo-nitzschia delicatissima* as a siderophore reducing the growth of *Skeletonema costatum* by giving competitive advantage under low iron conditions (Prince et al. 2013). Several dinoflagellate genera (e.g. *Alexandrium*, *Prorocentrum*, *Karlodinium*) and *Karenia brevis* induce allelopathic effects like growth reduction or cell lysis in other dinoflagellates, diatoms, cryptophytes and raphidophytes (Ma et al. 2011a; Prince et al. 2010; Tameishi et al. 2009). The haptophyte *Prymnesium parvum* causes cell lysis in the cryptophyte *Rhodomonas baltica* (Uronen et al. 2007), and the dinoflagellate *Cochlodinium polykrikoides* induces immobilization in diatoms (Lim et al. 2014). However, with the exception of karlotoxins (**7**-**13**) (Adolf et al. 2006) the involved allelochemicals were only preliminarily characterized. Also PUAs (e.g. **3**-**5**), which are well-known grazer defence metabolites, can induce allelopathic effects in a broad range of algal phyla (Ribalet et al. 2007a).

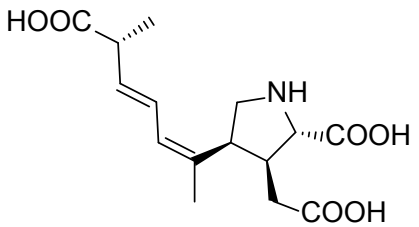

6

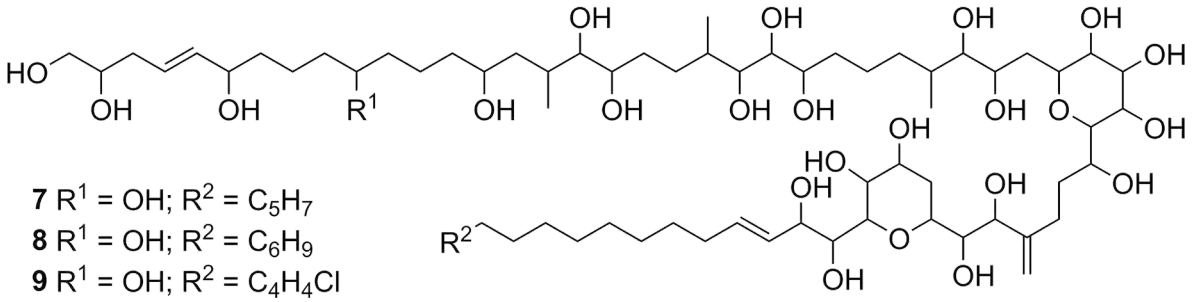

7 R^1 = OH; R^2 = C_5H_7
8 R^1 = OH; R^2 = C_6H_9
9 R^1 = OH; R^2 = C_4H_4Cl
10 R^1 = OH; R^2 = C_5H_6Cl
11 R^1 = OH; R^2 = C_6H_8Cl
12 R^1 = OSO_3H; R^2 = C_5H_7
13 R^1 = OSO_3H; R^2 = C_6H_9

7-13

Different predator-prey interactions are mediated by chemical cues, e.g. prey recognition and tracking, algal defence with effects on both predator behaviour and physiology, or predator avoidance. Predators can sense, track (Tiselius et al. 2013), and immobilize their prey (Blossom et al. 2012; Remmel and Hambright 2012). Prey quality can be recognized prior to ingestion (Barofsky et al. 2010; Martel 2009; Selander et al. 2011). Phytoplankton cells can defend themselves constitutively by permanent synthesis of well-known algal toxins such as saxitoxin (**14**) (*Alexandrium* sp.), brevetoxins (**15**-**22**) (*Karenia* sp., Waggett et al. (2012)), or nodularin (*Nodularia spumigena*), however, the ecological role and toxic mechanisms are poorly understood (Landsberg 2002; Turner and Tester 1997). Phytoplankton cells may also activate their chemical defence upon wounding by converting an inactive precursor into an active defence metabolite as demonstrated for the wound-activated release of

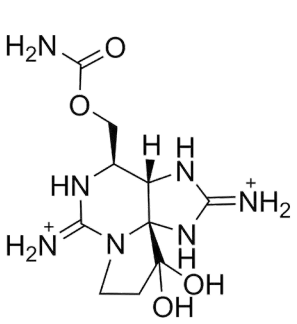

14

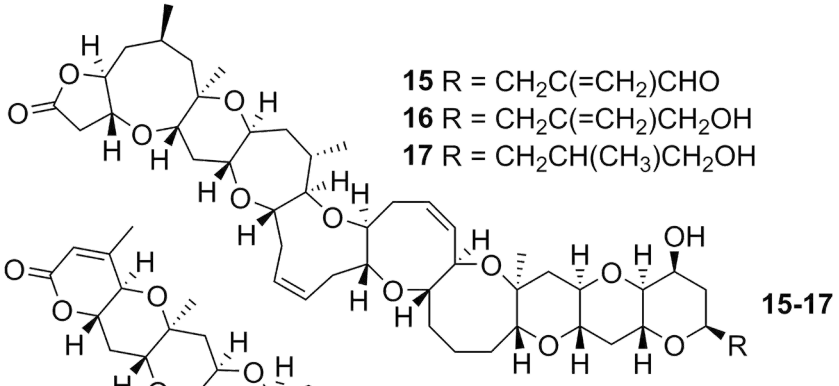

15 R = $CH_2C(=CH_2)CHO$
16 R = $CH_2C(=CH_2)CH_2OH$
17 R = $CH_2CH(CH_3)CH_2OH$

15-17

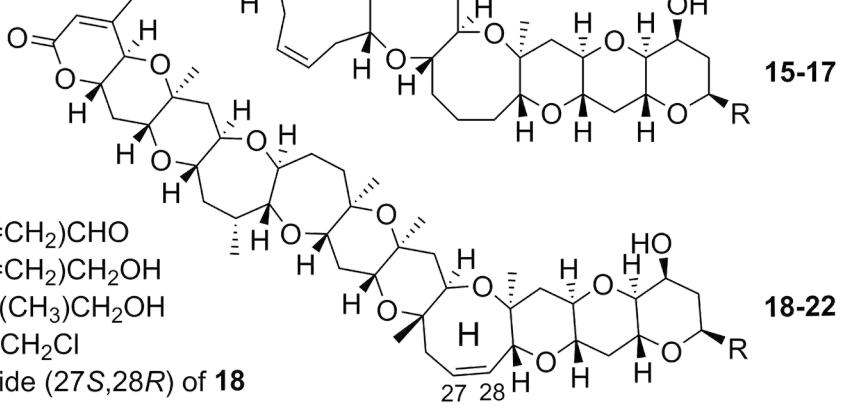

18 R = $CH_2C(=CH_2)CHO$
19 R = $CH_2C(=CH_2)CH_2OH$
20 R = $CH_2CH(CH_3)CH_2OH$
21 R = CH_2COCH_2Cl
22 H-ring epoxide (27*S*,28*R*) of **18**

18-22

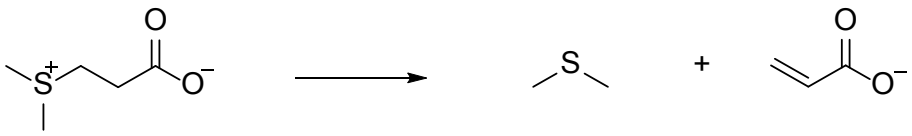

23 **24** **25**

dimethylsulfide (DMS, **24**) and acrylate (**25**) from dimethylsulfoniopropionate (DMSP, **23**) in *Emiliania huxleyi* (Wolfe et al. 1994; Wolfe et al. 2000), or for the oxylipin release from polyunsaturated fatty acids (PUFAs) in diatoms (see 1.1.3). In both cases their function as defence metabolites is, however, under discussion. Chemical defence may also be induced upon grazer contact as observed for *Alexandrium* sp. (Selander et al. 2015; Wohlrab et al. 2010) or *E. huxleyi* (Kolb and Strom 2013). Phytoplankton may avoid predation upon reception of (so far unknown) grazer cues by changes in motility (Harvey et al. 2013) and morphology, e.g. chain length (Bergkvist et al. 2012; Jiang et al. 2010; Selander et al. 2011) or colony formation (Long et al. 2007; Tang et al. 2008). The recently described copepodamides (**26**-**33**) are the first potential copepod cues that may mediate phytoplankton-copepod interactions (Selander et al. 2015).

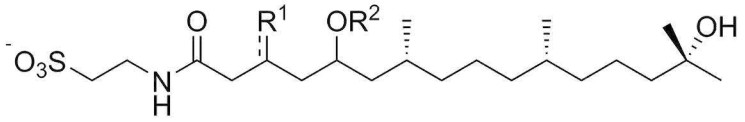

26-33

26 $R^1 = CH_3$; R^2 = docosahexaenoic acid
27 $R^1 = CH_3$; R^2 = eicosapentaenoic acid
28 $R^1 = CH_3$; R^2 = stearidonic acid
29 $R^1 = CH_3$; $R^2 = H$
30 $R^1 = CH_2$; R^2 = docosahexaenoic acid
31 $R^1 = CH_2$; R^2 = eicosapentaenoic acid
32 $R^1 = CH_2$; R^2 = stearidonic acid
33 $R^1 = CH_2$; $R^2 = H$

Parasitism describes interactions with benefits on the expense of the host. Algicidal effects mediated, for example, by proteases, troponoids and indole-derivatives were demonstrated for several bacteria already including *Kordia algicida*, *Phaeobacter gallaeciensis*, *Bacillus* sp. and *Shewanella* sp. (Jeong et al. 2003; Paul and Pohnert 2011; Pokrzywinski et al. 2012; Seyedsayamdost et al. 2011). Some parasites thereby rely on chemical cues like DMS to recognize and track their hosts (Garces et al. 2013). The sensitivity of the dinoflagellate host *Karlodinium veneficum* towards parasitic dinoflagellates is mediated via karlotoxins (**7-13**) and membrane sterol composition (Place et al. 2009). Membrane constituents like sterols and glycosphingolipids also

play an important role in the host-virus interaction of the haptophyte *Emiliania huxleyi*, in which they mediate, for example, programmed cell death in the host population (Rosenwasser et al. 2014; Vardi et al. 2012).

Facilitation describes interactions, in which one partner benefits with a positive (mutualism) or neutral effect (commensalism) for the interacting partner. The mutualistic interaction between the dinoflagellate *Scrippsiella trochoidea* and bacteria of the *Marinobacter* clade is mediated by the siderophore vibrioferrin (**34**) (Amin et al. 2009). Also facilitation of microalgal growth (Paul et al. 2009) and cyst germination (Bolch et al. 2011) has been described, the infochemicals are, however, still awaiting structure elucidation.

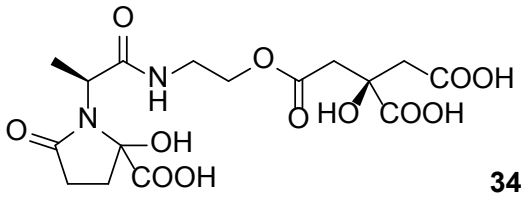

34

Whereas this happens on small spatial scales, a tritrophic interaction mediated via DMS (**24**) was observed between marine phytoplankton, herbivore copepods, and higher trophic level organisms. Upon copepod grazing, phytoplankton releases DMS (**24**) from DMSP (**23**). This attracts species that feed upon copepods such as birds or penguins (Amo et al. 2013; Savoca and Nevitt 2014). Such ecosystem-wide effects mediated by phytoplankton infochemicals are rarely investigated. So far, primarily the fate and role of microalgal toxins within the marine food web have been investigated (Schwartz et al. 2016). Phytoplankton toxicity is under the control of both biotic (con-specifics, grazers) and abiotic factors (nutrient availability, salinity, aeration). Toxins like nodularin, saxitoxin (**14**), gonyautoxins, brevetoxins (**15**-**22**) and domoic acid (**6**) as produced by cyanobacteria, dinoflagellates and diatoms are transferred to higher trophic levels including krill, fish, and seals, in which they may induce toxic effects. The investigation of phytoplankton chemical ecology on the community level is difficult to mimic with simplified laboratory-based experiments and requires more field-based research.

1.1.2 Elucidation of phytoplankton metabolic pathways

The investigation of infochemicals is often targeting metabolites that occur and act in the exometabolome of marine microalgae. However, the endometabolome and especially primary metabolites provide the basis for phytoplankton interactions as well (Fig. 3). Besides the investigation of biosynthetic pathways of certain infochemicals in the producing organisms, this also includes metabolic responses in the receiving organism and interactions with the abiotic environment mediated by e.g. nutrient concentrations that shape biotic interactions.

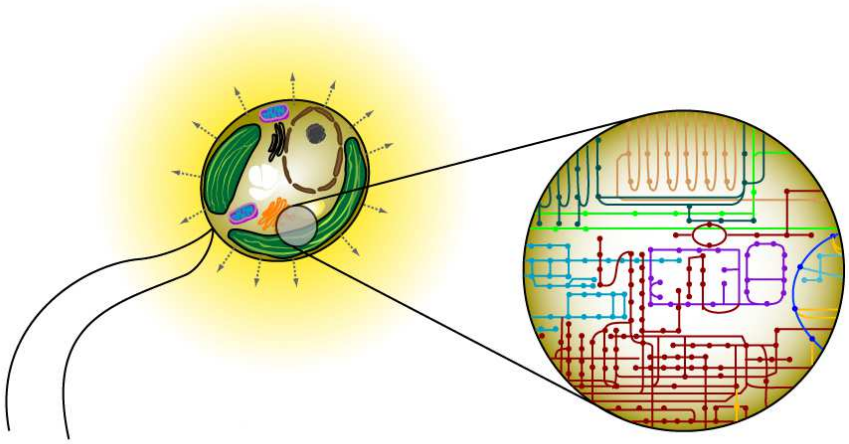

Fig. 3 Untargeted metabolite profiling sheds light on metabolic pathways and resulting primary and secondary metabolites, as well as excreted extracellular metabolites including signal molecules.

Metabolic diversity between taxa revealed by genome sequencing

Due to the polyphyletic origin of the marine phytoplankton (Fig. 2), differences in the primary and secondary metabolism exist between microalgal taxa. Recent advances in whole-genome sequencing technologies allowed the sequencing of several marine microalgae, including *Emiliania huxleyi*, *Thalassiosira pseudonana* (Armbrust et al. 2004), *Phaeodactylum tricornutum* (Bowler et al. 2008), and *Ostreococcus tauri* (Derelle et al. 2006), and even more genomes are in preparation. Already these genomes revealed novel potential metabolic pathways and a large number of genes and proteins with unknown functions (Tirichine and Bowler 2011). In diatoms, for example, there is evidence that metabolic pathways exist for the ornithine-urea-cycle, which is known for metazoa (Allen et al. 2011), and the Entner-Doudoroff glycolytic pathway, which is known for prokaryotes (Fabris et al. 2012). In the haptophyte *E. huxleyi* mannitol as major carbon storage of C_3 photosynthesis (Obata et al. 2013) and NAD-independent malate-oxidation (Rokitta et al. 2014) were elucidated. Whole-

genome sequencing thereby provides evidences that have to be confirmed by complementary analyses on the proteome, transcriptome or metabolome level.

Metabolic plasticity within species

Next to the metabolic diversity between taxa, substantial metabolic plasticity within species exists. Microalgal metabolism differs e.g. between the various life phases of one species. Thus, for example, many primary metabolites (citric acid, lactic acid, threonic acid, saccharides) were up-regulated in the haploid cell type of *Emiliania huxleyi*, whereas triacylglycerols were reduced, which may be due to the high energy demand of flagellar movement (Mausz and Pohnert 2015; Wördenweber et al. 2017). In contrast, diploid cells were characterized by higher levels of DMSP (**23**), which was proposed to be a response to higher osmotic needs during calcification (Wördenweber et al. 2017). Both life phases also differed in their sterol composition, being enriched either in ergosterol (haploid cells) or epibrassicasterol (diploid cells) (Mausz and Pohnert 2015). Microalgal metabolism also responds to various biotic and abiotic environmental factors like temperature, salinity, irradiance and nutrient concentrations. Viral infection of *E. huxleyi* induced fatty acid metabolism, production of viral-specific glycosphingolipids, and lead to a severe reduction in sterols and other terpenes (Rosenwasser et al. 2014). In response to light-dark-cycles, diurnal fluctuations in metabolite concentrations can occur. Trehalose, for example, exhibited strong diurnal fluctuations in the chlorophyte *Ostreococcus tauri* with accumulation at night due to starch degradation (Hirth et al. 2017). In the diatom *Skeletonema marinoi*, maltose and most amino acids accumulated during night, whereas only a few amino acids (e.g. proline) were more abundant during day (Vidoudez and Pohnert 2012). The observed diurnal variability in *S. marinoi* was even stronger during exponential growth.

Growth phase-specific marker metabolites

Phytoplankton cells develop their metabolic phenotype during growth, which has been documented on the metabolic level for only a few microalgal species so far: *Skeletonema marinoi* (Barofsky et al. 2010; Vidoudez and Pohnert 2012), *Emiliania huxleyi* (Mausz and Pohnert 2015), and *Synechococcus elongatus* (Fiore et al. 2015). Free amino acids and saccharides characterized the exponential growth of *S. marinoi* (Vidoudez and Pohnert 2012). In the stationary phase only a few metabolites had their maximum level, e.g. glucose, probably fuelling the lipid metabolism as further indicated by the accumulation of glycerol, inositol isomers and

lipids during stationary and declining growth. Induced catabolic reactions during growth decline gave rise to some known (e.g. sterols and other terpenes) and many unknown metabolites. Putrescine (**35**) increased throughout growth. In contrast, the exponential growth of *E. huxleyi* was characterized by carboxylic acids and mannitol, which appears to be the major carbohydrate storage molecule in this haptophyte (Mausz and Pohnert 2015). Amino acids were not regulated. During stationary growth, free fatty acids and putatively identified (di)galactosylglycerol increased indicating an active lipid metabolism. Declining growth was characterized by terpenes (e.g. α-tocopherol and sterols) but also by several mono- and disaccharides as putative breakdown products of structural polysaccharides. Growth of the cyanobacterium *S. elongatus* was characterized by an intracellular increase in DMSP (**23**), spermidine (**36**) and spermidine pathway-related metabolites, which also all belonged to the most abundant intracellular metabolites (Fiore et al. 2015).

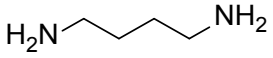

35

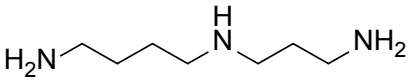

36

Already these three studies indicate general metabolic responses during growth (such as induced lipid metabolism under growth limitation), but also clear taxon-specific differences (such as mannitol as main carbohydrate storage molecule in *E. huxleyi*). For several growth phase-specific metabolites the function is not yet known (e.g. lumichrome), or they seem to be multifunctional without a specific recognized role (e.g. putrescine). Thus, further studies are necessary to discriminate between growth phase-related metabolites that are strain-specific, species-specific, or common among the phytoplankton clades. This may allow us in the future to discriminate phytoplankton bloom phases in natural environments.

1.1.3 Elucidation of phytoplankton infochemicals

Bioassay-guided fractionation

Even nowadays, bioassay-guided fractionation is a widely used approach to isolate and identify infochemicals in chemical ecology and new protocols are still developed (Cutignano et al. 2015). Active crude extracts are separated via (preparative) LC, GC, or thin-layer chromatography (TLC) based on chemical properties, fractionated manually or automatically, and the fractions are tested in bioassays for their ecological activity. This procedure is conducted in an iterative manner to purify and isolate the active compound(s) before final structure elucidation via MS or NMR spectroscopy. Different analytical platforms and bioassay set-ups are necessary to cope with the broad range in polarity, size, mode of action, and biosynthetic origin that can be expected for an unknown infochemical as reviewed by Weller (2012).

Many compounds that play a role in marine phytoplankton ecology have been elucidated by bioassay-guided fractionation. This applies especially to harmful algal bloom toxins that can induce negative effects in organisms at higher trophic levels like fish or humans. Toxin classes include alkaloids like domoic acid (**6**), tetrahydropurines like saxitoxin (**14**), macrocyclic imines like pinnatoxin A (**37**), linear and macrocyclic polyethers like karlotoxins (**7**-**13**), and ladder-frame polyethers like

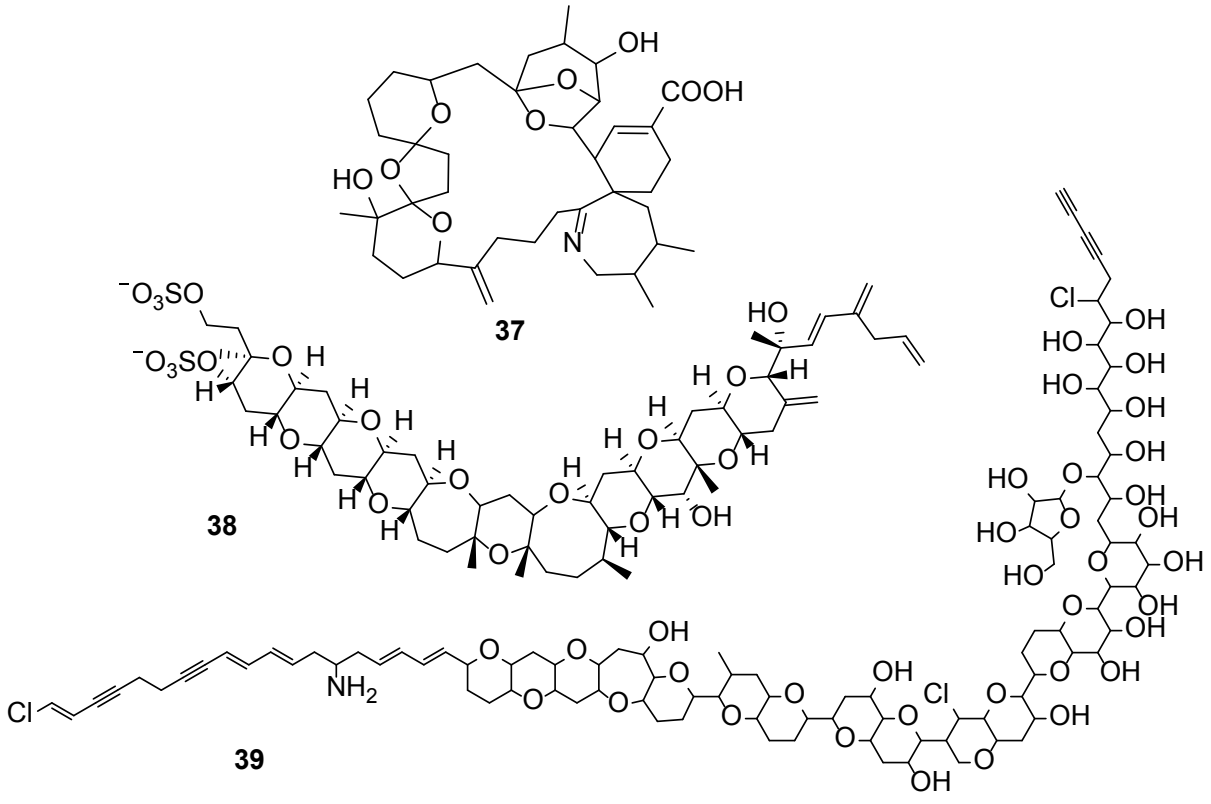

brevetoxins (**15**-**22**), yessetoxin (**35**), and prymnesin-2 (**36**) (Rasmussen et al. 2016). These phytoplankton toxins thereby demonstrate nicely the chemical diversity that can be expected in marine infochemical research spanning a wide range in molecular size and polarity.

The formerly proposed toxicity towards fish has been retracted recently for some phytoplankton metabolites (Blossom et al. 2014), and the responsible ichthyotoxic compounds could not be elucidated so far. This lack in identification of active compounds is exemplary for the infochemical research on marine phytoplankton in general (see 1.1.10), and may be due to the methodical limitations of bioassay-guided structure elucidation. The approach requires multiple sample purification and enrichment steps, and a well-designed bioassay. This is a solvent-demanding and time-consuming process with often low reproducibility. For marine samples a desalting step is needed. Especially unstable compounds and infochemicals with additive, antagonistic, or synergistic effects are difficult to elucidate via this approach and require for new analytical methodologies such as comparative metabolite profiling (see Chapter 1.2).

Targeted analytical approaches for polyunsaturated aldehydes and other oxylipins

Once a member of a compound class is identified that is biologically active (Miralto et al. 1999), targeted chemical analyses allow the discovery of additional members. Short-chained polyunsaturated aldehydes (PUAs; e.g. **3**-**5**) are a well-investigated infochemical compound class that plays, for example, a role in predator-prey interactions of marine phytoplankton. Upon cell wounding, PUAs are enzymatically cleaved from membrane-derived polyunsaturated fatty acids (PUFAs) and may be directly released into the grazer gut (Pohnert 2002; Wichard et al. 2007). PUAs can accumulate in the grazer gonads and react with proteins and DNA (Wolfram et al. 2014; Wolfram et al. 2015) leading to reproductive failure in the predator population. It thus reflects an activated chemical grazer defence strategy.

PUAs belong to the class of oxylipins - a diverse group of metabolites derived from fatty acid oxygenation (original definition by Gerwick et al. (1991): *'oxygenated compounds which are formed from fatty acids by reaction(s) involving at least one step of mono- or dioxygenase-catalyzed oxygenation*'). Catalyzed by lipoxygenases (LOXs), free PUFAs are thereby oxygenized with molecular oxygen to fatty acid hydroperoxides (FAHs). These can be further converted to e.g. PUAs, ω-oxo acids,

hydroxyacids, and halogenated, unsaturated, or alicyclic hydrocarbons (Fig. 4). Biological functions of some oxylipins have been reported for marine and freshwater microalgae (d'Ippolito et al. 2009; Fontana et al. 2007; Nanjappa et al. 2014; Pohnert and Boland 1996; Wang and Shimizu 1990; Wendel and Jüttner 1996; Wichard and Pohnert 2006).

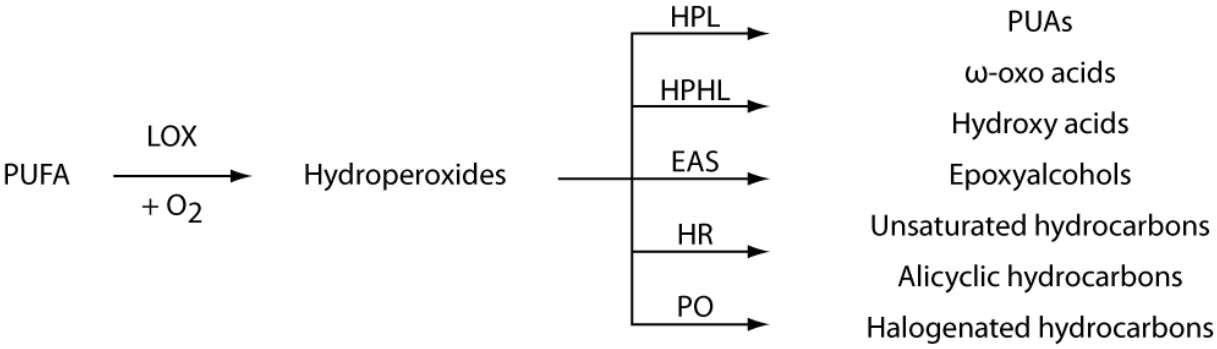

Fig. 4 Scheme of oxylipin-generating pathways that are known in phytoplankton. Free polyunsaturated fatty acids (PUFAs) are oxygenized by lipoxygenases (LOXs) to fatty acid hydroperoxides (FAHs). Different enzymes then lead to a variety of oxylipin products: HPL = hydroperoxide lyase, HPHL = hydroperoxide halolyase, EAS = epoxyalcohol synthase, HR = hydroperoxide reductase, PO = peroxidase.

The occurrence of PUAs depends on the presence of certain precursor fatty acids and the corresponding enzymes. For marine microalgae, the following PUAs are known with their biosynthetic pathways (Fig. 5): (2*E*,4*Z*)-hepta-2,4-dienal (**3**), (2*E*,4*Z*)-octa-2,4-dienal (**4**), (2*E*,4*Z*)-octa-2,4,7-trienal (**4b**), (2*E*,4*Z*)-deca-2,4-dienal (**5**), and (2*E*,4*Z*,7*Z*)-deca-2,4,7-trienal (**5b**). A wound-activated enzymatic pathway was proposed for their production (Pohnert 2002). In the first step, lipases release free fatty acids from membrane phospholipids and from chloroplast-derived glycolipids especially mono- and digalactosyldiacylglycerols (Cutignano et al. 2006; d'Ippolito et al. 2004; Pohnert 2002). In the second step, free PUFAs such as C16:3ω-4 (**40**), C16:4ω-1 (**41**), C20:4ω-6 (AA, **42**) and C20:5ω-3 (EPA, **43**) are oxygenated by LOX enzymes (Fig. 5). These are non-heme iron-containing dioxygenases that typically interact regio- and stereospecific with 1*Z*,4*Z*-pentadiene moieties within PUFAs (Schneider et al. 2007). Several LOXs are reported for marine diatoms, however, only 9-, 11- and 14-LOX seem to play a role for PUA formation (Andreou et al. 2009). In the third step, LOX-derived intermediate FAHs, for example (6*Z*,10*E*,12*Z*)-9-hydroperoxy-6,10,12-hexadecatrienoic acid (d'Ippolito et al. 2006), are further enzymatically transformed. Hydroperoxide lyases (HPLs) - haeme-containing monooxygenases - cleave FAHs substrate specific into two short-chained oxylipins like PUAs and shorter-chain fatty acid derivatives (Fig. 5). In higher plants this has been demonstrated to be

a homolytic cleavage releasing an aldehyde and a ω-oxo acid (Grechkin and Hamberg 2004). Diatom HPLs seem to follow another mechanism releasing hydroxy fatty acids like (8*Z*)-8-hydroxyoct-6-enoic acid (**44**) and (5*Z*,8*Z*)-10-hydroxydeca-5,8-dienoic acid (**45**, Fig. 5) (Barofsky and Pohnert 2007). Non-enzymatic isomerisation may result in ω-oxo acids. All enzymes are probably present in an active form in cell lysates as the whole reaction releases up to 4.1 fmol cell^{-1} of **5b** within seconds after loss of cellular integrity (Pohnert 2000).

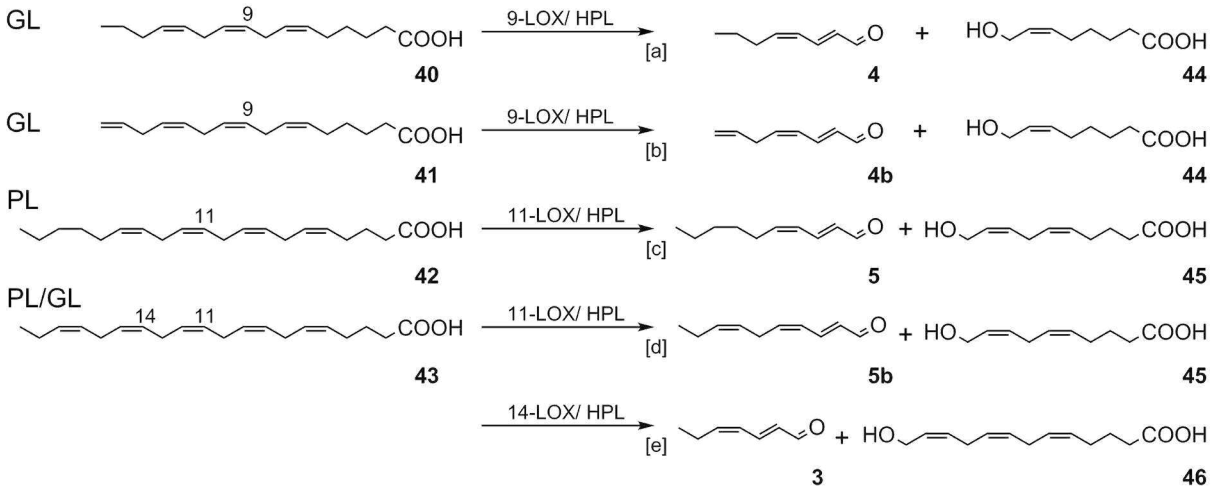

Fig. 5 Known biosynthetic pathways of polyunsaturated aldehydes in marine diatoms. Free polyunsaturated fatty acids as released from glycolipids (GL) or phospholipids (PL) and transformed by an enzymatic cascade into polyunsaturated aldehydes as described by a - d'Ippolito et al. (2003), a/b/d/e - d'Ippolito et al. (2004), b - Pohnert et al. (2004), c - Pohnert (2000), c/d/e - Pohnert (2002) and Barofsky and Pohnert (2007). LOX = lipoxygenase, HPL = hydroperoxide lyase.

PUA research has focused on marine diatoms in the past and *Skeletonema costatum* and *Thalassiosira rotula* often served as model organism (d'Ippolito et al. 2002a; d'Ippolito et al. 2002b; Miralto et al. 1999; Pohnert 2000). Observed species- and strain-specificity in PUA production (Pohnert et al. 2002) motivated the screening of >70 diatom strains, of which about 38% released PUAs with *T. rotula* being the most active species (Wichard et al. 2005a). Besides diatoms, PUA-production has been recorded within the following marine micro- and macroalgae: rhodophytes (de Alencar et al. 2017; Kajiwara et al. 1990), the chlorophyte *Ulva* sp. (Akakabe et al. 2003; Alsufyani et al. 2014), the phaeophyte *Laminaria* sp. (Boonprab et al. 2003; Goulitquer et al. 2009), and the haptophyte *Phaeocystis pouchetii* (Hansen et al. 2004). Thus, within marine phytoplankton so far only diatoms and *Phaeocystis pouchetii* are known to produce PUAs, whereas within freshwater phytoplankton diatoms, chrysophytes, synurids and cyanobacteria are known to release PUAs (Jüttner 1995).

Their role as chemical defence metabolites is due to their influence on the reproduction of copepods causing e.g. reduced fecundity and hatching success and malformation of nauplii. This was first observed for copepods fed with *Thalassiosira rotula* (Ianora and Poulet 1993; Poulet et al. 1994) and later confirmed in >30 copepod-diatom interactions (Ban et al. 1997). After observing reduced copepod viability during blooms of *Skeletonema costatum* and *Pseudo-nitzschia delicatissima*, Miralto et al. (1999) were the first that showed that the α,β,γ,δ-unsaturated aldehydes **5** and **5b** were responsible. Activity is dependent on the α,β-double bond conjugated to the aldehyde function representing a Michael-acceptor, which reacts non-specifically with nucleophiles (Adolph et al. 2003). Reactivity is influenced by side chain polarity (longer side chain length increases activity) with **5** being the most active PUA (Adolph et al. 2003). PUA accumulation in copepod gonads (Wolfram et al. 2014) and their nucleophile attack of e.g. proteins and DNA (Carvalho et al. 1998; Wolfram et al. 2015) may explain the deleterious effects on copepod grazers (reviewed in Ianora et al. (2003); Ianora and Miralto (2010); Paffenhöfer (2002)). PUAs also act on other phyla, e.g. fungi, echinoderms, molluscs and annelids (Adolph et al. 2004; Caldwell et al. 2002), including antimicrobial and allelopathic effects (Ribalet et al. 2007a; Ribalet et al. 2008). The observed toxicity towards diatoms themselves and PUA release directly before the declining growth phase both in field and laboratory studies indicates an additional role as infochemical during bloom succession (Casotti et al. 2005; Vardi et al. 2006; Vidoudez and Pohnert 2008; Vidoudez et al. 2011b).

Several analytical methods have been developed for the qualitative and quantitative analysis of marine dissolved (Vidoudez et al. 2011a) and particulate PUAs (d'Ippolito et al. 2002a; Spiteller and Spiteller 2000; Wichard et al. 2005b). Main challenges are thereby their low concentrations within biological samples and their inherent chemical instability. The first analyses that profiled diatom-derived PUAs were conducted by solid phase microextraction (SPME) and gas chromatography coupled mass spectrometry (GC-MS). Following Spiteller and Spiteller (2000), algal cultures were concentrated by centrifugation, cells disrupted by sonication, and PUAs extracted either from the cell-free liquid phase (Pohnert 2000) or headspace (Pohnert et al. 2002) with a polydimethylsiloxane (PDMS)-coated SPME fibre. Analytes were then directly evaporated in the GC injector. This allows the fast, direct, and sensitive detection of algal PUAs using mass spectrometry. Subsequent structure identification is facilitated by electron ionization (EI)-based fragmentation. However, precise quantitative

analyses are complicated as it is an equilibrium-based extraction influenced by e.g. salinity and temperature. Recent advances in on-fibre derivatization (Ma et al. 2011b) may stabilize these reactive analytes and may also enable sample storage. To overcome the limitations of SPME, a protocol was developed that used solvent extraction and chemical derivatization of PUAs for subsequent GC-MS analysis (d'Ippolito et al. 2002a; d'Ippolito et al. 2002b). PUAs were extracted from the aqueous phase using acetone and dichloromethane. Extracts were then dried, cleaned, concentrated, and derivatized to ethyl esters via a Wittig reaction with carbethoxyethylidene-triphenylphosphorane (CET-TPP, Fig. 6A). The protocol allows to stabilize PUAs and enables in combination with nuclear magnetic resonance (NMR) spectroscopy complete structure elucidation of purified samples. However, *Z*-*E*-isomerisation during extraction takes place and only aldehydes between C8-C16 can be determined. With a limit of detection (LOD) of approx. 100-200 µg aldehyde per biological sample using selected ion monitoring (SIM) the sensitivity is low and not sufficient for natural phytoplankton samples.

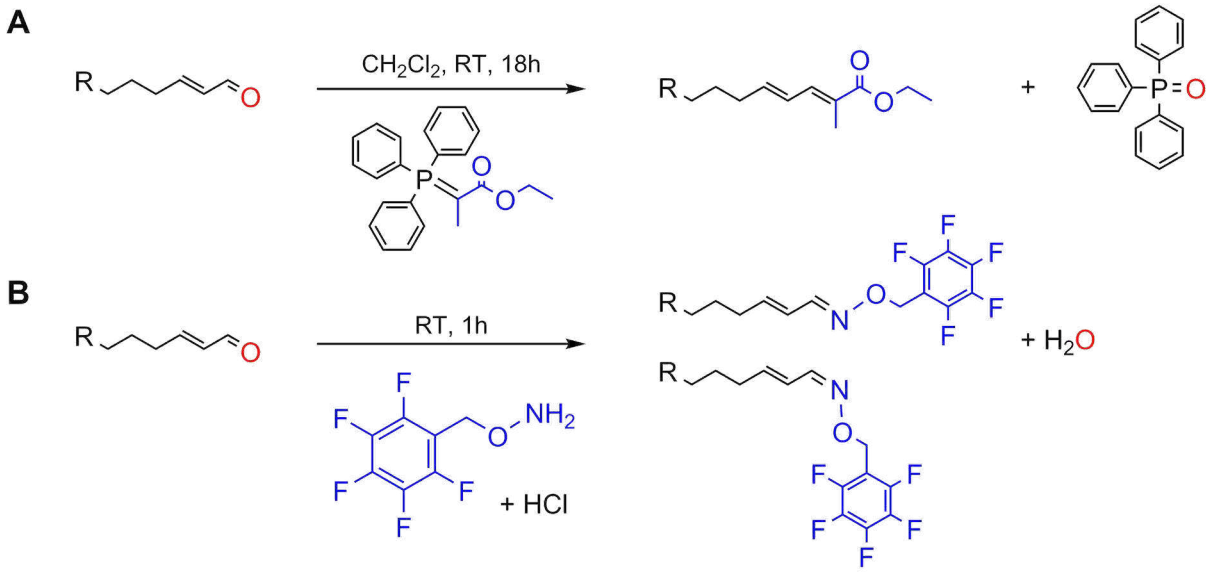

Fig. 6 Derivatization reactions for the targeted analysis of (polyunsaturated) aldehydes. (A) Wittig reaction with CET-TPP resulting in ethyl ester homologues of the aldehydes. (B) Oximation with PFBHA resulting in an *E*- and *Z*-isomer. RT = room temperature.

To improve the sensitivity for field-based studies, a protocol using *in situ* derivatization with *O*-(2,3,4,5,6-pentafluorobenzyl) hydroxylamine (PFBHA) was developed that allows a robust quantitative PUA analysis (Fig. 6B, Wichard et al. (2005b)). Algal samples are concentrated by filtration and re-suspended in buffered PFBHA solution. During sonication, the released PUAs are directly derivatized to pentafluorobenzyl-oximes, which are solvent-extracted, dried, and further concentrated for GC-MS

analysis. Two stable oximation products of each PUA stereoisomer are formed (Fig. 6B). With a LOD of <2000 cells in 1L of sample this method is sensitive enough for field experiments. The sensitivity can be further enhanced using chemical ionization (CI) instead of EI.

The PFBHA protocol also includes a method to detect ω-oxo acids, the second lyase product, after silylation of the acidic group. This demonstrates a general difficulty when investigating oxylipin metabolism: the chemical diversity in oxylipin substrates, intermediates and products requires several analytical methods and platforms for a comprehensive analysis of the metabolic pathways. Alsufyani et al. (2014) therefore combined fast screening of PUAs using the SPME method, exact quantification of PUAs using the PFBHA method, and investigation of the second HPL product using ultra-high pressure liquid chromatography (UHPLC)-MS. A protocol for the parallel analysis of PUAs and non-volatile oxylipins using one analytical platform still lacking.

1.2 The metabolomics toolbox

Metabolomics - the comprehensive and quantitative investigation of all metabolites (small molecules <1 kDa) produced by an organism under a given set of conditions (Fiehn 2001) - is a tool that has been repeatedly proposed to advance the research in chemical ecology (Prince and Pohnert 2010). The different aims in metabolomic analyses regarding e.g. analytical sensitivity, identification level, or metabolite coverage are thereby met by several sub-disciplines (Fiehn 2001). Thus, targeted metabolite analysis aims to quantify a small number of metabolites by a selective but sensitive and accurate method. Untargeted metabolite profiling aims to analyse one or a few subsets of metabolites or compound classes in a (semi-) quantitative way. And rapid untargeted metabolite fingerprinting aims to classify samples based on metabolite occurrence patterns gained by semi-quantitative analysis of endometabolomes. The corresponding classification of exometabolomes is defined as metabolite footprinting (Allen et al. 2003). Endometabolites are thereby all metabolites within the cells of an organism, whereas all metabolites released in the surrounding of a cell are termed exometabolites (Nielsen and Oliver 2005) (Fig. 3). All metabolomics approaches have to cope with the noisiness of metabolomes (high variability) and the need to relate interesting metabolites to functional roles in an ecological context.

1.2.1 Analytical strategies: an interdisciplinary overview

There is no technology existing yet that would allow the analysis of the whole metabolome at once, thus, complementary strategies have to be applied. A typical metabolomics workflow comprises the experimental design, sample processing, data acquisition using analytical instruments, computational data analysis, and biological interpretation or generation of new hypotheses (Fig. 7). Recent achievements in metabolomics research were mainly driven by the progress in analytical techniques and bioinformatics tools.

Especially in untargeted metabolomics the **design of the experiment** and sample size estimation are crucial for subsequent meaningful statistical analyses as a high co-linearity and variability exist in metabolite data (Hendriks et al. 2011). Decisions on metadata structure, biological and technical replication, and randomization have to be taken. Incubation experiments with stable-isotopically labelled metabolites may facilitate the unravelling of metabolic pathways (Weber et al. 2013). Approaches for

power analysis and sample size determination in metabolomics studies have already been proposed (Blaise et al. 2016) and should be further optimized.

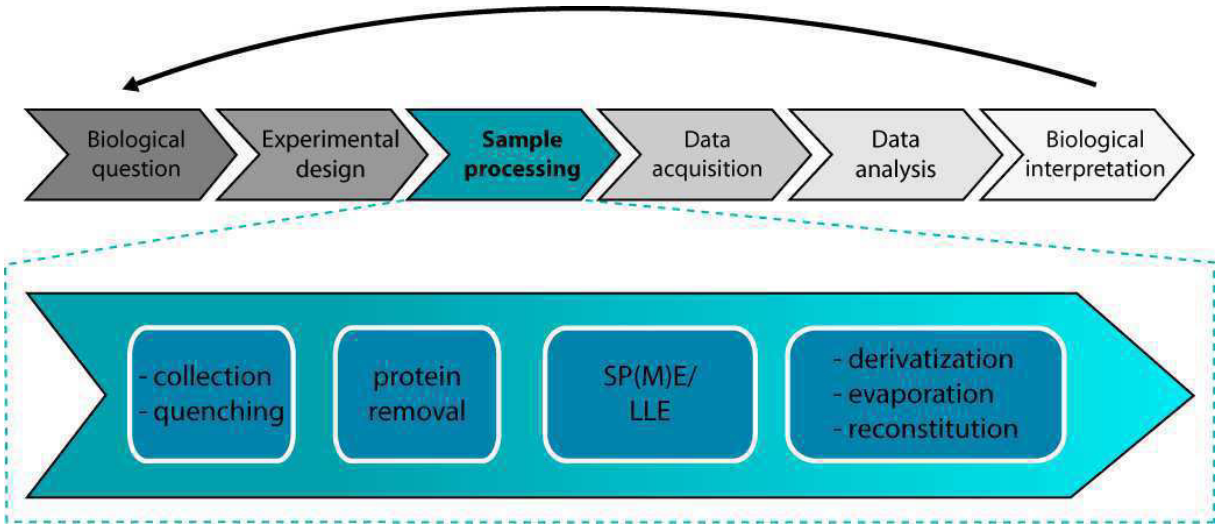

Fig. 7 Overview over metabolomics workflow highlighting sample processing steps. SP(ME) = solid-phase (micro)extraction. LLE = liquid-liquid extraction.

Sample collection and processing approaches have to be developed in line with the research question as they strongly determine the quality of the generated data and metabolite coverage (Dettmer et al. 2007; Villas-Bôas et al. 2005). Prior or immediately after rapid collection of the biomass and/or medium, enzyme activity and accordingly cell metabolism have to be interrupted ('quenched') by, for example, temperature or pH changes to prohibit any metabolite alterations. Metabolites are then extracted from the complex biological matrix using organic or aqueous solvents (liquid-liquid extraction) or solid-phase (micro)extraction (SP(M)E) to reduce interference by e.g. salts or proteins. Finally, metabolite concentrations are increased via solvent evaporation. Prior to GC-MS analysis, metabolites are derivatized to increase their volatility and thermal stability. Various protocols have been developed to optimize the sample collection and processing for specific study organisms (Patejko et al. 2017; van Gulik 2010; Winder et al. 2008), extracellular matrices (Pinu and Villas-Bôas 2017), or to improve derivatization conditions (Gullberg et al. 2004).

Several analytical platforms exist for **data acquisition**, each covering a different range in polarity and molecular weight as reviewed in Dunn et al. (2005) and Villas-Bôas et al. (2005). Metabolite detection can thereby be achieved using either MS, NMR, infrared (IR) or raman spectroscopy. Whereas the last three techniques are primarily used for high-throughput metabolite finger- and footprinting, mass spectrometry coupled to a chromatographic system is generally applied for metabolite profiling (Fig.

8). Gas chromatography (GC), liquid chromatography (LC) or capillary electrophoresis (CE) allow to separate metabolites in complex biological samples prior MS analysis. While instrumental sensitivity and resolution were continuously improved in recent years, the metabolite identification is still a major issue (Wolfender et al. 2015). In the past, LC-MS analyses were restricted due to the difficulty of relating obtained molecular masses to molecular formulas and chemical structures. However, achievements in chromatography (e.g. UHPLC, Guillarme et al. (2010)), mass spectrometry (e.g. high resolution mass spectrometry (HRMS), such as Orbitrap-MS and Fourier-transform ion cyclotron resonance mass spectrometry (FT-ICR-MS)), and data analysis tools (e.g. *in silico* fragmentation tools, Wolf et al. (2010)) greatly improved LC-MS-based untargeted metabolite profiling approaches. GC-MS offers larger identification efficiency in untargeted profiling approaches, which is due to the high chromatographic resolution and reproducible mass fragmentation. Metabolite fragmentation is based on EI at 70 eV and allows to compare fragmentation patterns with existing mass spectral data bases. Especially volatile, but also non-volatile, non-polar to medium-polar components can be analysed by GC-MS following appropriate derivatization steps (Fig. 8B).

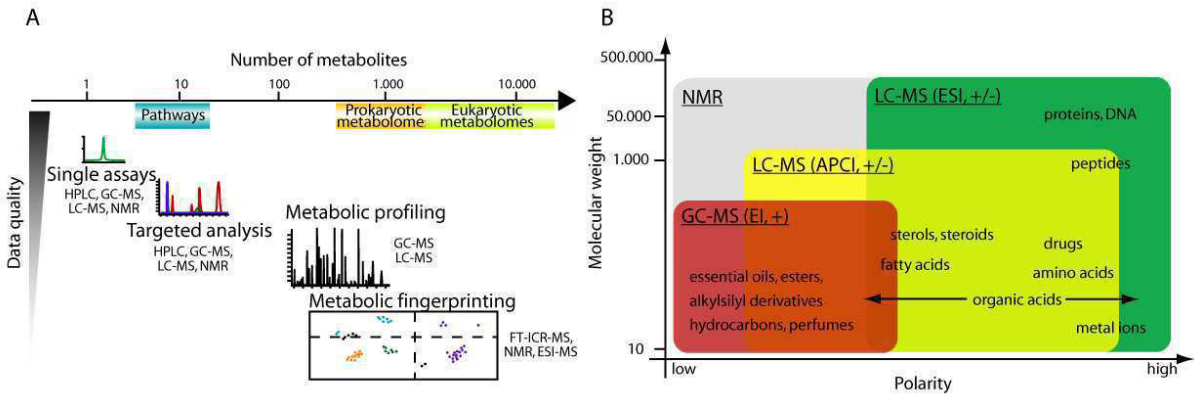

Fig. 8 Metabolomics approaches differ with regard to number of investigated metabolites and the accuracy in detection and quantification (A). The coverage of metabolites further depends on the analytical instrumentation discriminating towards metabolite polarity and molecular weight (B). Figures are adapted from Fernie et al. (2004), copyright license no. 4284021405305, and from Halket et al. (2005) , copyright license no. 4284030145796.

The broad and still developing field of **computational data analysis** includes platform-specific data extraction, data pre-processing, data analysis using e.g. uni- and multivariate statistical analyses, and validation steps (Alonso et al. 2015; Xi et al. 2014). Appropriate methods for data pre-processing (normalization, scaling, centring) have to be chosen (van den Berg et al. 2006). An increasing number of online and stand-alone software (Mahieu et al. 2016; Xia and Wishart 2016), as well as metabolite

databases (Vinaixa et al. 2016) facilitates statistical analyses and allows better metabolite identification. Aspects of standardization and quality control like data and metadata reporting (Fernie et al. 2011; Fiehn et al. 2008) have been targeted by e.g. the metabolomics standard initiative (Fiehn et al. 2007). The main application and main developments originate from human, microbial and plant sciences, and several model organisms and validated protocols exist already (e.g. Bolten et al. (2007); Lisec et al. (2006)). Metabolomics workflows have to meet several challenges with regard to their application in chemical ecology, e.g. the broad range of species in focus with only a few well-investigated model systems, or the low concentration of the metabolites of interest. Since the review of Prince and Pohnert (2010) on metabolomics in chemical ecology, many new analytical techniques have been developed, and a growing number of studies demonstrates the potential of metabolomics approaches to elucidate infochemicals and metabolic responses.

1.2.2 Untargeted metabolite profiling techniques for marine phytoplankton

The number of studies and thus also standards and protocols optimized for metabolomics investigations of marine algae in general, and for untargeted metabolite profiling of marine phytoplankton in particular, is still limited (Goulitquer et al. 2012). Method development for marine algae needs to address certain challenges: metabolic quenching is complicated by low phytoplankton abundances and harvesting techniques, high polysaccharide levels induce difficulties in cell disruption and homogenization, high salinity levels interfere during analyte detection, low metabolite concentrations in seawater require concentration steps via e.g. SPE, and large number of unknown structures and lack of (species-specific) databases for marine organisms hinders metabolite identification. Especially sample collection and sample processing steps have to be optimized and adjusted to the needs of the study organism. So far, rather few studies aimed to optimize protocols for the untargeted profiling of algal intra- and extracellular metabolites. Sample collection and separation of algal cells and medium highly depend on the study organism ranging from rapid filtration for pelagic microalgae (Vidoudez and Pohnert 2012), decanting and scraping for benthic microalgae (Nappo et al. 2008), to picking and thorough cleaning for macroalgal thalli. The effect of, for example, biomass-to-solvent ratio, extraction solvent composition, and derivatization time on the quality of metabolite profiles was investigated for the diatom *Skeletonema costatum* (Vidoudez and Pohnert 2012). However, additional studies evaluating the effect of these and other steps are also needed for other non-model organisms, followed by a critical review of the obtained results to compile the expertise in standardized protocols as has been done already for plants (Lisec et al. 2006; Veyel et al. 2014). In a first step, the current knowledge on metabolite profiling techniques of marine algae has to be compiled in a detailed protocol to guide and enhance future research.

1.2.3 Investigating phytoplankton communities: Meta-metabolomics

So far, metabolomics investigations of marine phytoplankton have been primarily conducted under controlled laboratory conditions using isolated microalgal cultures. However, many processes and mechanisms that are present in and responsible for phytoplankton dynamics in the field (e.g. bloom initiation, succession and decline) cannot be simulated under laboratory conditions. Natural marine environments are highly dynamic on small to large scales resulting also in a large spatial and temporal patchiness of phytoplankton communities. Environmental fluctuations occur with regard to e.g. water turbulence, temperature, nutrient concentration, light spectrum, light cycle, light intensity, and due to biological interactions with grazers and competitors. A simulation of the marine microbial environment is neither achieved by axenic (bacteria-free) nor xenic cultures with atypical species dominating. Also processes like sinking and buoyancy as encountered in natural environments is normally not targeted in laboratory set-ups. Thus, research in marine (chemical) ecology is to a large extent field-based and relies on the investigation of semi-natural mesocosm experiments (experimental water enclosures) or natural phytoplankton communities (Grice and Reeve 1982; Lalli 1990).

Recently, meta-approaches have been applied to marine phytoplankton communities with the goal to unravel complexity by whole-system sampling. Thus, in the *Tara* Oceans project (Karsenti et al. 2011) global metabarcoding revealed a large proportion of still undescribed eukaryotic taxa in the marine plankton (de Vargas et al. 2015). In addition, the shift from nomenclature ecology to trait-based ecology (McGill et al. 2006) motivated to go from taxonomic to functional interpretations using meta-genomics approaches complemented with meta-transcriptomics, meta-proteomics (Williams and Cavicchioli 2014), and meta-metabolomics that capture the spatial and temporal variation, signalling and communication in natural communities (Raes and Bork 2008) (Fig. 9).

Recently, the first meta-metabolomics studies have been conducted for marine phytoplankton communities. Llewellyn et al. (2015) investigated particulate organic matter between 0.7 µm and 200 µm at two stations in the English Channel via untargeted metabolite profiling of polar (using UHPLC-FT-ICR-MS) and lipid (using direct infusion (DI)-FT-ICR-MS) metabolites. Ray et al. (2016a) related copepod grazing in a semi-natural mesocosm experiment to phytoplankton bloom succession as described by intracellular metabolite profiles (using GC-TOF-MS). An increase in

meta-metabolomics investigations and in available sample and data analysis strategies in the next years may improve field investigations in marine chemical ecology.

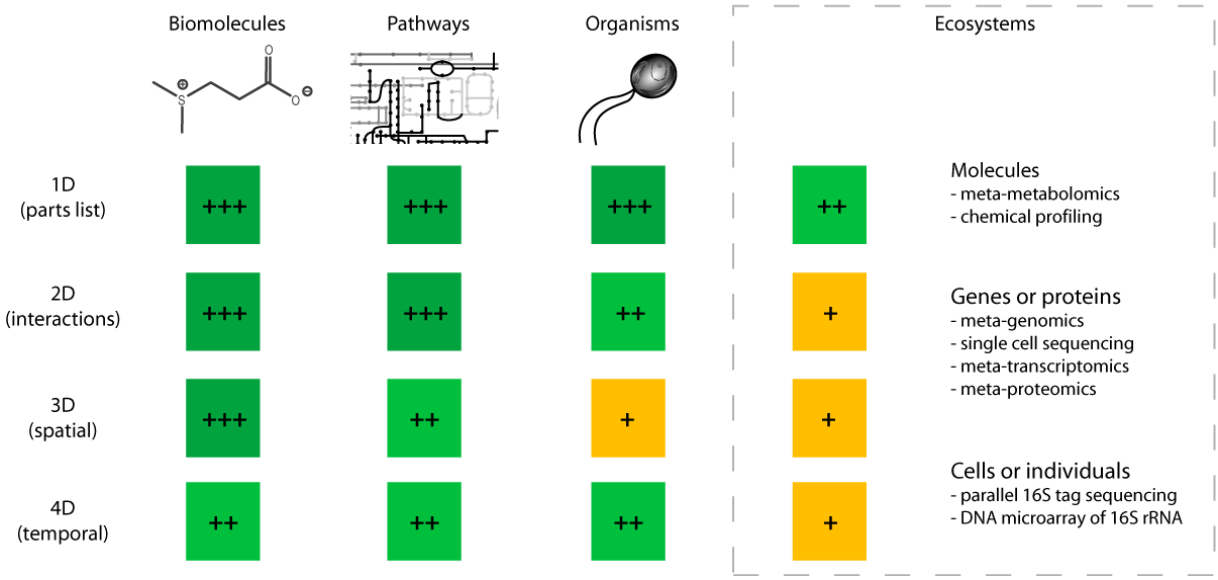

Fig. 9 Data availability for different spatial scales of systems biology ranging from biomolecules to pathways, organisms and ecosystems with regard to 4 dimensions that can be targeted (+++ ample data available, ++ some high-throughput data sets available, + few data sets available). Community analyses at the ecosystem level can be conducted at the molecular level (e.g. meta-metabolomics), at the genetic or protein level (metagenomics, -transcriptomics, -proteomics), or at the cellular level. Figure is adapted from Raes and Bork (2008), copyright license no. 4284030357097

2 Thesis objectives

Chemically mediated processes play an important role in the ecology of marine phytoplankton e.g. in sexual reproduction, interspecies competition, grazing defence, or host-virus interaction. Several involved metabolites and metabolic classes have already been elucidated and are under regular investigation, such as dimethylsulfoniopropionate (algae-bacteria interactions), polyunsaturated aldehydes (grazing defence), polyunsaturated fatty acids (food web), or glycosphingolipids (viral infection). This is, however, just a small fraction within the broad range of metabolites that are actually produced by the marine phytoplankton, especially with regard to the taxonomic diversity of protozoans from which primarily diatoms are so far under investigation. To cover a wider range of metabolites while analysing naturally occurring structures, metabolomics is well suited and rapidly developed in recent year in parallel with the underlying analytical techniques and data processing strategies. Thus, metabolomics offers new research possibilities in the field of chemical ecology, especially with regard to complex field situations, that are explored in this thesis.

Metabolomics in marine phycology: State of the art

Thus, the first aim of this thesis was to review the current expertise in metabolomics studies within the field of chemical ecology in general and of marine plankton ecology in particular (**Manuscript 1**). Further, I aimed to optimize and generalize the current methodological knowledge about endo- and exometabolic analyses of marine micro- and macroalgae, i.e. protocol details, technical considerations, and challenges, to facilitate a growing number of metabolomics investigations in plankton ecology in the future (**Manuscript 2**).

Metabolic diversity meets taxonomic diversity

Another objective of this thesis was to further expand the current knowledge about metabolic plasticity of microalgal cells with regard to algal taxonomy. Following the thorough endometabolic characterizations of the diatom *Skeletonema marinoi* and the haptophyte *Emiliania huxleyi* during growth, I investigated another haptophyte (*Phaeocystis pouchetii*) to indicate metabolic commonalities within algal lineages (**Manuscript 3**). As exometabolic investigations of microalgae are still in the minority, also a thorough extracellular metabolic characterization throughout growth was pursued for *Phaeocystis pouchetii* (**Manuscript 3**).

Meta-metabolomics in ecological field studies

Further, I explored the applicability of metabolomics investigations for field-based ecological studies. Thus, I aimed to find out whether laboratory-derived metabolic features or patterns that describe metabolic stages of unialgal cultures can be used in the characterization of metabolic states of mixed natural communities. Therefore, the occurrence of growth-regulated microalgal endometabolites within several phytoplankton communities in the Northeast Atlantic was studied (**Manuscript 3**). Untargeted metabolite profiling of phytoplankton bloom exometabolites was applied to facilitate the interpretation of a classical productivity study of marine bacterioplankton communities that is based on dilution (**Manuscript 4**).

Improving the analysis of 'known' metabolites for marine ecology

Motivated by the improved analytical possibilities provided by the orbitrap high resolution mass spectrometry technology, I finally aimed to re-investigate the qualitative and quantitative analysis of polyunsaturated aldehydes (PUAs), a well-known metabolic class that is regularly measured in marine ecology. Thus, my objective was to develop a targeted and untargeted metabolite profiling method for the parallel analysis of nonpolar PUAs and polar oxylipins on one analytical platform (**Manuscript 5**). Known PUA producers (*Skeletonema costatum*, *Thalassiosira rotula*) as well as an uncharacterized species (*Chaetoceros didymus*) were screened.

3 Publications

P1: Reprinted from C. Kuhlisch, G. Pohnert (2015) Metabolomics in chemical ecology, *Nat*. *Prod*. *Rep*., **32**, 937-955, doi: 10.1039/c5np00003c. Reproduced by permission of The Royal Society of Chemistry.

P2: Reprinted from C. Kuhlisch, G. Califano, T. Wichard, G. Pohnert, Metabolomics of intra- and extracellular metabolites from micro- and macroalgae using GC-MS and LC-MS in *Protocols for Macroalgae Research* (Eds.: B. Charrier, T. Wichard, C.R.K. Reddy), CRC Press, Taylor & Francis Group, ISBN-13: 978-1-4987-9642-2. (*re-submitted to CRC Press, December 2017*)

P3: Reprinted from C. Kuhlisch, J. Althammer, A. F. Sazhin, H. H. Jakobsen, J. C. Nejstgaard, G. Pohnert, Metabolomics-derived marker metabolites to characterize *Phaeocystis pouchetii* in natural plankton communities. (*submitted to Harmful Algae, December 2017)*.

P4: Reprinted from B. Pree, C. Kuhlisch, G. Pohnert, A. F. Sazhin, H. H. Jakobsen, M. L. Paulsen, M. E. Frischer, D. Stoecker, J. C. Nejstgaard, A. Larsen (2016) A simple adjustment to test reliability of bacterivory rates derived from the dilution method, *Limnol*. *Oceanogr*.: *Methods*, **14**, 114-123, doi:10.1002/lom3.10076. This is an open access article distributed under the terms of the Creative Commons Attribution License.

P5: Reprinted from C. Kuhlisch, M. Deicke, N. Ueberschaar, T. Wichard, G. Pohnert (2017) A fast and direct liquid chromatography-mass spectrometry method to detect and quantify polyunsaturated aldehydes and polar oxylipins in diatoms, *Limnol*. *Oceanogr*.: *Methods*, **15**, 70-79, doi: 10.1002/lom3.10143. Reproduced with permission from John Wiley and Sons via the Copyright Clearance Center, License number 4277440731059.

Publication P1:

"Metabolomics in chemical ecology"

C. Kuhlisch and G. Pohnert

Nat. *Prod*. *Rep*., 2015, **32**, 937-955.

Volume 32 | Number 7 | July 2015 | Pages 879–1156

NPR

Natural Product Reports

www.rsc.org/npr

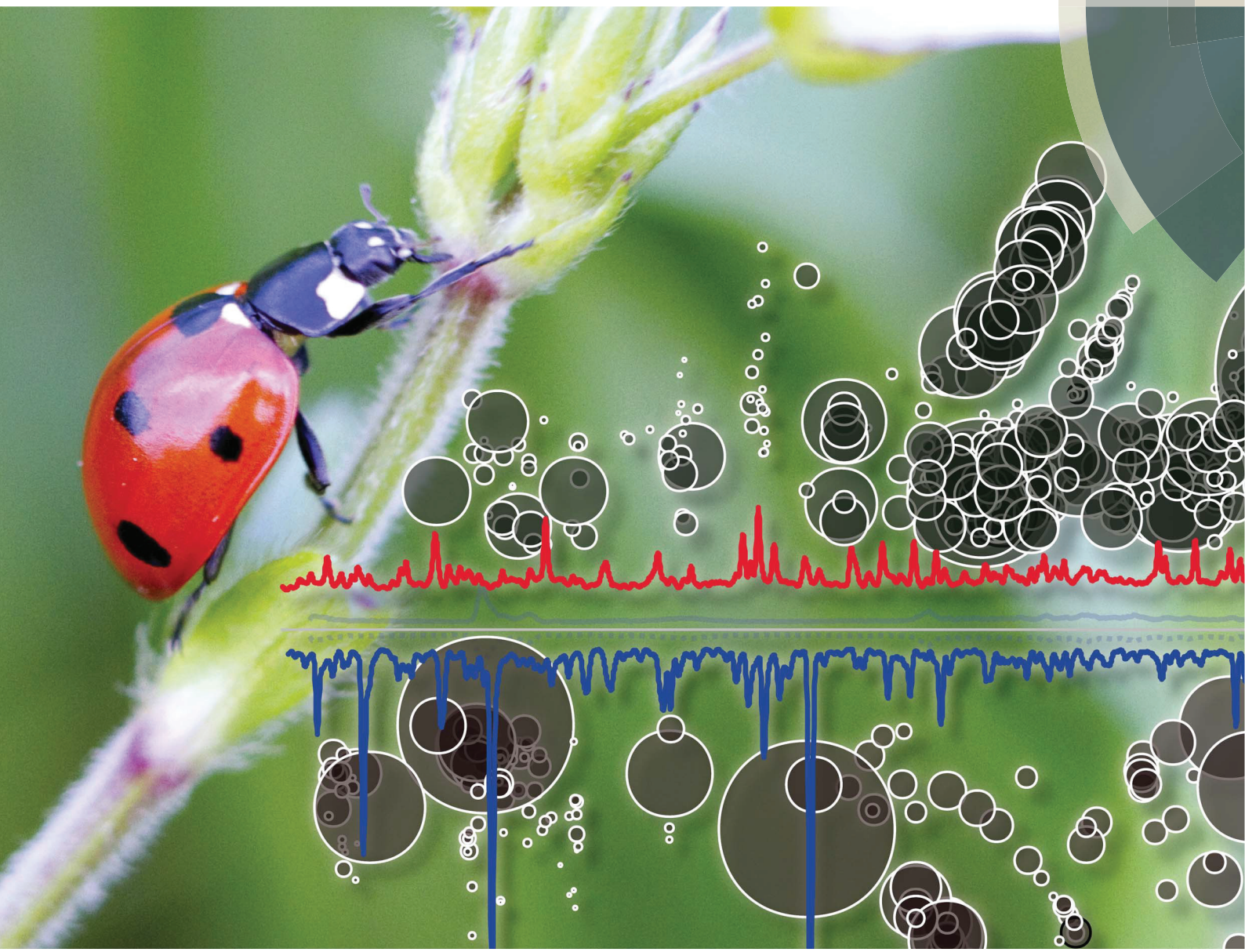

ISSN 0265-0568

ROYAL SOCIETY OF CHEMISTRY

REVIEW ARTICLE

Constanze Kuhlisch and Georg Pohnert

Metabolomics in chemical ecology

NPR

REVIEW

View Article Online
View Journal | View Issue

Cite this: *Nat. Prod. Rep.*, 2015, **32**, 937

Metabolomics in chemical ecology

Constanze Kuhlisch and Georg Pohnert*

Covering: up to December 2014

Chemical ecology elucidates the nature and role of natural products as mediators of organismal interactions. The emerging techniques that can be summarized under the concept of metabolomics provide new opportunities to study such environmentally relevant signaling molecules. Especially comparative tools in metabolomics enable the identification of compounds that are regulated during interaction situations and that might play a role as *e.g.* pheromones, allelochemicals or in induced and activated defenses. This approach helps overcoming limitations of traditional bioassay-guided structure elucidation approaches. But the power of metabolomics is not limited to the comparison of metabolic profiles of interacting partners. Especially the link to other –omics techniques helps to unravel not only the compounds in question but the entire biosynthetic and genetic re-wiring, required for an ecological response. This review comprehensively highlights successful applications of metabolomics in chemical ecology and discusses existing limitations of these novel techniques. It focuses on recent developments in comparative metabolomics and discusses the use of metabolomics in the systems biology of organismal interactions. It also outlines the potential of large metabolomics initiatives for model organisms in the field of chemical ecology.

Received 7th January 2015

DOI: 10.1039/c5np00003c

www.rsc.org/npr

1 Introduction

The ecological understanding of natural products that mediate interactions within and between organisms can be considered as the core of the discipline chemical ecology.[1] Knowledge of the nature of chemicals that mediate such interactions is central in this research area. The identification of active metabolites opens up possibilities from fundamental work in bioassays over general investigations of the physiology and ecology of an organism to the manipulation of entire ecosystems. Signaling molecules that mediate interactions between organisms have motivated many activities in basic research but also the commercial interest *e.g.* for pest control is a driving force in the search of such bioactive metabolites.[2] It is thus not surprising that the focus of numerous groups working in chemical ecology is the structure elucidation of these active principles. Since the early days of this discipline the central tool for such endeavors has been bioassay-guided structure elucidation. The work flow has first been successfully established for the identification of the insect pheromone bombykol (**1**) by Butenandt and colleagues in 1959.[3] It is based on the separation of an active crude extract by *e.g.* chromatography, selective extraction or crystallization and testing of the resulting fractions in bioassays. Active fractions are further purified and again tests of activity guide the further selection until a pure active compound can be submitted to structure elucidation.[4] This time-consuming and often tedious process can involve multiple rounds of separation and testing until the identification of a signal molecule is achieved. Besides the high workload the approach bears also the risk that activity of labile substances is lost during handling. Compounds that are only active in more complex formulations or specific mixtures, are also not recognized due to the involved purification steps and require combinatorial tests for activity verification.[5] Despite these drawbacks bioassay-guided structure elucidation was the main

Friedrich Schiller University, Institute of Inorganic and Analytical Chemistry, Lessingstr. 8, D-07743 Jena, Germany. E-mail: Georg.Pohnert@uni-jena.de; Fax: +49 3641 948 172; Tel: +49 3641 948 170

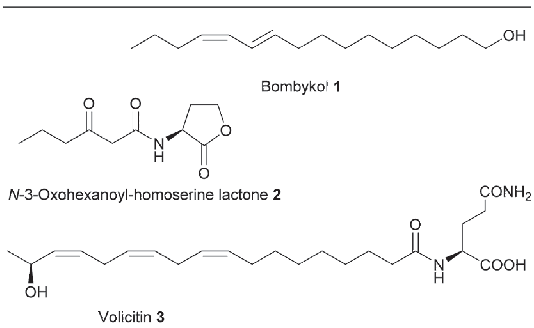

Scheme 1 Hallmark molecules in chemical ecology that were isolated by bioassay-guided structure elucidation. These include the first insect pheromone bombykol **1**, the bacterial quorum sensing signals of the acyl homoserine lactone family **2** and volicitin **3**, the first insect derived inducer of plant defense.

available technique for signal identification in chemical ecology over decades. Indeed, besides bombykol most hallmark molecules in chemical ecology have been identified by this approach (Scheme 1).[6,7]

With the advent of –omics techniques additional tools became available for the search for active principles. These include, among many others, the use of microarray methods, targeted knockout experiments based on the identification of candidate genes, and proteomics.[8–10] But especially metabolomics techniques provide a novel approach to the identification of molecules of relevance in chemical interactions. In fact, long before the discipline of metabolomics emerged, comparison of metabolic profiles that were created from extracts of organisms in different physiological states or ecological stress situations were used to spot candidate metabolites that are upregulated in an interaction context. This is *e.g.* demonstrated by the identification of volatiles in response to insect herbivory.[11] In a procedure that would today be categorized as metabolic profiling, volatiles in the headspace of plants were collected in controls and plants suffering herbivory. Comparison of gas chromatography/mass spectrometry (GC-MS) profiles led to the identification of several herbivory-induced compounds that could later be assigned to ecological functions in an indirect chemical defense. The collection and comprehensive analysis of plant volatiles from control organisms and those under herbivore pressure revealed not only the up regulation of terpenoid biosynthesis but also motivated further bioassays that led to a wide-ranging understanding of induced plant defenses. The involvement of the plant hormone jasmonic acid and its amino acid conjugates in the induction of metabolic pathways towards plant defensive metabolites was also discovered using such profiling tools.[12] It is striking to see that even in early publications figures are presented that would meet the reporting standards of modern metabolomics. Despite the fact that data mining tools were not as elaborate as today these studies enabled the investigation of regulatory patterns that allowed spotting candidate molecules or pathways relevant in species interactions.

Since these early days of metabolic profiling the discipline of metabolomics has emerged and matured. Even if some approaches are still in their infancy, the multiple facets of metabolomics are now emerging as central tools in chemical ecology for screening the pool of natural products and for the elucidation of regulative principles and pathways. Per definition the metabolome represents all metabolites of a given species, but comprehensive monitoring of such a structurally diverse set of compounds is technically often not feasible.[13] Thus several sub-disciplines have emerged that use the power of modern analytical instrumentation paired with elaborate statistical analysis suited mainly to recognize dynamic metabolic processes. Principal approaches and techniques in metabolomics have been reviewed extensively over the last years and will not be a subject of this contribution. We, however, want to refer to selected reviews for further reading concerning the general concepts in metabolomics,[13–16] specialized techniques

Constanze Kuhlisch received her M.Sc. in Marine Biology at the University of Rostock, Germany, in 2013. The same year she joined the research group of Georg Pohnert at the Friedrich-Schiller-University Jena where she started her PhD thesis investigating the chemical ecology of the bloom forming microalga Phaeocystis pouchetii.

Georg Pohnert gained a PhD in organic chemistry in the Group of Prof. W. Boland. In 1997 he joined the groups of Profs. Ganem and Wilson at the Cornell University as a postdoc. He was then appointed to a group leader position at the Max-Planck-Institute for Chemical Ecology in Jena, Germany. In 2005, he was appointed as assistant professor at the EPFL in Lausanne, Switzerland. He moved in 2007 to the Friedrich-Schiller-University in Jena where he was appointed as Full Professor in Instrumental Analytics. His research interests encompass various aspects of the chemically mediated interactions of marine organisms with focus on innovative analytical techniques.

that play an important role in chemical ecology including mass spectrometry[17,18] as well as nuclear magnetic resonance (NMR).[19–21] A wide array of statistical methods is applied routinely within metabolomics and already reviewed under different aspects including data pre-processing, uni- and multivariate analyses and visualization aspects.[22–24]

Comparative metabolomics provides the best-suited tools to unravel chemically mediated species interactions.[25] This approach will accordingly be the initial focus of this review. In contrast to previous studies where a targeted analysis of the induction of single compounds or specific groups of compounds was performed, comparative metabolomics allows to monitor global changes and to unravel multiple pathways that are affected by environmental stimuli using elaborate algorithms on complex data sets. Knowledge about the production of specific compounds or classes of metabolites during interaction situations might help to make educated guesses of their function. As a consequence this can motivate following bioassays to verify such hypotheses.[26] In addition, this review will cover concepts where multiple –omics techniques are combined in a systems biology approach to obtain a comprehensive picture of an organisms' response in interaction situations. We will also introduce aspects how the comprehensive metabolomics initiatives for model species might be fruitfully applied in the chemical ecology. Taken together, we aim to classify and evaluate metabolomics as a potential future driver in the search for the nature, role and regulation of signaling molecules.

2 The comparative metabolomics approach

This rather descriptive approach is the fundamental metabolomics tool in chemical ecology. Comparison of metabolomes for the investigation of chemical interactions does not necessarily require a comprehensive monitoring of as many compounds as possible. If the nature of a chemical interaction is known, the work plan can be dramatically simplified by a preselection of specific groups of analytes. Thus, for example the metabolomics-enabled search for airborne pheromones of insects would surely not require extraction of the insects themselves for a metabolic profiling but rather be restricted to a comprehensive monitoring of emitted volatiles in the headspace. In contrast, elucidation of plant defense metabolites might exclusively require monitoring metabolites in the plant's tissue or on its surface. Numerous specialized techniques have been introduced focusing on specific groups of the exometabolome (exuded metabolites) *e.g.* volatiles, surface associated metabolites or dissolved metabolites from aquatic organisms. But also the endometabolome (internal metabolites) within specific cells, tissue or the whole organism can be addressed selectively. Another way to perform a pre-selection is the inclusion of functional considerations in the initial analytical approach. Thus, it has been successfully demonstrated that the search for compounds acting as metallophores, which mediate metal complexation and uptake in microorganisms and thereby shape organismal interactions, can be pre-selected by biasing analytical techniques.[27,28] A pre-identification of metallophores in the exometabolome can be realized by recording liquid chromatography/mass spectrometry (LC-MS)-runs of the extracts in presence and absence of metals. The shift in masses resulting from the complexation of the metal can be used in a chemometric approach to pre-select only those metabolites relevant for metal interactions.[27,28] Alternatively, isotope-assisted data mining approaches were recently introduced that spot specific isotopic patterns of metals in complexes.[29] A preselection can also be made if specific pathways are suspected to be relevant in organismal interactions. This approach has *e.g.* been demonstrated for the elucidation of defense metabolites of the moss *Dicranum scoparium*. Here, initial evidence suggested that lipid-derived oxylipins mediate a wound activated chemical defense against herbivorous slugs.[30] Administration of stable isotope labeled fatty acids allowed to identify upregulated metabolites using automated routines of data mining thereby pointing towards a novel set of previously unrecognized highly reactive metabolites.[31] Genetic tools can make such pathway-associated approaches even more powerful. This was shown in the structure elucidation of myxoprincomide, a natural product from *Myxococcus xanthus*. The knockout of nonribosomal peptide synthetase (NRPS) genes and subsequent comparative metabolic profiling led to the identification of this novel metabolite of which the function in the natural environment is, however, still undetermined.[32] The emerging possibilities arising from the systematic pairing of metabolomics and genome mining opens up new avenues for the discovery of natural products.[33]

2.1 Comparative metabolomics in plant sciences

Plant interactions so far often have been studied by targeted analysis of a few model organisms. But especially within plant sciences comparative metabolomics has recently also been applied fruitfully. Metabolomics approaches using several platforms can be used on more diverse sets of plants to elucidate (common) interaction patterns. Plants can respond to a multitude of challenges by adapting their metabolic repertoire. These can include simple environmental stress situations, such as drought or light stress or infestation with pathogens and herbivory. But even herbivore interactions can be complex with different herbivores grazing on the same plant inducing different defense mechanisms at the same time. Thereby they also interact with each other in an indirect way *via* induced qualitative and quantitative changes of primary and secondary metabolites throughout the plant. All of these types of challenges can be addressed by comparative metabolomics. However the planning of experiments is crucial. For the understanding of simple responses the comparison of plant control and plants with grazer A might be sufficient. If a comprehensive picture of the defense potential of a plant shall be obtained additional investigations of the effects of a second grazer B as well as additional grazer A-grazer B-plant systems are required. On top, additional environmental stress factors can be considered to obtain a comprehensive picture.

A well-studied system is the grazing of aphids and root feeding nematodes on *Arabidopsis thaliana*. Single effects of each grazer have already been studied. Targeted analysis of glucosinolates in response to feeding bioassays have been introduced thereby paving the way for more complex experimental set-ups.[34] Such targeted profiling focuses on a small set of known candidate metabolites with similar chemical properties whereas untargeted approaches open up future perspectives in plant chemical ecology by uncovering previously unidentified lines of defense. Recently the mutual influence of

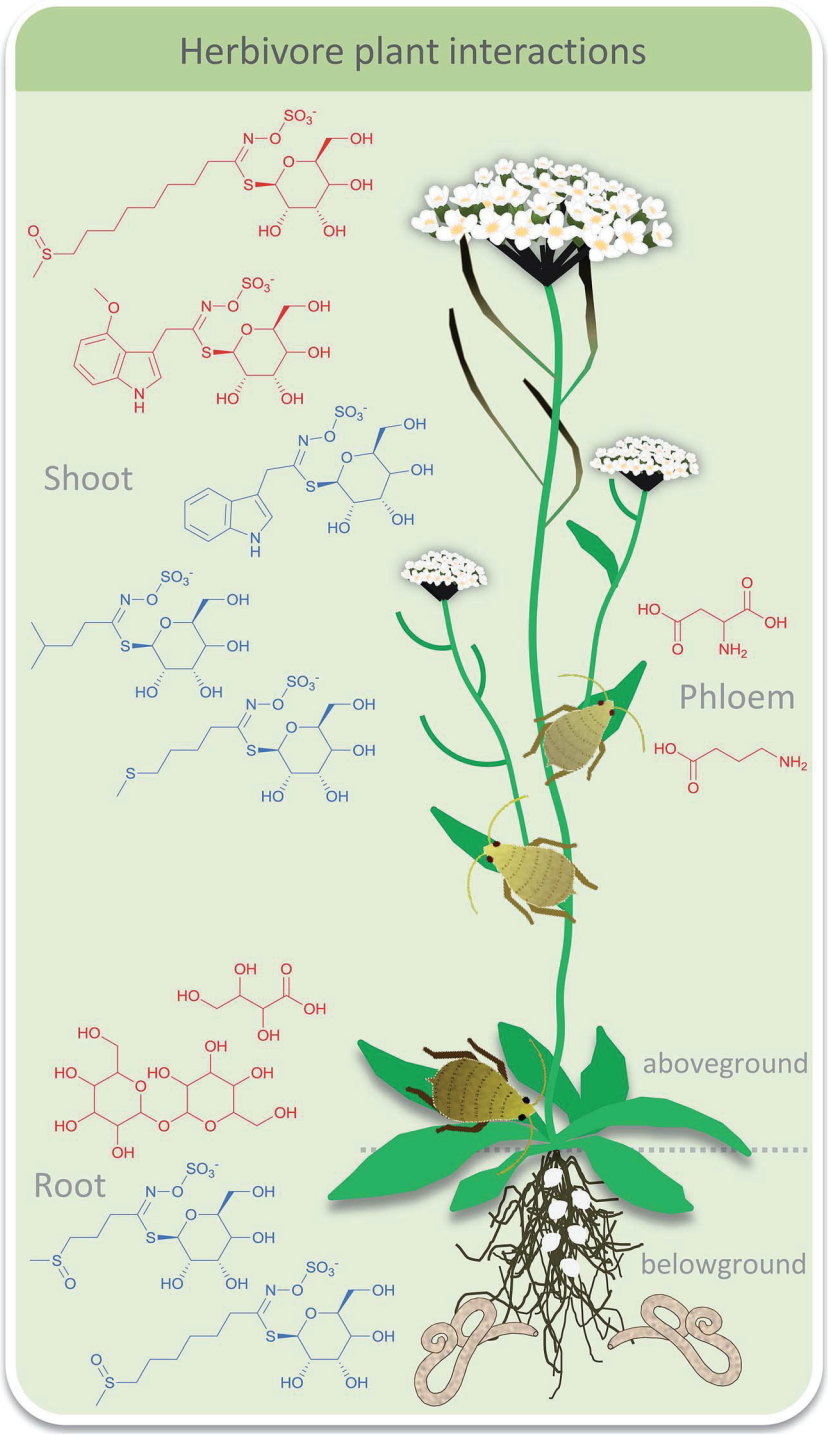

Fig. 1 Herbivore interactions of above ground feeding aphids and below ground feeding nematodes on *Arabidopsis thaliana* regulate aliphatic glucosinolates (Gls), amino acids and sugars. Selected up-(red) and down-regulated (blue) metabolites are depicted for the shoot (8-methylsulfinyloctyl Gls, 4-methoxyindol-3-ylmethyl Gls, indol-3-ylmethyl Gls, 3-methylbutyl Gls, 4-methylthiobutyl Gls), the phloem (aspartic acid, gamma-aminobutyric acid), and for the roots (erythronic acid, trehalose, 3-methylsulfinylpropyl Gls, 6-methoxysulfinylhexenyl Gls).

above- and below-ground herbivores that is mediated by plant chemistry was addressed.[34,35] Comparative metabolic profiling was used to monitor effects of grazing of the aphid *Brevicoryne brassicae* and the nematode *Heterodera schachtii* on *A. thaliana* (Fig. 1). Metabolic profiling of primary metabolites in the shoots by GC-MS and metabolic fingerprinting of shoot and root tissue by LC-MS were conducted and analyzed *via* multivariate statistics. Aphid grazing had a significant local effect in the shoot tissue. Only minor systemic effects were observed in the root tissue but changes of glucosinolates indicated an induced defense. As a consequence, aphid grazing led to reduced nematode infestation. In contrast, nematodes did not evoke any significant metabolite alterations locally or systemically thus having no influence on aphid population.[34] The confounding effect of nitrate fertilization in this plant-mediated herbivore interaction was considered in a follow-up study.[36] Again, only aphid grazing influenced nematodes but in a complex pattern. Under lower nitrate conditions aphid grazing increased nematode population whereas under higher nitrate fertilization nematodes were reduced as seen before. Metabolic profiling of root primary metabolites *via* GC-MS gave 88 compounds of which 54 could be identified. Multivariate statistics revealed that only marginal changes were observed under aphid grazing which might indicate a very sensitive reaction of nematodes. In a study where the specialist *B. brassicae* was replaced by the generalist *Myzus persicae* nematodes negatively influenced aphid abundance under lower nitrate availability.[37] Targeted metabolic profiling of amino acids and glucosinolates was conducted *via* GC-MS followed by principal component analysis (PCA) and multivariate analysis of variance (MANOVA). In response to nematode feeding the amino acid composition in the phloem changed as well as the glucosinolate composition in the leaves. The latter was correlated with aphid abundance.

The aspect of diurnality of changes in above- and below-ground metabolite patterns in response to herbivory was addressed in the wild tobacco plant *Nicotiana attenuata*.[38] Herbivory was simulated by wounding of the tobacco plants and administration of the oral secretion of the herbivorous caterpillar *Manduca sexta*. Metabolic fingerprinting showed that different compounds were oscillating in leaves compared to roots. In fact, only ten ions of 182 oscillating in leaves and 179 oscillating in roots (LC-MS) were rhythmic in both tissues. The response to simulated herbivory of seven selected metabolites was investigated in detail (unknown disaccharide, lyciumoside I, phenylalanine, tyrosine, coumaroyl tyramine, feruloyl putrescine, *N*-feruloyl tyramine, 12-oxo-phytodienoic acid, and jasmonic acid) and compared to transcript analyses, revealing a highly tissue-specific accumulation. It was concluded that the pronounced diurnal rhythm in the generalized and specialized metabolism that mediates the plant's responses to herbivory might play an important role in orchestrating its response to herbivory.

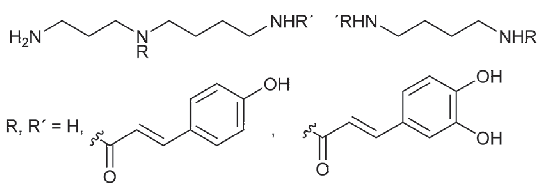

Scheme 2 Coumaroyl and caffeoyl spermidines and putrescines from *A. thaliana*. Specific positions of the residues were not assigned.[40]

The role of the plant hormone jasmonic acid (JA) for herbivore defense was addressed in a *Nicotiana attenuata* mutant.[39] If a jasmonate *O*-methyltransferase from *A. thaliana* is expressed in *N. attenuata*, it methylates JA, thereby acting as a sink for this plant hormone. This mutant was more vulnerable to grazing in the field. Targeted analyses of known defense compounds nicotine, diterpene glycosides and trypsin proteinase inhibitors but also untargeted metabolic profiling of volatile and non-volatile leaf metabolites was conducted. 42 of the most abundant and consistently detected volatile organic carbons (VOCs) in GC × GC/MS were compared between the mutant and the wild type after wounding. Early and late response VOCs could be separated clearly *via* PCA and partial least squares discriminant analysis (PLS-DA) due to increase of terpenes and hexenylesters and decrease of non-esterified green leaf volatiles during late response. In the late response mutants were separated from wild type due to reduced VOC emission (including *cis*-3-hexen-1-ol, *cis*-3-hexenyl-butyrate, -acetate, α-terpineol, *trans*-α-bergamotene and β-myrcene). Also the metabolic profiles (LC-MS) of secondary metabolites of mutant and wild type leaves were separated (PLS-DA) due to reduction of defense compounds such as nicotine, diterpene glycosides and phenylpropanoid–putrescine and –spermidine conjugates as well as some unknown metabolites in the mutant plants. This study convincingly demonstrated the multiple effects of jasmonic acid in a plant's defense and the power of metabolomics approaches to unravel such complex responses.

Gaquerel *et al.*[40] followed the effect of silencing of a hydroxycinnamoyl transferase (HCT)-like gene in *N. attenuata*, which was found to be induced in a previous transcript screening after herbivory.[41] Targeted analysis of well characterized herbivory-responsive caffeoyl- and feruloyl-based putrescine and spermidine phenolamides (PAs) did not show any pronounced silencing effects. However, an unknown PA-type did. This motivated an untargeted metabolomics approach using LC-MS. Up to 12% deregulation in insect-attacked leaves could be assigned to a diversion of coumaric acid units into the production of coumaroyl-containing PAs (Scheme 2). Samples could be separated according to genetic manipulation and herbivory treatment *via* PCA, and Venn diagrams showed increased metabolite numbers in silenced plants. All metabolites influenced by silencing were clustered hierarchically and annotation of the strongest regulated entries allowed the identification of several novel PA isomers and derivatives. The HTC-like gene thus encodes a coumaroylquinate-forming enzyme and mediates competition between the PA pathway and lignin production. This work is a nice example how metabolomics can be used to uncover a previously undescribed network of metabolites and help to unravel the interplay among herbivory and developmentally-controlled metabolic responses.

The herbivory effect of *Spodoptera* spp. on maize is well-investigated. Two recent studies now applied metabolomics to

mine for hitherto poorly characterized responses.[42,43] In those monocotyledonous plants 1,4-benzoxazin-3-ones (Bxs) are major defense compounds but the inducibility of specific metabolites of this class is rather poorly understood. Therefore Glauser *et al.*[42] used unbiased LC-MS-profiling to screen plant material before and after herbivory. PCA clearly separated the treatments and by investigating the loadings 2-β-D-glucopyranosyloxy-4,7-dimethoxy-1,4-benzoxazin-3-one (HDMBOA-Glc **4**) and 2-β-D-glucopyranosyloxy-4,7,8-trimethoxy-1,4-benzoxazin-3-one (HDM_2BOA-Glc **5**) appeared as strongest contributors to the separation in induced plants. Catabolism of these metabolites was addressed by monitoring also the digestive products in specialized and non-specialized herbivores. Since plants and herbivores differ in their Bxs-profiles digestive processes could be followed up based on PCA-evaluation of metabolic patterns. Consecutive analyses revealed the role of the highly dynamic activation of maize Bxs in chemical defense.

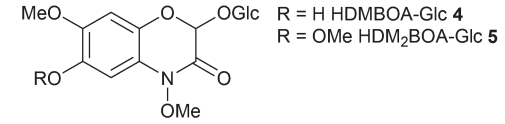

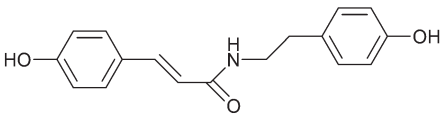

p-coumaroyltyramine **6**

Local and systemic responses to leaf herbivory by *S. littoralis* were the topic of a recent survey of secondary metabolites from maize leaves, sap, roots and root exudates.[43] A very comprehensive coverage using LC-MS in combination with unsupervised (PCA) and supervised (orthogonal (O)PLS-DA) data mining revealed more than 300 features in leaves and roots, 180 features in sap and 40 features in root exudates. Thirty-two differentially regulated compounds were identified from *Spodoptera littoralis*-infested maize seedlings and isolated for structure assignment by microflow NMR. Treatment-specific separation was only achieved for leaf samples and root exudates. Local leaf response consisted of an increase of lysophospholipids, azelaic acid, 1,3-benzoxazin-4-one derivatives, tryptophan and *N*-hydroxycinnamoyltyramines, whereas systemic response could be assigned to 1,3-benzoxazin-4-one derivatives increase in the sap and root exudates. Since *N*-hydroxycinnamoyltyramines were previously not identified in plant–herbivore interactions the authors tested the effect of the dominating *p*-coumaroyltyramine **6** on *S. littoralis*. This plant-derived natural product was metabolized by the larvae and increased larval growth, acting presumably as nitrogen source for the insect. The untargeted comparative metabolomics approach can thus lead to discovery of novel dynamically regulated metabolites and help to create novel hypotheses about herbivore–plant-interaction.

The interaction between the fungal endophyte *Fusarium verticillioides* and the pathogen *Ustilago maydis* which are both growing on maize has been the subject of several studies.[44,45] The endophyte thereby decreases the harmful effect of the pathogen.[46] LC-MS metabolic profiling of isolated partners as well as of co-cultures of the fungi revealed that most secondary metabolites are constitutively produced by each species.[44,45] Nevertheless the presence of *F. verticillioides* leads to reduction in *U. maydis* biomass. Comparative metabolomics was also employed to investigate leaf herbivory of *Manduca sexta* and *Helicoverpa zea* on tomato (*Solanum lycopersicum*) by GC-MS.[47,48] Metabolites were identified based on library searches resulting in 56 and 60 identified primary metabolites respectively and further analyzed *via* PCA and Venn diagrams. Primary metabolites throughout the plant (apex, leaves, stem, and roots) showed a species- and tissue-specific plant response. Induced metabolic changes were strong in the apex and root tissues as well as in damaged leaves confirming a whole-plant response to damage.

The metabolome of the endophytic fungus *Paraconiothyrium variabile* is of interest if the indirect interaction with its host plant *Cephalotaxus harringtonia* is concerned. *P. variabile* inhibits the phytopathogen *Fusarium oxysporum* thus providing protection for the host.[49] During an *in vitro* competition situation of both fungi LC-MS profiling and analysis with the powerful software XCMS[50] revealed, besides a comprehensive set of inactive constitutively produced metabolites, a series of induced compounds. These included 13-oxo-9,11-octadecadienoic acid **7**, 13-hydroperoxy-9,11-octadecadienoic acid, and several unknowns (Scheme 3). Interestingly, nanogram amounts of 13-oxo-9,11-octadecadienoic acid reduced the production of the mycotoxin beauvericin **8** in the phytopathogen *F. oxysporum* thereby promoting the idea of an induced interference mechanism.

Allelopathic interactions were investigated in a large study that addressed the effects of 16 Mediterranean plants on ovate goatgrass *Aegilops geniculata* using NMR-based comparative metabolic profiling.[51] Extracts of the 16 donor plants were characterized in terms of chemical composition. The effects of plant extracts on *A. geniculata* revealed a biological activity for most studied species probably due to phenolic compounds such as flavonoids and hydroxycinnamate derivatives. In

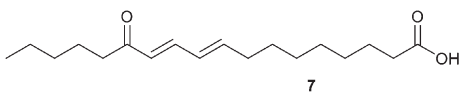

7

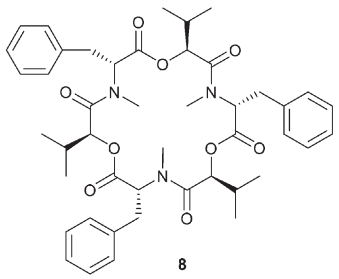

8

Scheme 3 13-Oxo-9,11-octadecadienoic acid **7** is upregulated in *Paraconiothyrium variabile* and suppresses formation of the mycotoxin beauvericin **8** in *Fusarium oxysporum*.

accordance to allelopathic activity, PCA analysis of NMR data of *A. geniculate* extracts clearly separated active treatment samples from controls and inactive treatment samples. This separation could be assigned to an increase in amino acids and organic acids and a decrease in oblongaroside, betaine, and *cis*-aconitic acid indicative for oxidative stress responses of the receiver plant. In accordance, hierarchical cluster analysis indicated three metabolite response groups: no, slight and strong metabolic changes due to treatment. This study is a nice example how such systemic approaches allow unravelling synergistic effects of allelopathic interactions that would have been difficult to spot in traditional bioassay-guided approaches.

Schweiger *et al.* analyzed the mutualistic interaction of arbuscular mycorrhiza (AM) with plant roots.[52] This ancient fungi–plant-symbiosis is widespread occurring in >80% of land plants. Common *vs.* species-specific responses in leaves of five model and non-model plant species (*Plantago lanceolata*, *P. major*, *Veronica chamaedrys*, *Medicago trunculatula*, *Poa annua*) to the generalist AM fungi *Rhizophagus irregularis* were investigated. A comparative metabolomics approach was selected involving the targeted metabolic profiling of carbohydrates, organic acids and sugar alcohols *via* GC-MS, of amino acids *via* HPLC-fluorescence detection, and the untargeted fingerprinting *via* LC-MS of methanolic leaf extracts. Between 18% and 45% of the polar metabolome was shared among species and designated as core metabolome with the rest being highly species/taxon-specific metabolites. Those species-specific differences would superimpose treatment effects and therefore these were analyzed separately for each plant. Besides a few common features in the dicotyledonous plants, responses were very species-specific even though the core metabolome would have allowed a common response pattern. The low conservation of responses indicates a long time of specific plant–fungus coevolution that leads to specific manifestations in the expressed metabolic response.

Metabolomics also allows the classification of responses of organisms by collecting "metabolic fingerprints" of a multitude of samples in defined states. Novel samples can then be compared to this data set allowing a categorization without any further ecological or physiological evaluation. This approach is especially used in plant sciences where stress responses are often analyzed by suitable interpretation of such metabolic patterns. Categorization of responses might also allow the identification of metabolites relevant in a specific interaction context thereby making this approach very valuable for the search of active metabolites in chemical ecology.

2.2 Comparative metabolomics in marine science

Especially in the chemical ecology of marine algae comparative metabolomics has recently gained importance *e.g.* to unravel anti-herbivory defense strategies,[53] allelopathic interactions,[54,55] bacteria–algae-symbioses,[56] or to discover algal pheromones.[57] However, compared to plants, defense strategies against herbivory are only poorly investigated in marine algae.[58,59] Other disciplines in marine chemical ecology currently start to use this emerging tool box as well.[60] Generally, the rather complex matrix of the seawater that carries signaling molecules represents a certain challenge if waterborne signals are concerned. In addition, there is no logical pre-selection for enrichment and extraction techniques of specific compound classes as it is the case for volatiles in insect signaling. It has been shown that the physical nature of metabolites that carry information in the seawater can range from highly polar zwitterionic metabolites[61] to entirely hydrophobic hydrocarbons.[62] The molecular weight is also not limiting the information content, since gases[63] and small molecules[64] as well as high molecular weight lipids[65] and proteins[66] can be active in interaction situations. Extraction techniques thus have to cover a broad spectrum of metabolites if those relevant in interactions shall be universally covered.

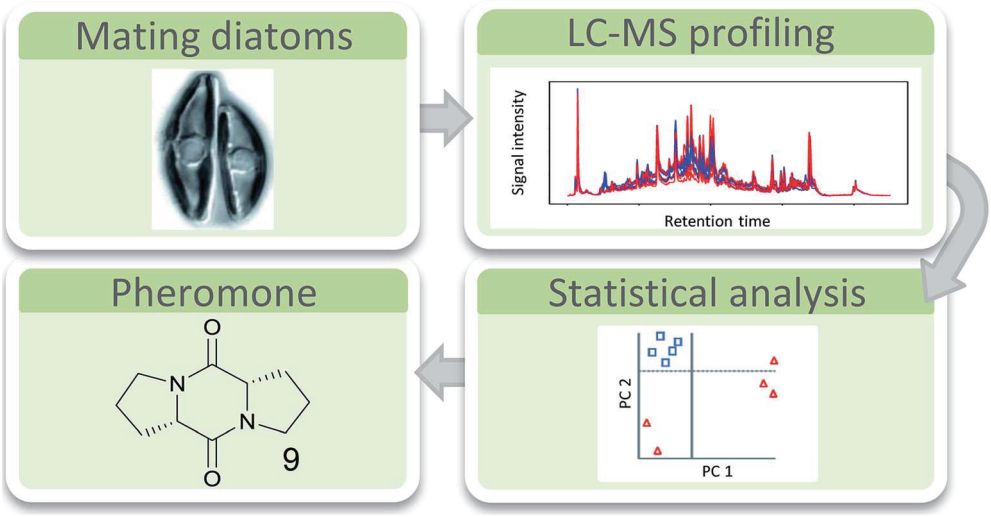

Fig. 2 The attraction pheromone di-L-prolyl diketopiperazine **9** was identified by comparative metabolomics of the diatom *S. robusta* (top left shows a mating pair). Cells with induced pheromone production were compared to control cells. LC-MS and statistical analysis pointed towards upregulated signals. The most prominent **9** was selected for purification and structure elucidation and proved to be as active as the natural product in bioassays.

Solid phase extraction and LC-MS analysis were suitable tools for the elucidation of the first diatom sex pheromone guided by comparative metabolomics.[67] The pennate diatom *Seminavis robusta* reproduces mainly asexually by cell division. Due to the rigid biomineralized cell wall of the diatoms this leads to a gradual cell size reduction in the population. If the cell size drops below a specific value, sexual reproduction of the alga is enabled. In this process pheromones are involved that activate the mating behavior and attract the partner cells of opposite mating types.[68] Comparative metabolic profiling of culture medium from cells that are not sexually active and those that call their mating partner revealed several upregulated metabolites as candidates for attraction pheromones.[67] The highest upregulated metabolite (>100 times) was isolated by fractionation and further bioassays confirmed its activity as mate attractant. Structure elucidation *via* MS(/MS), synthesis and co-injection proved di-L-prolyl diketopiperazine **9** as pheromone that was as active in bioassays as the natural pheromone (Fig. 2).

To unravel its chemical defense, the metabolome of the red alga *Gracilaria vermiculophylla* in response to herbivory by the generalist isopod *Idotea baltica* was studied using a combination of GC-MS and LC-MS metabolomics and bioassays.[53] Mechanical wounding significantly changed metabolic profiles as revealed by Permanova analysis, with some compounds being increased more than 100-fold. Metabolites that were upregulated in wounded tissue were predominantly eicosanoids (Scheme 4).

A detailed investigation of the data set by canonical analysis of principal coordinates (CAP) showed 11 upregulated metabolites in LC-MS and 8 upregulated metabolites in GC-MS data including prostaglandins, hydroxylated fatty acids, and arachidonic acid derived lactones. Isotopic labelling confirmed that most upregulated metabolites were derivatives of arachidonic acid. In subsequent bioassays five of the upregulated eicosanoids were tested for feeding deterrence. Only prostaglandin A2 **10** was deterrent while all other tested compounds rather attracted *Idotea*. This wound-activated defense differed from the induced defense which was systemically manifested in tissue neighboring feeding activity as revealed by CAP analysis in comparison to controls. While the activated response led to a change in eicosanoids, induced response affected mainly primary metabolites indicating a general stress effect, which calls for further investigations.

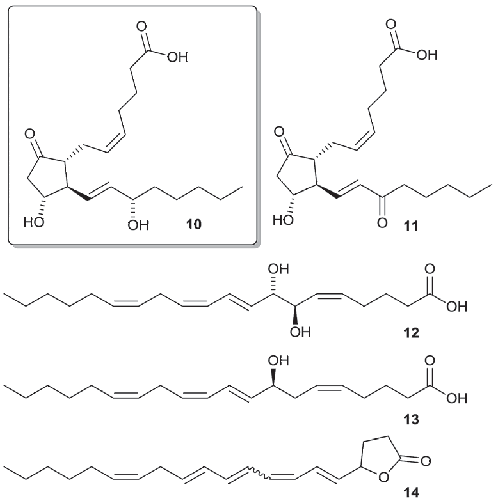

Scheme 4 Wound-activated produced eicosanoids (PGA_2 **10**, PGE_2 **11**, 7,8-di-HETE **12**, 8-HETE **13**, and a previously unknown lactone **14**) with the feeding deterrent prostaglandin A2 **10** framed.

Allelopathy is an important mediator of competition in plankton[69] and has been investigated focusing on the nature of allelopathic metabolites and the physiological response of the receiver.[54,55] In a comparative study of the interaction of the diatoms *Skeletonema costatum* and *Thalassiosira weissflogii* in co-culture it was observed that *S. costatum* promoted the growth of *T. weissflogii*. Comparative metabolic profiling *via* LC-MS revealed significant metabolic changes in the intra- and extracellular metabolome of both algae compared to monocultures. In the medium eight *S. costatum* specific metabolites and one *T. weissflogii* specific metabolite were found; their identification still remains an open task. Intracellular metabolomics in co-culture showed both up- and down-regulated metabolites in *S. costatum* whereas in *T. weissflogii* only downregulation was observed compared to the respective controls. This study demonstrates that even without physical contact non-toxic diatom cells can influence interaction partners by modulation of their endo- and exometabolome. In this context a novel approach to characterize exudates from aquatic autotrophs by stable-isotope metabolic footprinting might prove helpful for a thorough characterization of algal exudates from the complex seawater background.[70] Using a similar approach, the positive effect of the bacterium *Dinoroseobacter shibae* on the alga *Thalassiosira pseudonana* was investigated.[56] *D. shibae* slightly enhanced the growth of *T. pseudonana* in co-culture. Metabolic profiling of intracellular metabolites *via* GC-MS revealed more than 500 algal metabolites which could be separated according to treatment *via* principal coordinate analysis (PCO) and CAP. In accordance to the observed enhanced growth, algal primary metabolites were upregulated in presence of bacteria, among them amino acids such as serine, proline, phenylalanine and a glutamic acid derivative, as well as picolinic acid, some fatty acids and sugars. This study demonstrates a re-wiring of primary metabolism in the presence of bacteria, thereby underlying the complexity of plankton interactions.

2.3 Comparative metabolomics in nematode research

In nematode pheromone research comparative metabolic profiling has been applied mainly *via* MS/MS and NMR.[71,72] This field has recently been comprehensively reviewed elsewhere and thus this chapter will focus only on the general principles of metabolomics in the elucidation of signal molecules in this context.[73] The model organism *Caenorhabditis elegans* produces a class of glycolipids, the ascarosides, regulating diverse functions including development and behaviour.[74,75] Ascarosides (*e.g.* **15–20**) are built of the dideoxysugar ascarylose and fatty acid-derived side chains of varying length. Since bioassay-guided fractionation often was unsuccessful due to synergistic

functions of the metabolites that are lost during purification, comparative metabolomics proved to be the method of choice. The differential analysis by 2D-NMR spectroscopy (DANS) simplifies detection of ascarosides that are preferentially produced during interaction and regulation events.[76] For this purpose DQF-COSY NMR spectra of the wild type were overlaid with spectra of a signaling-deficient mutant, *daf-22*. Since the biosynthesis of certain mating and dauer pheromone components is abolished in *daf-22* worms a subtraction of the wild type and the mutant metabolome allowed identification of novel potentially active components. Major remaining signals represented mainly short-chained ascaroside structures including the four novel ascarosides ascr#6.1 **16**, ascr#6.2 **17**, ascr#7 **18**, and ascr#8 **19**.

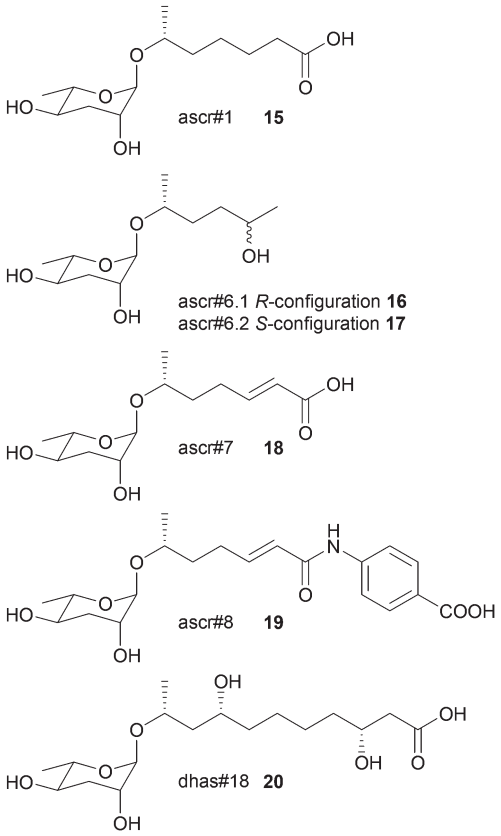

Additional HSQC- or HMBC-NMR, as well as HPLC-MS investigations and total synthesis confirmed the structures, and their function was verified in bioassays where ascr#8 proved to be a strong male-specific attractant and inducer of larval arrest.[76] Using LC-MS-based targeted metabolomics it could be shown that *C. elegans* males produce ascaroside signatures that differ from those of hermaphrodites. Even minor structural modifications profoundly affect the ascarosides' signaling properties.[77] These approaches proved to be fruitful in the elucidation of other functions and structures of ascarosides.[72,78,79] The sex-specific attraction of the nematode *Panagrellus redivivus* was initially investigated by bioassay-guided fractionation followed by LC-MS, 1D- and 2D-NMR, and total synthesis.[72] Males are attracted by ascr#1 (only produced by females) and females by dhas#18 (only produced by males). Targeted profiling of the exometabolomes of a mixed culture by LC-MS^2 revealed four more ascarosides (ascr#10, ascr#3, bhas#18, and bhas#10); however, a biological function could not be identified. Further comparative profiling of males, females and mixed cultures revealed highly sex-specific ascaroside production. Males only exhibited bhas#18 and dhas#18 whereas females exhibited at least 6 different ascarosides. The study suggests that ascarosides can have different functions in different nematode species and can even serve as allelochemicals.

The biosynthesis of ascarosides was elucidated by comparative LC-MS^2 profiling of wild type and several peroxisomal beta-oxidation mutants. Based on a series of elaborate experiments a working model of ascaroside biogenesis was proposed that involves an origin from very long side chain precursors that are transformed *via* peroxisomal beta-oxidation.[71] A picture arises of ascarosides as a modular library derived from carbohydrate metabolism, peroxisomal beta-oxidation and amino acid catabolism. Interested readers are referred to the contribution "combinatorial chemistry in nematodes: modular assembly of primary metabolism-derived building blocks" by Stephan H. von Reuss and Frank C. Schroeder within this issue of NPR.

DANS-based comparative metabolomics of *daf-12* and *daf-9 C. elegans* mutants revealed steroids with unexpected structural features that were further characterized after HPLC purification.[80] The compounds that are ligands of nuclear hormone receptors (NHR) of *C. elegans* extend our knowledge of transcriptional regulators in metazoans significantly (Fig. 3). More elaborate algorithms for comparative metabolic profiling *via* NMR have been already applied for comparison of the nematodes *Pristionchus pacificus* and *Panagrellus redivivus* and await application in the chemical ecology of this system.[81]

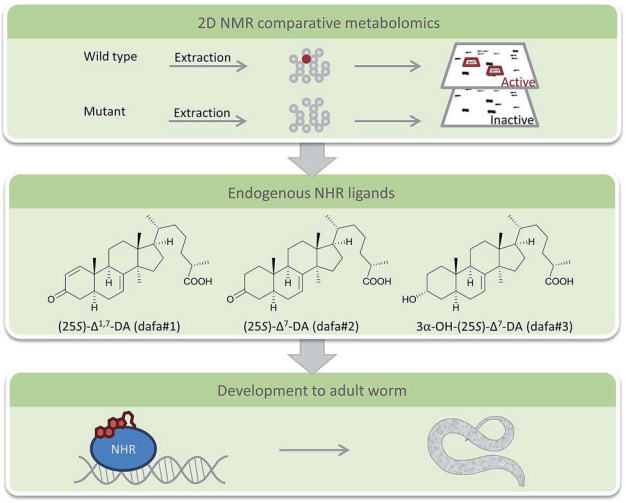

Fig. 3 Schematic work flow for the comparative NMR-metabolomics-based identification of novel steroids with signal properties from *C. elegans* wild type and mutant strains (NHR nuclear hormone receptors).

2.4 Comparative metabolomics unravels pheromones in social insects

Social insects like bees, ants, wasps or bumblebees use chemical signals for diverse chemical interactions such as nest-,[82] sex-,[83,84] or caste-recognition,[85–87] or as appeasement signal in mutualistic nest sharing.[88] Mainly cuticular hydrocarbons (CHCs) serve for chemical communication within and between species. These rather simple natural products are produced in complex mixtures that can hardly be resolved using traditional bioassay-guided fractionation. However, comparative metabolomics proves to be an ideal tool to spot relevant CHCs that are present in specific species or members of one species or that are regulated in interaction situations.

Reproduction in eusocial insects and thus development of reproductive queens and non-reproductive workers is regulated by pheromones which are primarily non-volatile, saturated hydrocarbons.[85] Comparative profiling of queen and worker cuticular extracts were investigated in the wasp *Vespula vulgaris*,[89] the bumblebee *Bombus terrestris*,[90] and the ant *Cataglyphis iberica*. Candidate pheromones were selected based on the assumption that they are more abundant in queens compared to workers.[85] The identified structures were tested in ovary regression and development bioassays and it was found that active compounds were all long-chain linear and methyl-branched saturated hydrocarbons (*n*-C27, *n*-C29, 3-MeC29 in the wasp and ant species, and *n*-C25 in the bumblebee).[85]

Primitively eusocial insects – such as permanently social polygynous epiponin wasps – can show caste flexibility until the adult stage. Queen selection either happens under physical attack[86] or peacefully.[91] Regarding the first case, after queen removal *Polybia micans* workers show aggression towards young, potential queen candidates. Prospective queens with larger ovaries also have higher amounts of queen caste-specific hydrocarbons thus probably increasing worker aggression. After a few days some are accepted and start as new queens. Comparative metabolic profiling of CHCs *via* GC-MS revealed a general dominance of linear alkanes but also showed differences between caste, age and reproductive status. C25 and 3-MeC25 could be identified as queen caste-specific. Further bioassays would be needed to confirm the potential roles. A similar but peaceful social behavior was found within the closely related *Synoeca surinama*, however dominant CHCs differ considerably.[91] Altogether 22 CHCs (alkenes or linear alkanes) were identified. Stepwise discriminate function analysis separated queens from >4 days old workers. C25 : 1 was increased in all queens in all colonies, whereas workers had longer hydrocarbons. Thus it seems that after queen removal, juvenile hormone modifies the CHC blend of young workers with an increase in C25 : 1 matching that of reproductive queens.

Worker reproduction in ants is reduced through policing behavior, such as physical aggression or egg eating. Based on the observation that CHCs regulate such aggression Smith *et al.* investigated the ant *Aphaenogaster cockerelli* where worker-produced eggs are not policed.[92] *A. cockerelli* has large colonies with only one queen and workers with active ovaries producing trophic eggs. CHCs were collected *via* solid phase micro-extraction from ants and *via* hexane extraction from eggs, measured by GC-MS and analyzed *via* nonmetric multidimensional scaling (nMDS). Interestingly, this species was found to have no distinct signaling pattern for worker-produced eggs which was confirmed by policing assays. In contrast, cuticular profiles of queens, workers and reproductive workers showed quantitative and qualitative differences which allow a separation *via* nMDS. These patterns were further investigated and confirmed *via* bioassays: reproductive cheaters could be mimicked by applying synthetic pentacosane, a compound typical of fertile individuals on nonreproductive workers. Pentacosane treatment induced nestmate aggression in colonies where queens were present.[93]

Within the trap-jaw ant *Odontomachus brunneus* large population differences within CHC profiles were observed that are potentially responsible for nest mate discrimination.[94] However, Z9 : C29 was found *via* nMDS as conserved fertility signal in queens across populations, a compound that was already recognized earlier. Social parasites such as the bumblebees *Bombus bohemicus* and *B. rupestris* use similar nest-specific signals (worker trail pheromones) to find their hosts.[95] Inter- and intraspecific odor variation of 45 hydrocarbons of nests of potential hosts were examined *via* GC-MS. PCA and discriminant function analysis (DFA) revealed interspecific and intercolonial differences in the odor bouquets of the host that were predominantly due to different patterns of alkenes. In Y-olfactometer choice tests *B. rupestris* showed a clear preference for the scent of its host proving that volatile signals enable parasite females to discriminate between potential host species.

In all these examples the power of statistical analysis of complex metabolic signatures could be demonstrated. While separation of the hydrocarbons and testing is tedious and would risk overlooking effects of specific mixtures, the recognition and evaluation of metabolic patterns helps to unravel the complex language of CHCs.

2.5 MS/MS networking in comparative metabolomics

The capacity to generate vast data sets also challenges the ability for downstream processing.[96] In the above mentioned examples the major goal was to eliminate signals of potentially irrelevant metabolites, but approaches to use MS-based molecular networking or other elaborate algorithms also allow to sketch more complex interaction networks by comprehensively evaluating metabolic patterns.[97] An emerging tool is MS/MS networking, a visualization method for MS/MS data sets where molecules are clustered with regard to similarities in their molecular ion mass and fragmentation pattern.[98] MS/MS spectra of complex mixtures of molecules are compared pair wise and their similarity is expressed as cosine of the normalized ratio of relative ion intensities (cosine similarity score). As a result structurally similar compounds with similar fragmentation patterns are located close to each other thus forming sub clusters of "molecular families" that share certain chemical properties. For identification of single nodes or whole sub clusters the network can be supplemented with standards and

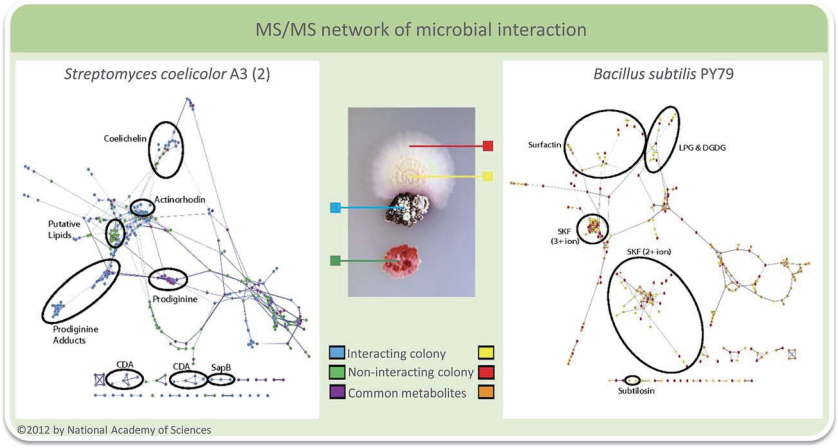

Fig. 4 Interacting *S. coelicolor* (blue) and *B. subtilis* (yellow) in comparison to samples from noninteracting bacteria (red and green). The molecular network of *S. coelicolor* is shown on the left and that of *B. subtilis* on the right. With permission from the National Academy of Sciences USA.[98]

database entries.[98] This identification differs from traditional approaches as MS/MS spectra are matched against other MS/MS spectra instead of matching them against protein sequences or molecular structures. Related or identical compounds are therefore detected before considering their possible identification. Instead of the traditional peak-by-peak identification consensus identifications from sets of spectra of related compounds are determined allowing a novel approach for classification.[96,97,99] Common metabolites in data sets of interaction studies as well as the global molecular diversity of single species or certain taxa can be easily visualized. Also biosynthetic considerations can be taken into account during data evaluation.[100–104] The software to generate MS/MS networks is freely available[105,106] and even quantitative data sets can be considered.[107]

To demonstrate the applicability of the MS/MS networking approach, several bacterial colonies were analyzed *in situ* on agar plates using nano desorption electrospray MS (DESI-MS).[98] Networks of metabolites from *Bacillus subtilis*, *Streptomyces coelicolor*, *S. marcescens*, *Mycobacterium smegmatis* and *Pseudomonas aeruginosa* demonstrated the ability to visualize species-dependent molecular diversity. But also time-dependent networks of *B. subtilis* colonies could be generated to gain insights into bacterial developmental processes. Most important in the context of this review is the fact that also microbial interactions could be visualized as shown for *S. coelicolor* and *B. subtilis* (Fig. 4). Molecular networking was able to confirm earlier reports that *B. subtilis* PY79 elicits pigment production in *S. coelicolor*, whereas *S. coelicolor* increases production of the cannibalistic factors SKF and SDP in PY79 in the region of interaction.[98]

The antifungal activity of *Pseudomonas* sp. SH-C52 – a strain that protects sugar beet plants from soil born fungi[108] – could be tentatively assigned to thanamycin **21** by generating a comparative MS/MS network of the wild type strain and two mutants. A partial structure of thanamycin **21** could be generated based on MS/MS data and analysis of the gene cluster. Since this initial report, MS/MS network-guided genome mining has been applied several times to facilitate the identification of non-ribosomal peptides (NRPs) and their associated gene clusters.[99,104]

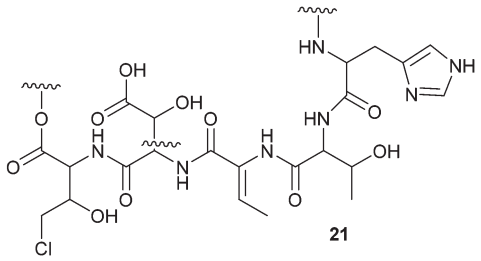

21

The antifungal activity of the octocoral symbiont *Bacillus amyloliquefaciens* against 13 different marine and terrestrial fungi was investigated using matrix-assisted laser desorption/ionization-imaging mass spectrometry (MALDI-IMS).[109] In side-by-side interactions of *B. amyloliquefaciens* with *Aspergillus fumigatus* and *A. niger* potential antifungal metabolites were measured and visualized using seeded MS/MS networking. Within the network members of the iturin-family were spotted that proved to be active in antifungal bioassays. The excreted metabolites of *Streptomyces coelicolor* during interaction with five other actinomycetes showed a high specificity with regard

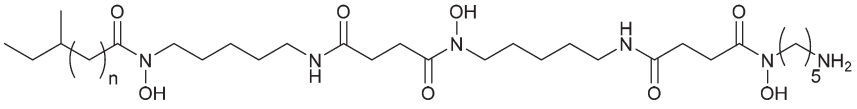

n=4 (**22**), 6 (**23**), 9 (**24**), 10 (**25**)

to the interacting partner.[110] By combining nano DESI-MS and MALDI-IMS one of the most comprehensive sets of molecules involved in microbial interactions to date was collected. Among the metabolites specific for the interaction a family of desferrioxamines **22–25** with acyl side chains of various lengths was triggered by siderophores from the neighboring actinomycetes. Altogether about 40% of all nodes within the spectral network were associated with the acyl-desferrioxamines **22–25** clearly characterizing the response of *S. coelicolor*. Besides the implications for the understanding of the chemical ecology of these strains, the study also outlines the importance of surveyed co-culturing in the search for new metabolites with potential pharmacological activity.

3 The systems biology approach

In contrast to the above mentioned reduction of complexity by pre-selecting specific groups of metabolites and by identifying single metabolites of relevance, systems biology approaches aim for a most comprehensive data collection and interpretation involving multiple-omics techniques.[111,112] Within this section the combination of metabolomics with transcriptomics or genomics to gather a more complex picture of the chemical ecology of organismal interactions will be presented. Such approaches can aim towards a full understanding of the biological processes connected to the production or perception of compounds involved in chemical ecology. This is a complex task, which not only depends on the identification of the compound itself but also on the investigation of the involved biochemical pathways and physiological responses on a gene, transcript, protein, and metabolite level using the entire omics-toolbox. Additionally, a link to ecology that can be provided in lab or field experiments is required to determine the role of the identified principles. Combining all these techniques is challenging but enables the unbiased generation of novel hypotheses and opens up new research avenues.[113]

Due to the advent of next generation sequencing technologies, genomic resources with a high degree of standardization can easily be obtained. However, the functional gene annotation that is relevant for the interconnection with metabolomics is lagging behind. In chemical ecology the understanding of dynamic metabolic networks is essential and it is therefore important to gather quantitative information using downstream-omics tools on the transcript, the protein or the metabolite level. A first challenging aspect for such an endeavor is the experimental design. Especially when taking the ecological situation of an organism into account elaborate incubation and sampling protocols are of key importance. Ideally, sampling should be performed in one step for all subsequent omics-technologies. In cases where time series are important this sampling should be minimal invasive to avoid disturbing the system. Substantial progress has been made and a recent protocol describes how one single sample can be used for analysis of metabolites, DNA, long and small RNA, and proteins *via* sequential isolation of those biomolecules.[114] Since the available biomass might be limiting, such a protocol ideally needs only minute amounts of sample. The introduced protocol requires only 50 mg fresh weight for a full sample set and has been tested using the plant species *Populus trichocarpa*, *Pinus radiata*, and *Arabidopsis thaliana*, as well as the microalga *Chlamydomonas reinhardtii*. Successful implementation in four different laboratories with different background in handling of such protocols showed the robustness of the method. Data integration and analysis of the different –omics data sets are still a major challenge. Several approaches have been introduced to correlate the different data sets, but are highly challenging to apply.[115,116] Thus often separate analysis of the respective data-sets and integration of the results is a more feasible approach as it is illustrated in the following examples.

The mode of infection and resistance of microalgae against a marine virus was addressed by Rosenwasser and collegues.[116] Those viruses can control some of the largest oceanic algal blooms of the coccolithophore *Emiliania huxleyi* and thereby deeply influence organismal interactions in the plankton. The interaction of the algal host and its specific double stranded DNA virus was observed in a set of infection experiments involving both, lytic and non-lytic virus strains. Global host and virus transcriptome profiling was conducted simultaneously with metabolome analyses to unravel cellular pathways affected by the viral infections. The transcript analysis proposed the regulation of several biochemical pathways of both the host and the virus. Also distinct shifts in metabolite composition during lytic and non-lytic infection were observed by comparative metabolic profiling.[116,117] In a combined weighted correlation network analysis that had to take into account a delay in metabolic compared to transcriptomic response, clusters from transcriptomics were correlated to metabolite levels. As many metabolites were correlated to one specific transcript expression pattern, integrated metabolic maps could be constructed. Especially during the early stages of viral infection a dynamic modulation of the host metabolism was observed. Based on the metabolic maps, a viral up regulation of algal fatty acid biosynthesis to help viral assembly, and a down regulation of host sphingolipid biosynthesis was observed. Viral influence on sphingolipids was already earlier identified in this system, thereby confirming the validity of the approach.[118] But in addition, several terpenes including a group of sterols were substantially down regulated in agreement with a reduction of all host genes related to the production of isopentenyl-pyrophosphate in the mevalonate pathway. This down regulation could be assigned to an antiviral response mechanism that was further confirmed by inhibition experiments. Subsequent targeted metabolic analyses revealed that the suppression of steroid formation interferes with viral replication that requires these metabolites. Viral replication in *E. huxleyi* thus depends on the host metabolic machinery to provide sterols, fatty acids and sphingolipids as building blocks for viral progeny formation.

Plankton interactions were also the subject of another recent study that combined metabolome and proteome analyses during a competition situation.[113] The sublethal allelopathic effects of the red-tide dinoflagellate *Karenia brevis* on two diatom competitors were addressed.[119] Therefore *Asterionellopsis glacialis*, a diatom species that co-occurs with the red

tide dinoflagellate and *Thalassiosira pseudonana* which may not have evolved resistance were challenged with *K. brevis* in co-cultivation experiments. In both diatoms the presence of the dinoflagellate caused changes in the metabolic and proteomic profiles. Up- and down regulated proteins and metabolites were identified tentatively and related to putative cell functions. Combining the proteomics and metabolomics results a molecular network was derived from which it was concluded that the naturally co-occurring species *A. glacialis* shows a more robust metabolism with only slight changes in co-cultivation. In contrast, allelopathy disrupted energy metabolism (glycolysis, photosynthesis) and impaired cellular protection mechanisms including cell membrane maintenance, osmoregulation and oxidative stress response in *T. pseudonana* (Fig. 5).[113] This study provided several novel hypotheses for the underlying mechanisms in sub lethal allelopathy that will surely be the subject of testing in the near future.

Successful combination of –omics approaches are also reported from the chemical ecology of higher plants.[120,121] The majority of trees form beneficial relationships with ectomycorrhizal (ECM) fungi.[122] After invasion an ECM-root tip is formed that can be considered as a type of symbiotic organ. The processes during invasive colonization of *Populus* root tips by the fungus *Laccaria bicolor* was the subject of a metabolomics/transcriptomics study by Tschaplinski *et al.*[120] This study could benefit from the availability of a genomic and transcriptomic data repository of the fungus. In addition, both, a compatible host *Populus trichocarpa* and a recalcitrant host *P. deltoides* were

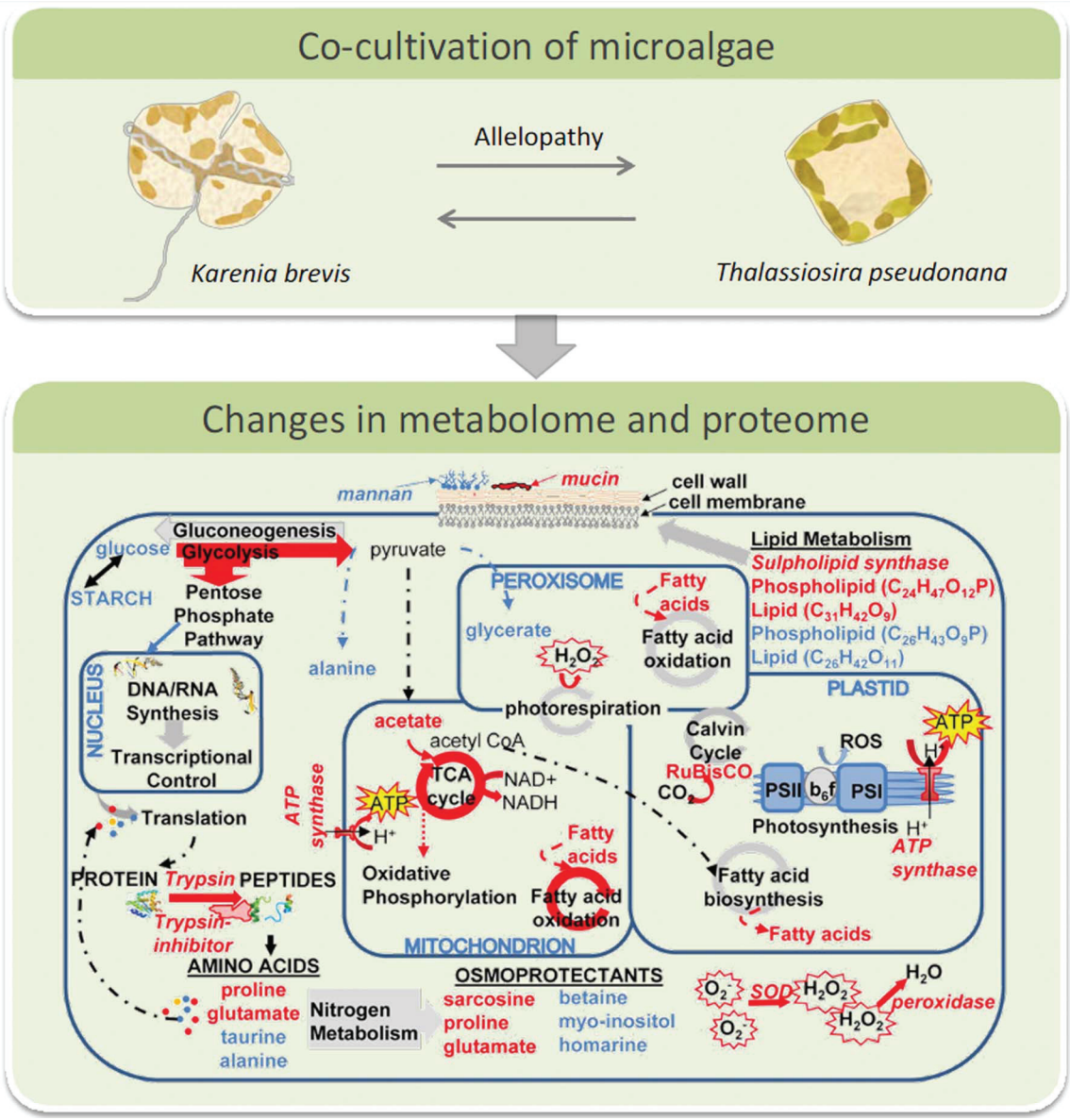

Fig. 5 Top: interacting microalgae *K. brevis* and *T. pseudonana* were investigated using a metabolomics/proteomics approach. Bottom: the network of cellular pathways, enzymes, and metabolites in *T. pseudonana* under the influence of *K. brevis* are depicted. Pathways and metabolites enhanced by allelopathy are indicated by red arrows and compound names, respectively and those suppressed by blue labels. Below panel is reproduced with permission from the National Academy of Sciences.[113]

accessible. The metabolic reprogramming that favors the formation of the ECM-root tip hybrid tissue in compatible interactions or that prevents the formation of such tissue in the recalcitrant host could be addressed by a combination of metabolomics and transcriptomics. In this case GC-MS proved to be the method of choice since data base supported evaluation of spectra allowed the tentative identification of regulated metabolites that could be brought into accordance with regulated pathways from transcriptomics.[120] The symbiotic metabolome is altered throughout the colonization process with shifts in aromatic acids and fatty acid metabolism. The mutualistic ECM relationship might require such suppression or moderation of host defenses, allowing for the fungus to integrate into the root tissues. Explorative mapping of the observed metabolic changes in the benzoate degradation pathway using the KEGG database[123,124] lead to a targeted transcriptome analysis. The results are in accordance with the fungus being the driver of metabolic reprogramming in the early stages of colonization. The challenge of ECM root tips of the recalcitrant *P. deltoides* with the fungus led to less pronounced metabolic shifts but plant defense related compounds such as tryptophan or salicin were elevated in the incompatible interaction. Targeted degradation assays further showed the capacity of the fungus to metabolize secreted defensive compounds. Thus diversity and half-life of plant defense compounds seem to be driving forces of the interaction.

An important tool for the deciphering of herbivory-induced gene-to-metabolite dynamics was introduced by Gulati *et al.*[125] The novel transcript and metabolite data classification tool for experiments with multiple factors such as treatment, tissue, genetic context, or time-series was tested on *Nicotiana attenuata* using 3 tissues, 2 stressors and a 6-point-time-series for transcriptome and metabolome data. The value of the approach was demonstrated by revisiting well-characterized changes of regulatory genes and the oxylipin pathway. But the dimensionality reduction approach is also applicable to unravel rewiring of gene and metabolite networks in an explorative manner. Dynamic metabolite–metabolite correlation networks were created to cluster biochemically connected metabolites (*e.g.* shikimate pathway derived amino acids correlated with phenylpropanoid pathway metabolites). This study underlines the high plasticity of herbivore responses and provides a nice functional genomics tool to find novel genes and metabolites involved in herbivore response as shown for oxylipin signaling and the 17-hydroxygeranyllinalool diterpene glycoside (17-HGL-DTG) pathway. The root metabolome of *N. attenuata* under the influence of leaf herbivory was addressed using this approach.[126] A multivariate time-series data analysis was used to evaluate leaf herbivory-elicited transcriptional and metabolic dynamics in the roots. Transient systemic responses in roots were detected. The semi-diurnal transcript oscillation was inverted and its major amplitude effects translated into root-specific secondary metabolite shifts.[126] Using the multifactorial approach described in Gulati *et al.*[125] tissue and treatment effects in a time-course data set could be analyzed that form the basis for further functional studies on the role of above ground herbivory on root metabolism.

The above examples might be considered as starting points of combined –omics studies in chemical ecology. These few publications that combined metabolomics with other –omics data sets to reveal basic principles of chemically mediated species interactions were all published within the last two years, thereby representing the start of a novel era in chemical ecology research. In other research areas relevant for the field, such as plant physiology, combined –omics approaches are also increasingly applied and several reviews already discussed the use of metabolomics, proteomics, transcriptomics and metabolic flux analyses as functional genomics tools.[127–130]

4 The comprehensive metabolome approach

This chapter will focus on the use of comprehensive metabolomics data of model species in chemical ecology and present an outline about the potential power of comprehensive data repositories. In the studies discussed so far the metabolome – the collection of all metabolites of an organism – has been covered only to some extent. Based on the hypothesis to be answered the focus of the study was on a certain subset of the metabolome. In such cases the exclusion of all other metabolites is crucial to increase the detection limit of the metabolites in focus. However, if the global metabolome response to species interactions is in focus of the study a comprehensive approach covering all present metabolites is needed.[116] Such comprehensive metabolomes are challenging since no protocol exists so far that enables the extraction and analysis of the chemical diverse array of metabolites at once. However, for certain model organisms, comprehensive collections of metabolites with the aim to obtain complete metabolomes are currently assembled. The field of chemical ecology could benefit from such collections since they would define the metabolic potential and answer the question of what is possible in chemical signaling. Another issue, not only in metabolomics but also in all other –omics fields,[121] is the identification and functional characterization of detected features, such as metabolites.[120,132] Here chemical ecology can provide novel structures and hints towards their function off the beaten track of primary metabolism. There is clearly a need for public large spectral data bases that not only cover metabolites of key species to support such initiatives. This also calls for the deposition of own compounds with the according metadata to allow for knowledge-sharing between laboratories.

It is estimated that about 5 million putative metabolites exist in the plant kingdom.[133] Besides the structural diversity, also spatial and temporal variability as well as broad concentration ranges limit a comprehensive coverage of the metabolome. Therefore it has been recommended repeatedly to combine knowledge obtained with different extraction protocols and analytical tools such as GC(× GC)-MS, LC-MS, NMR or FT-IR.[127,130] Standardized protocols addressing such combined approaches are however still under development.[134–136] For certain model organisms quite comprehensive annotated data repositories exist as it is the case for *Arabidopsis thaliana*,[137]

Escherichia coli,[138] and *Saccharomyces cerevisiae*.[139] Those repositories can serve as reference database not only for these species themselves but also for related organisms that might be of more interest in chemical ecology. http://PlantMetabolomics.org (PM) has been the first available online data repository covering over 3.100 compounds from *A. thaliana* wild type and 50 mutant lines that have been solely analyzed to accomplish this database.[137] The aim is to annotate each metabolite with its experimental metadata and abundance following standardizing procedures (MSI,[131] ArMet,[140] MIAMET[141]). PM is further linked to several other databases including KEGG and PubChem to allow searching for genetic, chemical and biosynthetic pathway information. Additionally, protocols, tutorials as well as diverse statistical tools are provided. The Yeast Metabolome Database (YMDB) provides over 2000 metabolites linked to 995 genes or proteins, 66 biochemical pathways and 916 chemical reactions.[139] 1540 NMR- and 951 MS spectra are linked to 750 compounds. Intra- and extracellular concentrations are given for 627 metabolites. This data has been collected from books, articles, other databases and own measurements, and is linked to metadata, images, references and other databases. The *E. coli* metabolome database (ECMDB) is the most recent annotated data repository for *E. coli* (primarily strain K-12).[138] It provides over 2600 metabolite entries with links to 1500 genes or proteins, 125 biochemical pathways and 2800 chemical reactions. It is also supplemented with 775 NMR spectra and 4035 MS spectra as well as intracellular concentration data for 800 compounds. But since *S. cervesiae* and *E. coli* serve mainly as model organisms in molecular biology and are rarely considered in chemical ecology these powerful data repositories address rather molecular biologists and system biologists.

Those data repositories are all species-specific, which is considered to be essential for the field of metabolomics as each organism has its own unique set of metabolites.[138] Facing this dilemma it remains to be answered how to integrate the diverse variety of species that are interesting for chemical ecologists. The closest related model organism with its associated database could be used but much of the power of the repositories would be lost. A remarkable concept for a general purpose, cross-species, cross-platform data repository for metabolomics data that can overcome these limitations is realized in the MetaboLights platform.[142,143] First results from studies in chemical ecology are already included[71] and a broad usage would open up vast possibilities for the search of secondary metabolites in organismal interactions.

Nevertheless, also chemical ecology can focus on model organisms, and several experiments on the chemical ecology of *A. thaliana*, *Caenorhabditis elegans* or *Drosophila melanogaster* have been conducted that can benefit from and contribute to the resources of joint metabolomics initiatives. Methods for the generation of comprehensive metabolomes of *e.g. D. melanogaster*[144] or *C. elegans*,[135] or at least standardized metabolomics methods for *e.g. Bacillus subtilis*[134] or *Staphylococcus aureus*[145] are suggested and it can be observed that even organisms that generated interest in the field of (chemical) ecology were promoted as models as it is the case with the tobacco plant *Nicotiana attenuata* or the unicellular diatom *Skeletonema costatum*. To assist metabolomics in chemical ecology standard operation procedures for such species with clear definition of specific protocols are needed as organism-specific characteristics can influence the extraction efficiency.[146] For example for *C. elegans* tissue disruption is a crucial step.[135] Tissue selection has also to be considered for more complex organisms since whole organism homogenates can be insufficient as was shown for *D. melanogaster*.[144] Sample collection, preparation, storage, analysis and data handling can thus introduce a variability that interferes with comparative efforts between laboratories. At the time being it is an unrealistic goal to reach a comprehensive coverage of the 'metabolome' for every organism interesting in chemical ecology. But intelligent use of existing repositories[147] normalized procedures and ethics of reporting and contributing to data bases[148] will help to make metabolomics an even more powerful tool. Of particular importance is the metabolomics standards initiative (MSI) that was conceived in 2005 with the goal to develop universal minimum standard requirements for metabolomics analyses. Primary minimal standards were published 2007 encompassing five different areas of metabolomics analyses.[131] Recommendations addressing the reporting of biological samples from mammals,[149] plants,[150] microbes,[151] and of environmental samples[152] were given, as well as for chemical analyses,[153] data processing,[154] data exchange structures,[155] and ontology.[156] To benefit from such initiatives, metabolomics researchers, also in chemical ecology, should stick wherever possible to these recommendations to make their work comparable.[131] Due to lacking open source file formats the COordination of Standards in MetabOlomicS (COSMOS) was initiated subsequently and might prove as a powerful tool to handle and compare data also in the field of chemical ecology.[142,157]

5 Conclusions

From the above discussed examples it can be concluded that metabolomics represents an emerging technique in chemical ecology that has the power to shape the discipline in several ways. For one, the identification of signaling molecules will be greatly facilitated by at least partially eliminating the need of bioassay-guided fractionation for the identification of active metabolites. In a systems biology context, metabolomics enables connecting chemically mediated interactions to regulative events on a protein or transcriptome level. With the emerging possibilities of data repositories and the categorization of metabolites from ever more model species, the discipline of metabolomics will become more mature and tasks such as de-replication, metabolite assignment and even structure elucidation that are tedious today will become routine. There is still a long way to go to establish metabolomics as standard technique in labs of biologists, but interdisciplinary approaches involving analytical chemists are already in place. In addition to the above outlined avenues, metabolomics also opens up new fields of research in chemical ecology. Thus, *e.g.* imaging techniques will allow to spot the point of interaction in microbial communities,[98,109] on surfaces and in the immediate

surroundings of plants and algae,[158–160] as well as in insects.[161] But also the metabolome of single cells might become of interest, especially when aspects of cooperative interactions or cheaters in microbial communities are concerned.[162–164] However the still limited capabilities of the available imaging techniques lead to smaller data-sets compared to other metabolomics techniques and quantification is still problematic. Novel concepts in metabolomics have the potential to allow the design of fundamentally new experiments in chemical ecology that will allow monitoring the ecological interactions of organisms in hitherto unrecognized complexity. One potential direction to go would be the space- and time resolved monitoring and manipulation of complex communities with the aim to identify the "chemical role" of each partner in set-ups that are a lot closer to the true ecology of the species than traditional, often over-simplified co-culturing approaches.

6 Acknowledgements

We thank the Volkswagen Foundation, the German Research Foundation (DFG) within the framework "Collaborative Research Centre CRC1127 Chemical Mediators in complex Biosystems" and the Jena School for Microbial Communication for funding.

7 References

1 http://www.chemecol.org.
2 S. M. Cook, Z. R. Khan and J. A. Pickett, in *Annual Review of Entomology*, Annual Reviews, Palo Alto, 2007, vol. 52, pp. 375–400.
3 A. Butenandt, R. Beckmann and E. Hecker, *Hoppe-Seyler's Z. Physiol. Chem.*, 1961, **324**, 71–83.
4 E. K. Prince and G. Pohnert, *Anal. Bioanal. Chem.*, 2010, **396**, 193–197.
5 J. Stokl, A. T. Dandekar and J. Ruther, *J. Chem. Ecol.*, 2014, **40**, 159–168.
6 T. Alborn, T. C. J. Turlings, T. H. Jones, G. Stenhagen, J. H. Loughrin and J. H. Tumlinson, *Science*, 1997, **276**, 945–949.
7 A. Eberhard, A. L. Burlingame, C. Eberhard, G. L. Kenyon, K. H. Nealson and N. J. Oppenheimer, *Biochemistry*, 1981, **20**, 2444–2449.
8 D. B. Wilburn, K. E. Bowen, P. W. Feldhoff and R. C. Feldhoff, *J. Chem. Ecol.*, 2014, **40**, 928–939.
9 K. Gase and I. T. Baldwin, *Plant Ecol. Divers.*, 2012, **5**, 485–490.
10 C. Tittiger, *J. Chem. Ecol.*, 2004, **30**, 2335–2358.
11 M. Dicke, *J. Plant Physiol.*, 1994, **143**, 465–472.
12 W. Boland, J. Hopke, J. Donath, J. Nuske and F. Bublitz, *Angew. Chem., Int. Ed.*, 1995, **34**, 1600–1602.
13 O. Fiehn, *Plant Mol. Biol.*, 2002, **48**, 155–171.
14 G. J. Patti, O. Yanes and G. Siuzdak, *Nat. Rev. Mol. Cell Biol.*, 2012, **13**, 263–269.
15 B. B. Aldridge and K. Y. Rhee, *Curr. Opin. Microbiol.*, 2014, **19**, 90–96.
16 E. M. Lenz and I. D. Wilson, *J. Proteome Res.*, 2007, **6**, 443–458.
17 C. Junot, F. Fenaille, B. Colsch and F. Becher, *Mass Spectrom. Rev.*, 2014, **33**, 471–500.
18 M. Ernst, D. B. Silva, R. R. Silva, R. Z. N. Vencio and N. P. Lopes, *Nat. Prod. Rep.*, 2014, **31**, 784–806.
19 K. Bingol and R. Bruschweiler, *Anal. Chem.*, 2014, **86**, 47–57.
20 S. L. Robinette, R. Bruschweiler, F. C. Schroeder and A. S. Edison, *Acc. Chem. Res.*, 2012, **45**, 288–297.
21 R. R. Forseth and F. C. Schroeder, *Curr. Opin. Chem. Biol.*, 2011, **15**, 38–47.
22 K. H. Liland, *Trends Anal. Chem.*, 2011, **30**, 827–84123.
23 E. Saccenti, H. C. J. Hoefsloot, A. K. Smilde, J. A. Westerhuis and M. M. W. B. Hendriks, *Metabolomics*, 2013, **10**, 361–374.
24 N. Gehlenborg, S. I. O'Donoghue, N. S. Baliga, A. Goesmann, M. A. Hibbs, H. Kitano, O. Kohlbacher, H. Neuweger, R. Schneider, D. Tenenbaum and A. C. Gavin, *Nat. Methods*, 2010, **7**, S56–S68.
25 J. Sardans, J. Penuelas and A. Rivas-Ubach, *Chemoecology*, 2011, **21**, 191–225.
26 D. D. Cheng, H. Kirk, P. P. J. Mulder, K. Vrieling and P. G. L. Klinkhamer, *New Phytol.*, 2011, **192**, 1010–1023.
27 M. Deicke, J.-P. Bellenger and T. Wichard, *J. Chromatogr. A*, 2013, **1298**, 50–60.
28 M. Deicke, J. F. Mohr, J.-P. Bellenger and T. Wichard, *Analyst*, 2014, **139**, 6096–6099.
29 O. Baars, F. M. M. Morel and D. H. Perlman, *Anal. Chem.*, 2014, **86**, 11298–11305.
30 E. Croisier, M. Rempt and G. Pohnert, *Phytochemistry*, 2010, **71**, 574–580.
31 M. Rempt and G. Pohnert, *Angew. Chem., Int. Ed.*, 2010, **49**, 4755–4758.
32 N. S. Cortina, D. Krug, A. Plaza, O. Revermann and R. Müller, *Angew. Chem., Int. Ed.*, 2012, **51**, 811–816.
33 D. Krug and R. Müller, *Nat. Prod. Rep.*, 2014, **31**, 768–783.
34 M. Kutyniok and C. Müller, *J. Exp. Bot.*, 2012, **63**, 6199–6210.
35 J. Hofmann, N. El Ashry Ael, S. Anwar, A. Erban, J. Kopka and F. Grundler, *Plant J.*, 2010, **62**, 1058–1071.
36 M. Kutyniok and C. Müller, *Oecologia*, 2013, **173**, 1367–1377.
37 M. Kutyniok, M. Persicke and C. Müller, *J. Chem. Ecol.*, 2014, **40**, 118–127.
38 S. G. Kim, F. Yon, E. Gaquerel, J. Gulati and I. T. Baldwin, *PLoS One*, 2011, **6**, e26214.
39 M. Stitz, I. T. Baldwin and E. Gaquerel, *PLoS One*, 2011, **6**, e25925.
40 E. Gaquerel, H. Kotkar, N. Onkokesung, I. Galis and I. T. Baldwin, *PLoS One*, 2013, **8**, e62336.
41 N. Onkokesung, E. Gaquerel, H. Kotkar, H. Kaur, I. T. Baldwin and I. Galis, *Plant Physiol.*, 2012, **158**, 389–407.
42 G. Glauser, G. Marti, N. Villard, G. A. Doyen, J.-L. Wolfender, T. C. J. Turlings and M. Erb, *Plant J.*, 2011, **68**, 901–911.
43 G. Marti, M. Erb, J. Boccard, G. Glauser, G. R. Doyen, N. Villard, C. A. M. Robert, T. C. J. Turlings, S. Rudaz and J.-L. Wolfender, *Plant, Cell Environ.*, 2013, **36**, 621–639.
44 A. E. Rodriguez Estrada, A. Hegeman, H. Corby Kistler and G. May, *Fungal Genet. Biol.*, 2011, **48**, 874–885.

45 W. Jonkers, A. E. Estrada, K. Lee, A. Breakspear, G. May and H. C. Kistler, *Appl. Environ. Microbiol.*, 2012, **78**, 3656–3667.
46 K. Lee, J. J. Pan and G. May, *FEMS Microbiol. Lett.*, 2009, **299**, 31–37.
47 A. Steinbrenner, S. Gómez, S. Osorio, A. Fernie and C. Orians, *J. Chem. Ecol.*, 2011, **37**, 1294–1303.
48 S. Gomez, A. D. Steinbrenner, S. Osorio, M. Schueller, R. A. Ferrieri, A. R. Fernie and C. M. Orians, *Entomol.Exp. Appl.*, 2012, **144**, 101–111.
49 A. Combès, I. Ndoye, C. Bance, J. Bruzaud, C. Djediat, J. Dupont, B. Nay and S. Prado, *PLoS One*, 2012, **7**, e47313.
50 C. A. Smith, E. J. Want, G. O'Maille, R. Abagyan and G. Siuzdak, *Anal. Chem.*, 2006, **78**, 779–787.
51 M. Scognamiglio, V. Fiumano, B. D'Abrosca, A. Esposito, Y. H. Choi, R. Verpoorte and A. Fiorentino, *Phytochemistry*, 2014, **106**, 69–85.
52 R. Schweiger, M. C. Baier, M. Persicke and C. Müller, *Nat. Commun.*, 2014, **5**, 3886.
53 G. M. Nylund, F. Weinberger, M. Rempt and G. Y. N. Pohnert, *PLoS One*, 2011, **6**, e29359.
54 E. K. Prince, K. L. Poulson, T. L. Myers, R. D. Sieg and J. Kubanek, *Harmful Algae*, 2010, **10**, 39–48.
55 C. Paul, A. Barofsky, C. Vidoudez and G. Pohnert, *Mar. Ecol.: Prog. Ser.*, 2009, **389**, 61–70.
56 C. Paul, M. Mausz and G. Pohnert, *Metabolomics*, 2013, **9**, 349–359.
57 J. Gillard, J. Frenkel, V. Devos, K. Sabbe, C. Paul, M. Rempt, D. Inzé, G. Pohnert, M. Vuylsteke and W. Vyverman, *Angew. Chem., Int. Ed.*, 2013, **52**, 854–857.
58 A. Ianora, M. Boersma, R. Casotti, A. Fontana, J. Harder, F. Hoffmann, H. Pavia, P. Potin, S. A. Poulet and G. Toth, *Estuaries Coasts*, 2006, **29**, 531–551.
59 E. Van Donk, A. Ianora and M. Vos, *Hydrobiologia*, 2011, **668**, 3–19.
60 S. Goulitquer, P. Potin and T. Tonon, *Mar. Drugs*, 2012, **10**, 849–880.
61 K. A. Fredrickson and S. L. Strom, *J. Plankton Res.*, 2009, **31**, 135–152.
62 G. Pohnert and W. Boland, *Nat. Prod. Rep.*, 2002, **19**, 108–122.
63 J. R. Seymour, R. Simo, T. Ahmed and R. Stocker, *Science*, 2010, **329**, 342–345.
64 B. Vanelslander, C. Paul, J. Grueneberg, E. K. Prince, J. Gillard, K. Sabbe, G. Pohnert and W. Vyverman, *Proc. Natl. Acad. Sci. U. S. A.*, 2012, **109**, 2412–2417.
65 C. Beemelmanns, A. Woznica, R. A. Aegado, A. M. Cantley, N. King and J. Clardy, *J. Am. Chem. Soc.*, 2014, **136**, 10210–10213.
66 C. Dreanno, K. Matsumura, N. Dohmae, K. Takio, H. Hirota, R. R. Kirby and A. S. Clare, *Proc. Natl. Acad. Sci. U. S. A.*, 2006, **103**, 14396–14401.
67 J. Gillard, J. Frenkel, V. Devos, K. Sabbe, C. Paul, M. Rempt, D. Inze, G. Pohnert, M. Vuylsteke and W. Vyverman, *Angew. Chem., Int. Ed.*, 2013, **52**, 854–857.
68 J. Frenkel, W. Vyverman and G. Pohnert, *Plant J.*, 2014, **79**, 632–644.
69 K. L. Poulson, R. D. Sieg and J. Kubanek, *Nat. Prod. Rep.*, 2009, **26**, 729–745.
70 R. J. M. Weber, E. Selander, U. Sommer and M. R. Viant, *Mar. Drugs*, 2013, **11**, 4158–4175.
71 S. H. von Reuss, N. Bose, J. Srinivasan, J. J. Yim, J. C. Judkins, P. W. Sternberg and F. C. Schroeder, *J. Am. Chem. Soc.*, 2012, **134**, 1817–1824.
72 A. Choe, T. Chuman, S. H. von Reuss, A. T. Dossey, J. J. Yim, R. Ajredini, A. A. Kolawa, F. Kaplan, H. T. Alborn, P. E. A. Teal, F. C. Schroeder, P. W. Sternberg and A. S. Edison, *Proc. Natl. Acad. Sci. U. S. A.*, 2012, **109**, 20949–20954.
73 F. C. Schroeder, *Chem. Biol.*, 2015, **22**, 7–16.
74 J. Srinivasan, F. Kaplan, R. Ajredini, C. Zachariah, H. T. Alborn, P. E. A. Teal, R. U. Malik, A. S. Edison, P. W. Sternberg and F. C. Schroeder, *Nature*, 2008, **454**, 1115–1146.
75 J. Srinivasan, S. H. von Reuss, N. Bose, A. Zaslaver, P. Mahanti, M. C. Ho, O. G. O'Doherty, A. S. Edison, P. W. Sternberg and F. C. Schroeder, *PLoS Biol.*, 2012, **10**, e1001237.
76 C. Pungaliya, J. Srinivasan, B. W. Fox, R. U. Malik, A. H. Ludewig, P. W. Sternberg and F. C. Schroeder, *Proc. Natl. Acad. Sci. U. S. A.*, 2009, **106**, 7708–7713.
77 Y. Izrayelit, J. Srinivasan, S. L. Campbell, Y. Jo, S. H. von Reuss, M. C. Genoff, P. W. Sternberg and F. C. Schroeder, *ACS Chem. Biol.*, 2012, **7**, 1321–1325.
78 N. Bose, J. M. Meyer, J. J. Yim, M. G. Mayer, G. V. Markov, A. Ogawa, F. C. Schroeder and R. J. Sommer, *Curr. Biol.*, 2014, **24**, 1536–1541.
79 A. Choe, T. Chuman, S. H. von Reuss, A. T. Dossey, J. J. Yim, R. Ajredini, A. A. Kolawa, F. Kaplan, H. T. Alborn, P. E. A. Teal, F. C. Schroeder, P. W. Sternberg and A. S. Edison, *Proc. Natl. Acad. Sci. U. S. A.*, 2012, **109**, 20949–20954.
80 P. Mahanti, N. Bose, A. Bethke, J. C. Judkins, J. Wollam, K. J. Dumas, A. M. Zimmerman, S. L. Campbell, P. J. Hu, A. Antebi and F. C. Schroeder, *Cell Metab.*, 2014, **19**, 73–83.
81 S. L. Robinette, R. Ajredini, H. Rasheed, A. Zeinomar, F. C. Schroeder, A. T. Dossey and A. S. Edison, *Anal. Chem.*, 2011, **83**, 1649–1657.
82 A.-M. Rottler, S. Schulz and M. Ayasse, *J. Chem. Ecol.*, 2013, **39**, 67–75.
83 A. Smith, W. Vanderpool, J. Millar, L. Hanks and A. Suarez, *Chemoecology*, 2014, **24**, 29–34.
84 S. E. F. Evison, R. S. Ferreira, P. D'Ettorre, D. Fresneau and C. Poteaux, *J. Chem. Ecol.*, 2012, **38**, 1441–1449.
85 A. Van Oystaeyen, R. C. Oliveira, L. Holman, J. S. van Zweden, C. Romero, C. A. Oi, P. d'Ettorre, M. Khalesi, J. Billen, F. Wackers, J. G. Millar and T. Wenseleers, *Science*, 2014, **343**, 287–290.
86 H. C. Kelstrup, K. Hartfelder, F. S. Nascimento and L. M. Riddiford, *J. Exp. Biol.*, 2014, **217**, 2399–2410.
87 E. Amsalem, J. Kiefer, S. Schulz and A. Hefetz, *J. Chem. Ecol.*, 2014, **40**, 900–912.
88 F. Menzel, J. Orivel, M. Kaltenpoth and T. Schmitt, *Chemoecology*, 2014, **24**, 105–119.
89 W. Bonckaert, F. P. Drijfhout, P. d'Ettorre, J. Billen and T. Wenseleers, *J. Chem. Ecol.*, 2012, **38**, 42–51.

90 A. Sramkova, C. Schulz, R. Twele, W. Francke and M. Ayasse, *Naturwissenschaften*, 2008, **95**, 515–522.
91 H. C. Kelstrup, K. Hartfelder, F. S. Nascimento and L. M. Riddiford, *Front. Zool.*, 2014, **11**, 78.
92 A. A. Smith, B. Holldobler and J. Liebig, *J. Chem. Ecol.*, 2008, **34**, 1275–1282.
93 A. A. Smith, B. Holldober and J. Liebig, *Curr. Biol.*, 2009, **19**, 78–81.
94 A. A. Smith, J. G. Millar, L. M. Hanks and A. V. Suarez, *J. Exp. Biol.*, 2013, **216**, 3917–3924.
95 E. Bunk, A. Sramkova and M. Ayasse, *Chemoecology*, 2010, **20**, 189–198.
96 A. Guthals, J. D. Watrous, P. C. Dorrestein and N. Bandeira, *Mol. BioSyst.*, 2012, **8**, 2535–2544.
97 J. Y. Yang, L. M. Sanchez, C. M. Rath, X. Liu, P. D. Boudreau, N. Bruns, E. Glukhov, A. Wodtke, R. de Felicio, A. Fenner, W. R. Wong, R. G. Linington, L. Zhang, H. M. Debonsi, W. H. Gerwick and P. C. Dorrestein, *J. Nat. Prod.*, 2013, **76**, 1686–1699.
98 J. Watrous, P. Roach, T. Alexandrov, B. S. Heath, J. Y. Yang, R. D. Kersten, M. van der Voort, K. Pogliano, H. Gross, J. M. Raaijmakers, B. S. Moore, J. Laskin, N. Bandeira and P. C. Dorrestein, *Proc. Natl. Acad. Sci. U. S. A.*, 2012, **109**, E1743–E1752.
99 D. D. Nguyen, C.-H. Wu, W. J. Moree, A. Lamsa, M. H. Medema, X. Zhao, R. G. Gavilan, M. Aparicio, L. Atencio, C. Jackson, J. Ballesteros, J. Sanchez, J. D. Watrous, V. V. Phelan, C. van de Wiel, R. D. Kersten, S. Mehnaz, R. De Mot, E. A. Shank, P. Charusanti, H. Nagarajan, B. M. Duggan, B. S. Moore, N. Bandeira, B. Ø. Palsson, K. Pogliano, M. Gutiérrez and P. C. Dorrestein, *Proc. Natl. Acad. Sci. U. S. A.*, 2013, **110**, E2611–E2620.
100 K. A. Aliferis and S. Jabaji, *PLoS One*, 2012, **7**, e42576.
101 F. Jourdan, Metabolomics Coming of Age with Its Technological Diversity, in *Advances in Botanical Res.*, ed. D. Rolin, 2013, vol. 67, pp. 557–591.
102 F. Jourdan, L. Cottret, L. Huc, D. Wildridge, R. Scheltema, A. Hillenweck, M. P. Barrett, D. Zalko, D. G. Watson and L. Debrauwer, *Metabolomics*, 2010, **6**, 312–321.
103 M. Sugimoto, M. Kawakami, M. Robert, T. Soga and M. Tomita, *Curr. Bioinf.*, 2012, **7**, 96–108.
104 W.-T. Liu, A. Lamsa, W. R. Wong, P. D. Boudreau, R. Kersten, Y. Peng, W. J. Moree, B. M. Duggan, B. S. Moore, W. H. Gerwick, R. G. Linington, K. Pogliano and P. C. Dorrestein, *J. Antibiot.*, 2014, **67**, 99–104.
105 P. Shannon, A. Markiel, O. Ozier, N. S. Baliga, J. T. Wang, D. Ramage, N. Amin, B. Schwikowski and T. Ideker, *Genome Res.*, 2003, **13**, 2498–2504.
106 M. E. Smoot, K. Ono, J. Ruscheinski, P. L. Wang and T. Ideker, *Bioinformatics*, 2011, **27**, 431–432.
107 J. R. Winnikoff, E. Glukhov, J. Watrous, P. C. Dorrestein and W. H. Gerwick, *J. Antibiot.*, 2014, **67**, 105–112.
108 R. Mendes, M. Kruijt, I. de Bruijn, E. Dekkers, M. van der Voort, J. H. M. Schneider, Y. M. Piceno, T. Z. DeSantis, G. L. Andersen, P. A. H. M. Bakker and J. M. Raaijmakers, *Science*, 2011, **332**, 1097–1100.
109 W. J. Moree, J. Y. Yang, X. Zhao, W.-T. Liu, M. Aparicio, L. Atencio, J. Ballesteros, J. Sanchez, R. G. Gavilan, M. Gutierrez and P. C. Dorrestein, *J. Chem. Ecol.*, 2013, **39**, 1045–1054.
110 M. F. Traxler, J. D. Watrous, T. Alexandrov, P. C. Dorrestein and R. Kolter, *mBio*, 2013, **4**, e00459-13.
111 K.-C. Tan, S. V. S. Ipcho, R. D. Trengove, R. P. Oliver and P. S. Solomon, *Mol. Plant Pathol.*, 2009, **10**, 703–715.
112 D. Yang, X. Du, Z. Yang, Z. Liang, Z. Guo and Y. Liu, *Eng. Life Sci.*, 2014, **14**, 456–466.
113 K. L. Poulson-Ellestad, C. M. Jones, J. Roy, M. R. Viant, F. M. Fernandez, J. Kubanek and B. L. Nunn, *Proc. Natl. Acad. Sci. U. S. A.*, 2014, **111**, 9009–9014.
114 L. Valledor, M. Escandon, M. Meijon, E. Nukarinen, M. J. Canal and W. Weckwerth, *Plant J.*, 2014, **79**, 173–180.
115 P. Langfelder, B. Zhang and S. Horvath, *Bioinformatics*, 2008, **24**, 719–720.
116 S. Rosenwasser, M. A. Mausz, D. Schatz, U. Sheyn, S. Malitsky, A. Aharoni, E. Weinstock, O. Tzfadia, S. Ben-Dor, E. Feldmesser, G. Pohnert and A. Vardi, *Plant Cell*, 2014, **26**, 2689–2707.
117 M. A. Mausz and G. Pohnert, *J. Plant Physiol.*, 2015, **172**, 137–148.
118 A. Vardi, B. A. S. Van Mooy, H. F. Fredricks, K. J. Popendorf, J. E. Ossolinski, L. Haramaty and K. D. Bidle, *Science*, 2009, **326**, 861–865.
119 E. K. Prince, T. L. Myers and J. Kubanek, *Limnol. Oceanogr.*, 2008, **53**, 531–541.
120 T. J. Tschaplinski, J. M. Plett, N. L. Engle, A. Deveau, K. C. Cushman, M. Z. Martin, M. J. Doktycz, G. A. Tuskan, A. Brun, A. Kohler and F. Martin, *Mol. Plant-Microbe Interact.*, 2014, **27**, 546–556.
121 J. Gulati, I. T. Baldwin and E. Gaquerel, *Plant J.*, 2014, **77**, 880–892.
122 A. Zuccaro, U. Lahrmann and G. Langen, *Curr. Opin. Plant Biol.*, 2014, **20**, 135–145.
123 http://www.genome.jp/kegg/.
124 P. E. Larsen, A. Sreedasyam, G. Trivedi, G. K. Podila, L. J. Cseke and F. R. Collart, *BMC Syst. Biol.*, 2011, **5**, 70.
125 J. Gulati, S. G. Kim, I. T. Baldwin and E. Gaquerel, *Plant Physiol.*, 2013, **162**, 1042–1059.
126 J. Gulati, I. T. Baldwin and E. Gaquerel, *Plant J.*, 2014, **77**, 880–892.
127 W. Weckwerth, *Annu. Rev. Plant Biol.*, 2003, **54**, 669–689.
128 M. Macel, N. M. van Dam and J. J. B. Keurentjes, *Mol. Ecol. Resour.*, 2010, **10**, 583–593.
129 K. Saito and F. Matsuda, *Annu. Rev. Plant Biol.*, 2010, **61**, 463–489.
130 W. Weckwerth, *Anal. Bioanal. Chem.*, 2011, **400**, 1967–1978.
131 O. Fiehn, D. Robertson, J. Griffin, M. van der Werf, B. Nikolau, N. Morrison, L. W. Sumner, R. Goodacre, N. W. Hardy, C. Taylor, J. Fostel, B. Kristal, R. Kaddurah-Daouk, P. Mendes, B. van Ommen, J. C. Lindon and S. A. Sansone, *Metabolomics*, 2007, **3**, 175–178.
132 R. Verpoorte, Y. H. Choi and H. K. Kim, *Phytochem. Anal.*, 2010, **21**, 2–3.
133 W. Weckwerth, *Planta Med.*, 2011, **77**, 1232–1232.

134 H. Meyer, H. Weidmann and M. Lalk, *Microb. Cell Fact.*, 2013, **12**, 13.
135 F. M. Geier, E. J. Want, A. M. Leroi and J. G. Bundy, *Anal. Chem.*, 2011, **83**, 3730–3736.
136 A. D. Hegeman, *Briefings Funct. Genomics*, 2010, **9**, 139–148.
137 P. Bais, S. M. Moon, K. He, R. Leitao, K. Dreher, T. Walk, Y. Sucaet, L. Barkan, G. Wohlgemuth, M. R. Roth, E. S. Wurtele, P. Dixon, O. Fiehn, B. M. Lange, V. Shulaev, L. W. Sumner, R. Welti, B. J. Nikolau, S. Y. Rhee and J. A. Dickerson, *Plant Physiol.*, 2010, **152**, 1807–1816.
138 A. C. Guo, T. Jewison, M. Wilson, Y. F. Liu, C. Knox, Y. Djoumbou, P. Lo, R. Mandal, R. Krishnamurthy and D. S. Wishart, *Nucleic Acids Res.*, 2013, **41**, D625–D630.
139 T. Jewison, C. Knox, V. Neveu, Y. Djoumbou, A. C. Guo, J. Lee, P. Liu, R. Mandal, R. Krishnamurthy, I. Sinelnikov, M. Wilson and D. S. Wishart, *Nucleic Acids Res.*, 2012, **40**, D815–D820.
140 H. Jenkins, N. Hardy, M. Beckmann, J. Draper, A. R. Smith, J. Taylor, O. Fiehn, R. Goodacre, R. J. Bino, R. Hall, J. Kopka, G. A. Lane, B. M. Lange, J. R. Liu, P. Mendes, B. J. Nikolau, S. G. Oliver, N. W. Paton, S. Rhee, U. Roessner-Tunali, K. Saito, J. Smedsgaard, L. W. Sumner, T. Wang, S. Walsh, E. S. Wurtele and D. B. Kell, *Nat. Biotechnol.*, 2004, **22**, 1601–1606.
141 R. J. Bino, R. D. Hall, O. Fiehn, J. Kopka, K. Saito, J. Draper, B. J. Nikolau, P. Mendes, U. Roessner-Tunali, M. H. Beale, R. N. Trethewey, B. M. Lange, E. S. Wurtele and L. W. Sumner, *Trends Plant Sci.*, 2004, **9**, 418–425.
142 C. Steinbeck, P. Conesa, K. Haug, T. Mahendraker, M. Williams, E. Maguire, P. Rocca-Serra, S. A. Sansone, R. M. Salek and J. L. Griffin, *Metabolomics*, 2012, **8**, 757–760.
143 K. Haug, R. M. Salek, P. Conesa, J. Hastings, P. de Matos, M. Rijnbeek, T. Mahendraker, M. Williams, S. Neumann, P. Rocca-Serra, E. Maguire, A. Gonzalez-Beltran, S. A. Sansone, J. L. Griffin and C. Steinbeck, *Nucleic Acids Res.*, 2013, **41**, D781–D786.
144 V. R. Chintapalli, M. Al Bratty, D. Korzekwa, D. G. Watson and J. A. T. Dow, *PLoS One*, 2013, **8**, e78066.
145 H. Meyer, M. Liebeke and M. Lalk, *Anal. Biochem.*, 2010, **401**, 250–259.
146 C. Vidoudez and G. Pohnert, *Metabolomics*, 2012, **8**, 654–669.
147 R. M. Salek, K. Haug, P. Conesa, J. Hastings, M. Williams, T. Mahendraker, E. Maguire, A. N. Gonzalez-Beltran, P. Rocca-Serra, S. A. Sansone and C. Steinbeck, *Database*, 2013, p.bat029.
148 J. Griss, A. R. Jones, T. Sachsenberg, M. Walzer, L. Gatto, J. Hartler, G. G. Thallinger, R. M. Salek, C. Steinbeck, N. Neuhauser, J. Cox, S. Neumann, J. Fan, F. Reisinger, Q. W. Xu, N. del Toro, Y. Perez-Riverol, F. Ghali, N. Bandeira, I. Xenarios, O. Kohlbacher, J. A. Vizcaino and H. Hermjakob, *Mol. Cell. Proteomics*, 2014, **13**, 2765–2775.
149 J. L. Griffin, A. W. Nicholls, C. A. Daykin, S. Heald, H. C. Keun, I. Schuppe-Koistinen, J. R. Griffiths, L. L. Cheng, P. Rocca-Serra, D. V. Rubtsov and D. Robertson, *Metabolomics*, 2007, **3**, 179–188.
150 O. Fiehn, L. W. Sumner, S. Y. Rhee, J. Ward, J. Dickerson, B. M. Lange, G. Lane, U. Roessner, R. Last and B. Nikolau, *Metabolomics*, 2007, **3**, 195–201.
151 M. J. van der Werf, R. Takors, J. Smedsgaard, J. Nielsen, T. Ferenci, J. C. Portais, C. Wittmann, M. Hooks, A. Tomassini, M. Oldiges, J. Fostel and U. Sauer, *Metabolomics*, 2007, **3**, 189–194.
152 N. Morrison, D. Bearden, J. G. Bundy, T. Collette, F. Currie, M. P. Davey, N. S. Haigh, D. Hancock, O. A. H. Jones, S. Rochfort, S. A. Sansone, D. Stys, Q. Teng, D. Field and M. R. Viant, *Metabolomics*, 2007, **3**, 203–210.
153 L. W. Sumner, A. Amberg, D. Barrett, M. H. Beale, R. Beger, C. A. Daykin, T. W. M. Fan, O. Fiehn, R. Goodacre, J. L. Griffin, T. Hankemeier, N. Hardy, J. Harnly, R. Higashi, J. Kopka, A. N. Lane, J. C. Lindon, P. Marriott, A. W. Nicholls, M. D. Reily, J. J. Thaden and M. R. Viant, *Metabolomics*, 2007, **3**, 211–221.
154 R. Goodacre, D. Broadhurst, A. K. Smilde, B. S. Kristal, J. D. Baker, R. Beger, C. Bessant, S. Connor, G. Calmani, A. Craig, T. Ebbels, D. B. Kell, C. Manetti, J. Newton, G. Paternostro, R. Somorjai, M. Sjostrom, J. Trygg and F. Wulfert, *Metabolomics*, 2007, **3**, 231–241.
155 N. W. Hardy and C. F. Taylor, *Metabolomics*, 2007, **3**, 243–248.
156 S. A. Sansone, D. Schober, H. J. Atherton, O. Fiehn, H. Jenkins, P. Rocca-Serra, D. V. Rubtsov, I. Spasic, L. Soldatova, C. Taylor, A. Tseng and M. R. Viant, *Metabolomics*, 2007, **3**, 249–256.
157 R. M. Salek, K. Haug and C. Steinbeck, *Gigascience*, 2013, **2**, 8.
158 A. L. Lane, L. Nyadong, A. S. Galhena, T. L. Shearer, E. P. Stout, R. M. Parry, M. Kwasnik, M. D. Wang, M. E. Hay, F. M. Fernandez and J. Kubanek, *Proc. Natl. Acad. Sci. U. S. A.*, 2009, **106**, 7314–7319.
159 K. Grosser, L. Zedler, M. Schmitt, B. Dietzek, J. Popp and G. Pohnert, *Biofouling*, 2012, **28**, 687–696.
160 D. Holscher, S. Dhakshinamoorthy, T. Alexandrov, M. Becker, T. Bretschneider, A. Buerkert, A. C. Crecelius, D. De Waele, A. Elsen, D. G. Heckel, H. Heklau, C. Hertweck, M. Kai, K. Knop, C. Krafft, R. K. Maddula, C. Matthaus, J. Popp, B. Schneider, U. S. Schubert, R. A. Sikora, A. Svatos and R. L. Swennen, *Proc. Natl. Acad. Sci. U. S. A.*, 2014, **111**, 105–110.
161 F. Kaftan, V. Vrkoslav, P. Kynast, P. Kulkarni, S. Bocker, J. Cvacka, M. Knaden and A. Svatos, *J. Mass Spectrom.*, 2014, **49**, 223–232.
162 A. Svatos, *Anal. Chem.*, 2011, **83**, 5037–5044.
163 C.-J. Shih, P.-Y. Chen, C.-C. Liaw, Y.-M. Lai and Y.-L. Yang, *Nat. Prod. Rep.*, 2014, **31**, 739–755.
164 B. B. Misra, S. M. Assmann and S. Chen, *Trends Plant Sci.*, 2014, **19**, 637–646.

Publication P2:

"Metabolomics of intra- and extracellular metabolites from micro- and macroalgae using GC-MS and LC-MS"

C. Kuhlisch, G. Califano, T. Wichard, and G. Pohnert

In: *Protocols for Macroalgae Research* (Eds.: B. Charrier, T. Wichard, C.R.E. Reddy), CRC Press, Taylor & Francis Group, ISBN-13: 978-1-4987-9642-2

In Press.

The final version of will be available in March 2018.

chapter eighteen

Metabolomics of intra- and extracellular metabolites from micro- and macroalgae using GC–MS and LC–MS

Constanze Kuhlisch, Gianmaria Califano, Thomas Wichard, and Georg Pohnert

Contents

18.1 Introduction

Metabolomics techniques aim to comprehensively extract, quantify, and evaluate metabolites from a given organism or community and have developed into an indispensable tool in life sciences (Allwood et al. 2011; Aldridge and Rhee 2014) (for more information, refer to a recent special issue in *Current Opinion in Chemical Biology*) (Schroeder and Pohnert 2017). Different approaches have been brought forward that allow us to answer a multitude of questions about the physiology of an organism and to generate new hypotheses about its response to stress (Goulitquer et al. 2012; Krug and Müller 2014). Among others, metabolomics allows us to map changes in primary metabolism that reflect the regulation of biochemical pathways to categorize samples by using metabolic fingerprinting techniques or to identify metabolites that are regulated in stress or interaction situations by comparative metabolic profiling. Especially, comparative metabolomics is suitable for the generation of hypotheses about the role of primary and secondary metabolites (Lee and Fiehn 2008; Kuhlisch and Pohnert 2015). Most commonly, mass spectrometric techniques are used for the recording of metabolomics data. With complex samples, mass spectrometry (MS) can be coupled to efficient separation techniques such as ultra performance liquid chromatography (UPLC) and gas chromatography (GC). By using such hyphenated analytical techniques, the profiling of hundreds of metabolites within minutes is feasible. Fundamental prerequirements for successful metabolomics investigations are the experiment planning, sample preparation, extraction, data recording, and the statistical evaluation of the results. In this contribution, we describe a very robust and validated protocol for the generation of metabolic data from marine organisms. Initially developed for the investigation of the diatom *Skeletonema marinoi*, the protocol was successfully adapted to the investigation of different algal taxa (Nylund et al. 2011; Vidoudez and Pohnert 2012; Mausz and Pohnert 2015), including flagellated gametes and thalli of the green macroalga *Ulva mutabilis* and water samples for exometabolomic profiling (Alsufyani et al. 2017). Even profiling of entire plankton communities is feasible without the need for further alterations (Kuhlisch et al. submitted), and it can be predicted that only minor adaptations to the protocol are required to make it suitable for a broad range of other (marine) organisms. By introducing a few additional experimental steps, the method that was initially developed for the investigation of the endometabolome (i.e., the intracellular metabolites) can also be used to monitor the exometabolome (i.e., the metabolites released into the surrounding seawater; see Barofsky et al. 2009 and Alsufyani et al. 2017). For high-quality

metabolomics, the sample preparation and handling are decisive, and we thus place here attention to fully document and describe the workflow. We also introduce one selected workflow for data analysis of comparative metabolomics datasets.

18.2 State of the art

In the past, qualitative and quantitative metabolite investigations were conducted by targeted chemical analyses of certain metabolites or metabolite classes (Gravot et al. 2010; Dittami et al. 2011). However, along with the improvement of hyphenated analytical techniques, the simultaneous and untargeted metabolic profiling of a broader range of substance classes including amino acids, organic acids, sugars, and fatty acids became feasible as reviewed in Dunn (2008). Complex biological extracts are thereby separated by, for example, GC, LC, or capillary electrophoresis, followed by their subsequent analysis using MS. Various available mass analyzers such as quadrupole, time of flight (TOF), and the Orbitrap provide a range of instruments with variable sensitivity, mass resolution, and mass accuracy. Besides LC–MS, one of the most common analytical platforms for metabolic profiling is GC–MS because of its high chromatographic resolution, sensitivity, and availability of reference libraries (Dunn 2008). Many experimental steps for GC–MS metabolic profiling were established in terrestrial plants and transferred to mammals and microbes (Fiehn 2008). Thus, the first protocols in plant sciences included plant specific protocols for enzyme quenching by liquid nitrogen, cell homogenization, and metabolite extraction in hot methanol before the separation of polar metabolites, evaporation for derivatization, GC–MS analysis, data processing, and statistical analysis. A two-step derivatization with optimized methoxylation conditions and *N*-methyl-*N*-trimethylsilyl-trifluoroacetamide (MSTFA) as silylation reagent was introduced, and DB-5ms columns were recommended for separation (Fiehn et al. 2000a, b; Roessner et al. 2000). Isotopically labeled primary metabolites (Fiehn et al. 2000a) and the polyol ribitol (Roessner et al. 2000) were introduced as internal standards (ISs) for semiquantitative metabolite analysis. In the following, several steps of the initial protocols were improved (Lisec et al. 2006) or adjusted to the needs of other study systems (Winder et al. 2008), especially for particularly error-prone steps such as metabolic quenching (Álvarez-Sánchez et al. 2010), or cell extraction, for which a one-phase-solvent mixture was proposed by Gullberg et al. (2004), who also sorted out the effect of oximation time and temperature during derivatization. Later, GC–TOF–MS systems came in focus,

which offer faster scan times compared with quadrupole-MS (Wagner et al. 2003). Furthermore, data processing and analysis strategies were evaluated, for example, handling of multiple derivatization products (Kanani and Klapa 2007), appropriate data-scaling methods (van den Berg et al. 2006), or the choice of uni- and multivariate statistical analyses (Saccenti et al. 2014).

Within the field of marine sciences, metabolomics approaches are still at their advent (Goulitquer et al. 2012). Metabolic profiling of microalgae was first established for the freshwater microalga *Chlamydomonas reinhardtii* (Bölling and Fiehn 2005), followed by the introduction of protocols for the investigation of the marine diatoms *Phaeodactylum tricornutum* (Allen et al. 2008), *Skeletonema marinoi* (Vidoudez and Pohnert 2012), and *Thalassiosira pseudonana* (Bromke et al. 2013). With *Gracilaria vermiculophylla* and *Gracilaria chilensis* (Nylund et al. 2011; Weinberger et al. 2011), the first marine macroalgae were profiled followed by the brown algae *Ectocarpus siliculosus*, *Laminaria digitata*, and *Lessonia spicata* (Ritter et al. 2014; Ritter et al. 2017). Some efforts have already been made to adjust experimental procedures to the needs of macroalgae. Thus, the robust cell wall structures were extracted after flash freezing in liquid nitrogen and thorough grinding with mortar and pestle. Prior to this, epibionts were removed gently if thalli were collected in the field. A challenge that has not been addressed thus far is the high morphological and chemical diversity of the diverse macroalgal taxa and life-cycle stages.

In contrast to the profiling of endometabolites of marine algae, rather few investigations exist, which cover exometabolites (Barofsky et al. 2009; Gillard et al. 2013; Becker et al. 2014; Longnecker et al. 2015). The methodology in this field is currently developing as reviewed in Minor et al. (2014). Main challenges are the separation of cells and surrounding medium without cell leakage and the extraction of dissolved metabolites. Thus, cells should be removed, for example, by gentle filtration over sand or GF/C filters (Barofsky et al. 2009; Alsufyani et al. 2017). The most common extraction method for dissolved metabolites in seawater is solid-phase extraction (SPE) as it is fast, simple, and removes the salt load of marine samples that would otherwise interfere with subsequent analytical processes. Metabolite coverage depends both on the choice of the SPE cartridge adsorbent and eluting solvents. Styrene divinylbenzene phases showed highest recoveries thus far, and we propose CHROMABOND® Easy cartridges due to their high recovery of m/z-retention time pairs (Barofsky et al. 2009).

In the following protocol, we focus on sample generation for GC–MS analysis in addition to LC–MS and give a brief overview of processes

in data treatment. Different sampling and extraction strategies for the diverse macroalgal life stages are presented. We also introduce a protocol for profiling the exometabolome of micro- and macroalgae.

18.3 Materials

18.3.1 Solvents

- Acetone (certified ACS, Fisher Chemical)
- Chloroform (for HPLC, HiPerSolv CHROMANORM® [≥99.8%, filtered through 0.2 µm, packed under N_2, stabilized with 0.6% ethanol], VWR)
- Ethanol (gradient grade for LC, LiChrosolv®; ≥99.9%, filtered through 0.2 µm, Merck)
- Hexane (for GC, SupraSolv® [≥98%], Merck; stored over 4 Å molecular sieve)
- Methanol (for HPLC, Chromasolv®Plus [≥99.9%], Sigma-Aldrich)
- Pyridine (for HPLC, Chromasolv®Plus [≥99.9%], Sigma-Aldrich; stored over 4 Å molecular sieve under argon)
- Tetrahydrofuran (THF; for HPLC, HiPerSolv CHROMANORM® [≥99.7%, filtered through 0.2 µm, packed under N_2, not stabilized], VWR; stored under argon)
- Water (for HPLC, Chromasolv®Plus [filtered through 0.2 µm], Sigma-Aldrich)
- Extraction solution (see Table 18.1 in Section 18.3.4)
- Column elution solution (see Table 18.2 in Section 18.3.4)
- Internal standard (IS) solution (see Table 18.3 in Section 18.3.4)
- Methoxyamine hydrochloride (98%, Sigma-Aldrich; hygroscopic and thus stored in a desiccator under argon and vacuum-dried before use)
- Retention time index (RI) solution (see Table 18.4 in Section 18.3.4)
- MSTFA (1 mL vials, Macherey–Nagel)

18.3.2 Equipment

- Fume hood
- Lab coat
- Safety goggles
- Chemical-resistant gloves (nitril or latex, dependent on solvent)
- Eppendorf® pipettes (1000, 100, and 10 µL, recently checked and calibrated)

- Filtration pump system with vacuum control and Nalgene® tubing (Figure 18.1)
- DURAN® filtering flasks (1 L, KECK™ assembly, Erlenmeyer shape) with rubber seals (Figure 18.1)
- DURAN® dismountable filter holders (ø 50 mm, 250 mL top manifold, sintered filter discs [Porosity 4], FKM seals, PP outlet funnel) (Figure 18.1a)
- Tweezers
- 25 mL glass beaker
- TissueLyser II (QIAGEN, max. speed: 30 frequencies s^{-1})
- Lyophilizer
- Polytetrafluoroethylene (PTFE) tubing (ø 0.8 mm, each ~30 cm) (Figure 18.1b)
- Vortex mixer
- Ultrasonic bath
- Centrifuge (with temperature control, up to 30,000 × g)
- Vacuum evaporation facility (desiccator) and vacuum diaphragm pump (down to 7 mbar, with vacuum control, connected to argon)
- Precision balance (±0.1 mg)

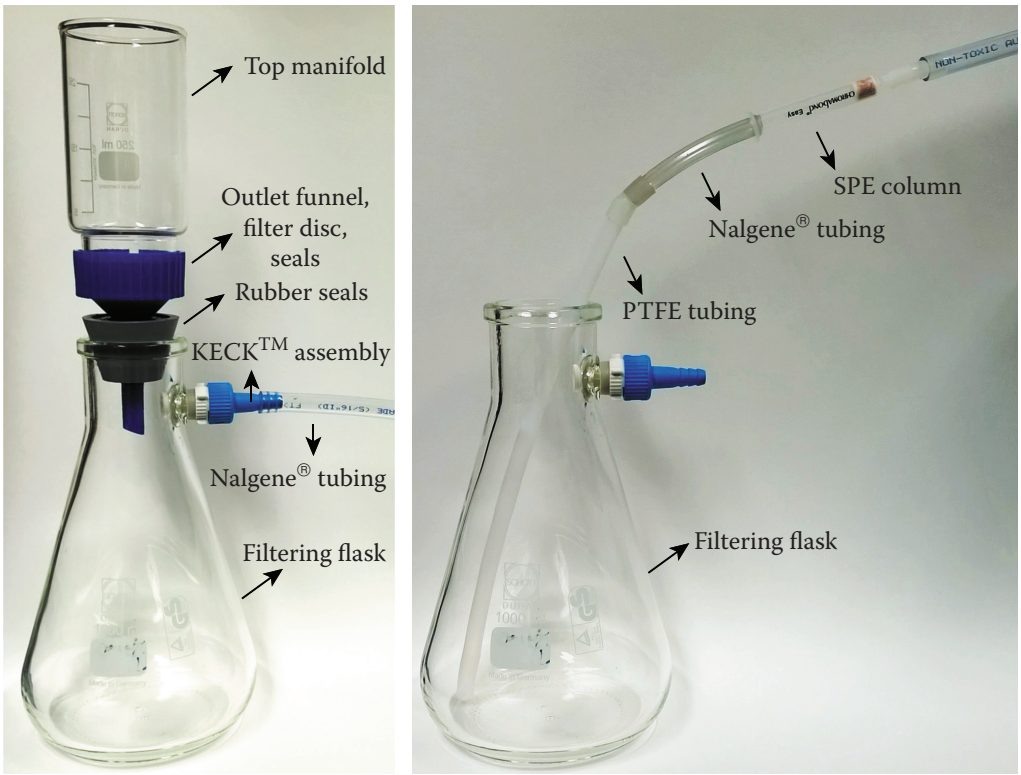

Figure 18.1 Setup of filtration system (a) and filtrate extraction system (b).

- Hamilton® glass syringes (100 µL)
- Heating block (for 1.5 mL vials)

18.3.3 Consumables

- Eppendorf® pipette tips (blue, yellow, and white)
- Eppendorf® centrifuge tubes (1.5 mL, 2 mL)
- Whatman® glass microfiber filters (ø 47 mm, grade GF/C)
- SPE columns CHROMABOND® Easy (3 mL, 200 mg, Macherey–Nagel)
- Metal beads (ø 3 mm, stainless steel)
- Centrifuge tubes (15 mL)
- Glass screw neck vials both 1.5 and 4 mL, the 1.5 mL vials have to fit GC–MS or LC–MS autosamplers
- Glass inserts for 1.5 mL vials (200 µL) with metal springs compatible with autosamplers
- Screw caps for 1.5 and 4 mL vials with septa (PTFE coated)
- Liquid nitrogen

18.3.4 Solution recipes

The following solutions have to be prepared in advance (Tables 18.1 through 18.4):

Table 18.1 Extraction solution

Composition	Final ratio (v:v:v)	Quantity to add (for 10 mL final solution)
Methanol	1	2 mL
Ethanol	3	6 mL
Chloroform	1	2 mL

Note: Prepare daily and precool at −20°C before use. During cell sampling, store on ice to ensure an ice-cold solution for extraction. The composition is optimized for diatom cells (*Skeletonema marinoi*) and was suitable for the extraction of other marine organisms but can be adjusted to ensure optimal metabolite extraction if using organisms with specific mechanical or chemical properties.

Table 18.2 Column elution solution

Composition	Final ratio (v:v:v)	Quantity to add (for 20 mL final solution)
Methanol	1	10 mL
THF	1	10 mL

Note: Store in inert containers (ideally glass sealed with PTFE caps). The composition can be adjusted to ensure optimal elution of the SPE column.

Table 18.3 Internal standard (IS) solution

Composition	Final concentration	Quantity to add (for 1 mL final solution)
Ribitol or $^{13}C_6$-sorbitol	4 mM	100 µL of stock solution at 40 mM
Water	–	900 µL

Note: Prepare a 40 mM stock solution by dissolving 24.9 mg ribitol (>99%, Sigma-Aldrich) in water. Store stock and working solution at −20°C in inert containers (ideally glass sealed with PTFE caps). Thaw before use. The polyol ribitol serves as IS in this protocol as it has not been reported from marine algae thus far. However, it has been shown in bacteria, fungi, plants, and green microalgae (Bieleski 1982). Here, isotopically labeled ISs are recommended such as $^{13}C_6$-sorbitol (Bölling and Fiehn 2005). Both the final concentration and composition of the IS can be adjusted with regard to the experiment.

Table 18.4 Retention time index (RI) solution

Composition	Final concentration	Quantity to add (for 1 mL final solution)
Decane, $C_{10}H_{22}$	1 mM	10 µL of stock solution at 100 mM
Pentadecane, $C_{15}H_{32}$	1 mM	10 µL of stock solution at 100 mM
Nonadecane, $C_{19}H_{40}$	1 mM	10 µL of stock solution at 100 mM
Docosane, $C_{22}H_{46}$	1 mM	10 µL of stock solution at 100 mM
Octacosane, $C_{28}H_{58}$	1 mM	100 µL of stock solution at 10 mM
Dotriacontane, $C_{32}H_{66}$	1 mM	100 µL of stock solution at 10 mM
Hexatriacontane, $C_{36}H_{74}$	0.5 mM	100 µL of stock solution at 5 mM
Hexane	–	660 µL

Note: Prepare stock solutions for *n*-alkanes from C_{10} to C_{36} (all >99%, Sigma-Aldrich) in hexane. Stock and working solutions are stored at −20°C and thawed before use. The *RI solution* is used to calculate system-independent retention times, which is, for example, necessary for comparison with externally measured reference compounds and thus metabolite identification. Final concentration and composition can be adjusted with regard to the experiment.

18.3.5 *Instrumental setup*

Common GC–MS (and LC–MS) instruments can be used. The described procedure can be easily adjusted to the available instrumentation.

GC–MS instrument: Agilent 6890N gas chromatograph, equipped with Agilent 7683B autosampler, coupled to Waters® Micromass GCT Premier™ mass spectrometer (orthogonal acceleration time-of-flight MS).

Injection parameters: 1 µL injection volume, split/splitless injector at 300°C, splitless to split 10 mode (can be adapted to sample and instrument properties), deactivated Agilent split liner (4 × 6.3 × 78.5 mm inner ø × outer ø × length) with glass wool.

GC parameters: Constant helium (5.0) flow at 1 mL min^{-1}, AGILENT J&W DB-5ms column (30 m, 0.25 mm internal diameter, 0.25 µm film thickness, 10 m Duraguard precolumn), oven temperature program: 60°C for 1 min, ramp to 310°C at 15°C min^{-1}, 310°C for 10 min.

MS parameters: Electron impact source (70 eV) at 300°C, scan rate of 5 scans s^{-1}, dynamic range extension mode, resolution of >6000 at m/z 501.97.

18.4 Experimental procedures

In the following section, all steps from sampling to statistical analysis are described in detail (Figure 18.2). Preceding steps such as the design of the experimental setup are not in focus of this protocol. It is, however,

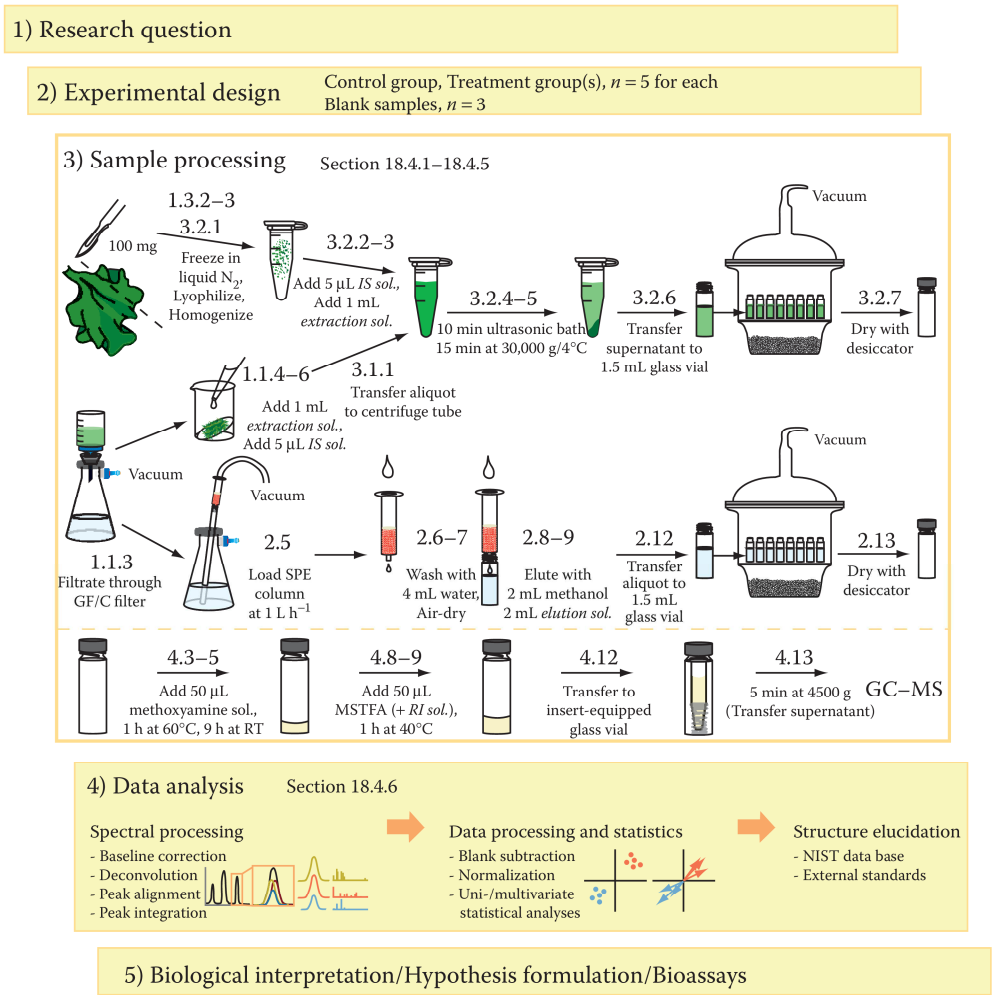

Figure 18.2 Metabolomics workflow for the analysis of intra- and extracellular metabolites of micro- and macroalgae by GC–MS. All numbers refer to steps within the protocol.

recommended to set up at least five biological replicates. Further, the sampling of blanks that should undergo identical treatment as the biological samples is essential for the later identification of contaminants.

18.4.1 Sampling and metabolic quenching

The presented protocol was originally developed for metabolite profiling of phytoplankton samples. Therefore, this section describes several strategies for collecting algal biomass depending on its origin, including a sampling of single-celled microalgae (Section 18.4.1.1), of single-cell stages of macroalgae (Section 18.4.1.2), and of the whole thalli (Section 18.4.1.3). As metabolites underlie diurnal fluctuations, the sampling time should be identical for all replicates. Until metabolic *quenching* (arresting the metabolic activity), all steps have to be conducted as rapidly as possible to prevent metabolic alterations.

18.4.1.1 Filtration of planktonic single-celled algae

- Gently shake the culture to homogeneously distribute the cells.
- Collect aliquots for cell counting (*Note 1*), bioassays, or collection of other metadata if needed.
- Filter a determined culture volume (*Note 2*) under reduced pressure (~600 mbar) through a GF/C filter. The filter should not run dry. Keep the filtrate at 4°C until SPE (see Section 18.4.2.).
- Immediately transfer the wet filter to a 25 mL glass beaker.
- Immediately quench the metabolism by quickly resuspending the cells in 1 mL cold (−10°C) extraction solution. Therefore, rinse cells as far as possible off the filter by repeatedly pipetting the *extraction solution* over the filter. Transfer the suspension into a 1.5 mL centrifuge tube.
- Add 5 µL *IS solution* and vortex 10 s.
- Store the sample on ice.
- Repeat steps 3–7 for all replicates. Continue with step 4 in Section 18.4.1.3.

18.4.1.2 Collection of algal gametes (of Ulva *spp.)*

- Once gametes swarm out of the gametangium, they gather toward the light. Collect, count, and transfer a volume equivalent to 5×10^6 gametes into 2 mL centrifuge tubes as described in Chapter 9 by Califano and Wichard (2018).
- *Optional*: Free swimming gametes can be sampled by centrifugation (*Note 3*).

- Once the gametes are attached to the 2 mL centrifuge tube wall or are pelleted after centrifugation, remove the growth medium with a pipette, and immediately freeze the sample in liquid nitrogen. Because of the low recovery rate of entire cells from surfaces, the tube in which the gametes were grown should also be used for extraction. Continue with step 4 in Section 18.4.1.3.

18.4.1.3 Collection of algal thalli

- Gently clean the thalli. First, scrape off epiphytes with a scalpel and then wash three times with autoclaved (filtered) seawater.
- Collect about 100 mg fresh weight of a specific tissue (e.g., blade tissue or rhizoid, cut with a scalpel) in a 2 mL centrifuge tube and immediately freeze in liquid nitrogen.
- Remove remaining water by lyophilization at 0.001 mbar at –50°C until completely dry.
- *Optional*: Samples can be stored at –20°C for a few days and –80°C for several weeks.
- Samples are ready for extraction (see Section 18.4.3.).

18.4.2 Solid-phase extraction of extracellular metabolites

The extraction of extracellular metabolites from the filtrates can be done in parallel for all replicates. Therefore, randomize the samples.

- Condition a CHROMABOND® Easy column directly before use. Therefore, pipette 4 mL methanol onto the column and let it flow by gravity into a waste vial.
- Wash the column with 4 mL water. Let it flow by gravity into a waste vial.
- Take out all filtrates from the fridge (step 3 in Section 18.4.1.1) and place them on ice.
- Connect the PTFE tube in line with the column. Place the PTFE tube into the filtration flask containing the filtrate and connect the column with the vacuum system.
- Pass the sample slowly through the column at a flow rate of ~1 L h^{-1}.
- Disconnect the column from the PTFE tube and wash the column with 4 mL water.
- Air-dry the column with the vacuum system. Dry column adsorbent is bright red again.
- Elute the column by gravity with 2 mL methanol into a 4 mL glass vial.

- Elute in the second step with 2 mL column elution solution into the same vial.
- Add 5 µL IS solution, close the vial, and vortex for 10 s.
- *Optional:* Samples can be stored at –20°C for a few days and at –80°C for several weeks.
- Transfer for each sample an aliquot of 1.5 mL into a 1.5 mL glass vial. For LC–MS see *Note 4.*
- Evaporate to dryness under vacuum using a desiccator (*Note 5*). Reduce the pressure from ambient pressure to 0 mbar considering solvent boiling points (*Note 6*).
- Vent the desiccator slowly with dry air or argon (*Note 7*) and immediately close all vials.
- Samples are ready for derivatization (see Section 18.4.4.).

18.4.3 Extraction of intracellular metabolites

The extraction of intracellular metabolites can be carried out in parallel for all replicates. Therefore, randomize the samples. Depending on the cell-wall morphology of the studied organism, different cell disruption methods might be suitable of which two are described in this section.

- *Optional*: Thaw samples from step 4 in Section 18.4.1.3 (or directly use samples from step 5 in Section 18.4.1.3).

18.4.3.1 Cell disruption by ultrasound treatment

- Vortex the samples for 30 s. Transfer an aliquot equivalent to ~5×10^7 cells into a new 1.5 mL centrifuge tube (*Note 2*).
- Add extraction solution to reach an adequate cell-to-solvent ratio that is ideally equivalent to a cell density of ~5×10^5 cells μL^{-1} solvent. Continue with step 4 in Section 18.4.3.2.

18.4.3.2 Cell disruption with a bead mill

- Place the centrifuge tubes in a precooled (–80°C) TissueLyser II tube support. Add two metal beads per tube, close again, and disrupt the cells using the TissueLyser II for 30 s at a frequency of 30 s^{-1} (*Note 8*). During this procedure, the sample will remain frozen.
- Add 5 µL IS solution.
- Add 1 mL extraction solution to each sample and vortex vigorously to homogenize the sample and allow a more uniform extraction.
- Place the samples for 10 min into an ultrasonic bath.
- Centrifuge the samples at 30,000 × g for 15 min at 4°C.
- Transfer the debris-free supernatants into 1.5 mL glass vials. For LC–MS analysis see *Note 4*.

- Evaporate to dryness under vacuum using a desiccator (*Note 5*). Reduce the pressure from ambient pressure to a 0 mbar setting considering solvent boiling points (*Note 6*).
- *Optional*: Traces of salt from the medium will precipitate as crystals that restrain water molecules. Thus, keep the pressure setting at 0 mbar for an additional hour to ensure an entirely dry sample.
- Vent the desiccator slowly with dry air or argon (*Note 7*) and immediately close all vials.
- Samples are ready for derivatization (see Section 18.4.4.).

18.4.4 Two-step-derivatization for GC–MS analysis

To analyze a broad range of metabolites by GC–MS, the volatility and thermostability of some substances classes need to be enhanced by derivatization. In a first step, ketones and aldehydes are derivatized to oximes, and then functional groups such as –OH, $-NH_2$, –SH, or –COOH as present in, for example, sugars, fatty acids, or amino acids are chemically derivatized by silylation. Directly use the dried samples from step 15 in Section 18.4.2 or step 10 in Section 18.4.3.2.

- Prepare the methoxyamine solution immediately before derivatization. Weigh 20 mg dried methoxyamine hydrochloride in a 1.5 mL glass vial.
- Add 1 mL pyridine, close the vial, and ensure complete dissolution by sonication in an ultrasonic bath for at least 5 min.
- Pipette 50 µL methoxyamine solution to each sample (a maximum of 20 samples is recommended, *Note 9*, and immediately close the vials. Vortex 60 s to redissolve the extract.
- Incubate at 60°C for 1 h.
- Subsequently incubate at room temperature for 9 h (up to 16 h, *Note 10*).
- Prepare the silylation solution. Therefore, remove a new vial of MSTFA from the fridge, and let it warm up to room temperature. Thaw and vortex the RI solution.
- Add with a glass syringe 40 µL RI solution to 1 mL MSTFA and vortex the vial. Rinse the syringe with hexane after use.
- Add with a glass syringe 50 µL silylation solution to each sample. Prevent any cross-contamination between samples. Rinse the syringe with acetone after use.
- Incubate at 40°C for 1 h (*Note 11*).
- Let the samples cool down to room temperature.
- *Optional*: In the case of condensation along the glass, briefly centrifuge the vials (~5 s).
- Transfer each sample into a glass insert and close the vial.

- Centrifuge all samples at 8000 × g for 5 min using 15 mL centrifuge tubes padded with a cloth as vial mounting. In the case of precipitate formation, transfer the supernatant into a new glass insert.
- Analyze the batch of samples immediately (*Note 9*) by GC–MS (see Section 18.4.5.).

18.4.5 GC–MS analysis

- Directly use the derivatized samples from step 24 in Section 18.4.4.
- Analyze each batch of samples in a random order to diminish, for example, a potential systematic effect of increasing time delay between silylation and injection. For analysis details, see the *Instrumental setup*.
- Run air injections before, in between, and after each batch to check for contaminations.
- Use a new glass liner every 21 injections or if air injections indicate contamination.
- For data analysis see Section 18.4.6.

18.4.6 Data analysis for GC–MS data

In the following protocol, a canonical analysis of principal coordinates (CAP, Anderson and Willis 2003) is used to investigate metabolic alterations. In comparison with other common multivariate statistical analyses, CAP is less sensitive to hidden correlations within the dataset (McCune et al. 2002), which are a direct result from metabolites generating multiple peaks, for example, due to different levels of derivatization. Alternatively, a range of online platforms is available offering different data processing and analysis strategies. These include MetaboAnalyst (Xia et al. 2009; see Figure 18.3e), XCMS Online (Tautenhahn et al. 2012; see Figure 18.3d), and Workflow4Metabolomics (Giacomoni et al. 2015). The following workflow is also applicable to LC–MS data after adaptation of the peak detection procedure (Alsufyani et al. 2017).

- Conduct a background-noise correction for each chromatogram using, for example, the CODA tool of MassLynx 4.1 (Waters, MCQ = 0.8, Smoothing window = 5).
- Convert the raw data files into NetCDF (.cdf), for example, by using the Databridge tool of MassLynx 4.1.
- Deconvolute all chromatograms with AMDIS 2.71 (nist, http://chemdata.nist.gov/, 2012) with the following parameters: minimum match factor = 30, type of analysis = simple, low/high m/z = auto,

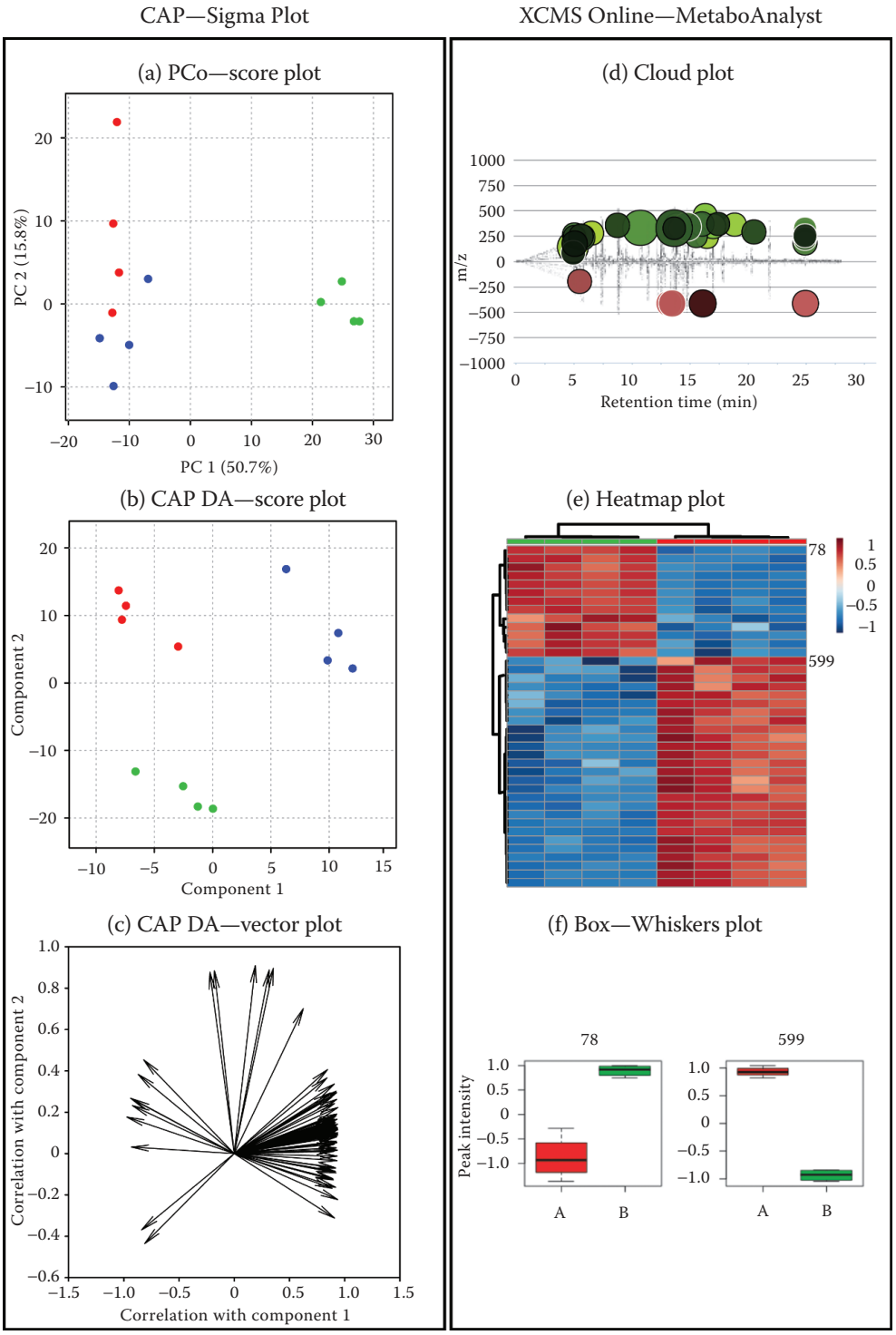

Figure 18.3 Statistical data analysis approaches for untargeted metabolomics datasets. A combination of unsupervised (a) and supervised (b, c) multivariate analyses with univariate analyses (d) is recommended. Selected metabolites of interest can be further described with heat maps (e) or box plots (f). (*Continued*)

***Figure 18.3* (Continued)** All plots were generated from a dataset that was obtained by GC–MS analysis of the macroalga *Ulva mutabilis* with either two (a–c) or three (d–f) treatment groups (n = 4). Score plots of (a) principal coordinate analysis and (b) CAP show the separation of sample groups. The vector plot of the CAP (c) and the *t*-test-based cloud plot (d, from XCMS Online) indicate characteristic metabolites. These selected metabolites can be visualized semiquantitatively with a heat map (e, from MetaboAnalyst) or box plots (f, from XCMS Online).

instrument type = quadrupole, component width = 32, omitted m/z = 147, 176, 193, 207, adjacent peak subtraction = 2, resolution = low, sensitivity = medium, shape requirement = low, column bleed = 207. Run one batch job each for extra- and intracellular samples.

- Integrate the deconvoluted peaks with MET-IDEA 2.08 (http://bioinfo.noble.org, 2012). Select the chromatogram with the highest number of deconvoluted components as ion file and the following parameters for peak integration: chromatography = GC, average peak width = 0.08, minimum peak width = 0.5, maximum peak width = 2, peak start/stop slope = 1.5, adjusted retention time accuracy = 0.25, peak overload factor = 0.9, MS = TOF, mass accuracy = 0.1, mass range = 0.3, lower mass limit = 100, ion per component = 1, exclude ion list = 73, 147, 281, 341, 415. In the output file, the peak area of each variable as described by model ion (m/z) and retention time (min) is listed for each sample.
- Import the peak area file in Excel (Microsoft® Office, 2010). For each variable, subtract the median area of all blanks from each sample. Remove variables with a resulting negative peak area.
- Normalize the data. Divide each peak area by the peak area of the IS of the same sample. For intracellular metabolites, normalize to extracted biomass (e.g., fresh weight) as well. For extracellular metabolites, normalize to the sum of all peak areas within one sample.
- Export the dataset as a text file for further statistical analysis. Sample and variable descriptors have to be omitted.
- Perform a CAP with CAP12 (Anderson and Willis 2003, http://www.esapubs.org/archive/ecol/E084/011/suppl-1.htm) by using the following parameters: transformation = none, standardization = none, distance measure = Bray–Curtis dissimilarity, discriminant analysis mode, number of principal coordinates axes chosen by the program, 999 random permutations test.
- Display the resulting sample coordinates as score plots and the metabolites as loading plot, for example, with SigmaPlot 13.0 (Systat Softwares). Evaluate the principal coordinate analysis score plot (Figure 18.3a) to detect sample outliers. Evaluate the CAP score plot

(Figure 18.3b) for correct sample groups. Use the correlation values of the original variables with the CAP axes to generate a vector plot (Figure 18.3c) and select highly correlated variables. Describe these variables by their m/z and t_R values (see Section 18.4.6).

- Compare the mass spectra of all highly correlated variables as extracted by AMDIS (see Section 18.4.6) with spectral libraries using MS Search 2.0 (NIST, http://chemdata.nist.gov/, 2005). A common commercial database is the NIST library. Other, noncommercial alternatives are available which often focus on specific metabolites, for example, the Golm-library for plant metabolites. Document the quality of spectral comparison with the *R*-match value.
- Compare the retention times of all highly correlated variables with externally measured reference compounds by calculating nonlinear retention indices (van den Dool and Kratz 1963). Follow Fiehn et al. (2008) for metabolomics standards initiative-compliant identification.

18.5 Notes

For a successful untargeted metabolomic approach, the personal security and sample protection against contaminants and chemical reactions with H_2O and O_2 are essential. It is thus recommended to wear personal protective equipment and work under fume hoods whenever necessary. Moreover, read the material safety data sheets (MSDS) of all reagents and follow the recommendations for correct disposal. As biological samples are rather complex, avoid any contamination by humans or lab equipment (e.g., fatty acids, plasticizers). It is thus advisable to wear gloves, use glass or PTFE whenever possible, and rinse lab equipment with solvents before use. For the same reason, blanks should be carried through the whole procedure. As the derivatization is moisture sensitive, all involved chemicals and samples have to be dry, which is especially challenging for salt water samples. Samples should be exposed to air as rarely as possible. Several metabolites are labile. Therefore, work should be carried out without longer interruptions.

Note 1: For subsequent data normalization, it is important to determine the amount of extracted biomass, for example, as cell count or fresh weight. For a quantitative comparison or differential screening, it is best to collect the same biomass among samples wherever possible.

Note 2: The sample volume should provide ~5×10^7 algal cells of a cell volume of ~100 μm^3 as tested for the diatom *Skeletonema marinoi*. With ~12 pg C $cell^{-1}$ (Menden-Deuer and Lessard 2000), this cell number equals ~0.6 mg C. For other organisms, the required cell numbers have to be determined in test runs or indirectly estimated on the basis of the amount of carbon per cell.

Note 3: Alternatively, algal cells can be sampled by centrifugation. Cold solvent quenching before centrifugation is necessary to prevent metabolic alterations during centrifugation (Bölling and Fiehn, 2005).

Note 4: At this stage, the samples can be directly used for LC–MS analysis as described in Barofsky et al. (2009) and Alsufyani et al. (2017) for extracellular extracts and in Barofsky et al. (2010) for cell extracts. Therefore, transfer an aliquot of 100 µL into insert-equipped glass vials and measure in one batch in randomized order.

Note 5: All solvents and water residues have to be evaporated before the derivatization. This can be achieved with a desiccator but also under a flow of nitrogen. Any sample contamination should, however, be prevented.

Note 6: Pressure reduction results similarly to heating in solvent boiling. In a desiccator, however, a boiling delay can occur. To avoid any loss of extract because of this uncontrolled boiling, reduce the pressure stepwise. Select the pressure steps at the boiling points of the different solvents as listed elsewhere.

Note 7: To vent the desiccator with dry air, mount a $CaCO_3$-filled column at the air inflow. Alternatively, argon can be used as shielding gas as it is denser than air and inert.

Note 8: The speed (or the frequency) of the grinding has to guarantee cell-wall disruption in a short period of time (before thawing) and has to be optimized for the respective tissue in test runs.

Note 9: The batch size is limited to maximum 20 samples because of the instability of the silylated samples. If, for example, standing in the autosampler of a GC–MS instrument at room temperature, decomposition would be substantial if more than 20 samples in a row would be measured (Kanani et al. 2008). As one GC–MS run lasts about 30 min, 20 samples can be analyzed within ~10 h. Biological replicates should be randomized within one batch.

Note 10: The oximation depends both on reaction temperature and time. To reduce the decomposition of, for example, sucrose and increase derivatization efficiency, an oximation for 1 h at 60°C and 16 h at room temperature was proposed by Gullberg et al. (2004). However, to be able to work up two batches per day, the latter time is reduced to 9 h without significant losses. With the addition of MSTFA, the oximation reaction is quenched because of silylation of the reactive amine group of methoxyamine.

Note 11: MSTFA is a strong trimethylsilyl group (TMS; $Si[CH_3]_3$) donor, and thus a common silylation reagent. During the silylation reaction, the active hydrogen of functional groups such as –OH, –NH, $–NH_2$ –SH, and –COOH are replaced by a TMS group. As each functional group has different reaction kinetics, a heating time of 1 h compromises silylation efficiency and required reaction times.

Acknowledgments

We gratefully thank Alina Hera for her help in the *Ulva mutabilis* analysis. Furthermore, we acknowledge Franziska Speck for testing protocol comprehensibility in the lab and Kathleen Thume for proofreading the manuscript. The current work was supported by the Jena School of Microbial Communication (CK, TW), by the Collaborative Research Center 1127 "Chemical Mediators in complex Biosystems" and CRC 1067 "AquaDiva" (TW, GP) and by the European Union's Horizon 2020 research and innovation program under the Marie Sklodowska-Curie grant agreement No. 642575 (GC, TW, and GP).

References

Aldridge, B. B., and K. Y. Rhee. 2014. Microbial metabolomics: Innovation, application, insight. *Curr. Opin. Microbiol.* 19:90–96.

Allen, A. E., J. Laroche, U. Maheswari et al. 2008. Whole-cell response of the pennate diatom *Phaeodactylum tricornutum* to iron starvation. *Proc. Nat. Acad. Sci.* 105 (30):10438–10443.

Allwood, J. W., R. C. De Vos, A. Moing et al. 2011. Plant metabolomics and its potential for systems biology research background concepts, technology, and methodology. *Methods Enzymol.* 500:299–336.

Alsufyani, T., A. Weiss, and T. Wichard. 2017. Time course exo-metabolomic profiling in the green marine macroalga *Ulva* (Chlorophyta) for identification of growth phase-dependent biomarkers. *Mar. Drugs* 15 (1):14. doi: 10.3390/md15010014.

Álvarez-Sánchez, B., F. Priego-Capote, and M. D. Luque de Castro. 2010. Metabolomics analysis II. Preparation of biological samples prior to detection. *TrAC, Trends Anal. Chem.* 29 (2):120–127.

Anderson, M. J., and T. J. Willis. 2003. Canonical analysis of principal coordinates: A useful method of constrained ordination for ecology. *Ecology* 84 (2): 511–525.

Barofsky, A., P. Simonelli, C. Vidoudez et al. 2010. Growth phase of the diatom *Skeletonema marinoi* influences the metabolic profile of the cells and the selective feeding of the copepod *Calanus* spp. *J. Plankton Res.* 32 (3):263–272.

Barofsky, A., C. Vidoudez, and G. Pohnert. 2009. Metabolic profiling reveals growth stage variability in diatom exudates. *Limnol. Oceanogr.: Methods* 7:382–390.

Becker, J., P. Berube, C. Follett et al. 2014. Closely related phytoplankton species produce similar suites of dissolved organic matter. *Front. Microbiol.* 5 (111). doi: 10.3389/fmicb.2014.00111.

Bieleski, R. L. 1982. Sugar alcohols. In *Plant Carbohydrates I: Intracellular Carbohydrates*, (Eds.) F. A. Loewus and W. Tanner, pp. 158–192. Berlin, Germany: Springer.

Bölling, C., and O. Fiehn. 2005. Metabolite profiling of *Chlamydomonas reinhardtii* under nutrient deprivation. *Plant Physiol.* 139 (4):1995–2005.

Bromke, M. A., P. Giavalisco, L. Willmitzer, and H. Hesse. 2013. Metabolic analysis of adaptation to short-term changes in culture conditions of the marine diatom *Thalassiosira pseudonana*. *PLoS One* 8 (6):e67340.

Califano, G., and T. Wichard. 2018. Preparation of axenic cultures in *Ulva* (Chlorophyta). In *Protocols for Macroalgae Research*, (Eds.) B. Charrier, T. Wichard, and C.R.K. Reddy, Chapter 9. Boca Raton, FL: CRC Press, Taylor & Francis Group.

Dittami, S. M., A. Gravot, D. Renault et al. 2011. Integrative analysis of metabolite and transcript abundance during the short-term response to saline and oxidative stress in the brown alga *Ectocarpus siliculosus*. *Plant Cell Environ.* 34 (4):629–642.

Dunn, W. B. 2008. Current trends and future requirements for the mass spectrometric investigation of microbial, mammalian and plant metabolomes. *Phys. Biol.* 5 (011001).

Fiehn, O. 2008. Extending the breadth of metabolite profiling by gas chromatography coupled to mass spectrometry. *TrAC-Trend. Anal. Chem.* 27 (3):261–269.

Fiehn, O., J. Kopka, P. Dormann, T. Altmann, R. N. Trethewey, and L. Willmitzer. 2000a. Metabolite profiling for plant functional genomics. *Nat. Biotechnol.* 18 (11):1157–1161.

Fiehn, O., J. Kopka, R. N. Trethewey, and L. Willmitzer. 2000b. Identification of uncommon plant metabolites based on a calculation of elemental compositions using gas chromatography and quadrupole mass spectrometry. *Anal. Chem.* 72 (15):3573–3580.

Fiehn, O., G. Wohlgemuth, M. Scholz et al. 2008. Quality control for plant metabolomics: Reporting MSI-compliant studies. *Plant J.* 53 (4):691–704.

Giacomoni, F., G. Le Corguille, M. Monsoor et al. 2015. Workflow4Metabolomics: A collaborative research infrastructure for computational metabolomics. *Bioinformatics* 31 (9):1493–1495.

Gillard, J., J. Frenkel, V. Devos et al. 2013. Metabolomics enables the structure elucidation of a diatom sex pheromone. *Angew. Chem. Int. Edit.* 52 (3):854–857.

Goulitquer, S., P. Potin, and T. Tonon. 2012. Mass spectrometry-based metabolomics to elucidate functions in marine organisms and ecosystems. *Mar. Drugs* 10 (4):849–880.

Gravot, A., S. M. Dittami, S. Rousvoal et al. 2010. Diurnal oscillations of metabolite abundances and gene analysis provide new insights into central metabolic processes of the brown alga *Ectocarpus siliculosus*. *New Phytol.* 188 (1):98–110.

Gullberg, J., P. Jonsson, A. Nordström, M. Sjöström, and T. Moritz. 2004. Design of experiments: An efficient strategy to identify factors influencing extraction and derivatization of *Arabidopsis thaliana* samples in metabolomic studies with gas chromatography-mass spectrometry. *Anal. Biochem.* 331 (2):283–295.

Kanani, H., P. K. Chrysanthopoulos, and M. I. Klapa. 2008. Standardizing GC-MS metabolomics. *J. Chromatogr. B: Anal. Technol. Biomed. Life Sci.* 871 (2):191–201.

Kanani, H. H., and M. I. Klapa. 2007. Data correction strategy for metabolomics analysis using gas chromatography-mass spectrometry. *Metab. Eng.* 9 (1): 39–51.

Krug, D., and R. Müller. 2014. Secondary metabolomics: The impact of mass spectrometry-based approaches on the discovery and characterization of microbial natural products. *Nat. Prod. Rep.* 31 (6):768–783.

Kuhlisch, C., J. Althammer, A. F. Sazhin, H. H. Jakobsen, J. C. Nejstgaard, and G. Pohnert. Metabolomics-derived marker metabolites to characterize *Phaeocystis pouchetii* in natural plankton communities. submitted.

Kuhlisch, C., and G. Pohnert. 2015. Metabolomics in chemical ecology. *Nat. Prod. Rep.* 32 (7):937–955.

Lee, D. Y., and O. Fiehn. 2008. High quality metabolomic data for *Chlamydomonas reinhardtii*. *Plant Methods* 4. doi: 10.1186/1746-4811-4-7.

Lisec, J., N. Schauer, J. Kopka, L. Willmitzer, and A. R. Fernie. 2006. Gas chromatography mass spectrometry-based metabolite profiling in plants. *Nat. Protocols* 1 (1):387–396.

Longnecker, K., M. C. K. Soule, and E. B. Kujawinski. 2015. Dissolved organic matter produced by *Thalassiosira pseudonana*. *Mar. Chem.* 168:114–123.

Mausz, M. A., and G. Pohnert. 2015. Phenotypic diversity of diploid and haploid *Emiliania huxleyi* cells and of cells in different growth phases revealed by comparative metabolomics. *J. Plant Physiol.* 172:137–148.

McCune, B., J. B. Grace, and D. L. Urban. 2002. *Analysis of Ecological Communities*. 2 ed., Vol. 28. Gleneden Beach, Oregon: MjM software design.

Menden-Deuer, S., and E. J. Lessard. 2000. Carbon to volume relationships for dinoflagellates, diatoms, and other protist plankton. *Limnol. Oceanogr.* 45 (3):569–579.

Minor, E. C., M. M. Swenson, B. M. Mattson, and A. R. Oyler. 2014. Structural characterization of dissolved organic matter: A review of current techniques for isolation and analysis. *Environ. Sci. Process Impacts* 16 (9):2064–2079.

Nylund, G. M., F. Weinberger, M. Rempt, and G. Pohnert. 2011. Metabolomic assessment of induced and activated chemical defence in the invasive red alga *Gracilaria vermiculophylla*. *PLoS One* 6 (12):e29359.

Ritter, A., L. Cabioch, L. Brillet-Guéguen et al. 2017. Herbivore-induced chemical and molecular responses of the kelps *Laminaria digitata* and *Lessonia spicata*. *PLoS One* 12 (3):e0173315.

Ritter, A., S. M. Dittami, S. Goulitquer et al. 2014. Transcriptomic and metabolomic analysis of copper stress acclimation in *Ectocarpus siliculosus* highlights signaling and tolerance mechanisms in brown algae. *BMC Plant Biol.* 14 (1):116.

Roessner, U., C. Wagner, J. Kopka, R. N. Trethewey, and L. Willmitzer. 2000. Technical advance: Simultaneous analysis of metabolites in potato tuber by gas chromatography-mass spectrometry. *Plant J.* 23 (1):131–142.

Saccenti, E., H. C. J. Hoefsloot, A. K. Smilde, J. A. Westerhuis, and M. M. W. B. Hendriks. 2014. Reflections on univariate and multivariate analysis of metabolomics data. *Metabolomics* 10 (3):361–374.

Schroeder, F., and G. Pohnert. 2017. Editorial overview: Omics techniques to map the chemistry of life. *Curr. Opin. Chem. Biol.* 36:v–vi.

Tautenhahn, R., G. J. Patti, D. Rinehart, and G. Siuzdak. 2012. XCMS Online: A web-based platform to process untargeted metabolomic data. *Anal. Chem.* 84 (11):5035–5039.

van den Berg, R. A., H. C. Hoefsloot, J. A. Westerhuis, A. K. Smilde, and M. J. van der Werf. 2006. Centering, scaling, and transformations: Improving the biological information content of metabolomics data. *BMC Genomics* 7:142. doi: 10.1186/1471-2164-7-142.

van den Dool, H., and P. D. Kratz. 1963. A generalization of retention index system including linear temperature programmed gas-liquid partition chromatography. *J. Chromatogr.* 11 (4):463–471.

Vidoudez, C., and G. Pohnert. 2012. Comparative metabolomics of the diatom *Skeletonema marinoi* in different growth phases. *Metabolomics* 8 (4):654–669.

Wagner, C., M. Sefkow, and J. Kopka. 2003. Construction and application of a mass spectral and retention time index database generated from plant GC-EI-TOF-MS metabolite profiles. *Phytochemistry* 62 (6):887–900.

Weinberger, F., U. Lion, L. Delage et al. 2011. Up-regulation of lipoxygenase, phospholipase, and oxylipin-production in the induced chemical defense of the red alga *Gracilaria chilensis* against epiphytes. *J. Chem. Ecol.* 37 (7):677–686.

Winder, C. L., W. B. Dunn, S. Schuler et al. 2008. Global metabolic profiling of *Escherichia coli* cultures: An Evaluation of methods for quenching and extraction of intracellular metabolites. *Anal. Chem.* 80 (8):2939–2948.

Xia, J. G., N. Psychogios, N. Young, and D. S. Wishart. 2009. MetaboAnalyst: A web server for metabolomic data analysis and interpretation. *Nucleic Acids Res.* 37:W652–W660.

Publication P3:

"Metabolomics-derived marker metabolites to characterize *Phaeocystis pouchetii* in natural plankton communities"

C. Kuhlisch, J. Althammer, A. Sazhin, H. H. Jakobsen, J. C. Nejstgaard, and G. Pohnert

Submitted to Harmful Algae.

The supplementary information is available via the Appendix and the embedded compact disc.

Metabolomics-derived marker metabolites to characterize *Phaeocystis pouchetii* in natural plankton communities

Constanze Kuhlisch[a], Julia Althammer[a,1], Andrey F. Sazhin[b], Hans H. Jakobsen[c], Jens C. Nejstgaard[d,2], Georg Pohnert[a *]

[a] Institute for Inorganic and Analytical Chemistry, Friedrich Schiller University Jena, Lessingstraße 8, 07743 Jena, Germany; constanze.kuhlisch@uni-jena.de

[b] P.P. Shirshov Institute of Oceanology, Russian Academy of Sciences, Nakhimovsky Prospect 36, Moscow, Russia; andreysazhin@yandex.ru

[c] Department of Bioscience, Aarhus University, Frederiksborgvej 399, 4000 Roskilde, Denmark; hhja@bios.au.dk

[d] Uni Research Environment, Uni Research AS, Postboks 7810, 5020 Bergen, Norway

* corresponding author, e-mail: georg.pohnert@uni-jena.de, Institute for Inorganic and Analytical Chemistry, Friedrich Schiller University Jena, Lessingstraße 8, 07743 Jena, Germany

[1] Present address: JenaBios GmbH, Löbstedter Straße 80, 07749 Jena, Germany; j.althammer@jenabios.de

[2] Present address: Leibniz-Institute of Freshwater Ecology and Inland Fisheries, Dep. 3, Alte Fischerhütte 2, 16775 Stechlin, Germany; nejstgaard@igb-berlin.de

Abstract

Phaeocystis pouchetii (Hariot) Lagerheim, 1893 regularly dominates phytoplankton blooms in the Arctic. Through grazing by herbivores and microbial activity it is considered to be a key resource for the entire marine food web but the actual relevance of biomass transfer to higher trophic levels is still under discussion. Cell physiology and algal nutritional state are considered to be responsible for the observed variability. However, no data have so far yielded insights into the state of *Phaeocystis* populations that would allow to test this hypothesis. Therefore, metabolic markers of different growth phases were determined in laboratory batch cultures using comparative metabolomics. Metabolites, expressed during exponential, early and late stationary growth of *P. pouchetii* were profiled using gas chromatography-mass spectrometry. Then, intra- and extracellular metabolites were characterized that correlate with the growth phases using multivariate statistical analysis. Within the endometabolome, free amino acids characterized exponential growth, whereas the early stationary phase was correlated with sugar alcohols, mono- and disaccharides. In the late stationary phase free fatty acids, sterols and terpenes increased. Within the exometabolome carboxylic acids were related to exponential growth, whereas adenosine and an indole derivative increased towards late stationary growth phase. These marker metabolites were then traced in *Phaeocystis* blooms during a cruise in the Barents Sea and North Norwegian fjords. About 50 endometabolites of *P. pouchetii* were detected in natural phytoplankton communities. Their relative abundances at *Phaeocystis*-dominated stations differed from diatom-dominated stations. Mannitol, *scyllo*-inositol, octadecan-1-ol, and several free fatty acids were characteristic for *Phaeocystis*-dominated blooms. Distinct metabolic profiles were detected in the nutrient-depleted community in the inner Porsangerfjord (<0.5 µM NO_3^-). High relative amounts of free mono- and disaccharides that are indicators for a limited culture were detected and mapped. This study therefore shows how variable physiology of plankton blooms can alter the metabolic landscape of entire communities.

Keywords

Arctic food web, DOM, POM, biomarker, bloom phase, meta metabolomics

Abbreviations

CAP canonical analysis of principal coordinates
IAA indole-3-acetic acid
IS internal standard
PCO principal coordinate analysis
PSII photosystem II
PUFA polunsaturated fatty acids
RI retention index
S/N signal to noise ratio
TCA tricarboxylic acid

1. Introduction

The marine microalga *Phaeocystis pouchetii* (Hariot) Lagerheim, 1893 is a key phytoplankton species in Arctic and high latitude areas, especially along the Norwegian coast and in the Barents Sea (Degerlund and Eilertsen, 2010). Several single celled stages are known or hypothesized within its life cycle (Rousseau et al., 2007; Whipple et al., 2007), however, most spring blooms are characterized by the colony stage of the alga (Rat'kova and Wassmann, 2002; Wassmann et al., 2005). Colonies develop from dividing single cells excreting a polysaccharide-rich mucus that builds the matrix for up to 600 cells (Verity et al., 2007a; Verity et al., 2007b). These carbohydrate-rich particles (Alderkamp et al., 2006) contribute not only to the microbial loop and vertical flux (Alderkamp et al., 2007; Reigstad and Wassmann, 2007), but also to the marine pelagic food web. Palatability and intake by grazers, nutritional value, and chemical defense strategies have been investigated intensively for decades (Nejstgaard et al. (2007) and references therein). *P. pouchetii* colonies are ingested by various grazers including dinoflagellates, ciliates, copepods, amphipods and fish. Other grazers avoid colonies or select specific colony size ranges. Size selection mechanisms as well as algal bloom phase-dependent biochemical mediation have been suggested (Estep et al., 1990; Hansen et al., 1994). Recent modeling of the Arctic marine ecosystem under climate warming predicted decreasing sea ice coverage and thickness that will influence phytoplankton community composition and biomass contribution (Slagstad et al., 2011; Wassmann and Reigstad, 2011). *P. pouchetii* may expand its distribution and occurrence as already observed locally (Lasternas and Agustí, 2010; Nöthig et al., 2015; Soltwedel et al., 2016). Within this context, the relevance of *P. pouchetii* biomass for trophic transfer in the Arctic food web needs closer investigation.

The role of *P. pouchetii* within the Arctic food web has been investigated under several laboratory, semi-natural and natural conditions with contradicting results (Nejstgaard et al., 2007). Senescent colonies in the East Greenland Current were not substantially grazed (Calbet et al., 2011) in contrast to previous observations (Estep et al., 1990; Huntley et al., 1987; Tande and Båmstedt, 1987). During blooms of *Phaeocystis* in mesocosms in Western Norway colonies were also not efficiently ingested by micro- and mesozooplankton, while single cells were actively grazed by microzooplankton (Nejstgaard et al., 2006; Ray et al., 2016a; Ray et al., 2016b). High rates of microzooplankton grazing on single cells and small colonies may even have even inhibited bloom-formation in North Norwegian fjords (Archer et al., 2000). In a study around Spitsbergen, Fram Strait and the Barents Sea, colonies were actively grazed by mesozooplankton but only ingested at low rates (Norrbin et al., 2009; Saiz et al., 2013). In conclusion, zooplankton grazing and ingestion may rely on *Phaeocystis* bloom phase and colony formation with a possible underlying modulating effect of the metabolite composition of the cells.

Phytoplankton cells do not represent steady-state chemical compartments. Metabolism, nutritional state, and exudate composition are highly plastic parameters that respond to environmental conditions (e.g. light intensity, water temperature, grazing). As shown for laboratory batch cultures of the diatoms *Skeletonema marinoi* and *Thalassiosira pseudonana*, and the haptophyte *Emiliania huxleyi*, the composition and release of metabolites from phytoplankton cells is growth phase-dependent (Barofsky et al., 2010; Barofsky et al., 2009; Mausz and Pohnert, 2015; Vidoudez and Pohnert, 2012). The responsiveness of herbivores to the variable metabolite composition can substantially influence grazing rates and thereby shape predator-prey interactions (Barofsky et al., 2010). Metabolic variability in endo- and exometabolomes is expected, but was never demonstrated in natural phytoplankton communities and could be a determining factor for *P. pouchetii* grazing.

The metabolic investigation of complex natural communities in contrast to defined monoclonal laboratory cultures is termed metametabolomics. Only a few studies exist that applied untargeted metabolite profiling on marine phytoplankton communities to search for novel metabolites (Longnecker et al., 2015a), characterize marine particulate organic matter (Llewellyn et al., 2015), or support metabarcoding studies (Ray et al., 2016a). The aim of the present work was to define intra- and extracellular marker metabolites for different growth phases of *Phaeocystis pouchetii* laboratory cultures using comparative metabolomics

(Kuhlisch and Pohnert, 2015). With these marker metabolites natural phytoplankton communities were analyzed and characterized in a metametabolomics approach.

2. Material and methods

2.1. Solvents

For sample processing, the following solvents were used: methanol, water, pyridine (HPLC grade, Sigma-Aldrich); chloroform, tetrahydrofuran (HPLC grade, VWR); ethanol (for LC, Merck); and hexane (for GC, Merck).

2.2. Algal cultivation

Phaeocystis pouchetii AJ01 (isolated 1994 from Raunefjord, Norway) was obtained from Aud Larsen (Bergen University, Norway). Cultures were grown in autoclaved, sterile-filtered f/2 medium (Guillard, 1975) at 6.7 ± 0.9°C, under a 14:10 h light:dark cycle, at 15-50 µmol photons s^{-1} m^{-2} provided by fluorescent tubes (Osram L15W/840 Lumilux Cool White). Cultures were shaken once daily. An exponentially growing stock culture was inoculated into three batches of 450 mL f/2 medium to a concentration of 3.1 ± 4.7 × 10^4 cells mL^{-1}. After 11 days cell densities reached 4.7 × 10^5 ± 5.5 × 10^4 cells mL^{-1} and cultures were combined to 1.5 L inoculation culture. In 2 L glass bottles 1.8 L cultures (n = 4) were set up at an initial cell density of 4.6 ± 3.3 × 10^3 cells mL^{-1}. Another bottle with 1.8 L f/2 medium was used as medium control.

2.3. Sampling of endo- and exometabolites

After 12 days (A), 26 days (B) and 47 days (C) of culturing, intra- and extracellular sampling of metabolites from all cultures and the medium control was conducted 2 h after onset of light. Therefore, aliquots of 0.5 L of the respective culture were collected in glass flasks and stored at culturing conditions until filtration. During filtration, samples were kept on ice and two samples were prepared in parallel. Samples were filtered through GF/C filters (ø 47 mm) at 650 mbar and the still wet filters immediately transferred to 25 mL glass beakers. One filter was required to pass the entire volume of all samples A, but due to increasing cell counts two or three filters, respectively, were required for cultures B and C. After filtration, cells were immediately re-suspended in 1 mL extraction mix (methanol:ethanol:chloroform, 1:3:1, *v*: *v*: *v*) and all suspensions of one culture were combined in 4 mL glass vials. Filtration took on average 20 min and the time between sampling and transfer to extraction mix was below 9 h. After adding 5 µL (C: 10 µL) 4 mM aqueous ribitol (>99%, Sigma-Aldrich) as internal standard (IS), samples were vortexed for 60 s and kept at -20°C until analysis 1 month after the end of the experiment. Filtrates were collected in glass flasks, stored at 4°C in the dark,

and processed immediately after the end of filtration according to Pree et al. (2016). Briefly, filtrates were passed at 500-600 mbar through Chromabond® Easy cartridges (Macherey-Nagel, 3 mL, 200 mg adsorbent) that were eluted with first methanol and then methanol:tetrahydrofuran (1:1, *v*: *v*). 5 µL IS were added (C) and samples were stored at -20°C until further analysis. All intra- and extracellular samples were further processed as one batch each in random order.

2.4. Metadata sampling

Every 2-3 days cultures were shaken and aliquots were sampled to determine chlorophyll *a* (Chl *a*) fluorescence, photosystem II (PSII) efficiency, cell abundance, bacterial abundance and inorganic nutrient concentrations according to Mausz and Pohnert (2015). Briefly, Chl *a* fluorescence and PSII efficiency were determined in a black well plate with a plate reader. F_0 (initial fluorescence) was measured after dark-incubation at 5°C and 30 s double orbital shaking. To determine cell abundance, samples were fixed with acidic Lugol's solution (Rodhe et al., 1958) at 1% final concentration and stored dark until they were investigated by light microscopy. At least 400 cells or at most 16 mm² were counted in a Fuchs-Rosenthal counting chamber in duplicates at ×400 magnification. Growth rates were calculated by iterative fitting of the logistic growth model ($N_t = \frac{KN_0e^{\mu t}}{K+N_0(e^{\mu t}-1)}$; N = population size, t = growth time, K = max. population size) to the observed cell abundances. To determine bacterial abundance, aliquots of 1 mL were fixed with glutaraldehyde at 0.5% final concentration, frozen in liquid nitrogen and stored at -80°C until flow cytometry analysis. After thawing, samples were diluted 1:50 with TE buffer (10 mM Tris-HCl, 1 mM EDTA, pH 8.0) and stained with SybrGold. 100 µL stained sample were mixed with 300 µL TE buffer and 100 µL Fluoresbrite™ Plain YG 1.0 µm Microspheres (Polysciences, Germany) and immediately measured in random order at 525 nm. Reference beads were calibrated with CountBright™ absolute counting beads (7 µm, Life technologies, USA) at 575 nm for 1 min with 10 µL min^{-1}. TE buffer was used as blank. To determine inorganic nutrient concentrations, filtered samples were fixed with 5 µL chloroform and stored at -20°C until analysis. Phosphate (PO_4^{3-}) was determined colorimetrically (Hansen and Koroleff, 2007) and nitrate (NO_3^-) with ion chromatography (Okada and Kuwamoto, 1985). Nitrite (NO_2^-) was analyzed colorimetrically following Parsons et al. (1984).

2.5. Metabolite extraction and derivatization

Samples were thawed and vortexed. For intracellular metabolite profiling, samples (0.5 mL per filter) were transferred into 1.5 mL centrifuge tubes (Eppendorf, Germany). Suspensions

were treated for 10 min in an ultrasonic bath, centrifuged (15 min, 30.000 g, 4°C), and supernatants were transferred to 1.5 mL glass vials. Samples were evaporated to dryness under vacuum before subsequent derivatization. For extracellular metabolite profiling, aliquots of 1.4 mL of the eluates from solid phase extraction were transferred to 1.5 mL glass vials (A/B: 2 µL IS were added) and evaporated to dryness. Samples were then derivatized with methoxyamine and MSTFA according to Vidoudez and Pohnert (2012). In cases where the IS peak was missing, samples were re-derivatized with 10 µL MSTFA and incubated for 30 min at 60°C followed by 30 min at 40°C.

2.6. Gas chromatography-mass spectrometry (GC-MS) measurements

Samples were run in random order on a Trace™ GC Ultra coupled to a ISQ™ LT and AS3000 II auto sampler (all ThermoScientific™) that was equipped with a DB-5ms column (Agilent J&W, 30 m, 0.25 mm internal diameter, 0.25 µm film thickness, 10 m Duraguard pre-column), and analyzed as described in Vidoudez and Pohnert (2012). New, deactivated glass liners (ThermoScientific™, 5 × 8 × 105 mm inner × outer diameter × length) with glass wool were used for every batch of 21 samples. Samples were injected using split 10 (intracellular) or splitless mode (1 min; extracellular). The electron impact source was set to 70 eV at 280°C. Resolution was 866 at *m/z* 502.20 (FWHM = 0.53).

2.7. Data processing and statistical analysis

Chromatograms were converted to NetCDF with the Xcalibur File Converter (ThermoScientific™) and then to RAW with MassLynx 4.1 DataBridge (Waters®) to allow background-noise correction with the MassLynx 4.1 CODA tool (Waters®, MCQ = 0.8, Smoothing window = 5). Signals were de-convoluted with AMDIS 2.71 (Nist) as one batch job each for intra- and extracellular samples. Peaks were integrated in MET-IDEA 2.08 using the chromatogram with the highest number of components as model ion file. For software settings see Vidoudez and Pohnert (2012), instrument type was set to 'quadrupole'. The resulting peak area table was imported in Microsoft® Excel. All peaks were deleted that corresponded to the IS, retention index (RI)-mix, and any signal that was negative after subtraction of the corresponding solvent blank in at least 4 samples of one day. Finally, data was peak sum normalized. A canonical analysis of principal coordinates (CAP) was performed according to Vidoudez and Pohnert (2012). Variables (loadings) were screened for significant correlation with the first two CAP axes using the Pearson correlation test ($k = 1$, $m = 2$, $\alpha = 0.01$). Score and loading plots were visualized in SigmaPlot 11.0 (Systat Softwares) and heat maps in MetaboAnalyst 3.0 (Xia and Wishart, 2016).

2.8. Metabolite identification

Metabolites were identified at different levels according to Sumner et al. (2007): metabolites, where both retention index and mass spectrum matched a chemical reference standard were classified as level 1 (L1), others were ranked by spectral similarity to a library compound (L2) or compound class (L3), or remained unidentified (L4). Selected reference standards (n >200) were derivatized as described above. Linear retention indices (Van den Dool and Kratz, 1963) were calculated and a match between compound and reference standard was accepted with ΔRI $\leq$26 (Koo et al., 2014). Mass spectra as extracted by AMDIS were manually compared to the following spectral libraries using MS Search 2.0 g (Nist): NIST 11 library version (mainlib, replib, nist_ri), Golm Metabolome Database libraries T_MSRI_ID (http://csbdb.de/csbdb/dload/dl_msri.html; 2004) and GMD_20111121_VAR5_ALK_MSP (http://gmd.mpimp-golm.mpg.de/download/; 2011), and an in-house library (175 compounds from several metabolite classes including algal extracts of *Skeletonema marinoi*). Mass spectra were regarded to match with a reverse match factor (R.Match) >800, or tagged with '?' if the factor was 700-800 and '??' if it was 600-700.

2.9. Sampling of natural phytoplankton communities

Phytoplankton communities including colony blooms of *P. pouchetii* were sampled in the Barents Sea and along the North Norwegian coast during the PHAEONIGMA cruise from 02-07th May 2013 on board of R/V *Håkon Mosby* (Figure 1, Table 1). Vertical profiles of temperature, salinity, depth, oxygen, Chl *a* fluorescence, transmission and irradiance were measured at each station with a CTD (Sea-Bird SBE 9) mounted to a rosette sampler with 12 Niskin bottles á 10 L.

Table 1 Overview over sample location, date and water depth of all seven PHAEONIGMA stations within the Barents Sea and adjacent North Norwegian fjords.

#	Station description	Latitude	Longitude	Date	Sample depths
1	Arctic water	75° 48.15 N	20° 03.63 E	02/05/2013	5 m, 16 m, 31 m
2	Polar front	74° 42.51 N	19° 59.49 E	02/05/2013	6 m, 15 m, 30 m
3	Atlantic water	72° 45.50 N	20° 02.78 E	03/05/2013	6 m, 32 m, 58 m
4	Inner Porsangerfjord	70° 20.95 N	25° 15.57 E	04/05/2013	5 m, 20 m, 40 m
5a	Outer Porsangerfjord	70° 51.19 N	26° 05.36 E	04/05/2013	5 m, 20 m, 41 m
5b	Outer Porsangerfjord	70° 51.06 N	26° 04.70 E	06/05/2013	5 m, 20 m, 40 m
6	Ullsfjord	69° 55.79 N	19° 53.53 E	07/05/2013	5 m, 33 m, 50 m

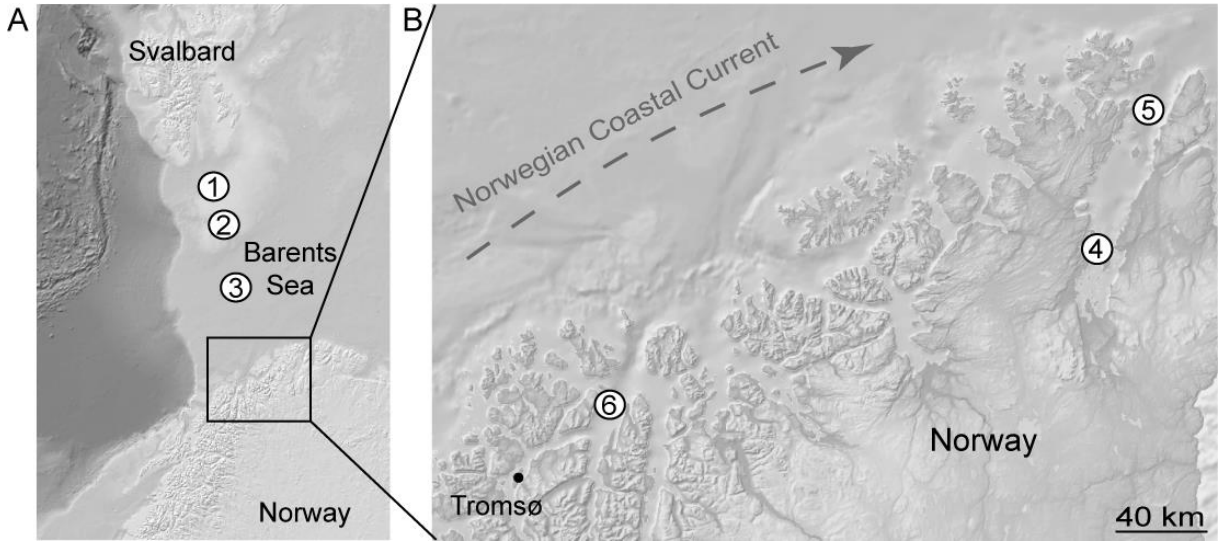

Figure 1 Phytoplankton sampling sites in the Barents Sea and North Norwegian fjords during the PHAEONIGMA cruise. A) Barents Sea transect: 1- Arctic water, 2- Polar front, 3- Atlantic water. B) North Norwegian fjord stations: 4- Inner Porsangerfjord, 5- Outer Porsangerfjord, 6- Ullsfjord, Maps adapted from www.norgeskart.no.

Samples for the analysis of dissolved inorganic nutrients, phytoplankton and *Phaeocystis* colonial cell abundance were taken as described in Pree et al. (2016). Briefly, nitrate, nitrite, phosphate and silicate concentrations were determined colorimetrically using a continuous flow analyzer (Skalar San+ Autoanalyzer) according to an ISO17025 accredited procedure (Hansen and Koroleff, 2007). For epifluorescence microscopy, a subsample of 50 mL was stained with 20 µL primulin (250 µg mL^{-1} working solution with 0.1 M TRIS HCl at pH 4), after 3 min fixed with 25% glutaraldehyde and 70% glycerol to a final concentration of 3.6% glutaraldehyde and 10% glycerol (*v*%), filtered onto black filters (Nucleopore, 0.4 µm), mounted on glass slides, and stored at -20°C until cell enumeration and carbon estimation (Sazhin et al., 2007). *Phaeocystis* colonial cell abundance was determined for subsamples of 20 mL with a FlowCAM II™ (Fluid Imaging technologies, ME, USA) equipped with a ×4 objective and a FC300 flow cell (Fluid Imaging technologies) as in Jonasdottir et al. (2011). Colonial cell number was calculated from individual images of colonies by a grey scale area calibrated regression as outlined in Ray et al. (2016b).

Water samples for metabolite analysis were collected above, at, and below the Chl *a* maximum (Table 1), and transferred to 10 L containers (Nalgene™). Intracellular metabolites were sampled in triplicates by filtering in parallel 2-6 L at 600 mbar through GF/C filters (ø 47 mm). Larger zooplankton was removed from the filtration units with a pipette. Cells were re-suspended in 1.2 mL extraction mix as described above. The average time between

sampling and quenching was about 12 h since filtration took about 8-10 h. Filtration and extraction was performed in a 10°C cold room. Samples were stored on board at -20°C until transportation on ice to Jena, Germany, and at -80°C until GC-MS analysis 1 year later.

2.10. GC-MS analysis of natural phytoplankton samples

Samples were thawed, diluted with extraction mix to 1.7 mL, and 5 µL IS were added. Aliquots of 0.7 mL per sample were processed in random order as described above for intracellular samples. Derivatization was achieved according to Vidoudez and Pohnert (2012) in a reduced volume of 25 µL methoxymation solution and 25 µL silylation solution. Samples with weak IS peak were re-derivatized with MSTFA as described above. GC-MS measurements were conducted using a 6890N GC equipped with a 7683B auto sampler (Agilent) coupled to a Micromass GCT Premier™ (Waters®) mass spectrometer. The GC was operated with glass liners (Agilent, 4 × 6.3 × 78.5 mm inner × outer diameter × length), split 1, and 250° injector temperature. The MS was used with 300°C source temperature and dynamic range extension mode. Resolution was >6.000 at *m/z* 501.97.

2.11. Comparison of laboratory- and field-derived endometabolomes

To qualitatively compare the endometabolites of *P. pouchetii* strain AJ01 with those of the natural communities, all GC-MS raw files were converted to NetCDF (MetaboLights MTBLSxxx) and further processed with MetaboliteDetector 2.0 (Hiller et al., 2009). Using 'RI Calibration Wizard' the peaks of all added RI compounds and the IS were once assigned to calibrate the system and calculate RI values for all deconvoluted features (for parameters see Supplementary Table 1, 2). This was done separately for each data set. Using 'Batch quantification' the features of both data sets were quantified within all chromatograms (for parameters see Supplementary Table 3). The resulting file was exported to Microsoft® Excel, features with <3 matches within the entire data set and an average S/N ratio <10 were removed, and all remaining features (n = 214) manually checked for false or missing matches based on RI and mass spectrum. A presence-absence data table for laboratory, field and control samples was generated and plotted as Venn diagram using convex curves (Rodgers et al., 2010). Features shared between laboratory and field but not control samples were visualized as semi-quantitative box plots using MetaboAnalyst 3.0 (Xia and Wishart, 2016), and as cruise transect section plots using Ocean Data View 4.7.10 (Schlitzer, 2016) with DIVA gridding and automatic scale lengths. Spearman rank correlation coefficients and their MC estimated p-values and 95%-CI limits were calculated for selected metabolites and environmental parameters (Supplementary Table 4).

3. Results

3.1. Growth of Phaeocystis pouchetii *AJ01 in batch cultures*

The metabolic plasticity of *P. pouchetii* cells was investigated by comparing endo- and exometabolomes of different growth phases. To prevent potential overlaying effects of morphological plasticity, a strain with just one morphotype was selected. *P. pouchetii* strain AJ01 consists solely of diploid, flagellated cells, and showed no colony formation in culture since isolation (Jacobsen and Veldhuis, 2005). Batch cultures were set up and monitored every 2-3 days throughout a period of 47 days, and sampled three times for intra- and extracellular metabolite profiling. All cultures showed logistic growth (Figure 2A). Light microscopy confirmed one flagellated single cell type during the whole growth period. Data were in accordance with reports on synchronized cell divisions taking place during dark phase (Jacobsen and Veldhuis, 2005). Directly after inoculation, the cultures remained in lag-phase for 4 days showing no significant changes in cell abundance or Chl *a* fluorescence (Figure 2A). During this time span PSII efficiency increased, indicating recovery of the cells after transfer to the fresh medium (Figure 2B, left panel). During the following 12 days cell numbers and Chl *a* fluorescence increased significantly between sampling days (t-test, $\alpha = 0.05$) indicating exponential growth, and PSII efficiency remained at 0.31-0.35 ± 0.02. Metabolites were sampled at day 12. The average specific growth rate ($\mu = 0.38 \pm 0.04$ d^{-1}) is in agreement with recently observed rates of the same strain (Pfaff et al., 2016). During the following 20 days, cell abundances leveled off at about 2×10^6 cells mL^{-1} indicating the stationary growth phase. Chl *a* fluorescence slightly increased further, whereas PSII efficiency first decreased to 0.1 ± 0.04 at day 29 (= early stationary growth, sampled at day 26), and then remained low until day 46. During the last two days the fluorescence decreased significantly (t-test, $\alpha = 0.05$) and PSII efficiency dropped to 0.04 ± 0.01 while no significant changes in cell abundance occurred (= late stationary growth, sampled at day 47). Nutrient concentrations can explain this growth development (Supplementary Figure 1). During lag and exponential growth neither nitrate nor phosphate were limiting, nitrite was below detection limit. Nitrate decreased from about 800 to 600 µM at the end of the experiment, thus cultures never became N-limited. Nitrite increased from day 22 onwards to 4.5 µM. For other algae it has been shown that low irradiance levels can restrict the cellular nitrite reduction followed by nitrite excretion (Collos, 1998; Lomas and Lipschultz, 2006).

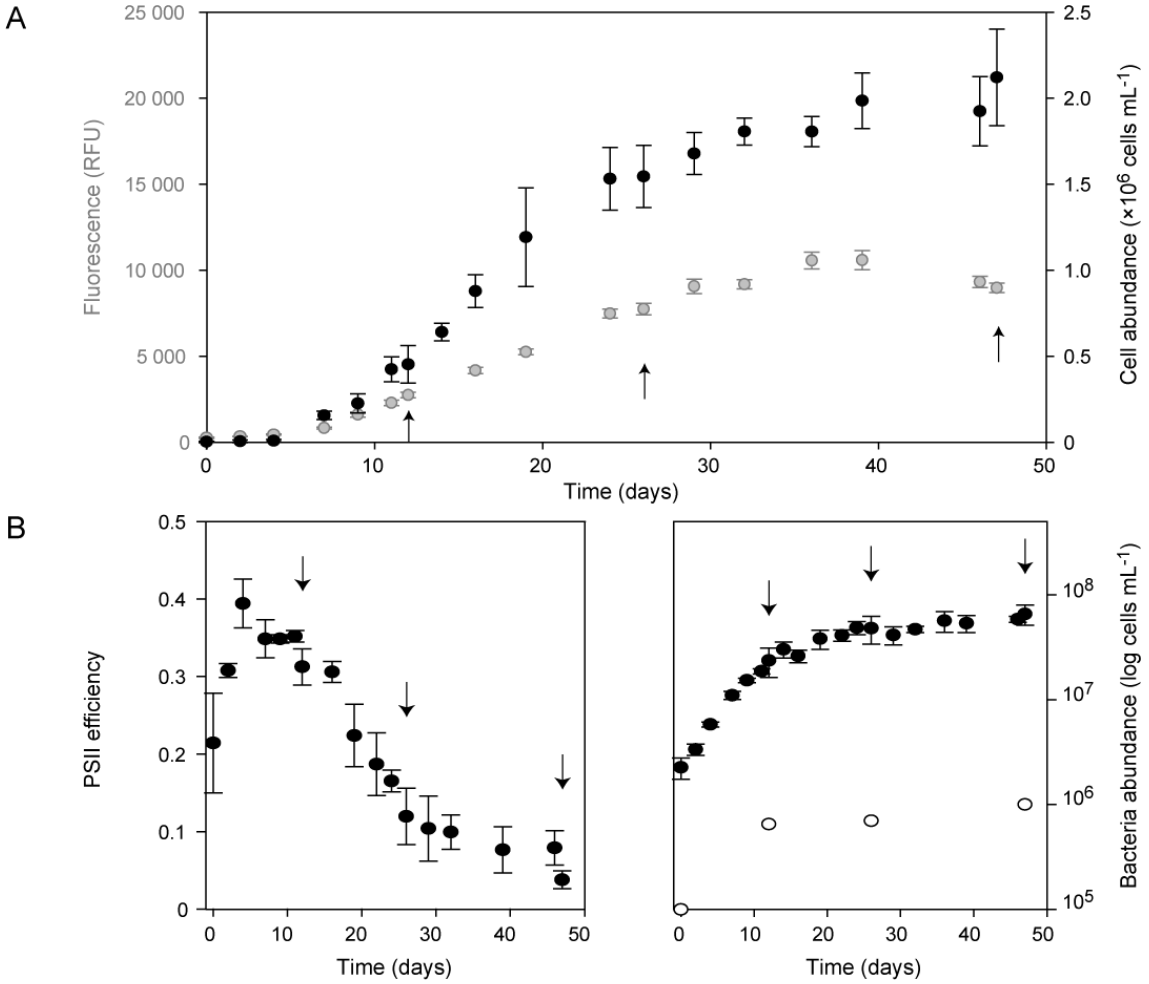

Figure 2 *Phaeocystis pouchetii* AJ01 growth-associated parameters as average ± standard deviation (n = 4). A) Cell abundance (cells mL^{-1}; black) and Chl *a* fluorescence (RFU = relative fluorescence units; grey). B) Algal PSII efficiency (left panel) and bacterial abundance (cells mL^{-1}; right panel) within the cultures (filled circles) or control (open circles). Arrows indicate sampling days of intra- and extracellular metabolites.

Thus, light seems to have been limiting thereby inducing the stationary growth phase. Phosphate fell below 5 µM at day 29 (<1 µM at day 36) and may have limited algal growth during the last two weeks of the experiment. All cultures were xenic with an initial bacterial background of 2×10^6 bacteria mL^{-1} increasing exponentially during algal exponential growth and leveling off around 5×10^7 bacteria mL^{-1} (Figure 2B, right panel). Even though bacteria can influence algal growth and metabolism (Cole, 1982; Paul et al., 2013), xenic cultures were investigated as algae naturally co-occur with bacteria. The use of one inoculation culture should have induced the same effects in all algal cultures. Bacterial metabolites can contribute to the extracted algal profile, however, with an average biovolume of 0.2 μm^3 for bacteria (Sherr et al., 2001) and 65 μm^3 for *P. pouchetii* (Vogt et al., 2012) the effect of bacterial cells that may remain on GF/C filters (Morán et al., 1999) is regarded to be negligible.

3.2. Growth phase-specific intracellular metabolites

Metabolic pathways are underlying substantial quantitative and qualitative changes during growth. In batch cultures physiological adaptations occur simultaneously with the developing growth environment. In total 518 features were detected by AMDIS and integrated by MET-IDEA. After data pre-processing, 477 features remained for data analysis: 458 ± 6 for exponential growth, 431 ± 27 for early and 398 ± 57 for late stationary growth (n = 4). Multivariate statistical analysis of the sum normalized peak areas allowed to differentiate all three growth phases. Initially, an unsupervised principal coordinate analysis (PCO) was conducted, with the first two axes explaining 78% sample variation (data not shown). Using the PCO axes a supervised CAP was conducted (Figure 3A). The replicates of each growth phase grouped together, whereas the growth phases were separated via two axes (eigenvalues: axis 1 = 0.948, axis 2 = 0.836; squared canonical correlations: axis 1 = 0.898, axis 2 = 0.698). Separation of the growth phases was confirmed by cross validation (1 out of 12 samples misclassified) and permutation test (n = 9999, p = 0.0004 for trace statistic). Based on a critical value of 0.708 (test of multiple correlation using t; n = 12), 225 metabolites were significantly correlated with the CAP axes (Figure 3B) from which 107 were highly correlated (>0.8). After removal of features with a retention time <5 min and artifacts (contaminants,

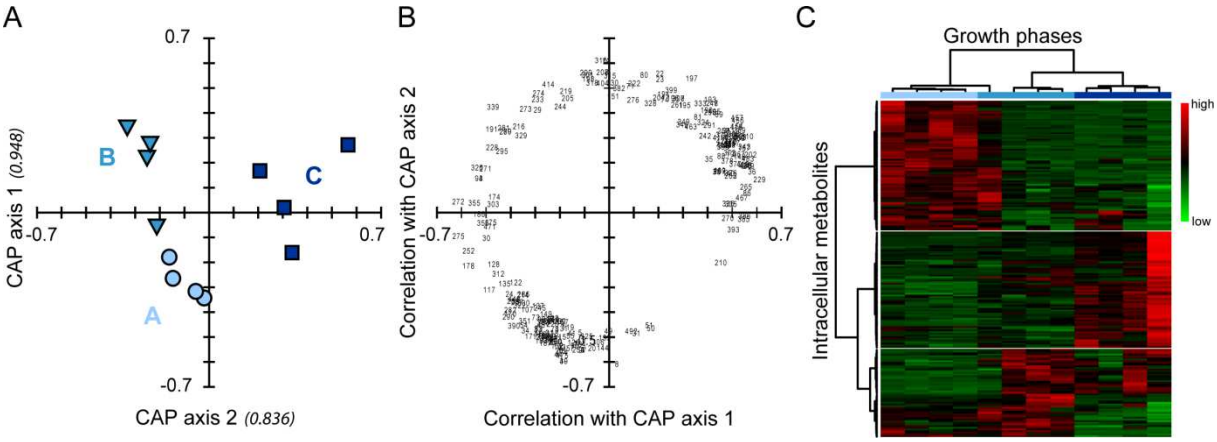

Figure 3 [Colour] Endometabolic changes of *Phaeocystis pouchetii* AJ01 laboratory batch cultures during growth (n = 4). Separation is based on canonical analysis of principal coordinates (CAP); axis eigenvalues are given in parentheses. A) Score plot of the growth phases: exponential phase (A, bright blue circle), early stationary phase (B, blue triangle), late stationary phase (C, dark blue square). B) Loading plot (scaled to score plot) of correlated intracellular metabolites (>0.708) depicted with their tabulated number (Supplementary Table 5). C) Heat map of correlated intracellular metabolites (area analyte/peak sum) indicating high (red) or low (green) relative concentrations in the growth phases. For better visualization metabolites and samples are clustered hierarchically using the Pearson distance measure and Ward cluster algorithm.

S/N <10, doublets), 88 features remained for identification. From those 31% were identified (L1, n = 27), 3% putatively annotated (L2, n = 3), 41% putatively assigned to metabolite classes (L3, n = 36), and 25% remained unknown (L4, n = 22). Most metabolites belonged to the class of saccharides, sugar alcohols, and sugar acids (n = 31), followed by fatty acids and derivatives (n = 11), and amino acids (n = 9). Many metabolites had their highest relative concentration in the exponential phase (n = 32), e.g. amino acids, pyrrole-2-carboxylic acid and threonic acid, or in the late stationary phase (n = 33), e.g. xylose, maltose, sterols, and α-tocopherol, whereas only 12 metabolites were correlated with the early stationary phase, e.g. glycerol and *scyllo*-inositol (Figure 3C).

Saccharides, sugar acids and sugar alcohols were the most pronounced regulated substance class and showed strong interphase variation. Most saccharides were significantly correlated with the late stationary phase with either constantly increasing relative concentrations (e.g. xylose, ribose, maltose, met. 204, 323, 413), or strong up-regulation in both early and late stationary phase (e.g. glyceraldehyde, met. 231). Most of the sugar alcohols (glycerol, *scyllo*-inositol, met. 285, 291, 293, 343), 1,6-anhydro-β-D-glucose, and three unidentified saccharides (putatively identified (di)galactosylglycerol, met. 238, 428) were correlated with the early stationary phase. One unidentified sugar alcohol (met. 275) was up-regulated in the late stationary phase. In this phase, mannitol showed a strong down-regulation, as did two pentafuranoses (met. 186, 194) and one sugar acid (putatively identified as quinic acid, Supplementary Figure 2). Most sugar acids (threonic acid, met. 195, 197, 294, 302) and two unknown saccharides (met. 364, 403) were significantly correlated with the exponential phase with decreasing relative concentrations towards the late stationary phase. Most fatty acids and derivatives - the second most pronounced regulated substance class - were correlated with the late stationary growth (putative hexanoic acid, arachidonic acid (AA), eicosapentaenoic acid (EPA), 1-palmitoyl-glycerol, met. 381, 387, 392), or both the early and late stationary phase (putative octadecadienoic- and octadecatrienoic acid). The only exception were tetra- and hexadecanoic acid which showed higher relative concentrations in the exponential (tetra-) and early stationary phase (hexa-). Also an unidentified alcohol (met. 155), three hydrocarbons (putative dodecatriene, met. 389, 433), and two sterols (24-methylcholesta-5,22-dien-3β-ol, met. 452) were significantly correlated with the late stationary phase. In contrast, amino acids (serine, glycine, alanine, valine, threonine, pyroglutamic acid, a proline-derivative) were correlated with the exponential phase and decreased towards the late stationary phase. Other

metabolites were either correlated with the exponential (pyrrole-2-carboxylic acid, met. 86, 330) or late stationary growth (α-tocopherol, putative phenol, met. 261, 267, 319, 322).

3.3. Growth phase-specific extracellular metabolites

In total 884 features were extracted from all chromatograms. After data pre-processing, 807 features remained for data analysis: 530 ± 47 for the exponential phase (n = 3), 543 ± 109 for the early and 489 ± 131 for the late stationary phase (n = 4). Statistical analysis of the sum normalized peak areas differentiated the growth phases (Figure 4A). The first two axes of the unsupervised PCO explained 75% of the sample variation. In the supervised CAP two axes separated the growth phases (eigenvalues: axis 1 = 0.977, axis 2 = 0.862; squared canonical correlations: axis 1 = 0.955, axis 2 = 0.744). Group separation was confirmed by cross validation (0 out of 12 samples misclassified) and a permutation test (n = 9999, p = 0.0001 for trace statistic). Based on a critical value of 0.735 (test of multiple correlation using t; n=11), 287 features were significantly correlated with the CAP axes (Figure 4B). After removal of features with a retention time <5.6 min and artifacts, 89 features remained for identification. From those 10% were identified (L1, n = 9), 16% putatively annotated (L2, n = 14), 20% putatively assigned to metabolite classes (L3, n = 18), and 54% remained unknown (L4, n = 48). The most abundant substance class was carboxylic acids (n = 11), followed by saccharides (n = 6), fatty acids (n = 2) and alcohols (n = 2). Hydrocarbons and sugar alcohols were represented with one metabolite each, and a large number of metabolites belonged to other classes (n = 15). Many metabolites had their highest relative concentration in the exponential phase (n = 30), e.g. succinic acid, putatively identified hydroxybutanoic acid, and a lumichrome-like metabolite, or in the late stationary phase (n = 26), e.g. ribose, adenosine, putatively identified guanosine, and an indole derivative. Only 19 metabolites were correlated with the early stationary phase, e.g. glycolic acid, glycerol, and nonanoic acid (Figure 4C).

Carboxylic acids were the most abundant regulated metabolites in the exometabolome and correlated with the exponential to early stationary growth (e.g. succinic acid, fumaric acid, glycolic acid, pyruvic acid, and putative hydroxybutanoic acid). Saccharides were correlated with the exponential (met. 69, 71, 602) or late stationary growth (ribose, putative ribofuranose). The sugar alcohol glycerol, the fatty acid nonanoic acid, and the putatively identified alcohol 1-octanol were correlated with the early stationary growth. An unknown indole derivative, different from the monitored indole-3-ethanol, -acetic acid, -propanoic acid, and -butanoic acid (Supplementary Figure 3), was correlated with the late stationary phase and increased throughout growth.

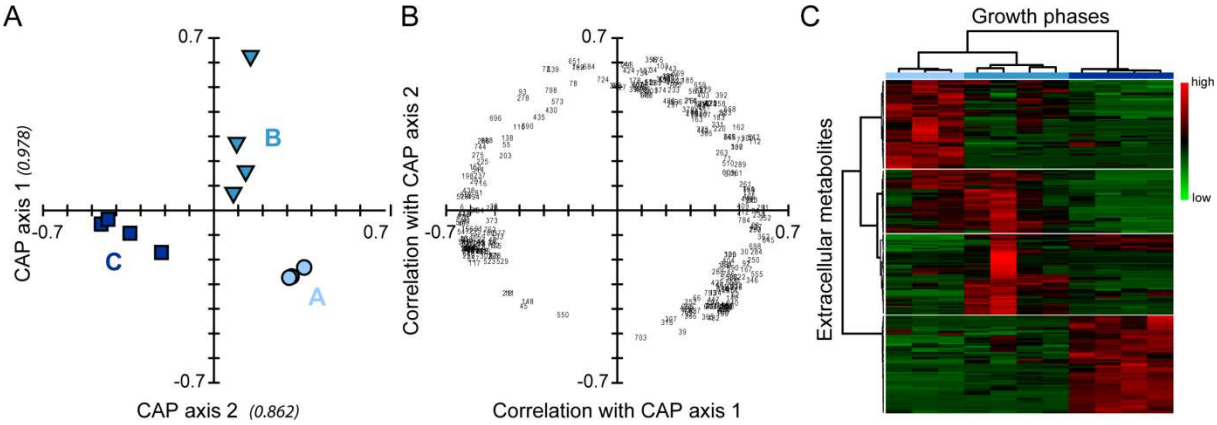

Figure 4 [Colour] Exometabolic changes in *Phaeocystis pouchetii* AJ01 laboratory batch cultures during growth (n = 4). Separation is based on canonical analysis of principal coordinates (CAP); axis eigenvalues are given in parentheses. A) Score plot of growth phases: exponential phase (A, bright blue circles), early stationary phase (B, blue triangles), late stationary phase (C, dark blue squares). B) Loading plot (scaled to score plot) of correlated extracellular metabolites (>0.735) depicted with their tabulated number (Supplementary Table 6). C) Heat map of correlated extracellular metabolites (area analyte/peak sum) indicating high (red) or low (green) relative concentrations in the growth phases. For better visualization metabolites and samples are clustered hierarchically using the Pearson distance measure and Ward cluster algorithm.

3.4. Phaeocystis pouchetii *in natural phytoplankton communities*

Phytoplankton communities were sampled along a transect in the Barents Sea (stations 1-3; Figure 1) and along the North Norwegian coast (stations 4-6; Figure 1) capturing different bloom scenarios (Figure 5). The northernmost station in the Barents Sea (station 1) was located at the ice edge with low water temperatures, slight stratification, non-limiting nutrients, and a biomass-rich, diatom-dominated algal bloom (*Gyrosigma tenuirostrum*, *Thalassiosira* spp., *Odontella aurita*). *P. pouchetii* showed minor abundance, colonies were not observed. Station 2 was located near Bjørnøya in the polar front region characterized by a well-mixed water column down to the shelf and low algal biomass again dominated by diatoms (*Thalassiosira* spp., *Fragilariopsis oceanica*, *O. aurita*) and low abundance of *P. pouchetii* as described for station 1. The southernmost station in the Barents Sea (station 3) was located within the Atlantic water inflow represented by elevated temperatures and salinities, a well-stratified water column, and high nutrient concentrations. The phytoplankton bloom was dominated by diatoms (*Thalassiosira* spp., *Skeletonema costatum*, *Chaetoceros* spp.) and *P. pouchetii* which was present with high abundance of colonies (5 µm cell size). Station 4 was located in the inner Porsangerfjord and was characterized by a shallow mixed upper layer and a highly stratified bottom layer with limiting nutrient concentrations (at Chl *a* maximum: 0.22 µM silicate, 0.05 µM phosphate, nitrate below detection level). The algal

bloom was dominated by *P. pouchetii* (about 50% biomass) in high abundance of colonies (5 µm cell size). The second most biomass-rich taxon was diatoms (*Thalassiosira* spp., *Thalassiosira nordenskioldii*, *Chaetoceros socialis*). Station 5a and 5b were both located in the outer Porsangerfjord with a shallow mixed upper layer, a well stratified layer below, and a bottom layer (>140 m depth) with increasing temperature and salinity. The Chl *a* maximum was shallow (0-20 m) with reduced to limiting nutrient concentrations (<0.12 µM phosphate, <0.7 µM nitrate). The phytoplankton community was dominated by *P. pouchetii* (up to 85% of the biomass) present with high abundance of colonies (5 µm cell size). The southernmost station was located in the outer Ullsfjord (station 6) with a mixed upper layer and stratified water below. Nutrients were reduced towards the surface, nitrate and phosphate even limiting (at 5 m depth: below detection limit). Algal biomass was low with a deep Chl *a* maximum at 30-40 m depth slowly decreasing towards the bottom. The population was dominated by ciliates, flagellates and *P. pouchetii*. Colony abundance increased with depth and cell sizes varied in contrast to previous stations between 2-6 µm with a high proportion of large cells (40% at 6 µm). In summary, *P. pouchetii* characterized the phytoplankton communities at stations 3-6 present with high abundance of colonies primarily at 5 µm cell size. These stations were therefore well-suited to test if growth phase-specific endometabolites as determined for *P. pouchetii* AJ01 could be detected in the field and used to characterize the physiological state of algal blooms.

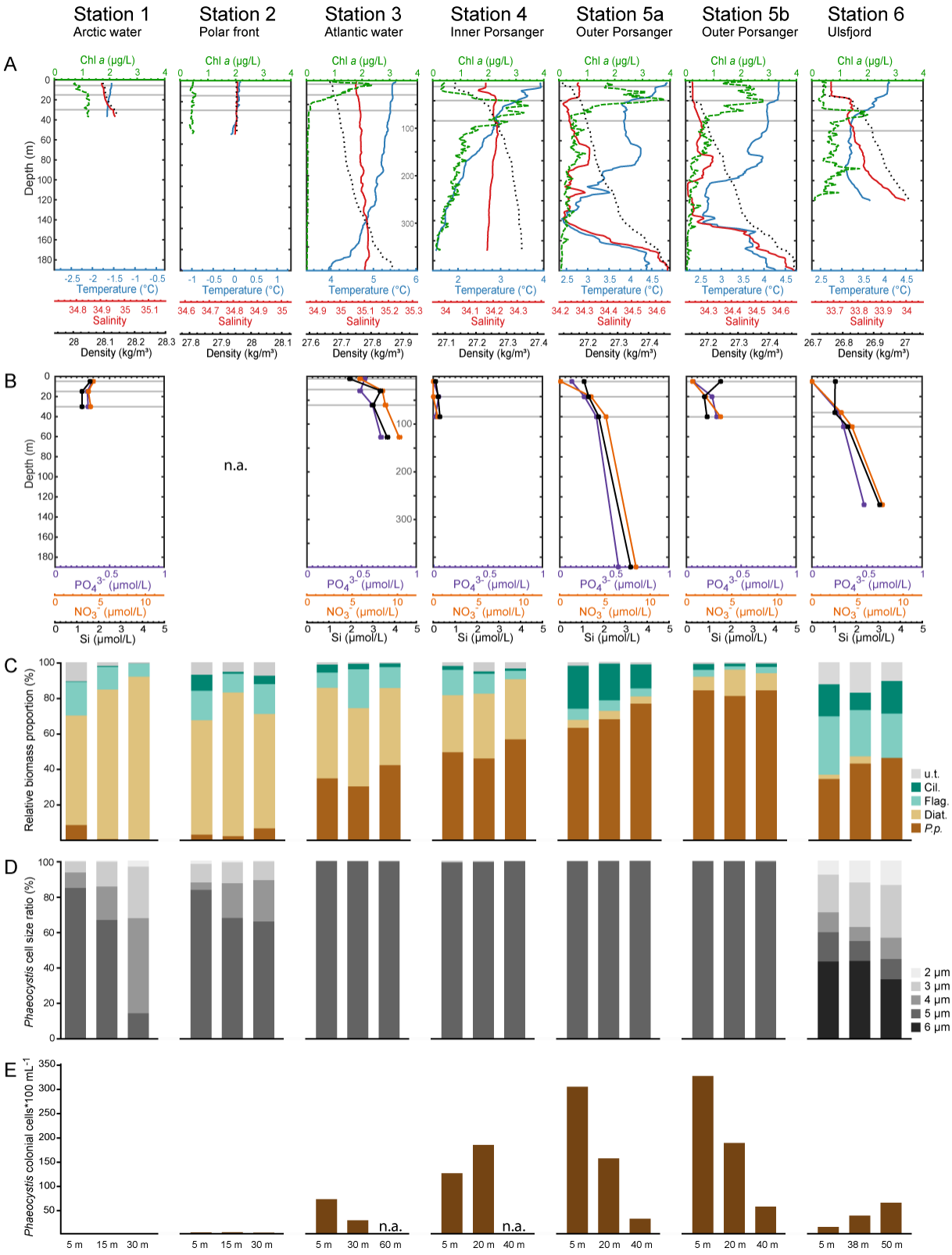

Figure 5 [Colour] PHAEONIGMA cruise data with stations sampled along a transect in the Barents Sea (Station 1-3) and in North Norwegian fjords (Station 4-6) as indicated in Figure 1 Depth profiles of water temperature (blue; °C), salinity (red), density (dashed line; kg m^{-3}) and Chl *a* (green; µg L^{-1}) as determined *in situ* with a CTD. B) Depth profiles of dissolved inorganic nutrient concentrations (µmol L^{-1}) of phosphate (violet), nitrate (orange) and silicate (black). C)-E) Phytoplankton community characteristics above, at and below the Chl *a*

maximum as determined by microscopy and FlowCAM. C) Relative biomass (mg C m^{-3}) of phytoplankton taxa: *Phaeocystis pouchetii* (*P.p.*), diatoms (diat.), flagellates (flag.), ciliates (cil.), unknown taxa (u.t.). D) Proportion of different cell sizes of *P. pouchetii* ranging from 2 µm (light grey) to 6 µm (dark grey). E) Abundance (×100 mL^{-1}) of *P. pouchetii* colonial cells. Grey horizontal lines indicate sampling depths for metabolite profiling. n.a. = not available.

3.5. Metametabolome analysis of natural phytoplankton communities

In total, 572 features were extracted by MetaboliteDetector 2.0 (Hiller et al., 2009) from laboratory and field data. From these, 192 features were removed as contaminants since they were only found in control samples, and another 198 features were identified as artifacts. Manual verification revealed that 30% of the remaining features were also present in control samples. These were excluded as well from further discussion. Thus, 47 features were unique for *Phaeocystis* cultures, 29 features were unique for field samples, and 51 features were shared between laboratory and field samples (Figure 6A, Supplementary Table 7). About 50% of the metabolites that occurred both in *P. pouchetii* cultures and in the field were growth phase-dependent in the cultures, 25% were not regulated, and for the remaining regulation is unknown. Three main occurrence patterns were found in the field based on hierarchical cluster analysis of average normalized peak areas per station (Pearson distance measure, Ward cluster algorithm, Supplementary Figure 4): high metabolite abundance at diatom-dominated stations, at *P. pouchetii*-dominated stations except station 4, and at station 4 (Figure 6B). Within the *P. pouchetii*-associated metabolites are the sugar alcohols mannitol ($r_s = 0.55$, p-value = 0.01) and *scyllo*-inositol (Figure Figure 6B, $r_s = 0.64$, p-value = 0.002), the fatty acids octadecatetraenoic acid and docosahexaenoic acid, 24-methylcholesta-5,22-dien-3β-ol (Figure 6B), and a putative 1-stearoyl-glycerol. The fatty acids hexadecanoic acid, octadecanoic acid (Figure 6B), octadecenoic acid, the alcohol octadecan-1-ol, and several unknown metabolites formed a subclade with higher abundance at station 3 and lower at station 6. In the clade with high metabolite abundance at the nutrient-limited station 4 are primarily mono- and disaccharides (ribose, a pentose, a hexose (Figure 6B), maltose ($r_s = -0.51$, p-value = 0.03), met. 403, 413), as well as fatty acids and derived metabolites (hexadecenoic and polyunsaturated octadecanoic acid, 1-myristoyl-glycerol (Figure 6B), 1-palmitoyl-glycerol) and phytol. Within the diatom-associated metabolites are threonic acid, several saccharides (erythrose, met. 138, 254, 256, 352, hexitol (Figure 6B)), the fatty acids EPA ($r_s = 0.54$, p-value = 0.01) and met. 322, and three phytol-like structures. Thus, from the *P. pouchetii* endometabolites especially saccharides, sugar alcohols, fatty acids and derived metabolites, sterols and terpenes were re-detected in the field with three main occurrence patterns.

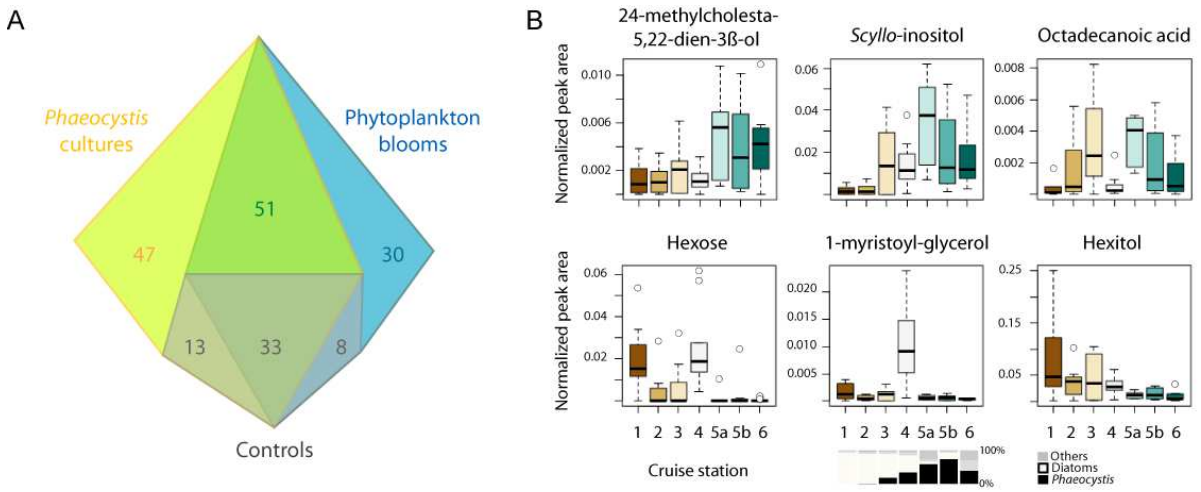

Figure 6 Occurrence of *Phaeocystis pouchetii* endometabolites within natural phytoplankton communities of the Barents Sea and North Norwegian fjords. A) Area-proportional Venn diagram of unique and shared metabolites between *P. pouchetii* laboratory cultures (n = 12), natural phytoplankton communities (n = 58), and controls (n = 7). B) Box-Whisker plots showing abundance of selected shared metabolites (as peak area/peak sum) at Barents Sea (1-3) and North Norwegian fjord stations (4-6; n = 8-9, averaged over all depths). The depicted metabolites are representative for different occurrence patterns e.g. *Phaeocystis* dominance (top row). Insert shows relative biomass of phytoplankton taxa at the respective sites.

4. Discussion

4.1. Growth-specific endometabolites of P. pouchetii

It has long been expected that metabolic plasticity of phytoplankton may profoundly influence zooplankton grazing and transfer rates, especially for haptophytes such as *Phaeocystis* (reviewed in Nejstgaard et al. (2007)). However, until recently thorough metabolite analyses of the prey have not been included in grazing studies. When included, it has indeed been shown that phytoplankton species such as the diatom *Skeletonema marinoi* can switch from an avoided to a highly ingested food source in different growth phases in accordance with changes of their metabolome (Barofsky et al. 2010). Endometabolomic plasticity has still only been demonstrated for rather few microalgal taxa including diatoms (Vidoudez and Pohnert, 2012) and haptophytes (Mausz and Pohnert, 2015). This study on *P. pouchetii* is the first report of endometabolomic plasticity of a dominant Arctic and Boreal haptophyte. Physiological changes in batch cultures of *P. pouchetii* were characterized using untargeted metabolomics. Growth phases as determined by cell abundance and Chl *a* fluorescence were associated with distinct endometabolic states. Most pronounced were alternations in amino acid, fatty acid and carbohydrate metabolism.

The exponential growth was characterized by high abundance of free amino acids reflecting high metabolic activity towards proteins under nitrogen-replete conditions. This increased amount of free amino acids during intense growth has previously also been reported from diatoms and higher plants (Bromke, 2013). Elevated glutamate levels might be directly linked to NH_4^+ incorporation. Alanine, which is formed from glutamate, is up-regulated as well. Serine and glycine represent photorespiration products, threonine is derived from the tricarboxylic acid (TCA) cycle via aspartate, and valine from glycolytic pyruvate (Bromke, 2013). The dominance of these amino acids in the early growth phase thus indicates active carbon and nitrogen acquisition. The composition of free amino acids in *P. pouchetii* differs from other marine microalgae (Mausz and Pohnert, 2015; Vidoudez and Pohnert, 2012), which may indicate taxon specificity in nitrogen assimilation and amino acid metabolism. The observed pattern can be used as specific physiological marker for actively growing *Phaeocystis* cells. Pyrrole-2-carboxylic acid is linked to amino acid metabolism via proline and is involved in pyrrole biosynthesis (Walsh et al., 2006). Even though this carboxylic acid has been reported for *Emiliania huxleyi* (Mausz and Pohnert, 2015) and *Ostreococcus taurii* (Hirth et al., 2017), its role in microalgal metabolism, particularly during exponential growth, in not known. Threonic acid, an oxidation product of ascorbic acid, was also present in higher amounts during exponential phase. Ascorbic acid is a well-known antioxidant in chloroplasts that scavenges reactive oxygen species. Oxidation of dehydroascorbic acid can be a source for the observed threonic acid (Foyer and Shigeoka, 2011; Parsons et al., 2011). It may thus mark the oxidative stress during high photosynthetic activity.

Characteristic for the exponential and even more the early stationary growth of *P. pouchetii* were mannitol and a quinic acid like metabolite. Mannitol has been found in several stramenopiles e.g. phaeophyta and chrysophyta but not in diatoms (Dittami et al., 2011a), and can thus be considered as a further specific metabolic marker. It acts as an osmolyte and antioxidant in phaeophyta (Davison and Reed, 1985; Dittami et al., 2011b), and is the main short-term carbon storage molecule in *E. huxleyi* (Obata et al., 2013). Mannitol may thus also play a role in carbon assimilation of *P. pouchetii*. It would further indicate active photosynthesis under growth limitation. The quinic acid like metabolite showed high mass spectral similarity to a reference standard, however, retention indices were not alike (Supplementary Figure 2). As quinic acid is related to the shikimate pathway fueling the biosynthesis of e.g. aromatic amino acids, mycosporine-like amino acids, and indole derivatives, a further chemical characterization is recommended.

Mono- and disaccharides as well as sugar alcohols such as glycerol, pentitols, and *scyllo*-inositol, reflecting an active carbohydrate metabolism, characterized early stationary growth. The presence of polyols may indicate interconversion of monosaccharide building blocks via pentitols (Loewus, 1971). *Myo*-inositol is most commonly reported and plays diverse roles e.g. in signaling, phosphate storage, or synthesis of oligosaccharides, glycerophospholipids, and indole-3-acetic acid (IAA) conjugates. In *P. pouchetii myo*-inositol was present in small amounts and not regulated. Instead, the stereoisomer *scyllo*-inositol was elevated at early stationary phase. This isomer has been previously reported for the haptophyte *Pavlova* with unknown function (Kobayashi et al., 2007). Inositol isomers are metabolized from *myo*-inositol and e.g. involved in phosphor storage (Loewus and Murthy, 2000). Glycerol, which may be derived from glycolysis, is involved in lipid metabolism (Xue et al., 2017).

Induced lipid metabolism during early and late stationary growth is also reflected by the elevated presence of glyceraldehyde and two methylated C18-polyunsaturated fatty acids (PUFAs). Glyceraldehyde may be derived from hexoses fueling the TCA cycle and potentially also the lipid metabolism via interconversion to glycerol. C18-PUFAs are synthesized from C18:0 via C18:1ω9 (Mühlroth et al., 2013). *Phaeocystis* is known to contain high amounts of C14:0, C16:0, C18:0 and C18-PUFAs (especially C18:1ω9 and C18:5ω3) in the polar lipid fraction which is mainly derived from cell membranes (Hamm et al., 2001). The role and occurrence of free and methylated fatty acids is, in contrast, poorly understood (Hirth et al., 2017). However, the general trend of up-regulated lipid metabolism with the onset of stationary growth is in accordance with earlier reports on this metabolite class under light, nutrient, or osmotic stress (Roessler, 1990).

In late stationary growth mono- and disaccharides, free fatty acids, hydrocarbons, sterols and alcohols became dominant. These metabolites provide evidence for an active metabolism of carbohydrates, lipids and derived structures. Within the life cycle of *Phaeocystis*, monosaccharides play a role as precursors and intermediates in regular cell metabolism, whereas disaccharides are involved in the synthesis of polysaccharides for carbon storage, cell wall and mucus formation (Alderkamp et al., 2007). Thus, uncoupling of Calvin and TCA cycle during stationary phase may lead to an accumulation of carbohydrates. Monosaccharide accumulation may further reflect the catabolism of storage polysaccharides, as enhanced degradation of the storage compound glucan would go ahead with a direct transformation of glucose. The main sterol in *P. pouchetii* is 24-methylcholesta-5,22-dien-3β-ol (Hamm et al., 2001; Nichols et al., 1991), that was found in elevated quantities during later growth phases.

Also the membrane antioxidant α-tocopherol is most abundant in the late stationary phase. Both metabolites are relevant for membrane stability during declining growth (see Mausz and Pohnert (2015); Vidoudez and Pohnert (2012) and references therein). The polyamine putrescine, that marked the declining growth of *Skeletonema marinoi* and *Alexandrium tamarense* (Lu and Hwang, 2002; Vidoudez and Pohnert, 2008), was neither detected in *P. pouchetii* nor in *E. huxleyi* or other haptophytes (Hamana and Niitsu, 2006; Mausz and Pohnert, 2015). This demonstrates different strategies in metabolic stress response within algal lineages during bloom decline.

The growth physiology of *P. pouchetii* is thus reflected in the endometabolites, such as amino acids, fatty acids and carbohydrates. Besides general metabolic responses (e.g. α-tocopherol), also taxon-specific responses are observed (e.g. *scyllo*-inositol, putrescine).

4.2. Growth-specific exometabolites of **P. pouchetii** *as physiological markers*

Marine phytoplankton releases diverse mixtures of dissolved organic matter (DOM) composed of amino acids, peptides, carbohydrates, fatty acids, lipids and nucleic acids by both passive leakage and active exudation (Thornton, 2014). Algal exometabolomes may thus reveal qualitative and quantitative differences with regard to species composition (Becker et al., 2014), growth phase (Barofsky et al., 2009; Longnecker et al., 2015b), or associated bacteria (Alsufyani et al., 2017). Growth phase-dependent changes have been rarely investigated for marine microalgae (Barofsky et al., 2009; Granum et al., 2002). *P. pouchetii* is the first haptophyte which is profiled on the exometabolite level during growth.

Within the exometabolome of *P. pouchetii*, several of the released metabolites were growth phase-dependent. Compared to the endometabolomes, a smaller fraction of the detected signals could be identified based on reference compounds and library-based identification. Since the identification of metabolites discriminates for "known" compounds that are well-investigated and included in libraries, mainly primary metabolites or those close to primary metabolism are covered. The proportion of these "knowns" is lower in the open water compared to the cellular content, potentially as a result from exudation of secondary metabolites with specialized functions (Pohnert et al., 2007). In addition, primary metabolites might be degraded or otherwise transformed once released into the environment and therefore not be identified by library-based approaches.

Some of the identified metabolites or metabolite classes have already been observed and discussed earlier for microalgae, such as short chain alcohols and fatty acids (Kambourova et al., 2004). Glycerol has been suggested as algal derived carbon source for associated bacteria

(Alsufyani et al., 2017). Putatively identified lumichrome - known as algal quorum sensing agonist of associated bacteria (Meyer et al., 2017) - was elevated during exponential growth. This compound was also found in *E. huxleyi* based on intracellular metabolite profiling (Mausz and Pohnert, 2015), a release mechanism as observed here would explain a plausible function in the interaction of the alga with the bacterial community (Rajamani et al., 2008). In the following, the extracellular occurrence of carboxylic acids, 3-alkylindoles and nucleosides is addressed.

Several carboxylic acids were detected in the exometabolome of *P. pouchetii*, e.g. succinic acid, pyruvic acid and glycolic acid that are all indicators for high metabolic activity. Succinic acid is an intermediate of the TCA cycle showing highest abundance during exponential growth which would be in accordance with the overflow hypothesis of DOM release under excess carbon fixation (Thornton, 2014). Release can also be high during growth phase transitions due to imbalance situations, which may explain that elevated amounts of pyruvic acid were detected extracellularly during exponential and early stationary phase. Pyruvic acid fuels the TCA cycle and fatty acid synthesis, and plays a role in carbon assimilation via β-carboxylation in the chloroplast (Tsuji et al., 2009). Succinic and pyruvic acid are involved in carbon as well as nitrogen metabolism and a clear association to one of the two is therefore not possible (Zhang et al., 2016). Glycolic acid is formed as photorespiration intermediate of actively photosynthesizing algae under high light intensities, high O_2 or low CO_2, and is excreted into the medium in exchange with bicarbonate (Tolbert and Zill, 1956). It was most abundant during early stationary phase reflecting active photosynthesis and high cell numbers. Taken together this group of compounds clearly shows that *P. pouchetii* releases substantial amounts of reduced carbon into the surrounding environment that might directly fuel microbial proliferation associated with blooms.

An indole derivative that increased in abundance throughout growth was also identified in the metabolomics survey (Supplementary Figure 3). Indole-3-acetic acid (IAA) is a well-known plant growth and development hormone. It is excreted by marine bacteria promoting algal growth (Amin et al., 2015) or killing their algal host (Segev et al., 2016), and by the alga *E. huxleyi* with a putative intraspecific signaling function (Labeeuw et al., 2016). Elevated IAA levels inhibit algal growth and may thus control population density comparable to quorum sensing in bacteria (Piotrowska-Niczyporuk and Bajguz, 2014). Several other indole derivatives are known from plants and may be involved in microalgal growth regulation as well (Lau et al., 2009; Ludwig-Müller, 2000). Further investigations are needed to elucidate

the exact chemical identity, origin and role of the extracellular indole derivative in *P. pouchetii* cultures.

In the late stationary phase the purine nucleosides adenosine and putative guanosine were elevated. Extracellular nucleosides have already been observed for *Synechococcus* sp. (Fiore et al., 2015). However, origin, role and fate of these metabolites can only be hypothesized. Their increase during late stationary phase may be associated with enhanced membrane permeability due to autocatalytic cell death (Franklin et al., 2012), DNA degradation, or the release of other precursor molecules, such as cAMP (Francko and Wetzel, 1980). Extracellular nucleosides and related metabolites can be re-incorporated by diatoms (Werner, 1971) and play a signaling role in the reproduction and wound response of macroalgae (Huidobro-Toro et al., 2015; Torres et al., 2008). Production and fate of extracellular metabolites are further closely linked to associated bacteria (Buchan et al., 2014).

The growth physiology of *P. pouchetii* is thus reflected in the exometabolome by the occurrence of e.g. carboxylic acids and ribonucleosides. In addition, molecules such as a 3-alkylindole and lumichrome-like metabolite with putative signaling functions are constituents of algal exometabolomes, and point towards a potentially complex signaling chemistry. The present study therefore paves the way to a more comprehensive interpretation of the metabolite interactions during bloom development and decay in *P. pouchetii*.

4.3. Physiological marker metabolites in natural plankton assemblages

Metabolite profiles of phytoplankton blooms depend on algal taxonomy, environmental factors, and the inherent algal physiology (Mayzaud et al., 1989; Nichols et al., 1989). The relevance of traditional chemotaxonomy approaches has recently been questioned, since metabolic variability during growth phases of one species might be more substantial than differences between species (Barofsky et al., 2010; Bell et al., 2010; White et al., 2015). This substantial plasticity is documented in this study in both, laboratory and field experiments. Previous work linked fatty acids to trophic relationships as discussed in Dalsgaard et al. (2003), and potential senescence markers are reviewed by Rontani (2001). But very few studies indeed provide a direct link of metabolic variability in the field with algal performance, as demonstrated for the resistance to viral infection in *E. huxleyi* (Vardi et al., 2009). Our data now allow surveying metabolic markers of growth phase-dependent physiology in the field using an unbiased metabolomics approach and pave the way to a better understanding of phenotypic variability in the plankton.

At all cruise stations *Phaeocystis* was detected and, in accordance, many of the endometabolites identified in laboratory cultures were also detected in all investigated natural phytoplankton communities in variable concentration. A diverse metabolic landscape shaped by the abundance of various phytoplankton in different growth phases was recognized at the cruise stations (Figure 7). Overlaying influences of e.g. irradiance and bacterial metabolism additionally modulate the observed metametabolome. Light attenuates with water depth, which has a strong impact on the photosynthetic activity of all algal cells and on the release of metabolites such as hexose that decreases in greater depth (Figure 7B). Also reduced nutrient concentrations of e.g. NO_3^- and PO_4^{3-} influence algal physiology and metabolism. Accordingly, in the inner Porsangerfjord (Station 4, Figure 7C) distinct endometabolite profiles were observed with increased levels of e.g. several mono- and disaccharides as well as hexadecenoic acid, 1-myristoyl-, and 1-palmitoyl-glycerol, and phytol. This distinct pattern may be a result of nutrient limitation and the resulting stress metabolism as observed during the late growth phase in laboratory cultures. In addition, the decline of the diatom bloom (*Chaetoceros* spp.) as indicated by high bacterial production (0.31 µg C L^{-1} h^{-1}) and abundance of heterotrophic flagellates (e.g. *Gyrodinium lachryma*) may be reflected in the metabolic maps.

Several metabolites were most abundant at the stations dominated in biomass by *Phaeocystis* (Figure 7E). Their differential distribution within these blooms reflects different bloom phases. Mannitol, which is not reported in diatoms (Dittami et al., 2011a), showed an interesting pattern: it was lower at stations 5a/b with high biomass contribution of *Phaeocystis* (>60%) and higher at stations with low *Phaeocystis* biomass (15-35%). Elevated mannitol levels during exponential and early stationary growth in *P. pouchetii* would thus correspond to an earlier bloom phase with high carbon acquisition at station 3. Stations 4-5 were dominated by *P. pouchetii* in a stationary bloom phase. The high carbon assimilation at station 6 may be attributed to physiological changes: colony abundance was low and increased with depth. Cell sizes ranged from 2-6 µm with a high proportion of 6 µm cells (ca. 50%) and a relative increase of smaller cells with depth (Figure 5). This indicates bloom senescence with sinking colonies that induces the release of flagellated single cells (Reigstad et al., 2000; Rousseau et al., 1994). Station 3 was also characterized by several free fatty acids reflecting active lipid metabolism, whereas stations 5-6 showed high levels of octadecan-1-ol and the sterol 24-methylcholesta-5,22-dien-3β-ol. This sterol is a marker for late stationary growth in the *Phaeocystis* laboratory cultures and was relative to *Phaeocystis* biomass highest

at station 6 and lowest at station 4 confirming again the determination of different bloom phases at the cruise stations. The occurrence of a few metabolites was either highly correlated with the biomass of diatoms (Figure 7D, EPA) or of *Phaeocystis* (Figure 7E, C18:1) and therefore rather reflects algal taxonomy than physiology.

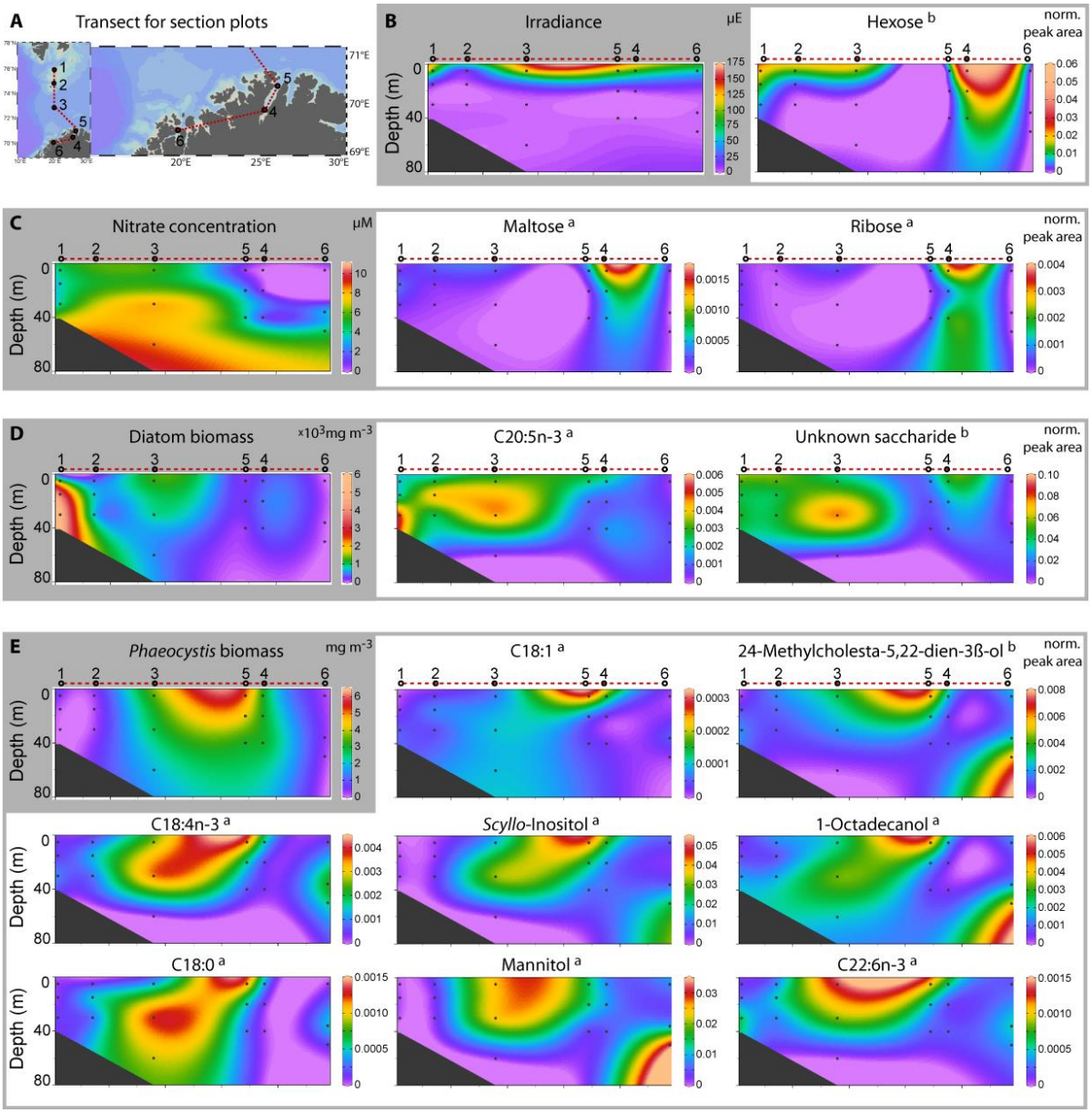

Figure 7 [Colour] Abundance of *P. pouchetii* and endometabolites within phytoplankton communities in the Barents Sea and North Norwegian fjords. A) Transect along the PHAEONIGMA cruise stations 1-6 as used for section plots. B-E) Section plots of metabolites, species composition, and environmental parameters (shaded in grey). Metabolites with similar occurrence patterns are grouped in grey boxes.

4.4. Conclusion

Taken together, a diverse metabolic landscape in natural phytoplankton blooms can be linked to physiological conditions of *P. pouchetii* using the information of endometabolites of laboratory cultures. The physiological response of phytoplankton cultures and communities to irradiance, nutrient concentrations, and bloom phase is reflected in their (meta)metabolite profiles and can be discriminated from species-specific metabolites. Characterization of the physiological state of *Phaeocystis* blooms in addition to classical methods such as microscopy, pigment analysis, or targeted analyses of fatty acids, dimethylsulfoniopropionate or polyunsaturated aldehydes can give direct information on food quality and may help in the interpretation of zooplankton grazing variability (Estep et al., 1990; Ray et al., 2016a; Ray et al., 2016c). Bloom states and metabolic states might also serve as predictors for bloom succession and toxicity of harmful algae.

5. Acknowledgements

We gratefully acknowledge Aud Larsen (Bergen, Norway) for kindly providing us strain *Phaeocystis pouchetii* AJ01, Katharina Eick (Jena, Germany) for flow cytometry analysis, JenaBios GmbH (Jena, Germany) for phosphate and nitrate analysis of the laboratory samples and E. Kuhlisch for statistical support. Further we thank the whole crew of R/V *Håkon Mosby* for their assistance onboard, A. Larsen and Marc E. Frischer as cruise leaders, and all fellow scientists. This work was supported by Jena School of Microbial Communication (C.K.); VELUX Foundation Grant VKR022608 (H.J.); and Deutsche Forschungsgemeinschaft (CRC 1127 "ChemBioSys"). The research cruise in 2013 was funded by the Research Council of Norway research project ‘A novel cross-disciplinary approach to solve an old enigma: the food-web transfer of the mass-blooming phytoplankter *Phaeocystis pouchetii*’ (Phaeonigma, project no. 204479/F20).

6. References

Alderkamp, A.C., Buma, A.G.J., van Rijssel, M., 2007. The carbohydrates of *Phaeocystis* and their degradation in the microbial food web. Biogeochemistry 83(1-3), 99-118.

Alderkamp, A.C., Nejstgaard, J.C., Verity, P.G., Zirbel, M.J., Sazhin, A.F., van Rijssel, M., 2006. Dynamics in carbohydrate composition of *Phaeocystis pouchetii* colonies during spring blooms in mesocosms. J. Sea Res. 55(3), 169-181.

Alsufyani, T., Weiss, A., Wichard, T., 2017. Time course exo-metabolomic profiling in the green marine macroalga *Ulva* (Chlorophyta) for identification of growth phase-dependent biomarkers. Mar. Drugs 15(1), doi: 10.3390/md15010014.

Amin, S.A., Hmelo, L.R., van Tol, H.M., Durham, B.P., Carlson, L.T., Heal, K.R., Morales, R.L., Berthiaume, C.T., Parker, M.S., Djunaedi, B., Ingalls, A.E., Parsek, M.R., Moran, M.A., Armbrust, E.V., 2015. Interaction and signalling between a cosmopolitan phytoplankton and associated bacteria. Nature 522(7554), 98-101.

Archer, S.D., Verity, P.G., Stefels, J., 2000. Impact of microzooplankton on the progression and fate of the spring bloom in fjords of northern Norway. Aquat. Microb. Ecol. 22(1), 27-42.

Barofsky, A., Simonelli, P., Vidoudez, C., Troedsson, C., Nejstgaard, J.C., Jakobsen, H.H., Pohnert, G., 2010. Growth phase of the diatom *Skeletonema marinoi* influences the metabolic profile of the cells and the selective feeding of the copepod *Calanus* spp. J. Plankton Res. 32(3), 263-272.

Barofsky, A., Vidoudez, C., Pohnert, G., 2009. Metabolic profiling reveals growth stage variability in diatom exudates. Limnol. Oceanogr.: Methods 7, 382-390.

Becker, J., Berube, P., Follett, C., Waterbury, J., Chisholm, S.W., DeLong, E., Repeta, D., 2014. Closely related phytoplankton species produce similar suites of dissolved organic matter. Front. Microbiol. 5(111), doi: 10.3389/fmicb.2014.00111.

Bell, T.G., Poulton, A.J., Malin, G., 2010. Strong linkages between dimethylsulphoniopropionate (DMSP) and phytoplankton community physiology in a large subtropical and tropical Atlantic Ocean data set. Global Biogeochem. Cycles 24(3).

Bromke, M.A., 2013. Amino acid biosynthesis pathways in diatoms. Metabolites 3(2), 294-311.

Buchan, A., LeCleir, G.R., Gulvik, C.A., Gonzalez, J.M., 2014. Master recyclers: features and functions of bacteria associated with phytoplankton blooms. Nat. Rev. Microbiol. 12(10), 686-698.

Calbet, A., Saiz, E., Almeda, R., Movilla, J.I., Alcaraz, M., 2011. Low microzooplankton grazing rates in the Arctic Ocean during a *Phaeocystis pouchetii* bloom (Summer 2007): Fact or artifact of the dilution technique? J. Plankton Res. 33(5), 687-701.

Cole, J.J., 1982. Interactions between bacteria and algae in aquatic ecosystems. Annu. Rev. Ecol. Syst. 13, 291-314.

Collos, Y., 1998. Nitrate uptake, nitrite release and uptake, and new production estimates. Mar. Ecol.: Prog. Ser. 171, 293-301.

Dalsgaard, J., St. John, M., Kattner, G., Müller-Navarra, D., Hagen, W., 2003. Fatty acid trophic markers in the pelagic marine environment. Adv. Mar. Biol. 46, 225-340.

Davison, I.R., Reed, R.H., 1985. The physiological significance of mannitol accumulation in brown algae: the role of mannitol as a compatible cytoplasmic solute. Phycologia 24(4), 449-457.

Degerlund, M., Eilertsen, H.C., 2010. Main species characteristics of phytoplankton spring blooms in NE Atlantic and Arctic waters (68–80° N). Estuaries Coasts 33(2), 242-269.

Dittami, S.M., Aas, H.T.N., Paulsen, B.S., Boyen, C., Edvardsen, B., Tonon, T., 2011a. Mannitol in six autotrophic stramenopiles and *Micromonas*. Plant Signaling Behav. 6(8), 1237-1239.

Dittami, S.M., Gravot, A., Renault, D., Goulitquer, S., Eggert, A., Bouchereau, A., Boyen, C., Tonon, T., 2011b. Integrative analysis of metabolite and transcript abundance during the short-term response to saline and oxidative stress in the brown alga *Ectocarpus siliculosus*. Plant Cell Environ. 34(4), 629-642.

Estep, K.W., Nejstgaard, J.C., Skjoldal, H.R., Rey, F., 1990. Predation by copepods upon natural populations of *Phaeocystis pouchetii* as a function of the physiological state of the prey. Mar. Ecol.: Prog. Ser. 67(3), 235-249.

Fiore, C.L., Longnecker, K., Kido Soule, M.C., Kujawinski, E.B., 2015. Release of ecologically relevant metabolites by the cyanobacterium *Synechococcus elongates* CCMP 1631. Environ. Microbiol. 17(10), 3949-3963.

Foyer, C.H., Shigeoka, S., 2011. Understanding oxidative stress and antioxidant functions to enhance photosynthesis. Plant Physiol. 155(1), 93-100.

Francko, D.A., Wetzel, R.G., 1980. Cyclic adenosine-3'-5'-monophosphate - production and extracellular release from green and blue-green-algae. Physiol. Plant. 49(1), 65-67.

Franklin, D.J., Airs, R.L., Fernandes, M., Bell, T.G., Bongaerts, R.J., Berges, J.A., Malin, G., 2012. Identification of senescence and death in *Emiliania huxleyi* and *Thalassiosira pseudonana*: Cell staining, chlorophyll alterations, and dimethylsulfoniopropionate (DMSP) metabolism. Limnol. Oceanogr. 57(1), 305-317.

Granum, E., Kirkvold, S., Myklestad, S.M., 2002. Cellular and extracellular production of carbohydrates and amino acids by the marine diatom *Skeletonema costatum*: diel variations and effects of N depletion. Mar. Ecol. Prog. Ser. 242, 83-94.

Guillard, R.R.L., 1975. Culture of phytoplankton for feeding marine invertebrates, Culture of marine invertebrate animals. Springer US, pp. 29-60.

Hamana, K., Niitsu, M., 2006. Cellular polyamines of lower eukaryotes belonging to the phyla Glaucophyta, Rhodophyta, Cryptophyta, Haptophyta and Percolozoa. J. Gen. Appl. Microbiol. 52(4), 235-240.

Hamm, C., Reigstad, M., Riser, C.W., Mühlebach, A., Wassmann, P., 2001. On the trophic fate of *Phaeocystis pouchetii*. VII. Sterols and fatty acids reveal sedimentation of *P. pouchetii*-derived organic matter via krill fecal strings. Mar. Ecol. Prog. Ser. 209, 55-69.

Hansen, B., Bjørnsen, P.K., Hansen, P.J., 1994. The size ratio between planktonic predators and their prey. Limnol. Oceanogr. 39(2), 395-403.

Hansen, H.P., Koroleff, F., 2007. Determination of nutrients, Methods of Seawater Analysis. Wiley-VCH Verlag GmbH, pp. 159-228.

Hiller, K., Hangebrauk, J., Jäger, C., Spura, J., Schreiber, K., Schomburg, D., 2009. MetaboliteDetector: Comprehensive analysis tool for targeted and nontargeted GC-MS based metabolome analysis. Anal. Chem. 81(9), 3429-3439.

Hirth, M., Liverani, S., Mahlow, S., Bouget, F.-Y., Pohnert, G., Sasso, S., 2017. Metabolic profiling identifies trehalose as an abundant and diurnally fluctuating metabolite in the microalga *Ostreococcus tauri*. Metabolomics 13(6), 68.

Huidobro-Toro, J.P., Donoso, V., Flores, V., Santelices, B., 2015. ATP and related purines stimulate motility, spatial congregation, and coalescence in red algal spores. J. Phycol. 51(2), 247-254.

Huntley, M., Tande, K., Eilertsen, H.C., 1987. On the trophic fate of *Phaeocystis pouchetii* (Hariot). 2. Grazing rates of *Calanus hyperboreus* (Krøyer) on diatoms and different size categories of *Phaeocystis pouchetii*. J. Exp. Mar. Biol. Ecol. 110(3), 197-212.

Jacobsen, A., Veldhuis, M.J.W., 2005. Growth characteristics of flagellated cells of *Phaeocystis pouchetii* revealed by diel changes in cellular DNA content. Harmful Algae 4(5), 811-821.

Jonasdottir, S.H., Dutz, J., Koski, M., Yebra, L., Jakobsen, H.H., Vidoudez, C., Pohnert, G., Nejstgaard, J.C., 2011. Extensive cross-disciplinary analysis of biological and chemical control of *Calanus finmarchicus* reproduction during an aldehyde forming diatom bloom in mesocosms. Mar. Biol. 158(9), 1943-1963.

Kambourova, R., Bankova, V., Petkov, C., 2004. Extracellular lipophilic substances of green alga *Scenedesmus*. C. R. Acad. Bulg. Sci. 57(11), 11: 77.

Kobayashi, Y., Torii, A., Kato, M., Adachi, K., 2007. Accumulation of cyclitols functioning as compatible solutes in the haptophyte alga *Pavlova* sp. Phycol. Res. 55(2), 81-90.

Koo, I., Shi, X., Kim, S., Zhang, X., 2014. *iMatch2*: Compound identification using retention index for analysis of gas chromatography-mass spectrometry data. J. Chromatogr. A 1337, 202-210.

Kuhlisch, C., Pohnert, G., 2015. Metabolomics in chemical ecology. Nat. Prod. Rep. 32(7), 937-955.

Labeeuw, L., Khey, J., Bramucci, A.R., Atwal, H., de la Mata, A.P., Harynuk, J., Case, R.J., 2016. Indole-3-acetic acid is produced by *Emiliania huxleyi* coccolith-bearing cells and triggers a physiological response in bald cells. Front. Microbiol. 7, 828.

Lasternas, S., Agustí, S., 2010. Phytoplankton community structure during the record Arctic ice-melting of summer 2007. Polar Biol. 33(12), 1709-1717.

Lau, S., Shao, N., Bock, R., Jürgens, G., De Smet, I., 2009. Auxin signaling in algal lineages: fact or myth? Trends Plant Sci. 14(4), 182-188.

Llewellyn, C.A., Sommer, U., Dupont, C.L., Allen, A.E., Viant, M.R., 2015. Using community metabolomics as a new approach to discriminate marine microbial particulate organic matter in the western English Channel. Prog. Oceanogr. 137, Part B, 421-433.

Loewus, F., 1971. Carbohydrate interconversions. Ann. Rev. Plant Physiol. 22, 337-364.

Loewus, F.A., Murthy, P.P.N., 2000. Myo-Inositol metabolism in plants. Plant Sci. 150(1), 1-19.

Lomas, M.W., Lipschultz, F., 2006. Forming the primary nitrite maximum: Nitrifiers or phytoplankton? Limnol. Oceanogr. 51(5), 2453-2467.

Longnecker, K., Futrelle, J., Coburn, E., Kido Soule, M.C., Kujawinski, E.B., 2015a. Environmental metabolomics: Databases and tools for data analysis. Mar. Chem. 177, Part 2, 366-373.

Longnecker, K., Kido Soule, M.C., Kujawinski, E.B., 2015b. Dissolved organic matter produced by *Thalassiosira pseudonana*. Mar. Chem. 168, 114-123.

Lu, Y.H., Hwang, D.-F., 2002. Polyamine profile in the paralytic shellfish poison-producing alga *Alexandrium minutum*. J. Plankton Res. 24(3), 275-279.

Ludwig-Müller, J., 2000. Indole-3-butyric acid in plant growth and development. Plant Growth Regul. 32(2), 219-230.

Mausz, M.A., Pohnert, G., 2015. Phenotypic diversity of diploid and haploid *Emiliania huxleyi* cells and of cells in different growth phases revealed by comparative metabolomics. J. Plant Physiol. 172, 137-148.

Mayzaud, P., Chanut, J.P., Ackman, R.G., 1989. Seasonal changes of the biochemical composition of marine particulate matter with special reference to fatty acids and sterols. Mar. Ecol. Prog. Ser. 56(1/2), 189-204.

Meyer, N., Bigalke, A., Kaulfuss, A., Pohnert, G., 2017. Strategies and ecological roles of algicidal bacteria. FEMS Microbiol. Rev. 41(6), 880-899.

Morán, X.A.G., Gasol, J.M., Arin, L., Estrada, M., 1999. A comparison between glass fiber and membrane filters for the estimation of phytoplankton POC and DOC production. Mar. Ecol. Prog. Ser. 187, 31-41.

Mühlroth, A., Li, K., Røkke, G., Winge, P., Olsen, Y., Hohmann-Marriott, M.F., Vadstein, O., Bones, A.M., 2013. Pathways of lipid metabolism in marine algae, co-expression network, bottlenecks and candidate genes for enhanced production of EPA and DHA in species of Chromista. Mar. Drugs 11(11), 4662-4697.

Nejstgaard, J.C., Frischer, M.E., Verity, P.G., Anderson, J.T., Jacobsen, A., Zirbel, M.J., Larsen, A., Martinez-Martinez, J., Sazhin, A.F., Walters, T., Bronk, D.A., Whipple, S.J., Borrett, S.R., Patten, B.C., Long, J.D., 2006. Plankton development and trophic transfer in seawater enclosures with nutrients and *Phaeocystis pouchetii* added. Mar. Ecol. Prog. Ser. 321, 99-121.

Nejstgaard, J.C., Tang, K.W., Steinke, M., Dutz, J., Koski, M., Antajan, E., Long, J.D., 2007. Zooplankton grazing on *Phaeocystis*: a quantitative review and future challenges. Biogeochemistry 83(1-3), 147-172.

Nichols, P.D., Palmisano, A.C., Rayner, M.S., Smith, G.A., White, D.C., 1989. Changes in the lipid composition of Antarctic sea-ice diatom communities during a spring bloom: an indication of community physiological status. Antarct. Sci. 1(2), 133-140.

Nichols, P.D., Skerratt, J.H., Davidson, A., Burton, H., McMeekin, T.A., 1991. Lipids of cultured *Phaeocystis pouchetii* - Signatures for food-web, biogeochemical and environmental studies in Antarctica and the Southern-Ocean. Phytochemistry 30(10), 3209-3214.

Norrbin, F., Eilertsen, H.C., Degerlund, M., 2009. Vertical distribution of primary producers and zooplankton grazers during different phases of the Arctic spring bloom. Deep-Sea Res. Part II-Top. Stud. Oceanogr. 56(21-22), 1945-1958.

Nöthig, E.-M., Bracher, A., Engel, A., Metfies, K., Niehoff, B., Peeken, I., Bauerfeind, E., Cherkasheva, A., Gäbler-Schwarz, S., Hardge, K., Kilias, E., Kraft, A., Mebrahtom Kidane, Y., Lalande, C., Piontek, J., Thomisch, K., Wurst, M., 2015. Summertime plankton ecology in Fram Strait - a compilation of long- and short-term observations. Polar Res. 34(1), 23349.

Obata, T., Schoenefeld, S., Krahnert, I., Bergmann, S., Scheffel, A., Fernie, A.R., 2013. Gas-chromatography mass-spectrometry (GC-MS) based metabolite profiling reveals mannitol as a major storage carbohydrate in the coccolithophorid alga *Emiliania huxleyi*. Metabolites 3(1), 168-184.

Okada, T., Kuwamoto, T., 1985. Potassium hydroxide eluent for nonsuppressed anion chromatography of cyanide, sulfide, arsenite, and other weak acids. Anal. Chem. 57(4), 829-833.

Parsons, Harriet T., Yasmin, T., Fry, Stephen C., 2011. Alternative pathways of dehydroascorbic acid degradation *in vitro* and in plant cell cultures: novel insights into vitamin C catabolism. Biochem. J. 440(3), 375-385.

Parsons, T., Maita, Y., Lalli, C., 1984. Manual of chemical and biological methods for seawater analysis, Manual of chemical and biological methods for seawater analysis. Pergamon.

Paul, C., Mausz, M.A., Pohnert, G., 2013. A co-culturing/metabolomics approach to investigate chemically mediated interactions of planktonic organisms reveals influence of bacteria on diatom metabolism. Metabolomics 9(2), 349-359.

Pfaff, S., Gustavs, L., Reichardt, A., Jaskulke, R., Ewald, H., Gäbler-Schwarz, S., Karsten, U., 2016. Ecophysiological plasticity in the Arctic phytoplankton species *Phaeocystis pouchetii* (Prymnesiophyceae, Haptophyta). Algol. Stud. 151(1), 87-102.

Piotrowska-Niczyporuk, A., Bajguz, A., 2014. The effect of natural and synthetic auxins on the growth, metabolite content and antioxidant response of green alga *Chlorella vulgaris* (Trebouxiophyceae). Plant Growth Regul. 73(1), 57-66.

Pohnert, G., Steinke, M., Tollrian, R., 2007. Chemical cues, defence metabolites and the shaping of pelagic interspecific interactions. Trends Ecol. Evol. 22(4), 198-204.

Pree, B., Kuhlisch, C., Pohnert, G., Sazhin, A.F., Jakobsen, H.H., Paulsen, M.L., Frischer, M.E., Stoecker, D., Nejstgaard, J.C., Larsen, A., 2016. A simple adjustment to test reliability of bacterivory rates derived from the dilution method. Limnol. Oceanogr.: Methods 14(2), 114-123.

Rajamani, S., Bauer, W.D., Robinson, J.B., Farrow, J.M., Pesci, E.C., Teplitski, M., Gao, M., Sayre, R.T., Phillips, D.A., 2008. The vitamin riboflavin and its derivative lumichrome activate the LasR bacterial quorum sensing receptor. Molecular plant-microbe interactions : MPMI 21(9), 10.1094/MPMI-1021-1099-1184.

Rat'kova, T.N., Wassmann, P., 2002. Seasonal variation and spatial distribution of phyto- and protozooplankton in the central Barents Sea. J. Mar. Syst. 38(1-2), 47-75.

Ray, J.L., Althammer, J., Skaar, K.S., Simonelli, P., Larsen, A., Stoecker, D., Sazhin, A., Ijaz, U.Z., Quince, C., Nejstgaard, J.C., Frischer, M., Pohnert, G., Troedsson, C., 2016a. Metabarcoding and metabolome analyses of copepod grazing reveal feeding preference

and linkage to metabolite classes in dynamic microbial plankton communities. Mol. Ecol. 25(21), 5585-5602.

Ray, J.L., Skaar, K.S., Simonelli, P., Larsen, A., Sazhin, A., Jakobsen, H.H., Nejstgaard, J.C., Troedsson, C., 2016b. Molecular gut content analysis demonstrates that *Calanus* grazing on *Phaeocystis pouchetii* and *Skeletonema marinoi* is sensitive to bloom phase but not prey density. Mar. Ecol.: Prog. Ser. 542, 63-77.

Ray, J.L., Skaar, K.S., Simonelli, P., Larsen, A., Sazhin, A., Jakobsen, H.H., Nejstgaard, J.C., Troedsson, C., 2016c. Molecular gut content analysis demonstrates that *Calanus* grazing on *Phaeocystis pouchetii* and *Skeletonema marinoi* is sensitive to bloom phase but not prey density. Mar. Ecol. Prog. Ser. 542, 63-77.

Reigstad, M., Wassmann, P., 2007. Does *Phaeocystis* spp. contribute significantly to vertical export of organic carbon? Biogeochemistry 83(1-3), 217-234.

Reigstad, M., Wassmann, P., Ratkova, T., Arashkevich, E., Pasternak, A., Oygarden, S., 2000. Comparison of the springtime vertical export of biogenic matter in three northern Norwegian fjords. Mar. Ecol. Prog. Ser. 201, 73-89.

Rodgers, P., Flower, J., Stapleton, G., Howse, J., 2010. Drawing area-proportional venn-3 diagrams with convex polygons, In: Goel, A.K., Jamnik, M., Narayanan, N.H. (Eds.), Diagrammatic Representation and Inference: 6th International Conference, Diagrams 2010, Portland, OR, USA, August 9-11, 2010. Proceedings. Springer Berlin Heidelberg, Berlin, Heidelberg, pp. 54-68.

Rodhe, W., Vollenweider, R.A., Nauwerck, A., 1958. The primary production and standing crop of phytoplankton, In: Traverso, A.A. (Ed.), Perspectives in Marine Biology. University of California Press, pp. 299-322.

Roessler, P.G., 1990. Environmental control of glyerolipid metabolism in microalgae: Commercial implicatioins and future research directions. J. Phycol. 26(3), 393-399.

Rontani, J.-F., 2001. Visible light-dependent degradation of lipidic phytoplanktonic components during senescence: a review. Phytochemistry 58(2), 187-202.

Rousseau, V., Chretiennot-Dinet, M.J., Jacobsen, A., Verity, P., Whipple, S., 2007. The life cycle of *Phaeocystis*: state of knowledge and presumptive role in ecology. Biogeochemistry 83(1-3), 29-47.

Rousseau, V., Vaulot, D., Casotti, R., Cariou, V., Lenz, J., Gunkel, J., Baumann, M., 1994. The life-cycle of *Phaeocystis* (Prymnesiophyceae) - Evidence and hypotheses. J. Mar. Syst. 5(1), 23-39.

Saiz, E., Calbet, A., Isari, S., Anto, M., Velasco, E.M., Almeda, R., Movilla, J., Alcaraz, M., 2013. Zooplankton distribution and feeding in the Arctic ocean during a *Phaeocystis pouchetii* bloom. Deep Sea Res., Part I 72, 17-33.

Sazhin, A.F., Artigas, L.F., Nejstgaard, J.C., Frischer, M.E., 2007. The colonization of two *Phaeocystis* species (Prymnesiophyceae) by pennate diatoms and other protists: a significant contribution to colony biomass. Biogeochemistry 83(1-3), 137-145.

Schlitzer, R., 2016. Ocean Data View, https://odv.awi.de.

Segev, E., Wyche, T.P., Kim, K.H., Petersen, J., Ellebrandt, C., Vlamakis, H., Barteneva, N., Paulson, J.N., Chai, L., Clardy, J., Kolter, R., 2016. Dynamic metabolic exchange governs a marine algal-bacterial interaction. eLife 5, e17473.

Sherr, B., Sherr, E., del Giorgio, P., 2001. Enumeration of total and highly active bacteria. Methods Microbiol. 30, 129-159.

Slagstad, D., Ellingsen, I.H., Wassmann, P., 2011. Evaluating primary and secondary production in an Arctic Ocean void of summer sea ice: an experimental simulation approach. Prog. Oceanogr. 90(1–4), 117-131.

Soltwedel, T., Bauerfeind, E., Bergmann, M., Bracher, A., Budaeva, N., Busch, K., Cherkasheva, A., Fahl, K., Grzelak, K., Hasemann, C., Jacob, M., Kraft, A., Lalande, C., Metfies, K., Nöthig, E.-M., Meyer, K., Quéric, N.-V., Schewe, I., Włodarska-Kowalczuk, M., Klages, M., 2016. Natural variability or anthropogenically-induced variation? Insights from 15 years of multidisciplinary observations at the Arctic marine LTER site HAUSGARTEN. Ecol. Indic. 65, 89-102.

Sumner, L.W., Amberg, A., Barrett, D., Beale, M.H., Beger, R., Daykin, C.A., Fan, T.W.M., Fiehn, O., Goodacre, R., Griffin, J.L., Hankemeier, T., Hardy, N., Harnly, J., Higashi, R., Kopka, J., Lane, A.N., Lindon, J.C., Marriott, P., Nicholls, A.W., Reily, M.D., Thaden, J.J., Viant, M.R., 2007. Proposed minimum reporting standards for chemical analysis. Metabolomics 3(3), 211-221.

Tande, K.S., Båmstedt, U., 1987. On the trophic fate of *Phaeocystis pouchetii*. 1. Copepod feeding rates on solitary cells and colonies of *Phaeocystis pouchetii*. Sarsia 72(3-4), 313-320.

Thornton, D.C.O., 2014. Dissolved organic matter (DOM) release by phytoplankton in the contemporary and future ocean. Eur. J. Phycol. 49(1), 20-46.

Tolbert, N.E., Zill, L.P., 1956. Excretion of glycolic acid by algae during photosynthesis. The Journal of biological chemistry 222(2), 895-906.

Torres, J., Rivera, A., Clark, G., Roux, S.J., 2008. Participation of extracellular nucleotides in the wound response of *Dasycladus ermicularis* and *Acetabularia acetabulum* (Dasycladales, Chlorophyta). J. Phycol. 44(6), 1504-1511.

Tsuji, Y., Suzuki, I., Shiraiwa, Y., 2009. Photosynthetic carbon assimilation in the coccolithophorid *Emiliania huxleyi* (Haptophyta): Evidence for the predominant operation of the C3 cycle and the contribution of β-carboxylases to the active anaplerotic reaction. Plant Cell Physiol. 50(2), 318-329.

Van den Dool, H., Kratz, P.D., 1963. A generalization of the retention index system including linear temperature programmed gas-liquid partition chromatography. J. Chromatogr. A 11, 463-471.

Vardi, A., Van Mooy, B.A., Fredricks, H.F., Popendorf, K.J., Ossolinski, J.E., Haramaty, L., Bidle, K.D., 2009. Viral glycosphingolipids induce lytic infection and cell death in marine phytoplankton. Science 326(5954), 861-865.

Verity, P.G., Whipple, S.J., Nejstgaard, J.C., Alderkamp, A.C., 2007a. Colony size, cell number, carbon and nitrogen contents of *Phaeocystis pouchetii* from western Norway. J. Plankton Res. 29(4), 359-367.

Verity, P.G., Zirbel, M.J., Nejstgaard, J.C., 2007b. Formation of very young colonies by *Phaeocystis pouchetii* from western Norway. Aquat. Microb. Ecol. 47(3), 267-274.

Vidoudez, C., Pohnert, G., 2008. Growth phase-specific release of polyunsaturated aldehydes by the diatom *Skeletonema marinoi*. J. Plankton Res. 30(11), 1305-1313.

Vidoudez, C., Pohnert, G., 2012. Comparative metabolomics of the diatom *Skeletonema marinoi* in different growth phases. Metabolomics 8(4), 654-669.

Vogt, M., O'Brien, C., Peloquin, J., Schoemann, V., Breton, E., Estrada, M., Gibson, J., Karentz, D., Van Leeuwe, M.A., Stefels, J., Widdicombe, C., Peperzak, L., 2012. Global marine plankton functional type biomass distributions: *Phaeocystis* spp. Earth Syst. Sci. Data 4(1), 107-120.

Walsh, C.T., Garneau-Tsodikova, S., Howard-Jones, A.R., 2006. Biological formation of pyrroles: Nature's logic and enzymatic machinery. Nat. Prod. Rep. 23(4), 517-531.

Wassmann, P., Ratkova, T., Reigstad, M., 2005. The contribution of single and colonial cells of *Phaeocystis pouchetii* to spring and summer blooms in the north-eastern North Atlantic. Harmful Algae 4(5), 823-840.

Wassmann, P., Reigstad, M., 2011. Future Arctic Ocean seasonal ice zones and implications for pelagic-benthic coupling. Oceanography 24(3), 220-231.

Werner, D., 1971. The life cycle with sexual phase in the marine diatom *Coscinodiscus asteromphalus*. III. Differentiation and spermatogenesis. Arch. Mikrobiol. 80(2), 134-146.

Whipple, S.J., Patten, B.C., Verity, P.G., Frischer, M.E., Long, J.D., Nejstgaard, J.C., Anderson, J.T., Jacobsen, A., Larsen, A., Martinez-Martinez, J., Borrett, S.R., 2007. Gaining integrated understanding of *Phaeocystis* spp. (Prymnesiophyceae) through model-driven laboratory and mesocosm studies. Biogeochemistry 83(1-3), 293-309.

White, D.A., Widdicombe, C.E., Somerfield, P.J., Airs, R.L., Tarran, G.A., Maud, J.L., Atkinson, A., 2015. The combined effects of seasonal community succession and adaptive algal physiology on lipid profiles of coastal phytoplankton in the Western English Channel. Mar. Chem. 177, 638-652.

Xia, J., Wishart, D.S., 2016. Using MetaboAnalyst 3.0 for comprehensive metabolomics data analysis. Curr. Protoc. Bioinformatics 55, 14. 10. 11-14. 10. 91.

Xue, L.-L., Chen, H.-H., Jiang, J.-G., 2017. Implications of glycerol metabolism for lipid production. Prog. Lipid Res. 68, 12-25.

Zhang, Y., Liu, Y., Cao, X., Gao, P., Liu, X., Wang, X., Zhang, J., Zhou, J., Xue, S., Xu, G., Tian, J., 2016. Free amino acids and small molecular acids profiling of marine microalga *Isochrysis zhangjiangensis* under nitrogen deficiency. Algal Res. 13, 207-217.

Publication P4:

"A simple adjustment to test reliability of bacterivory rates derived from the dilution method"

B. Pree, C. Kuhlisch, G. Pohnert, A. F. Sazhin, H. H. Jakobsen, M. Lund Paulsen, M. E. Frischer, D. Stoecker, J. C. Nejstgaard, and A. Larsen

Limnol. Oceanogr.: Methods, 2016, **14**, 114-123.

The supplementary information of this publication is available in the Appendix.

LIMNOLOGY
and
OCEANOGRAPHY: METHODS

ASLO

Limnol. Oceanogr.: Methods 00, 2015, 00–00

doi: 10.1002/lom3.10076

A simple adjustment to test reliability of bacterivory rates derived from the dilution method

Bernadette Pree,*[1] Constanze Kuhlisch,[2] Georg Pohnert,[2] Andrey F. Sazhin,[3] Hans Henrik Jakobsen,[4] Maria Lund Paulsen,[1] Marc E. Frischer,[5] Diane Stoecker,[6] Jens C. Nejstgaard,[7] Aud Larsen[8]

[1]Department of Biology, University of Bergen, Bergen, Norway
[2]Institute for Inorganic and Analytical Chemistry, Friedrich Schiller University Jena, Jena, Germany
[3]Laboratory of Plankton Ecology, P.P. Shirshov Institute of Oceanology, Russian Academy of Sciences, Moscow, Russia
[4]Department of Bioscience, Aarhus University, Roskilde, Denmark
[5]Skidaway Institute of Oceanography, University of Georgia, Savannah, Georgia
[6]Horn Point Laboratory, University of Maryland Center for Environmental Science, Cambridge, Maryland
[7]Department 3, Experimental Limnology, Leibnitz-Institute of Freshwater Ecology and Inland Fisheries (IGB), Stechlin, Germany
[8]Uni Research Environment and Hjort Centre for Marine Ecosystem Dynamics, Bergen, Norway

Abstract

Quantification of grazing losses of marine heterotrophic bacteria is critical for understanding nutrient and carbon pathways in aquatic systems. The dilution method is a commonly used experimental approach for quantifying bacterivory. However, valid estimates of grazing rates obtained using this method depend on several methodological assumptions including that the method does not influence specific growth rates of bacteria. Here, we hypothesize that filtration during the set-up of a dilution experiment has the potential to release allelochemicals from phytoplankton cells and thereby stimulate or inhibit bacterial growth with the consequence of biased grazing estimates. We tested this hypothesis during a natural *Phaeocystis pouchetii* bloom at two different locations within an Arctic fjord. Results from the dilution experiments suggest higher gross growth rate and grazing impact for bacteria in the outer fjord compared with the inner fjord. However, specific growth rates estimated by bacterial production cell^{-1} were significantly elevated in dilutions of water from the outer fjord but not the inner fjord. The analysis of dissolved metabolites in the seawater from both experiments prior and after filtration revealed altered metabolic profiles after filtration at both stations. As unaffected specific growth of prey on dilution is one of three fundamental assumptions of the dilution method, we conclude that it is important that empirically estimated bacterial specific growth rates be routinely included when using the dilution method to quantify bacterivory.

Marine heterotrophic prokaryotes (subsequently referred to as bacteria) are important players on a global scale in biogeochemical processes, such as nutrient uptake, carbon cycling and remineralization. Whereas methods for determination of bacterial abundance, community composition and activity are well established today, quantification of bacterial interactions with other components of the microbial food web and their dynamics remain a major challenge in the field. Grazing by heterotrophic nanoflagellates (HNF) and microzooplankton on bacteria is, together with viral lysis, the main cause of bacterial mortality (Proctor and Fuhrman 1990; Sherr and Sherr 1994; Suttle 2007). Direct measurement of bacterivory is challenging and a range of experimental methods have evolved, which can be categorized into three approaches. First, the use of fluorescent-labeled (Sherr et al. 1987) or radio-labeled (Lessard and Swift 1985) bacteria, second, the use of size fractionation (Wright and Coffin 1984) or dilution (Anderson and Rivkin 2001; Evans et al. 2003; Pearce et al. 2010; Pearce et al. 2011) to uncouple predator and prey, and third, the direct inspection of food vacuoles of predators (Dolan and Simek 1999). Often, the different approaches give results which are not necessarily

Additional Supporting Information may be found in the online version of this article.

*Correspondence: bernadette.pree@uib.no

Table 1. Definitions of bacterial growth rates (d^{-1}).

Net growth rate (k)	Change of bacterial numbers over time in presence of grazers and viruses, often referred to as *apparent growth* (Landry and Hassett 1982)
Gross growth rate (μ)	Change of bacterial numbers over time in absence of grazers and viruses, in dilution experiments μ corresponds to the *y*-axis intercept (Landry et al. 1995)
Specific growth rate ($\mu_{specific}$)	Rate of biomass production per unit biomass as estimated from leucine incorporation (biomass per time unit per volume) of bacterial abundance (biomass or cell concentration per volume). Due to short incubation time (1 h typically), it is usually used as an estimate for gross growth rate (Ducklow 2000; Kirchman 2001), and sometimes referred to as *independent growth measure* (e.g., Pasulka et al. 2015)

comparable because each approach contains shortcomings not resolved yet (Vaque et al. 1994).

In comparison to the methods using labeled bacteria or food vacuole inspection, the major advantage of size fractionation and the dilution technique is their ability to estimate both grazing and growth of the prey community (net and gross growth). In size fractionation experiments growth and grazing are based only on comparison between predator-free incubations and untreated incubations. The dilution method includes a gradient of dilution with predator-free water and thereby, theoretically results in a more accurate estimate of grazing and growth rates.

The dilution method (Landry and Hassett 1982) was designed to estimate growth and grazing losses of phytoplankton but has also been applied to determination of bacterial growth and bacterivory (Anderson and Rivkin 2001; Evans et al. 2003; Pearce et al. 2010, 2011). For both prey organisms, weaknesses of the dilution method include the need for experimental manipulation and the typically long incubation time of 24 h (Landry 1994; Schmoker et al. 2013). Several studies revealed that preparation of dilutions by addition of whole seawater (WSW) to filtered seawater (FSW) can result in changed grazer behavior (Moigis 2006), differences in bacterial community composition (Agis et al. 2007), and enrichment of organic and inorganic nutrients (Ferguson et al. 1984). During some phytoplankton blooms, such as *Phaeocystis pouchetii* which is known to release organic material [review by Alderkamp et al. (2007)], preparation of FSW can cause release of dissolved metabolites that can inhibit phytoplankton growth in diluted treatments (Stoecker et al. 2015). Measurements of bacterivory may be more sensitive to experimental manipulation and long incubation times than measurements of herbivory because of the great potential of bacteria to be both stimulated and/or inhibited by released metabolites or nutrients and the relatively rapid response times of bacteria compared with phytoplankton assemblages.

In this study, we applied the dilution technique to measure bacterivory during a *P. pouchetii* bloom in coastal Arctic waters. Two locations within a fjord (inner and outer fjord, subsequently referred to as IF and OF) were selected for setting-up dilution experiments. We tested the hypotheses that (1) 0.2 μm filtration of seawater during the set-up of a dilution experiment alters the metabolic profile of the water with a chance to release allelochemicals and as a consequence (2) the addition of 0.2 μm filtered water to the diluted treatments impacts specific growth of bacteria (see Table 1 for definition of bacterial growth) and thereby violating one of the central assumptions of the dilution technique (Landry and Hassett 1982). To address these hypotheses, we measured bacterial concentrations and bacterial production (Smith and Azam 1992) in the WSW and diluted treatments as well as comparing metabolic profiles of the WSW and the FSW used for dilution.

This combination of biological and chemical measurements allowed us to evaluate the reliability of the dilution technique for measuring bacterivory during *P. pouchetii* blooms and to recommend procedures for applying the dilution technique to measurement of bacterivory.

Materials and procedures

Theoretical outline of dilution method for bacterivory

The dilution technique uses incubations of WSW and dilutions (typically 1–4 dilutions in fraction 10%, 25%, 50%, 75% of sample to WSW) to derive estimates of net growth rate (= apparent growth rate, k) at different densities of grazers based on bulk measurements of biomass or cell counts. Landry and Hassett (1982) state 3 crucial assumptions of the method, first that growth rate of prey (μ) is not affected by dilution, second, that grazing loss (g) is proportional to grazer abundance (D=dilution factor). Third, growth of prey is assumed to be exponential, as described in Eq. 1 (Landry and Hassett 1982), where k is apparent growth rate and P_t and P_0 biomass/concentration of prey at the end and start of the incubation.

$$k = \frac{1}{t} \ln \left(\frac{P_t}{P_0} \right) \quad (1)$$

When these three assumptions are met, linear regression analysis of net growth rates of prey against dilution factor results in an reliable estimate of grazing (g, slope) and growth of the prey population in absence of any grazing (μ,

y-axis intercept) as shown in Eq. 2 (Landry and Hassett 1982).

$$k = \mu - (g \times D) \quad (2)$$

Several studies have tested whether these assumptions are met when using the dilution method for herbivory, as reviewed in Schmoker et al. (2013), but only a few studies have tested these assumptions with bacteria as prey organisms despite increased use of the dilution method to quantify bacterivory. Tremaine and Mills (1987) addressed each of the three assumptions when using the method for bacterivory and tested the first assumption by including different concentrations of dissolved organic carbon (DOC) in the dilutions to simulate potential increase in DOC in the diluent due to shear stress on cells during filtration. They found increased growth with increasing carbon concentrations, although not statistically significant. Berninger and Wickham (2005) also tested the first assumption by including one set of replicates with amended nutrients to ensure no nutrient limitation was given. However, specific growth of bacteria may not only be affected by dissolved nutrients or organic matter in the seawater but also by presence or absence of dissolved metabolites caused by release from phytoplankton cells or adsorbance/breakdown during filtration. Here, we argue that 0.2 μm filtration during the preparation of dilutions alters concentrations of dissolved metabolites and consequently affects specific growth rate of bacteria. We suggest that cell specific rates of incorporation of radioactive precursors, such as leucine, can be used as index of specific growth as shown in Eq. 3 (Ducklow 2000).

$$\mu_{\text{specific}} = \frac{BP_t}{P_t} \quad (3)$$

where μ_{specific} is converted from leucine uptake (BP_t, biomass d^{-1} $cell^{-1}$) of bacterial mass (P_t, biomass $cell^{-1}$ at the end of the experiment). Bacterial production measurement is a measure of "gross production" of biomass (Ducklow 2000; Kirchman 2001), and can serve as a relatively simple control during the dilution method to test the underlying assumption that specific growth of bacteria is not affected by dilution.

Study sites and sampling

The study was carried out during the PHAEONIGMA project cruise in May 2013 on board of R/V *Håkon Mosby*. Water for dilution experiments was collected at two different locations in the Porsangerfjord (ca. 70°32′N 26°31′E), northern Norway at the maximum fluorescence depth (20 m). The first experiment was conducted on 4–5th May 2013 in IF and the second experiment on 6–7th May in OF.

At the time of sampling there was an ongoing bloom of colonial *P. pouchetii* as assessed on board by FlowCAM imaging using a color FlowCAM (ver. VS IV) with the same settings as described in Jonasdottir et al. (2011). We estimated cell numbers using a calibrated regression between manually counted number of cells per colony and colony grey scale area (ABD) according to Jakobsen and Carstensen (2011). Cell carbon was then estimated assuming a *Phaeocystis* cell-volume of 60 μm^3 $cell^{-1}$ and the generic volume to carbon scaling of Menden-Deuer and Lessard (2000). *Phaeocystis* single cells (motile and nonmotile stages) and other phytoplankton were identified and enumerated by epifluorescence microscopy as described in Sazhin et al. (2007). In brief, samples were stained with primuline, fixed with 3.6% glutaraldehyde and gently filtered onto black Nucleopore filters (0.4 μm) and stored at −20°C until analysis.

Chlorophyll *a* (Chl *a*) was assessed in triplicate water samples (200–250 mL) according to Parsons et al. (1984). Water was filtered onto 47 mm 0.2 μm polycarbonate filters, and immediately frozen. Prior to measurement of fluorescence, Chl *a* was extracted in 90% acetone overnight at 4°C, and analyzed using a Turner Designs AU fluorometer.

Concentrations of dissolved inorganic nutrients (i.e., PO_4^{3-}, NO_3^- and dissolved Si), were determined by colorimetric continuous flow analysis by a Skalar San Plus autoanalyzer. Analysis procedures were done on routine basis following a standard ISO17025 accredited procedure according to the methods described by Hansen and Koroleff (1999). The precision was 0.06 μM, 0.1 μM and 0.2 μM for PO_4^{3-}, NO_3^- and dissolved Si, respectively.

Experimental set-up

Before dilution experiments, all containers, bottles, filters and tubing were soaked in 10% HCl and rinsed with ultra pure water. Water for dilution experiments was collected with Niskin (5 L) bottles attached to a CTD-rosette and transferred into 20 L containers (Nalgene). The experiments consisted of four dilutions in duplicates, in the proportions of 10%, 25%, 50%, and 70% of sample relatively to the sum of sample and filtered seawater, and triplicates of whole seawater (100%, WSW). Routinely in dilution experiments, nutrients (10 μM NO_3, 0.6 μM PO_4) were added to all dilutions, to avoid mineral nutrient limitation, except of another set of triplicates of WSW without nutrient addition, serving as control. Filtered seawater (FSW) was obtained by prefiltration through a 35 μm mesh and then gravity filtration through 0.2 μm sterile inline filter (Whatman Polycap capsule). Dilutions were prepared in 20 L Nalgene containers, and subsequently syphoned into experimental bottles (2.4 L) in a staggered way to ensure homogenous water masses between the replicates. All experimental bottles were incubated at in situ temperature (4–5°C) and light conditions ($\sim$ 6% surface irradiance) in a large volumetric container on-deck with running seawater pumped from ca. 2.5 m depth in the bow of the ship. Initial sampling for flow cytometry and bacterial production was done from remaining water from all dilutions and WSW and after 24 h of incubation from experimental bottles.

Bacteria net growth (k, d^{-1}) was calculated for each dilution and WSW treatments as in Eq. 1. Grazing (g) and gross growth rate (μ) of bacteria were calculated by linear regression analysis of net growth rate against dilution factor. Specific growth rates of bacteria were derived as shown in Eq. 3. Single analysis of variance (ANOVA) was used to test for significant differences ($p < 0.05$) among mean values of specific growth rates in the dilutions and WSW. For linear regression, ANOVA and calculation of diversity indices R-studio (including vegan-package, Oksanen et al. (2015)) was used.

Abundance of bacteria and heterotrophic nanoflagellates

Bacteria were enumerated using a FACSCalibur flow cytometer (BD, Biosciences, Franklin Lakes, New Jersey, U.S.A.) equipped with an air-cooled laser providing 15 mW at 488 nm with standard filter set-up. Samples for bacterial counts were fixed in glutaraldehyde (0.5% final conc.) for 30 min at 4°C, frozen in liquid nitrogen and stored at −80°C until further analysis. For analysis samples were thawed and diluted 5- to 100-fold in TE buffer (Tris 10 mM, EDTA 1mM, pH 8). Samples were stained with a green fluorescent nucleic-acid dye (SYBR Green I) for 10–15 min in the dark and run in the flow cytometer with the discriminator at green fluorescence and a flow rate of 30 μL min^{-1}. Bacterial population determination was based on scatter plot observations of the side-scatter signal vs. the green fluorescence signal of SYBR Green I. The cell numbers were calculated from the instrument flow rate based on volumetric measurements. For calculation of specific growth rates bacterial concentrations were converted to biomass using a carbon content of 20 fg C $cell^{-1}$ (Lee and Fuhrman 1987).

Abundances of HNF were determined on an Attune® Focusing Flow Cytometer (Applied Biosystems by Life technologies) with a syringe-based fluidic system and a 20 mW 488 nm laser. Samples were fixed and stored in the same manner as bacterial samples and were stained with SYBR Green I for 2 h in the dark and run in the flow cytometer with discrimination on basis of green and red fluorescence, side-scatter and forward-scatter following the protocol of Zubkov et al. (2007). Volumes of 800 μL were run using a flow rate of 200 μL min^{-1}.

Bacterial production

Bacterial production (BP) was determined by incorporation of ^{3}H-leucine as described in Smith and Azam (1992). Triplicate samples were incubated with ^{3}H-leucine (60 nM final concentration) for 1 h in the dark at in situ temperature in a water bath on-deck with continuous water flow. Protein synthesis was terminated by adding trichloroacetic acid (TCA) to a final concentration of 5%. A fourth sample served as control and was fixed with TCA before isotope addition. After incubation all samples were centrifuged (10 min) and the supernatant was removed and washed with TCA. The pellets were washed twice by adding 5% TCA followed by centrifugation. After removing the supernatant, scintillation cocktail (Ecoscint) was added and samples were radio assayed in a Tri-Carb 2900TR scintillation counter (PerkinElmer Life and Analytical Sciences, Waltham, Massachusetts). Disintegrations per minute (DPMs) from killed controls were subtracted from the average of live DPM. Incorporation rates of leucine were converted to bacterial production assuming a conversion factor of 1797 as the grams of protein produced per mole of incorporated leucine and 0.86 as the weight ratio (g: g) of total C: protein in bacteria (Simon and Azam 1989).

Dissolved metabolites within seawater

Sampling for metabolic profiles was done at both stations at Chl *a* maximum (IF, OF, $n = 3$) and during set-up of the dilution experiments of both unfiltered (IF-WSW, OF-WSW) and 0.2 μm gravity filtered sea water (IF-FSW, OF-FSW). Until processing water was kept in carboys in the dark at 15°C. For metabolic foot printing all particulate matter from 2–3 L WSW was gently removed under vacuum (600 mbar, GF/C filter) in analytical duplicates. Dissolved metabolites were absorbed to inline installed Chromabond® EASY solid phase extraction cartridges (Macherey-Nagel) which were conditioned with 4 mL methanol and rinsed with 4 mL ultra pure water prior sample loading (Barofsky et al. 2009). Loaded cartridges were rinsed again with 4 mL ultra pure water, dried with a vacuum pump, and gravity eluted with 2 mL methanol and 2 mL methanol: tetrahydrofuran (1: 1 v/v; Chromasolv® Plus, Sigma Aldrich; HiPerSolv, VWR). Samples were stored at −20°C until transport on ice to Jena, Germany, and at −80°C until analysis approximately 1 yr later. After thawing, 5 μL 4 mM aqueous ribitol were added as internal standard and an aliquot of 1.5 mL per sample was dried under vacuum. Derivatization was done by adding 50 μL methoxyamine solution (20 mg mL^{-1} methoxyamine hydrochloride in pyridine, Chromasolv® Plus, Sigma Aldrich), incubation at 60°C for 1 h and room temperature for 11 h, and subsequent addition of 50 μL *N*-methyl-*N*-(trimethylsilyl) trifluoroacetamide for 1 h at 40°C. Immediate GC-MS analysis and further data processing were performed as described by Vidoudez and Pohnert (2012). The DB-5ms column had a length of 30 m attached to a 4.6 m pre-column, source temperature was set to 250°C, and the split to 1. Chromatogram deconvolution was performed using AMDIS 2.71 with a smoothing window of five scans and peak integration using MET-IDEA 2.08 with a lower mass limit of 50. Artifacts found also in solvent controls were excluded using Excel 2010. The effect of 0.2 μm gravity filtration and station differences were investigated with a canonical analysis of principal coordinates (CAP) and the strongest treatment correlated peaks were putatively identified with the spectral library NIST 2011.

Assessment

Different conditions in IF and OF: background information

At the time of sampling, phytoplankton community of Porsangerfjord was dominated by colonial cells of *P. pouchetii*, accounting for 82% (IF) and 94% (OF) of the total carbon of phytoplankton at Chl *a* maximum (20 m). Chl *a*

Table 2. Overview of biological parameters and nutrient concentrations at IF and OF at Chl *a* max (20 m).

	IF	OF
Chl *a* (μg L^{-1})	6.3 ± 1.5	6.0 ± 1.7
Bacteria (mL^{-1})	7.4×10^5	2.0×10^5
HNF (mL^{-1})	615	1249
$\mu_{specific}$ (d^{-1})	1.0	0.6
Dissolved Si (μM)	0.22	0.81
NO_3^- (μM)	0.00	2.10
PO_4^{3-} (μM)	0.05	0.23

concentrations were similar at both stations (6.3 ± 1.5 μg Chl *a* L^{-1} in IF, 6.0 ± 1.7 μg Chl *a* L^{-1} in OF, Table 2). However, microscopy revealed higher diversity of phytoplankton community (based on carbon estimates) in IF than in OF (1.24 Shannon index in IF and 0.91 in OF). The diatom *Thalassiosira* spp. accounted for the major difference in phytoplankton assemblage of those two stations and was only present in IF and not in OF. Nutrient concentrations of dissolved Si, NO_3^-, and PO_4^{3-} at 20 m depth were low and close to detection limit in IF but higher in OF (Table 2). Together these findings indicate that phytoplankton community at IF was at the reminiscence of a diatom bloom whereas in OF there was a monospecific *P. pouchetii* bloom.

Bacteria and HNF varied in terms of abundance in these different bloom situations (Table 2). In IF bacteria concentration at 20 m depth was 7.4×10^5 mL^{-1} and HNF abundance was 615 mL^{-1}. In OF, bacteria concentration was 3.7 × lower (2.0×10^5 mL^{-1}) and HNF abundance 2 × higher (1249 mL^{-1}). Bacterial specific growth was 1.0 d^{-1} in IF and 0.6 d^{-1} in OF. Microzooplankton abundances were low at both stations (1 mL^{-1}) and consisted of ciliates only.

Dilution experiments

Following the method of Landry and Hassett (1982) the regression line provided an estimate of gross growth rate of bacteria of 0.58 d^{-1} at IF and 0.75 d^{-1} at OF. Estimates of grazing mortality were also higher in OF (0.19 d^{-1}) than IF (0.06 d^{-1}, Fig. 1). Bacterial growth in controls of WSW was not significantly different to WSW with nutrient amendment and therefore is not shown ($p > 0.05$, Table 3).

Apparent growth rates were not significantly related to dilution factor in any of the two experiments ($p > 0.05$, Table 3) and linear regression line yielded low R^2 values ($R^2 = 0.13$ in IF, $R^2 = 0.29$ in OF) a commonly observed problem when using dilutions for bacterivory (Berninger and Wickham 2005) and herbivory (Calbet and Saiz 2013).

Specific growth at the start of the experiment (Fig. 2a) was not affected by dilution and was higher in IF (1.1 ± 0.2 d^{-1}) than in OF (0.7 ± 0.2 d^{-1}). However, at the end of the experiment (24 h) specific growth increased by a factor of 9 in dilutions of 10% and 25% compared with WSW during the experiment in OF, corresponding to a maximum of 13.2 d^{-1} in the 10% dilution (Fig. 2b). In dilutions of IF specific growth rates remained at the same level as at the start of the experiment (1.2 ± 0.2 d^{-1}).

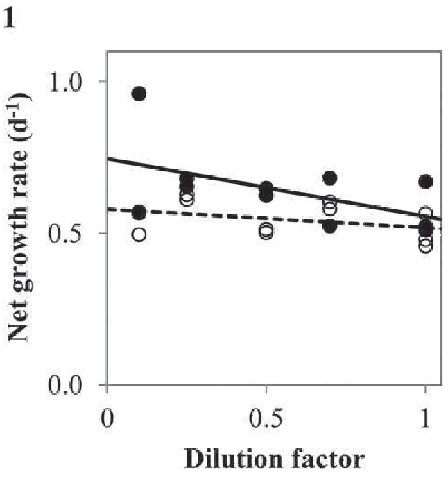

Fig. 1. Net growth rates of bacteria (d^{-1}) derived from initial and final (24 h) cell counts from IF and OF. Grazing and gross growth rates were higher in OF ($\mu_{gross} = 0.75$ d^{-1}, $g = 0.19$ d^{-1}, $R^2 = 0.29$) than in IF ($\mu_{gross} = 0.58$ d^{-1}, $g = 0.06$ d^{-1}, $R^2 = 0.13$). Filled circles and solid line symbolize samples from OF, open circles and dashed line from IF.

Table 3. *p*-values of statistical analysis (ANOVA and regression) of dilution experiments.

ANOVA, *p*-values	IF	OF
Regression total bacteria abundance	0.264	0.090
WSW (+nutrients), WSW (−nutrient)	0.211	0.869
Regression LNA bacteria abundance	0.939	0.013
Regression HNA bacteria abundance	0.292	0.010

It should be noted that bacterial production measurements by ^{3}H-leucine uptake is controversial due to the conversions to carbon content of a "typical" bacterial cell (Ducklow 1993). In spite of this controversy we assume a constant conversionfactor for all dilutions and WSW to show how dilution affects bacterial carbon incorporation. Another issue is that leucine might act as fertilizer for bacterial growth, as it is labile and especially in oligotrophic conditions stimulating growth. For this study, we consider this a negligible problem, since incubation is only 1 h, and if leucine acted as a carbon source for C-limited bacteria, it would have had the same effect in all bottles and not change the overall result. Moreover, enrichment bioassays performed with water from both stations (Fig. 1 in Supporting Information) show that C addition in form of glucose did not increase bacterial production significantly for any of them, suggesting that C was in fact not limiting.

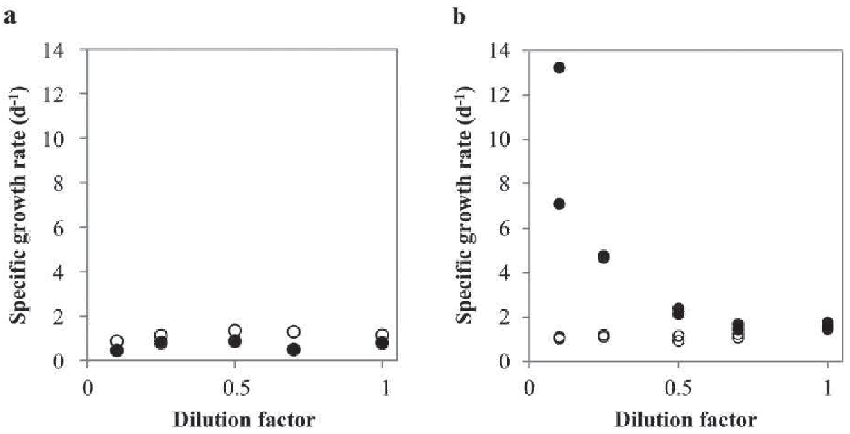

Fig. 2. Specific growth rates of bacteria (d^{-1}) at the start (**a**) and at the end (24 h, **b**) of the experiment in dilutions and WSW. Open circles display samples from IF, filled circles from OF.

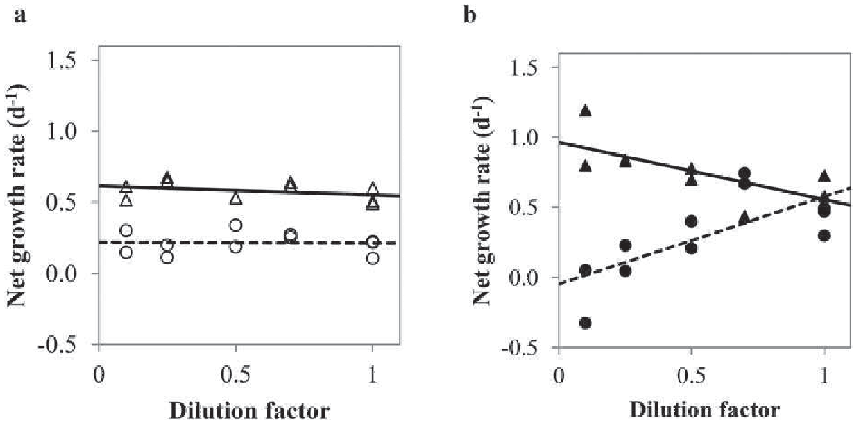

Fig. 3. Net growth rates (d^{-1}) of HNA (triangles and solid lines) and LNA (circles and dashed lines) bacteria in IF (**a**) and OF (**b**). In IF, HNA, and LNA bacteria had similar net growth in all dilutions and WSW, whereas in OF, HNA, and LNA had opposite trends.

How the differences in specific growth rates in OF affect the net growth rates of bacteria we can only speculate at this stage. One possible inference could be that bacteria in dilutions of OF did not only increase in numbers during incubation, but also in biomass and/or additionally changed community composition. Interestingly, flow cytometer plots indicated a shift in bacterial community or activity. Scatter plots of samples from WSW at the start of the dilution experiments showed two distinct populations of bacteria (Fig. 2 in Supporting Information), corresponding to different (high and low) nucleic-acid staining properties, called HNA and LNA bacteria (Li et al. 1995; Gasol et al. 1999). During 24 h of incubation, HNA and LNA bacteria developed differently at the two stations. To illustrate this change, we repeated the calculations for HNA and LNA bacteria separately (Eq. 1) and performed linear regression analysis against dilution factor. We did not aim to derive growth or grazing rates from these calculations but to demonstrate the difference in HNA and LNA bacteria in dilutions compared with WSW. For bacteria from IF (Fig. 3a), the regression lines are more or less parallel to each other for both populations and similar to the one derived from total community counts. In OF (Fig. 3b), the discrimination into HNA and LNA bacteria revealed that HNA and LNA bacteria developed differently in dilutions. Linear regression of HNA and LNA bacteria against dilution factor was significant ($p < 0.05$) for OF but not for IF (Table 3).

Gasol et al. (1999) found a similar increase in abundances of HNA bacteria in size fractionation experiments when grazers were absent (0.8 μm filtered water). They suggested that HNA bacteria are large and active cells preferable grazed on and as a consequence of reduced grazing pressure HNA bacteria increased. We find one case where HNA and LNA developed similar in the dilution experiment (IF) and one case

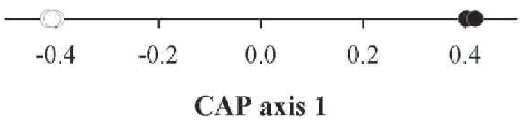

Fig. 4. Score plot of a canonical analysis of principal coordinates (CAP) showing a clear separation of seawater samples from the Chl *a* maximum at IF (open circles) compared with OF (filled circles) based on relative abundances of dissolved metabolites ($n = 3$). [Eigenvalues 0.99986, squared correlations 0.99972, misclassification error 66.67%].

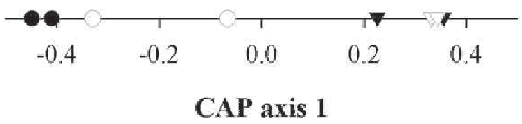

Fig. 5. Score plot of a canonical analysis of principal coordinates (CAP) showing a clear separation of WSW samples (circles) compared with 0.2 μm gravity filtered seawater samples (triangles) based on the relative abundances of dissolved metabolites in IF (open symbols) and OF (filled symbols) ($n = 2$). [Eigenvalues 0.9421, squared correlations 0.88755, misclassification error 25%].

where they showed opposite net growth along a gradient of dilutions with filtered seawater (OF). Filtered seawater is not only predator free but also contains a different level of metabolites released from phytoplankton cells during filtration or reduced during filtration compared with unfiltered seawater. Therefore, we cannot determine whether HNA bacteria in dilutions of OF grow better due to decreased grazing or due to change in concentrations of metabolites. We did not examine community composition and we cannot tell whether HNA and LNA are different phylogenetic groups (Zubkov et al. 2001; Vila-Costa et al. 2012) or whether this discrimination is due to different levels of bacterial activity from the same taxa (Li et al. 1995). However, the increase of specific growth rate in OF corresponds well with the increase of HNA bacteria numbers in OF and most importantly constitutes a violation of one of the basic assumptions of the dilution method (Landry and Hassett 1982).

Whereas we found increased growth rates of bacteria in dilutions with FSW in OF, Pasulka et al. (2015) recently described decreased specific growth of bacteria in dilutions prepared for estimating viral lysis (30 kDA filtrate) and grazing on picophytoplankton. Pasulka and colleagues were not aiming for retrieving rates for bacterivory from their experiments but suggest that altered growth of bacteria in dilutions have an impact on the other communities like picophytoplankton and consequently the grazing rates. Findings of Pasulka et al. (2015) provide additional support of the main objective of this study, which is to show, that dilution method needs modifications and cautionary use when applying it for bacterivory estimates.

Dynamics within grazer community during incubation are important to consider during dilution experiments because, e.g., if there is a trophic cascade within grazers during incubations, grazing rates become biased (Calbet and Saiz 2013). In our study, ciliate abundances were similar and low (1 mL^{-1}) at both stations, and although HNF concentrations were different in IF and OF, (Table 2) their growth rates during the experiments (Fig. 3 in Supporting Information) were similar in dilutions and WSW suggesting that there was neither a strong trophic cascade nor an effect of dissolved metabolites on HNFs.

Filtration altered sea water chemistry

The profiles of metabolites in seawater (exometabolome) of IF and OF can be separated with a CAP when using IF/OF as groups (Fig. 4). By subtraction of chromatographic profiles of control samples it was made sure that only metabolites in the seawater and no contaminations contributed to this difference. This result is in line with the other parameters previously used to indicate different bloom status despite similar Chl *a* concentrations at the two stations (Table 2).

For dilution experiments at both sampling sites significant differences in the metabolic profile of the seawater were observed when comparing FSW and WSW (Fig. 5). Thus, filtration has a clear impact on the metabolic composition of seawater masking the initial differences of metabolic profiles of seawater of IF and OF (Fig. 4).

The GC-MS metabolic profiling approach allows to tentatively assign structures to compounds that cause the separation into distinct groups. The 0.2 μm gravity filtration reduced some contaminations (phthalates, sebacic acid, siloxanes) but also saccharides (galactosyl-glycerol, disaccharides; Table 4a). This can be due to an adsorption effect on the filter or depletion due to a lack of stability of metabolites during filtration. Further, we also detected several metabolites that were more abundant after filtration (Table 4b), possibly released due to stress and disruption of cells during filtration. Unfortunately most metabolites remain unknown, however, some fatty acids and dodecanol could be tentatively assigned by spectral library search.

Discussion

The main objective of this study was to provide a relatively simple adjustment of the dilution method to test the first basic assumption of Landry and Hassett (1982) by measuring bacterial production additional to abundance. We provide results of two dilution experiments used to derive bacterivory rates where in one case (IF) specific growth rates were not affected by dilution and another case (OF) where these were significantly affected. Chemical analysis revealed differences in metabolic profiles of metabolites in seawater from the two stations as well as a change in metabolic profiles caused by the filtration. Bacteria growth might be affected by release of allelochemicals but also by the adsorption of metabolites, such as saccharides due to filtration. For

Table 4. Heat map of dissolved seawater metabolites with highest correlation to the CAP axis separating WSW and FSW as groups for both the inner (IF) and outer (OF) Porsangerfjord station. Yellow: more abundant, blue less abundant.

a) Putative metabolites which decreased or depleted during filtration.

	WSW		FSW	
Putative metabolites	**IF**	**OF**	**IF**	**OF**
-				
Terephthalic acid				
Galactosylglycerol				
-				
Glycerol				
Sebacic acid?				
-				
-				
-				
Phthalate?				
-				
Isooctylphthalate				
Siloxane				
-				
-				
MUFA?				
Disaccharide?				
-				
-				
Disaccharide?				

b) Which are only present or increased after filtration.

	WSW		FSW	
Putative metabolites	**IF**	**OF**	**IF**	**OF**
-				
-				
-				
Dodecanoic acid				
-				
-				
-				
-				
-				
-				
-				
-				
-				
Dodecanol				
Decanoic acid				
-				
-				
-				
-				
Ditertbutylphenol?				

MUFA, monounsaturated fatty acid.
"-", unknown metabolite.
"?", reverse match in comparison with NIST library < 800.

an in-depth evaluation a structure determination of the relevant metabolites causing the differences would be required but this was clearly beyond the scope of this work.

Obviously, our study is limited to dilution experiments during a *P. pouchetii* bloom and further studies under different conditions are needed. Nevertheless, *Phaeocystis* sp. is an important primary producer as it seasonally forms dense blooms at higher latitudes and may dominate the pelagic biomass at certain periods (reviewed by Verity et al. 2007). Moreover, change of metabolic profiles when filtering seawater for dilution experiments is not only an issue during blooms of *Phaeocystis* but has also been shown during other phytoplankton blooms such as *Skeletonema marinoi* (Stoecker et al. 2015).

Analysis of metabolic profiles before and after filtration during the set-up of dilution experiments is desirable but not always feasible due to high workload and costs. However, the suggested modification of including BP measurements as a proxy of specific growth when using dilution method for bacterivory helps to unravel uncertainties coming along with the method and to understand whether derived bacterivory rates are reliable or not. In terms of additional costs/efforts the suggested modification is minor, also, only little volume of the incubation bottles is needed for BP measurements (<10 mL).

For previous studies of bacterivory using dilution method based on flow cytometric analysis, one could reanalyze the scatter plots and check whether two different populations (HNA, LNA) are distinguishable. Further, if they developed differently during incubation in dilutions and WSW the assumption can be drawn that either bacterial community or bacteria specific growth was affected by filtration and bacterivory rates are biased.

Comments and recommendations

We recommend including measurements of BP to the protocol of the dilution method for bacterial grazing to test and validate the effect of dilution with 0.2 μm filtered water on bacteria specific growth rates. By that, one can identify the circumstances under which the dilution technique provides reliable estimates for bacterivory and minimize the uncertainty the impact filtration might have on bacterial growth. In case of different specific growth rates in dilutions and WSW the derived grazing rates are inaccurate. If future studies show that in the majority of dilution experiments specific growth rates differ between WSW and dilutions, alternative methods not using a filtration step should be preferred. At the same time, improvement of the filtration protocol, by combining biological and chemical measurements, is a necessity for further developing the dilution method toward more accurate estimates of bacterivory rates.

References

Agis, M., A. Granda, and J. R. Dolan. 2007. A cautionary note: Examples of possible microbial community dynamics in dilution grazing experiments. J. Exp. Mar. Biol. Ecol. **341**: 176–183. doi:10.1016/j.jembe.2006.09.002

Alderkamp, A. C., A. G. J. Buma, and M. Van Rijssel. 2007. The carbohydrates of *Phaeocystis* and their degradation in the microbial food web. Biogeochemistry **83**: 99–118. doi:10.1007/s10533-007-9078-2

Anderson, M. R., and R. B. Rivkin. 2001. Seasonal patterns in grazing mortality of bacterioplankton in polar oceans: A bipolar comparison. Aquat. Microb. Ecol. **25**: 195–206. doi:10.3354/ame025195

Barofsky, A., C. Vidoudez, and G. Pohnert. 2009. Metabolic profiling reveals growth stage variability in diatom exudates. Limnol. Oceanogr.: Methods **7**: 382–390. doi:10.4319/lom.2009.7.382

Berninger, U.-G., and S. Wickham. 2005. Response of the microbial food web to manipulation of nutrients and grazers in the oligotrophic Gulf of Aqaba and northern Red Sea. Mar. Biol. **147**: 1017–1032. doi:10.1007/s00227-005-1565-1

Calbet, A., and E. Saiz. 2013. Effects of trophic cascades in dilution grazing experiments: From artificial saturated feeding responses to positive slopes. J. Plankton Res. **35**: 1183–1191. doi:10.1093/plankt/fbt067

Dolan, J. R., and K. Simek. 1999. Diel periodicity in *Synechococcus* populations and grazing by heterotrophic nanoflagellates: Analysis of food vacuole contents. Limnol. Oceanogr. **44**: 1565–1570. doi:10.4319/lo.1999.44.6.1565

Ducklow, H. W. 1993. Bacterioplankton distributions and production in the northwestern Indian Ocean and Gulf of Oman, September 1986. Deep-Sea Res. Part II Top. Stud. Oceanogr. **40**: 753–771. doi:10.1016/0967-0645(93)90056-S

Ducklow, H. W. 2000. Bacterial production and biomass in the oceans. *In* D. L. Kirchman [ed.], Microbial ecology of the oceans. John Wiley and Sons.

Evans, C., S. D. Archer, S. Jacquet, and W. H. Wilson. 2003. Direct estimates of the contribution of viral lysis and microzooplankton grazing to the decline of a *Micromonas* spp. population. Aquat. Microb. Ecol. **30**: 207–219. doi:10.3354/ame030207

Ferguson, R. L., E. N. Buckley, and A. V. Palumbo. 1984. Response of marine bacterioplankton to differential filtration and confinement. Appl. Environ. Microbiol. **47**: 49–55.

Gasol, J. M., U. L. Zweifel, F. Peters, J. A. Fuhrman, and A. Hagstrom. 1999. Significance of size and nucleic acid content heterogeneity as measured by flow cytometry in natural planktonic bacteria. Appl. Environ. Microbiol. **65**: 4475–4483.

Hansen, H. P., and F. Koroleff. 1999. Determination of nutrients, p. 159–228. *In* K. Grasshoff [ed.], Methods of seawater analysis. Wiley-VCH Verlag GmbH.

Jakobsen, H. H., and J. Carstensen. 2011. FlowCAM: Sizing cells and understanding the impact of size distributions on biovolume of planktonic community structure. Aquat. Microb. Ecol. **65**: 75–87. doi:10.3354/ame01539

Jonasdottir, S. H., and others. 2011. Extensive cross-disciplinary analysis of biological and chemical control of *Calanus finmarchicus* reproduction during an aldehyde forming diatom bloom in mesocosms. Mar. Biol. **158**: 1943–1963. doi:10.1007/s00227-011-1705-8

Kirchman, D. 2001. Measuring bacterial biomass production and growth rates from leucine incorporation in natural aquatic environments, p. 227–238. *In* J. H. Paul [ed.], Methods in microbiology. Academic Press.

Landry, M. R. 1994. Methods and controls for measuring the grazing impact of planktonic protists. Mar. Microb. Food Webs **8**: 37–57.

Landry, M. R., and R. P. Hassett. 1982. Estimating the grazing impact of marine micro-zooplankton. Mar. Biol. **67**: 283–288. doi:10.1007/BF00397668

Landry, M. R., J. Kirshtein, and J. Constantinou. 1995. A refined dilution technique for measuring the community grazing impact of microzooplankton, with experimental tests in the central equatorial Pacific. Mar. Ecol. Prog. Ser. **120**: 53–63. doi:10.3354/meps120053

Lee, S., and J. A. Fuhrman. 1987. Relationships between biovolume and biomass of naturally derived marine bacterioplankton. Appl. Environ. Microbiol. **53**: 1298–1303.

Lessard, E. J., and E. Swift. 1985. Species-specific grazing rates of heterotrophic dinoflagellates in oceanic waters, measured with a dual-label radioisotope technique. Mar. Biol. **87**: 289–296. doi:10.1007/BF00397808

Li, W. K. W., J. F. Jellett, and P. M. Dickie. 1995. DNA distributions in planktonic bacteria stained with TOTO or TO-PRO. Limnol. Oceanogr. **40**: 1485–1495. doi:10.4319/lo.1995.40.8.1485

Menden-Deuer, S., and E. J. Lessard. 2000. Carbon to volume relationships for dinoflagellates, diatoms, and other protist plankton. Limnol. Oceanogr. **45**: 569–579. doi:10.4319/lo.2000.45.3.0569

Moigis, A. G. 2006. The clearance rate of microzooplankton as the key element for describing estimated non-linear dilution plots demonstrated by a model. Mar. Biol. **149**: 743–762. doi:10.1007/s00227-005-0202-3

Oksanen, J., F. G. Blanchet, R. Kindt, P. Legendre, P. R. Minchin, R. B. O'Hara, L. G. Simpson, P. Solymos, M. H. H. Stevens, and H. Wagner 2015. vegan: Community Ecology Package. R package version 2.3-0. http://CRAN.R-project.org/package=vegan.

Parsons, T. R., Y. Maita, and C. M. Lalli. 1984. A manual of chemical and biological methods for seawater analysis. Pergamon Press.

Pasulka, A. L., T. J. Samo, and M. R. Landry. 2015. Grazer and viral impacts on microbial growth and mortality in

the southern California Current Ecosystem. J. Plankton Res. **37**: 320–336. doi:10.1093/plankt/fbv011

Pearce, I., A. T. Davidson, P. G. Thomson, S. Wright, and R. Van Den Enden. 2010. Marine microbial ecology off East Antarctica (30-80 degrees E): Rates of bacterial and phytoplankton growth and grazing by heterotrophic protists. Deep-Sea Res. Part II Top. Stud. Oceanogr. **57**: 849–862. doi:10.1016/j.dsr2.2008.04.039

Pearce, I., A. T. Davidson, P. G. Thomson, S. Wright, and R. Van Den Enden. 2011. Marine microbial ecology in the sub-Antarctic Zone: Rates of bacterial and phytoplankton growth and grazing by heterotrophic protists. Deep-Sea Res. Part II Top. Stud. Oceanogr. **58**: 2248–2259. doi:10.1016/j.dsr2.2011.05.030

Proctor, L. M., and J. A. Fuhrman. 1990. Viral mortality of marine bacteria and cyanobacteria. Nature **343**: 60–62. doi:10.1038/343060a0

Sazhin, A., L. F. Artigas, J. Nejstgaard, and M. Frischer. 2007. The colonization of two *Phaeocystis* species (Prymnesiophyceae) by pennate diatoms and other protists: A significant contribution to colony biomass, p. 137–145. *In* M. A. van Leeuwe, J. Stefels, S. Belviso, C. Lancelot, P. G. Verity and W. W. C. Gieskes [eds.], Phaeocystis, major link in the biogeochemical cycling of climate-relevant elements. Springer Netherlands.

Schmoker, C., S. Hernández-León, and A. Calbet. 2013. Microzooplankton grazing in the oceans: Impacts, data variability, knowledge gaps and future directions. J. Plankton Res. **35**: 691–706. doi:10.1093/plankt/fbt023

Sherr, B. F., E. B. Sherr, and R. D. Fallon. 1987. Use of monodispersed, fluorescently labeled bacteria to estimate in situ protozoan bacterivory. Appl. Environ. Microbiol. **53**: 958–965.

Sherr, E. B., and B. F. Sherr. 1994. Bacterivory and herbivory: Key roles of phagotrophic protists in pelagic food webs. Microb. Ecol. **28**: 223–235. doi:10.1007/BF00166812

Simon, M., and F. Azam. 1989. Protein content and protein synthesis rates of planktonic marine bacteria. Mar. Ecol. Prog. Ser. **51**: 201–213. doi:10.3354/meps051201

Smith, D. C., and F. Azam. 1992. A simple, economical method for measuring bacterial protein synthesis rates in seawater using 3H-leucine. Mar. Microb. Food Webs **6**: 107–114.

Stoecker, D. K., and others. 2015. Underestimation of microzooplankton grazing in dilution experiments due to inhibition of phytoplankton growth. Limnol. Oceanogr. **60**: 1426–1438. doi:10.1002/lno.10106

Suttle, C. A. 2007. Marine viruses—major players in the global ecosystem. Nat. Rev. Microbiol. **5**: 801–812. doi:10.1038/nrmicro1750

Tremaine, S. C., and A. L. Mills. 1987. Tests of the critical assumptions of the dilution method for estimating bacteriovory by microeucaryotes. Appl. Environ. Microbiol. **53**: 2914–2921.

Vaque, D., J. M. Gasol, and C. Marrase. 1994. Protists grazing rates: the significance of methodology and ecological factors. Mar. Ecol. Prog. Ser. **109**: 263–274. doi:10.3354/meps109263

Verity, P. G., C. P. Brussaard, J. C. Nejstgaard, M. A. Van Leeuwe, C. Lancelot, and L. K. Medlin. 2007. Current understanding of *Phaeocystis* ecology and biogeochemistry, and perspectives for future research. Biogeochemistry **83**: 311–330. doi:10.1007/s10533-007-9090-6

Vidoudez, C., and G. Pohnert. 2012. Comparative metabolomics of the diatom *Skeletonema marinoi* in different growth phases. Metabolomics **8**: 654–669. doi:10.1007/s11306-011-0356-6

Vila-Costa, M., J. M. Gasol, S. Sharma, and M. A. Moran. 2012. Community analysis of high- and low-nucleic acid-containing bacteria in NW Mediterranean coastal waters using 16S rDNA pyrosequencing. Environ. Microbiol. **14**: 1390–1402. doi:10.1111/j.1462-2920.2012.02720.x

Wright, R. T., and R. B. Coffin. 1984. Measuring microzooplankton grazing on planktonic marine bacteria by its impact on bacterial production. Microb. Ecol. **10**: 137–149. doi:10.1007/BF02011421

Zubkov, M. V., B. M. Fuchs, P. H. Burkill, and R. Amann. 2001. Comparison of cellular and biomass specific activities of dominant bacterioplankton groups in stratified waters of the Celtic Sea. Appl. Environ. Microbiol. **67**: 5210–5218. doi:10.1128/AEM.67.11.5210-5218.2001

Zubkov, M., P. H. Burkill, and J. N. Topping. 2007. Flow cytometric enumeration of DNA-stained oceanic planktonic protists. J. Plankton Res. **29**: 79–86. doi:10.1093/plankt/fbl059

Acknowledgments

We thank the captain and the crew of R/V *Håkon Mosby* for great support during the cruise. Julia Althammer is acknowledged for her help during sampling and extraction on board and for fruitful discussion. Thanks to T. Frede Thingstad and Jessica L. Ray for helpful discussions. The study is conducted as part of the NFR project 204479/F20, "PHAEONIGMA: A novel cross-disciplinary approach to solve an old enigma: the food-web transfer of the mass-blooming phytoplankter *Phaeocystis*" and also supported by MINOS (ERC grant 250254, salary BP and AL).

Submitted 12 June 2015
Revised 19 August 2015
Accepted 5 October 2015

Associate editor: Steven Wilhelm

Publication P5:

"A fast and direct liquid chromatography-mass spectrometry method to detect and quantify polyunsaturated aldehydes and polar oxylipins in diatoms"

C. Kuhlisch, M. Deicke, N. Ueberschaar, T. Wichard, and G. Pohnert

Limnol. Oceanogr.: Methods, 2017, **15**, 70-79.

The supplementary information of this publication is available in the Appendix.

Corrigendum

Figure 2c contains a fragment with the value *m*/*z* 57.0342. The assigned sum formula in the publication was $C_4H_7O^+$. However, this is not the correct sum formula and instead should be assigned to $C_3H_5O^+$.

LIMNOLOGY
and
OCEANOGRAPHY: METHODS

ASLO

Limnol. Oceanogr.: Methods 15, 2017, 70–79

doi: 10.1002/lom3.10143

A fast and direct liquid chromatography-mass spectrometry method to detect and quantify polyunsaturated aldehydes and polar oxylipins in diatoms

Constanze Kuhlisch, Michael Deicke, Nico Ueberschaar, Thomas Wichard, Georg Pohnert*
Institute for Inorganic and Analytical Chemistry, Friedrich Schiller University Jena, Jena, Germany

Abstract

Polyunsaturated aldehydes (PUAs) are a group of microalgal metabolites that have attracted a lot of attention due to their biological activity. Determination of PUAs has become an important routine procedure in plankton and biofilm investigations, especially those that deal with chemically mediated interactions. Here we introduce a fast and direct derivatization free method that allows quantifying PUAs in the nanomolar range, sufficient to undertake the analysis from cultures and field samples. The sample preparation requires one simple filtration step and the initiation of PUA formation by cell disruption. After centrifugation the samples are ready for measurement without any further handling. Within one chromatographic run this method additionally allows us to monitor the formation of the polar oxylipins arising from the cleavage of precursor fatty acids. The robust method is based on analyte separation and detection using ultra high performance liquid chromatography-atmospheric pressure chemical ionization mass spectrometry (UHPLC-APCI MS) and enables high throughput investigations by employing an analysis time of only 5 min. Our protocol thus provides an alternative and extension to existing PUA determinations based on gas chromatography-mass spectrometry (GC-MS) with shorter run times and without any chemical derivatization. It also enables researchers with widely available LC-MS analytical platforms to monitor PUAs. Additionally, non-volatile oxylipins such as ω-oxo-acids and related compounds can be elucidated and monitored.

Polyunsaturated aldehydes (PUAs) are short-chained $\alpha,\beta,\gamma,\delta$-unsaturated aldehydes which came into focus of marine biologists due to their high bioactivity (Miralto et al. 1999). These fatty acid-derived metabolites are mainly produced by planktonic and benthic microalgae. As PUAs can play important roles in the interaction and regulation of algae-herbivore relationships, they have become a common parameter, determined along with other metadata in many studies. Being produced on cell damage of microalgae (Pohnert 2000; Pohnert 2002) PUAs have been made responsible for numerous effects on the grazer reproductive success such as the inhibition of copepod egg hatching or the action as causative agents for abnormal larval morphology (Miralto et al. 1999; Ianora et al. 2004; Poulet et al. 2007). However, the ecological relevance of these findings is still under discussion (Wichard et al. 2008). PUAs were not only found to be responsible for influencing diatom-copepod interactions, they also play a role in, e.g., intraspecific signaling and programmed cell death, allelopathy, and bacteria-phytoplankton interactions (Adolph et al. 2004; Vardi et al. 2006; Ribalet et al. 2008; Ribalet et al. 2014). Mainly diatoms are considered as important sources for PUAs but also other marine organisms, such as the brown alga *Dictyopteris* sp. and the green alga *Ulva* sp., as well as terrestrial plants and mosses produce $\alpha,\beta,\gamma,\delta$-unsaturated aldehydes (Noordermeer et al. 2001; Schnitzler et al. 2001; Stumpe et al. 2006; Alsufyani et al. 2014).

Biosynthetically, algal PUAs are derived from C_{16} and C_{20} polyunsaturated fatty acids (PUFAs) in a wound-activated process. These precursor fatty acids are enzymatically released within seconds after cell damage from phospholipids (Pohnert 2002) or glycolipids (d'Ippolito et al. 2004; Cutignano et al. 2006) and transformed to PUAs by a lipoxygenase (LOX)-hydroperoxide lyase (HPL) or a LOX-halolyase cascade (Pohnert 2000; d'Ippolito et al. 2004; Wichard and Pohnert 2006). Hexadecatrienoic acid (C16 : 3ω4) serves as precursor for 2*E*,4*Z*-octadienal (**3**), hexadecatetraenoic acid (C16 : 4ω1) for 2*E*,4*Z*,7-octatrienal (**5**), arachidonic acid (C20 : 4ω6) for 2*E*,4Z-decadienal (**4**), and eicosapentaenoic acid (C20 : 5ω3) for both 2*E*,4Z-heptadienal (**2**) and 2*E*,4*Z*,7Z-decatrienal (**6**) (Pohnert 2000; d'Ippolito et al. 2003; d'Ippolito et al. 2004; Pohnert et al. 2004). Besides PUAs, a multitude of other oxylipins are produced by diatoms such as hydroxy-, keto-, epoxyhydroxy-fatty acid derivatives (*see* Cutignano et al. 2011 and references

*Correspondence: georg.pohnert@uni-jena.de

Additional Supporting Information may be found in the online version of this article.

therein), some of which are also biologically active (Ianora et al. 2011). Variability in the content of precursor molecules and enzyme activity leads to species-, strain- and even clone-specific oxylipin profiles that are further modulated by environmental factors (Wichard et al. 2005a; Ribalet et al. 2007; Taylor et al. 2009; Dittami et al. 2010; Gerecht et al. 2011). In addition, the physiological state of the cells determines their PUA profile (Vidoudez and Pohnert 2008).

To qualitatively or quantitatively analyze the oxylipin composition of diatoms from laboratory cultures and field samples several methods have been developed (Wendel and Jüttner 1996; Pohnert 2000; d'Ippolito et al. 2002a; Wichard et al. 2005b; Cutignano et al. 2011). Especially in field experiments, the low concentration and the inherent instability of PUAs requires elaborated sample preparation and sensitive detection methods for the direct determination of PUAs in filtered seawater samples (Vidoudez et al. 2011). Methods monitoring PUAs by gas chromatography-mass spectrometry (GC-MS) include the enrichment of the volatile PUA-containing oxylipin fraction by adsorption to resin and subsequent headspace GC-MS (Wendel and Jüttner 1996) or the more convenient solid phase micro extraction coupled to GC-MS (Pohnert 2000; Spiteller and Spiteller 2000). The rather labile aldehydes can be further stabilized by chemical derivatization (d'Ippolito et al. 2002a; Wichard et al. 2005b). Using pentafluorobenzylhydroxylamine (PFBHA), PUAs can be trapped in the aqueous phase without interfering with the enzymatic oxylipin production (Wichard et al. 2005b). This has been proven as a very robust and reliable method used by several laboratories (Taylor et al. 2007; Morillo-Garcia et al. 2014; Lavrentyev et al. 2015). Derivatization is followed by extraction using hexane giving highly reproducible results in GC-MS. Alternatively, high performance liquid chromatography (HPLC)-separation of PUA-derived dinitrophenylhydrazones has been introduced on liquid–liquid extracts of PUAs (Edwards et al. 2015). Recent studies focusing on oxylipin profiles of diatoms not only analyzed the volatile oxylipins using GC-MS but also screened for non-volatile oxylipins such as fatty acid hydroperoxides, hydroxy-, epoxyhydroxy fatty acids or ω-oxo-acids using liquid chromatography-mass spectrometry (LC-MS) (Barreiro et al. 2011; Ianora et al. 2015).

Our goal was to overcome the time-consuming derivatization processes by elaborating a method for the direct detection and quantification of PUAs and non-volatile oxylipins by ultra high performance liquid chromatography (UHPLC)-HRMS in a fast procedure not requiring extraction or derivatization steps, suitable for high sample capacities.

Materials and procedures

Reagents

2*E*,4*E*-hexadienal (**1**, 95%), 2*E*,4*E*-heptadienal (**2**, $\geq$97%), 2*E*,4*E*-octadienal (**3**, $\geq$95%), 2*E*,4*E*-decadienal (**4**, 85%), methanol (CHROMASOLV® Plus, for HPLC), and water (CHROMASOLV® Plus, for HPLC) were purchased from Sigma-Aldrich (Germany). Vanillin (VEB Laborchemie Apolda, Germany) was used as internal standard (IS).

Algal cultivation and enumeration

The marine diatom *Chaetoceros didymus* Na20B4 was obtained from W. Kooistra (Stazione Zoologica Anton Dohrn, Naples, Italy). The strains *Skeletonema costatum* RCC75 and *Thalassiosira rotula* RCC776 were obtained from the Roscoff Culture Collection (RCC, Roscoff, France). Stationary cultures were inoculated in artificial seawater (Maier and Calenberg 1994) in polystyrene culture flasks (Sarstedt, Germany) and grown without agitation at 11.3 ± 0.42°C under an illumination of 15 μmol photons m^{-2} s^{-1} on a 14 : 10 light : dark cycle (OSRAM Lumilux Cool White L36W/840). After 2 weeks the cultures reached 1–4 $\times$ 10^5 cells mL^{-1} (Table 1) and were aliquoted into four replicates with 40 mL each. For cell enumeration 1.5 mL of each culture were fixed with 10 μL mL^{-1} acid Lugol's solution (Rodhe et al. 1958).

Cell abundance of *C. didymus* was determined with a Nannoplankton Chamber (PhycoTech Inc., St. Joseph, MI) and of *S. costatum* and *T. rotula* with a Fuchs-Rosenthal hemocytometer (Laboroptik, Friedrichsdorf, Germany) using a Leica DM2000 microscope (Heerbrugg, Switzerland). At least 400 cells or 16 mm^2 were counted in four replicates.

Sample preparation

For cell harvesting, 40 mL of each replicate were concentrated by filtration on Whatman® GF/C filters (ø 47 mm) under reduced pressure (600 mbar). Cells were rinsed off the filter with 0.5 mL artificial seawater. The suspensions were transferred to 1.5 mL Eppendorf-tubes and 5 μL vanillin (700 μmol L^{-1} in MeOH : H_2O; 1 : 1; *v* : *v*) were added as IS. After 10 s vortexing, PUA formation was initiated by 1 min pulsed (50%) ultrasound treatment in an ice-cold water bath using a Bandelin Sonopuls HD 2070 (Berlin, Germany). Tubes were closed and incubated for 10 min in a water bath at room temperature to complete PUA formation (Pohnert 2000). Samples were cooled for 2 min in an ice-bath before adding 270 μL methanol. These cell lysates were centrifuged with an Eppendorf centrifuge 5415 D (9,300 rcf; 3 min), supernatants transferred to 1.5 mL glass vials, sealed air tight with a Teflon septum, and subsequently measured by UHPLC-HRMS. Aliquots of 40 mL artificial seawater were processed as described above as blank samples.

UHPLC-HRMS Orbitrap measurements

UHPLC was carried out using a Thermo Scientific (Bremen, Germany) UltiMate HPG-3400 RS binary pump and a WPS-3000 auto sampler which was set to 10°C and which was equipped with a 25 μL injection syringe and a 100 μL sample loop. The injection volume was set to 10 μL. The chromatography column Phenomenex (Aschaffenburg, Germany) Kinetex® C-18 RP (50 $\times$ 2.1 mm; 1.7 μm) was kept at 25°C within

Table 1. Cell abundance of harvested diatom cultures as mean cell abundance ± SD (cells mL^{-1}; $n = 4$).

Algal species	Strain	Mean cell abundance ± SD (cells mL^{-1})
Chaetoceros didymus	Na20B4	$1.9 \times 10^5 \pm 1.9 \times 10^4$
Skeletonema costatum	RCC75	$4.0 \times 10^5 \pm 3.5 \times 10^4$
Thalassiosira rotula	RCC776	$9.7 \times 10^4 \pm 8.6 \times 10^3$

the column compartment TCC-3200 and elution was carried out using a gradient (Table 2). Eluent A was water with 2% acetonitrile and 0.1% formic acid (*v* : *v*). Eluent B was acetonitrile with 0.1% formic acid (*v* : *v*). The UHPLC was coupled to a Thermo Scientific™ Q Exactive plus™ hybrid quadrupole-Orbitrap mass spectrometer equipped with an atmospheric pressure chemical ionization (APCI) source. To minimize source contamination a solvent delay was set at the beginning (0.0–0.2 min) and end (3.5–5.0 min) of the chromatographic run. For monitoring of the PUAs **1**–**4** a targeted selective ion monitoring (tSIM) in the positive ionization mode was used with the following parameters: $[M + H]^+$; m/z = x (Table 3) ± 0.2; resolution = 70,000; AGC target = 5×10^4; maximum IT = 254 ms. For untargeted monitoring of other relevant oxylipins such as **5**–**9** a simultaneous full scan was set to: m/z = 70–500; resolution = 70,000; AGC target = 5×10^6; maximum IT = 254 ms. Further settings were: sheath gas flow rate = 40 arbitraty units; aux gas flow rate = 15 arbitraty units; sweep gas flow rate = 0 arbitraty units; discharge current = 8.0 μA; capillary temperature = 350°C; S-lens RF level = 33; vaporizer temperature = 360°C; acquisition time frame = 0.5–3.5 min. MS^2 experiments were recorded with stepped normalized collision energy of 15, 30, and 45 selected by the calculated mass ± 0.2 m/z starting at 50 m/z.

Quantification

Peak detection and integration were carried out using the Thermo Scientific™ Xcalibur™ 3.0.63 Quan Browser software with the following settings: mass tolerance = 10 ppm; mass precision = 5 decimals; compounds = C_6H_8O (**1**), $C_7H_{10}O$ (**2**), $C_8H_{12}O$ (**3**), $C_{10}H_{16}O$ (**4**), $C_8H_{10}O$ (**5**), $C_{10}H_{14}O$ (**6**); adduct = $[M + H]^+$; retention time window = 3 s; signal = XIC from tSIM experiment for the dienals (**1**–**4**) and XIC from full scan experiment for dienals (**1**–**4**) and trienals (**5**–**6**); peak detection algorithm = ICIS (Smoothing = 1); peak detection method = highest peak. Area ratios of each analyte relative to the IS were determined and the analyte concentration per volume or cell calculated via calibration curves and cell abundances. After blank subtraction all replicates were averaged.

Table 2. Gradient for UHPLC-HRMS measurement.

Time (min)	Flow (mL min^{-1})	Solvent B (%)	Curve*
0.0	0.400	35	5
0.5	0.400	35	5
3.0	0.675	100	8
4.0	0.675	100	8
4.1	0.675	35	5
5.0	0.400	35	5

Eluent A was water with 2% acetonitrile and 0.1% formic acid. Eluent B (= Solvent B) was acetonitrile with 0.1% formic acid. Curve 1–9 with 5 = linear gradient and 6–9 concave upward (Fig. 1a).
*Instrument parameter setting linear or non-linear solvent gradients.

Calibration, limit of detection (LOD), and limit of quantification (LOQ)

A PUA stock solution of 2*E*,4*E*-dienals (**1**–**4**; all 100 μmol L^{-1} in MeOH) was generated from commercial standards (*see* "Reagents").

Seven calibration solutions were freshly prepared independently for an all-in-one-quantification in the range from 1×10^{-8}–5×10^{-5} mol L^{-1} (MeOH : H_2O; 35 : 65; *v* : *v*) using vanillin as IS (5 μL of a 700 μmol L^{-1} solution in MeOH : H_2O; 1 : 1; *v* : *v*), and subsequently analyzed by UHPLC-HRMS in six technical replicates. The injection volume was set to 10 μL. The average peak area ratio analyte/IS was plotted against the nominal concentration of each analyte for the working range of 1×10^{-8}–1×10^{-5} mol L^{-1}. Each calibration in the data set was tested to be normally distributed, free of outliers and homoscedasticity was proven for the whole concentration range. A Mandel test was applied to test the linear model against the quadratic model. No statistically significant differences demonstrated linearity.

The LOD and LOQ were estimated by the lowest analyzed concentration that gave a signal-to-noise (S/N) ratio equal to or greater than 3 (LOD) and 10 (LOQ). The noise range directly before the eluting peak was evaluated. Whenever the analyzed concentrations did not match a S/N of 10 the LOQ was interpolated by linear regression of the three lowest calibration concentrations.

Precision and sample stability

The precision of the instrument was determined by re-injection of a quality control sample (QCS) at the beginning ($n = 6$, QCS_{start}) and end ($n = 6$, QCS_{end}) of the entire measurement regime. As QCS acted a freshly prepared sample of *S. costatum* as described (*see* above). Homoscedasticity of the peak area ratios of IS and selected PUAs (**2**–**4**) was proven for the QCS_{start} and QCS_{end} samples using the *F*-test ($\alpha = 5\%$).

Sample stability of the cell free samples was determined by re-capping the vials after injection and re-measurement after 7 days of storage at 5°C in darkness. This was exemplary conducted for *S. costatum* and *T. rotula* for all quantifiable

Table 3. PUA structures and diagnostic UHPLC-HRMS data as m/z $[M + H]^+$.

Chemical species	Structure	m/z $[M + H]^+$	LOD (mol L^{-1})	LOQ (mol L^{-1})
2*E*,4*Z*-hexadienal (**1**)	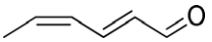	97.06479	1.0×10^{-8}	5.0×10^{-8}
2*E*,4*Z*-heptadienal (**2**)	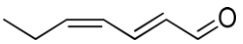	111.08044	$<1.0 \times 10^{-8}$*	2.3×10^{-8}
2*E*,4*Z*-octadienal (**3**)	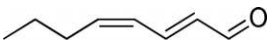	125.09609	5.0×10^{-8}	1.4×10^{-7}
2*E*,4*Z*,7-octatrienal (**5**)	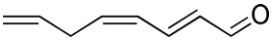	123.08044	n.d.	n.d.
2*E*,4*Z*-decadienal (**4**)	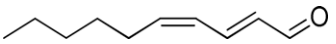	153.12739	$<1.0 \times 10^{-8}$*	1.9×10^{-8}
2*E*,4*Z*,7*Z*-decatrienal (**6**)	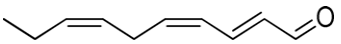	151.11174	n.d.	n.d.

Limit of detection (LOD; in mol L^{-1}) and quantification (LOQ; in mol L^{-1}) as determined for the corresponding 2*E*,4*E*-isomers. n.d. = not determined. *S/N at the lowest analyzed concentration of 1×10^{-8} M was 5 (**2**) and 6 (**4**).

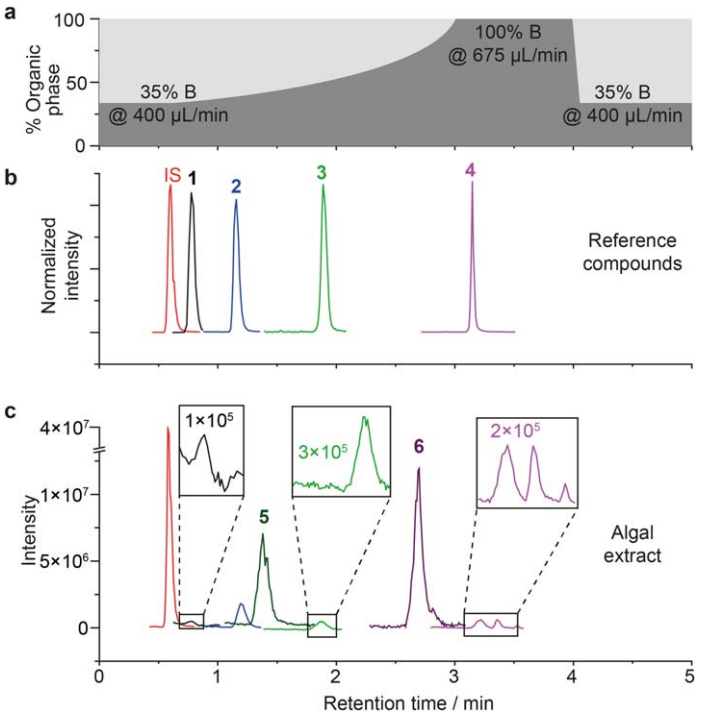

Fig. 1. UHPLC-HRMS analysis of polyunsaturated aldehydes including the gradient used for chromatography. (**a**) Gradient program for liquid chromatography (dark grey: organic phase (B); bright grey: aqueous phase). (**b**) Extracted ion chromatograms of the internal standard vanillin (IS, in red), and the authentic standards 2*E*,4*E*-hexadienal (**1**, in black), 2*E*,4*E*-heptadienal (**2**, in blue), 2*E*,4*E*-octadienal (**3**, in green), and 2*E*,4*E*-decadienal (**4**, in magenta) measured within one single run. Intensities are normalized to equal signal response. (**c**) Extracted ion chromatograms of a cell free extract of *Thalassiosira rotula* RCC776 harboring dienals (**1**–**4**) and the trienals octatrienal (**5**) and decatrienal (**6**) (color code see (**b**), trienals are in a darker color shade than their corresponding dienals). Note: In cell free extracts *E*/*Z*-isomers of PUAs are detected, resulting in more than one peak per aldehyde.

analytes. Sample stability over prolonged time was estimated by re-measurement of *T. rotula* extracts after 113 days storage at −20°C.

Assessment

Sample preparation

The sample preparation was modified according to former protocols (Wichard et al. 2005b) to achieve a fast analytical workflow allowing cell enrichment, cell wounding, incubation for wound-activated PUA production, and removal of suspended cell material within 20 min before UHPLC-HRMS measurement. The novel analytical approach allows determining PUAs within the complex cell-free algal lysate matrix without work- and time-intensive derivatization procedures as introduced by d'Ippolito et al. (2002a), Wichard et al. (2005b), or Edwards et al. (2015).

UHPLC-HRMS Orbitrap measurements

For quantification, a fast reversed-phase ultra-high performance liquid chromatography (RP-UHPLC) method was developed to separate PUAs. An elaborate curve-shaped 2.5 min gradient followed by a column wash with 100% organic eluent and re-equilibration of one minute was performed to achieve an optimal separation of the analytes. All analyzed compounds were baseline separated (Fig. 1b). The very short overall measurement time compared to former approaches (d'Ippolito et al. 2002a; Wichard et al. 2005b) now provides the opportunity of high sample throughput analyses, e.g., for monitoring experiments covering PUAs as well as other PUFA breakdown products. APCI proved to be superior compared to heated electro spray ionization (HESI). Sensitivity for the rather nonpolar short-chain aldehydes using HESI was two to three times lower compared to APCI (data not shown). For the dienals (**1**–**4**) targeted SIM analyses were used to enable maximum performance. For the analysis of trienals (**5**–**6**) and non-volatile oxylipins (**7**–**9**) a parallel analysis in full scan mode was executed. Hereby also potential unknown compounds may be identified. All method parameters were tested and verified with purchased dienal standards to ensure the adequate performance within all measurements.

Table 4. Mean concentration ± SD [fmol cell^{-1}] of the sums of the isomeric hexa- (**1**), hepta- (**2**), octa- (**3**), and decadienal (**4**), and of octa- (**5**) and decatrienal (**6**) in the exponentially growing marine diatom strains *Chaetoceros didymus* Na20B4 ($n = 4$), *Skeletonema costatum* RCC75 ($n = 4$), and *Thalassiosira rotula* RCC776 ($n = 3$).

	PUA concentration (fmol cell^{-1})					
Algae	**1**	**2**	**3**	**4**	**5**[a]	**6**[a]
C. didymus	n.d.	0.01 ± 0.001	n.d.	*	n.d.	n.d.
S. costatum	n.d.	0.48 ± 0.13	0.25 ± 0.09	*	0.08 ± 0.03	0.024 ± 0.005
T. rotula	*	0.18 ± 0.04	0.17 ± 0.03	0.03 ± 0.01	0.42 ± 0.08	1.08 ± 0.41

* = detected. n.d. = not detected.
[a]Trienal concentration as estimated if similar response factor as for the corresponding dienal is assumed.

Calibration, LOD, and LOQ

The statistical tests of normal distribution and trends passed for all calibration standards. As data showed no homoscedasticity over the working range of 1×10^{-8} mol L^{-1} to 1×10^{-5} mol L^{-1} a weighted linear regression was applied (1/y, Miller and Miller 2005). No significant difference was determined between the weighted linear and quadratic regression. According to this result the weighted linear model was accepted and used for quantification.

For each dienal LOD and LOQ were estimated based on the lowest analyzed concentration that on average gave S/N > 3 or 10, respectively (Table 3). The LOD ranged from 1 to 5×10^{-8} mol L^{-1} for the different analytes with the highest instrumental sensitivity for 2*E*,4*E*-decadienal.

Precision and sample stability

The precision of the instrument was successfully verified by homoscedasticity of re-measured QCS at the beginning (QCS_{start}) and end (QCS_{end}) of the entire measurement regime.

Re-measurement of samples after storage of seven days at reduced temperatures (5°C) and darkness resulted in a recovery rate of > 91% for all quantified compounds. Thus sample stability for 1 week was demonstrated. After additonal prolonged sample storage of 113 days at −20°C a recovery of > 84% for the dienals and of 50–77% for the trienals was determined (Supporting Information **S8**).

Dienal analysis in diatom cultures

Laboratory cultures of marine microalgae in exponential growth phase were investigated to evaluate the applicability of the new UHPLC-HRMS method for the detection and quantification of PUAs with two conjugated double bonds (dienals). Cultures of the bloom forming diatoms *C. didymus*, *S. costatum*, and *T. rotula* were analyzed. For the latter two species, PUA production was already quantified using a GC-MS method following derivatization (Wichard et al. 2005a). Concentrations determined in Wichard et al. (2005a) served as reference. *C. didymus* was investigated for the first time with regard to PUA production. Besides **2**, **3**, and **4** that are regularly recorded in diatoms also hexadienal (**1**) was detected.

Dienals were detected and quantified in all three diatom strains (Table 4). Heptadienal (**2**) was present in highest amounts in *S. costatum* (0.48 ± 0.13 fmol cell^{-1}) followed by octadienal (**3**) with 0.25 ± 0.09 fmol cell^{-1}. Decadienal (**4**) was present in quantifiable amounts only in *T. rotula* (0.03 ± 0.01 fmol cell^{-1}). Values for *S. costatum* can be compared to those from Wichard et al. (2005b) who investigated the same strain using PFBHA-derivatization. As in our study heptadienal (**2**) was the most dominant PUA with ca. 0.1 fmol cell^{-1} followed by octadienal (**3**) thus indicating the validity of the approach. In general, all results presented here are in accordance with earlier investigations and are well within the range of already observed species-, strain-, and culture dependent variability (Pohnert et al. 2002; Wichard et al. 2005a). Hexadienal (**1**) was detected in traces in *T. rotula* which is to our knowledge the first record of **1** in marine diatoms. Co-injection with an authentic standard confirmed the first evidence of the formation of hexadienal (**1**) by *T. rotula*. This detection of a low abundant, previously unknown metabolite supports the power of the direct PUA determination introduced here. Decadienal (**4**) was for the first time detected in traces in *S. costatum*.

Decadienal (**4**) was present in three of the four possible isomeric forms. The peak corresponding to the reference standard (2*E*,4*E*-isomer, $t_R = 3.14$ min) was followed by two peaks with identical mass ($t_R = 3.30$ min, $t_R = 3.45$ min) presumably corresponding to the 2*E*,4*Z*- and 2*Z*,4*E*-isomers since the fourth possible isomer with 2*Z*,4*Z* geometry has not been found in diatoms. We could not observe baseline separation of the isomers of **2** and **3**, which might be caused by their lower polarity and thereby shorter retention times. We therefore have to consider both isomers contributing to the integration for quantification. The origin of the different isomers is not fully understood; it was assigned to the release of isomeric mixtures by diatoms (Miralto et al. 1999) but also was discussed to be caused by isomerization occurring during sample processing (d'Ippolito et al. 2002a,b). Because our method induces minimum stress during sampling and the pure standards show only one signal without contribution of isomerization during the experimental procedure (Fig. 1b), we conclude that the production of isomeric mixtures by diatoms is more likely the explanation for the phenomenon.

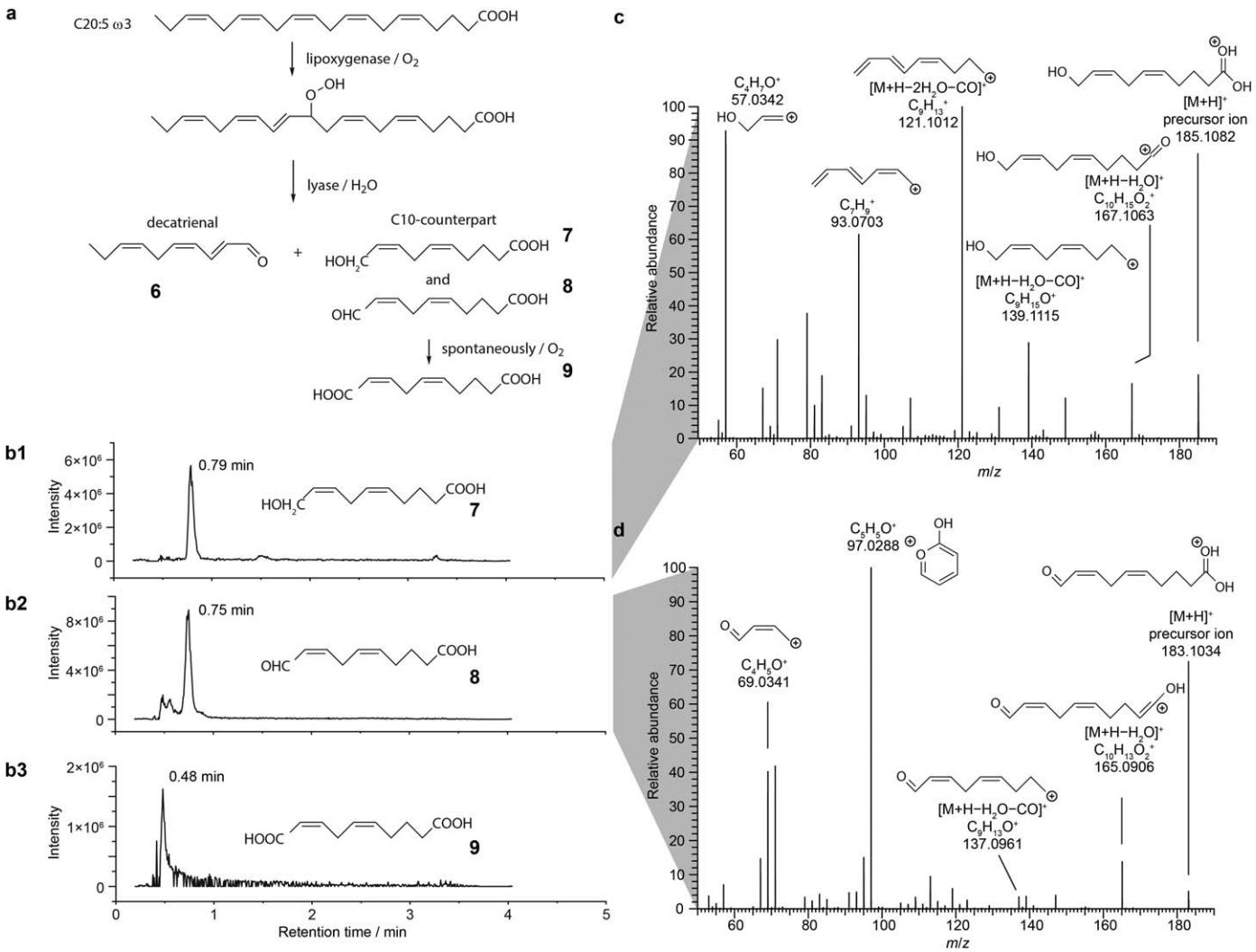

Fig. 2. UHPLC-HRMS analysis of polar eicosapentaenoic acid-derived products. (**a**) Lipoxygenase-mediated oxygenation and hydroperoxide lyase cleavage of eicosapentaenoic acid. All known (Barofsky and Pohnert 2007) and in this context newly observed products are listed. (**b**) Representative extracted ion chromatograms from a culture of *Thalassiosira rotula* RCC776 from the products **7** (**b1**), **8** (**b2**), and **9** (**b3**). (**c**) MS^2 spectrum of **7** obtained from **b1** including the main fragments. (**d**) MS^2 spectrum of **8** obtained from **b2** including the main fragments. Detailed fragmentation trees including the assignment to the spectra can be found in the Supporting Information (**S4**–**S7**).

Trienal analysis in diatom cultures

Trienals, PUAs with three double bonds, such as 2*E*,4*Z*,7-octatrienal (**5**) and 2*E*,4*Z*,7*Z* -decatrienal (**6**) are also released by marine algae and show comparable or even higher activity compared to dienals (Miralto et al. 1999; Jüttner 2005; Romano et al. 2010). For **5** and **6** no commercial standards are available and thus chromatograms were screened in full scan mode. Chromatographic runs were evaluated by monitoring the calculated accurate masses of the trienals (Table 3; for extracted mass spectra *see* Supporting Information **S1**). Both trienals were assigned to intense peaks eluting ca. 0.5 min earlier compared to the dienals of identical chain length (Fig. 1c). Decatrienal (**6**) was confirmed by analysis of its MS^2 spectrum (Supporting Information **S2**–**S3**). Peak shapes indicate the occurrence of isomers that are not baseline separated. The trienals **5** and **6** were thus determined as sum of all isomers and detected in quantifiable amounts in *T. rotula* and *S. costatum* but not in *C. didymus*. The trienal concentration can be estimated by comparison of the peak areas in full scan mode and assuming similar response factors as for the corresponding dienals (Table 4). Due to the fact that these values are not supported by referencing to synthetic standards different response factors in the MS might lead to a slight overestimation of one of the groups. The relative proportion of trienals compared to the dienals was as low as 12% in *S. costatum* and as high as 80% in *T. rotula*. *S. costatum* contained more octatrienal (**5**) compared to decatrienal (**6**), while **6** was the major PUA in *T. rotula*. The relative

proportions of these metabolites are in accordance with previous investigations using derivatization-based methods (d'Ippolito et al. 2002a; Wichard et al. 2005a,b).

Non-volatile oxylipins in diatom cultures

During the formation of PUAs from fatty acids a second product is released in diatoms namely short-chain hydroxylated fatty acids: 6*E*-8-hydroxyoct-6-enoic acid accompanying **3** and **5**, and 5*Z*,8*Z*-10-hydroxydeca-5,8-dienoic acid (**7**) accompanying **4** and **6** (Fig. 2a; Barofsky and Pohnert 2007). Analogous to these metabolites, formation of heptadienal (**2**) from eicosapentaenoic acid would result in 5*Z*,8*Z*,11*Z*-13-hydroxytrideca-5,8,11-trienoic acid, a metabolite that has not been detected so far in diatom lysates. As no commercial standards are available for these oxylipins the chromatograms were screened in full scan mode and monitored for the calculated accurate masses of these oxylipins. An intense peak eluting at around 0.79 min (Fig. 2, b1) could be assigned to **7** and was fully confirmed by its high resolution mass and by the evaluation of the according MS^2 spectrum (Fig. 2c). The presence in quantifiable amounts in *T. rotula* but not in *C. didymus* and *S. costatum* is in accordance with the high amounts of decatrienal (**6**) released by *T. rotula* (Table 4). Additionally, a concomitantly eluting peak at 0.75 min (Fig. 2, b2) was tentatively assigned to the corresponding ω-oxo-acid 5*Z*,8*Z*-10-oxodeca-5,8-dienoic acid (**8**) based on evaluation of the accurate mass and the MS^2 spectrum (Fig. 2d). The ω-oxo-acid may be formed as a shunt product of the lyase which seems to produce similarly to known P450 enzymes the corresponding oxo analogue (Noordermeer et al. 2001; Grechkin and Hamberg 2004). Supporting this hypothesis is the fact that evidence for the oxidation product, namely the dicarboxylic acid (**9**) was found (Fig. 2, **b3**) which easily can be obtained as oxidation product from **8** on air contact.

Discussion

The developed method provides a sensitive technique to measure and identify oxylipins including dienals, trienals, as well as ω-oxidized-acids within complex biological matrices. In contrast to previously published methods it can monitor the wide array of diatom-derived oxylipins within one single chromatographic run. This will enable mechanistic studies of fatty acid metabolism in diatoms and other oxylipin-producing organisms. The method will also facilitate investigations on the activity of the hitherto poorly investigated polar oxylipins derived from LOX-HPL reactions, thereby opening up new fields of research. Especially the fact that no bias is introduced due to the lack of the need for extraction procedures, the method provides direct access to the wound-activated metabolism of diatoms. The first identification of hexadienal (**1**) in diatom extracts shows that the untargeted measurement of previously unidentified compounds is possible in parallel to targeted PUA analysis. In addition it demonstrates that the newly introduced method allows for sensitive detection of novel products that were previously overseen, presumable due to their problematic extraction or derivatization. Small required sample volumes compared to existing methods (d'Ippolito et al. 2002a) and the short analysis time make this method ideal for higher throughput surveys of cellular PUA concentrations in naturally occurring phytoplankton assemblages as well as cultures. Due to the high plasticity of the parameter "PUA" such high throughput analyses will enable a close monitoring of PUA in diatoms under the influence of abiotic and biotic stressors. A quantitative comparison of the performance of the newly introduced protocol and previous approaches is hindered by the fact that neither, d'Ippolito et al. (2002a) nor Edwards et al. (2015) report limits of detection. Compared to Wichard et al. (2005b) our method is more sensitive (1.7×10^{-8} mol L^{-1} vs. 7.2×10^{-8} mol L^{-1} determined in GC-EI-MS mode). In case of sensitivity problems, the method would easily allow a lowering of the LOD by scaling up the volume of filtered samples to increase the analyte signal intensities. Compared to derivatization-based methods we avoid handling of potentially toxic metabolites and extraction protocols using organic solvents. Further, in contrast to PFBHA-derivatized PUAs where each isomer results in two peaks we only detect one signal per analyte resulting in less complex chromatograms. However, PFBHA treatment traps PUAs and allows the detection of even highly reactive metabolites that might be overlooked using our protocol. In conclusion, we provide a fast and direct determination of PUAs that is as sensitive as established protocols based on derivatization. We are able to pick up and quantify all PUAs previously detected in the phytoplankton species investigated here as well as other novel apolar and polar oxylipins. We also introduce the use of wide spread LC-MS analytical platforms and provide an alternative for labs that do not have access to GC-MS methods.

Comments and recommendations

In this study laboratory cultures of marine diatoms were investigated. To apply the method on field samples the UHPLC-HRMS measurements can be used without further adjustment.

The sensitivity is determined by the amount of PUA-producing cells on the GF/C filter and their PUA production. Sensitivity can thus easily be increased by filtration of more biomass. In case of samples containing larger particles or herbivores an additional filtration step removing those might be required. The method allows high throughput investigations and our monitoring of stability indicates that usage of a cooled (5°C) auto sampler would be sufficient for accurate measurements of larger sample sets. If prolonged storage time is required, as in the case of field experiments, sample instability could easily be compensated using standards that are processed and stored under identical conditions

as the field samples. In this study cell damage and the following PUA production were achieved by ultrasound treatment, which was adjusted to diatom cells. For other phytoplankton members with non-silicified cell walls the ultrasound treatment can be modulated accordingly to achieve sufficient cell damage; alternative methods like repeated freezing and thawing cycles might be utilized for cell disruption. Mass spectrometers that provide accurate mass measurements are recommended to filter out the background noise of the complex sample matrix to obtain high analyte sensitivities. However, even nominal mass resolution together with the added selectivity by chromatographic retention time is sufficient for the determination of PUAs. In these cases, additional specificity might be brought in using MS^2 protocols. When analyzing high salinity matrices a routine cleaning of the corona discharge needle is recommended as salt precipitation influences the analyte ionization.

References

Adolph, S., and others. 2004. Cytotoxicity of diatom-derived oxylipins in organisms belonging to different phyla. J. Exp. Biol. **207**: 2935–2946. doi:10.1242/jeb.01105

Alsufyani, T., A. H. Engelen, O. E. Diekmann, S. Kuegler, and T. Wichard. 2014. Prevalence and mechanism of polyunsaturated aldehydes production in the green tide forming macroalgal genus *Ulva* (Ulvales, Chlorophyta). Chem. Phys. Lipids **183**: 100–109. doi:10.1016/j.chemphyslip.2014.05.008

Barofsky, A., and G. Pohnert. 2007. Biosynthesis of polyunsaturated short chain aldehydes in the diatom *Thalassiosira rotula*. Org. Lett. **9**: 1017–1020. doi:10.1021/ol063051v

Barreiro, A., and others. 2011. Diatom induction of reproductive failure in copepods: The effect of PUAs versus non volatile oxylipins. J. Exp. Mar. Biol. Ecol. **401**: 13–19. doi:10.1016/j.jembe.2011.03.007

Cutignano, A., and others. 2006. Chloroplastic glycolipids fuel aldehyde biosynthesis in the marine diatom *Thalassiosira rotula*. ChemBioChem. **7**: 450–456. doi:10.1002/cbic.200500343

Cutignano, A., N. Lamari, G. d'Ippolito, E. Manzo, G. Cimino, and A. Fontana. 2011. Lipoxygenase products in marine diatoms: A concise analytical method to explore the functional potential of oxylipins. J. Phycol. **47**: 233–243. doi:10.1111/j.1529-8817.2011.00972.x

d'Ippolito, G., I. Iadicicco, G. Romano, and A. Fontana. 2002a. Detection of short-chain aldehydes in marine organisms: The diatom *Thalassiosira rotula*. Tetrahedron Lett. **43**: 6137–6140. doi:10.1016/S0040-4039(02)01283-2

d'Ippolito, G., and others. 2002b. New birth-control aldehydes from the marine diatom *Skeletonema costatum*: Characterization and biogenesis. Tetrahedron Lett. **43**: 6133–6136. doi:10.1016/s0040-4039(02)01285-6

d'Ippolito, G., G. Romano, T. Caruso, A. Spinella, G. Cimino, and A. Fontana. 2003. Production of octadienal in the marine diatom *Skeletonema costatum*. Org. Lett. **5**: 885–887. doi:10.1021/ol034057c

d'Ippolito, G., and others. 2004. The role of complex lipids in the synthesis of bioactive aldehydes of the marine diatom *Skeletonema costatum*. Biochim. Biophys. Acta Mol. Cell Biol. Lipids **1686**: 100–107. doi:10.1016/j.bbalip.2004.09.002

Dittami, S. M., T. Wichard, A. M. Malzahn, G. Pohnert, M. Boersma, and K. H. Wiltshire. 2010. Culture conditions affect fatty acid content along with wound-activated production of polyunsaturated aldehydes in *Thalassiosira rotula* (Coscinodiscophyceae). Nova Hedwigia **136**: 231–248. doi:10.1127/1438-9134/2010/0136-0231

Edwards, B. R., K. D. Bidle, and B. A. S. van Mooy. 2015. Dose-dependent regulation of microbial activity on sinking particles by polyunsaturated aldehydes: Implications for the carbon cycle. Proc. Natl. Acad. Sci. USA **112**: 5909–5914. doi:10.1073/pnas.1422664112

Gerecht, A., G. Romano, A. Ianora, G. d'Ippolito, A. Cutignano, and A. Fontana. 2011. Plasticity of oxylipin metabolism among clones of the marine diatom *Skeletonema marinoi* (Bacillariophyceae). J. Phycol. **47**: 1050–1056. doi:10.1111/j.1529-8817.2011.01030.x

Grechkin, A. N., and M. Hamberg. 2004. The "heterolytic hydroperoxide lyase" is an isomerase producing a short-lived fatty acid hemiacetal. Biochim. Biophys. Acta Mol. Cell Biol. Lipids **1636**: 47–58. doi:10.1016/j.bbalip.2003.12.003

Ianora, A., and others. 2004. Aldehyde suppression of copepod recruitment in blooms of a ubiquitous planktonic diatom. Nature **429**: 403–407. doi:10.1038/nature02526

Ianora, A., and others. 2011. Impact of the diatom oxylipin 15*S*-HEPE on the reproductive success of the copepod *Temora stylifera*. Hydrobiologia **666**: 265–275. doi:10.1007/s10750-010-0420-7

Ianora, A., and others. 2015. Non-volatile oxylipins can render some diatom blooms more toxic for copepod reproduction. Harmful Algae **44**: 1–7. doi:10.1016/j.hal.2015.02.003

Jüttner, F. 2005. Evidence that polyunsaturated aldehydes of diatoms are repellents for pelagic crustacean grazers. Aquat. Ecol. **39**: 271–282. doi:10.1007/s10452-005-3419-9

Lavrentyev, P. J., G. Franze, J. J. Pierson, and D. K. Stoecker. 2015. The effect of dissolved polyunsaturated aldehydes on microzooplankton growth rates in the Chesapeake Bay and Atlantic coastal waters. Mar. Drugs **13**: 2834–2856. doi:10.3390/md13052834

Maier, I., and M. Calenberg. 1994. Effect of extracellular Ca^{2+} and Ca^{2+}-antagonists on the movement and chemoorientation of male gametes of *Ectocarpus siliculosus* (Phaeophyceae). Bot. Acta **107**: 451–460. doi:10.1111/j.1438-8677.1994.tb00820.x

Miller, J. N., and J. C. Miller. 2005. Statistics and chemometrics for analytical chemistry. Pearson Education.

Miralto, A., and others. 1999. The insidious effect of diatoms on copepod reproduction. Nature **402**: 173–176. doi:10.1038/46023

Morillo-Garcia, S., and others. 2014. Potential polyunsaturated aldehydes in the Strait of Gibraltar under two tidal regimes. Mar. Drugs **12**: 1438–1459. doi:10.3390/md12031438

Noordermeer, M. A., G. A. Veldink, and J. F. G. Vliegenthart. 2001. Fatty acid hydroperoxide lyase: A plant cytochrome P450 enzyme involved in wound healing and pest resistance. ChemBioChem **2**: 494–504. doi:10.1002/1439-7633(20010803)2:7/8<494::AID-CBIC494>3.0.CO;2-1

Pohnert, G. 2000. Wound-activated chemical defense in unicellular planktonic algae. Angew. Chem. Int. Ed. **39**: 4352–4354. doi:10.1002/1521-3773(20001201)39:23<4352::AID-ANIE4352>3.0.CO;2-U

Pohnert, G. 2002. Phospholipase A_2 activity triggers the wound-activated chemical defense in the diatom *Thalassiosira rotula*. Plant Physiol. **129**: 103–111. doi:10.1104/pp.010974

Pohnert, G., and others. 2002. Are volatile unsaturated aldehydes from diatoms the main line of chemical defence against copepods?. Mar. Ecol.: Prog. Ser. **245**: 33–45. doi:10.3354/meps245033

Pohnert, G., S. Adolph, and T. Wichard. 2004. Short synthesis of labeled and unlabeled 6*Z*,9*Z*,12*Z*,15-hexadecatetraenoic acid as metabolic probes for biosynthetic studies on diatoms. Chem. Phys. Lipids **131**: 159–166. doi:10.1016/j.chemphyslip.2004.04.011

Poulet, S. A., A. Cueff, T. Wichard, J. Marchetti, C. Dancie, and G. Pohnert. 2007. Influence of diatoms on copepod reproduction. III. Consequences of abnormal oocyte maturation on reproductive factors in *Calanus helgolandicus*. Mar. Biol. **152**: 415–428. doi:10.1007/s00227-007-0701-5

Ribalet, F., T. Wichard, G. Pohnert, A. Ianora, A. Miralto, and R. Casotti. 2007. Age and nutrient limitation enhance polyunsaturated aldehyde production in marine diatoms. Phytochemistry **68**: 2059–2067. doi:10.1016/j.phytochem.2007.05.012

Ribalet, F., L. Intertaglia, P. Lebaron, and R. Casotti. 2008. Differential effect of three polyunsaturated aldehydes on marine bacterial isolates. Aquat. Toxicol. **86**: 249–255. doi: 10.1016/j.aquatox.2007.11.005

Ribalet, F., and others. 2014. Phytoplankton cell lysis associated with polyunsaturated aldehyde release in the Northern Adriatic Sea. PLoS One **9**: e85947. doi:10.1371/journal.pone.0085947

Rodhe, W., R. A. Vollenweider, and A. Nauwerck. 1958. The primary production and standing crop of phytoplankton, p. 299–322. *In* A. A. Traverso [ed.], Perspectives in marine biology. Univ. of California Press.

Romano, G., A. Miralto, and A. Ianora. 2010. Teratogenic effects of diatom metabolites on sea urchin *Paracentrotus lividus* embryos. Mar. Drugs **8**: 950–967. doi:10.3390/md8040950

Schnitzler, I., G. Pohnert, M. E. Hay, and W. Boland. 2001. Chemical defense of brown algae (*Dictyopteris* spp.) against the herbivorous amphipod *Ampithoe longimana*. Oecologia. **126**: 515–521. doi:10.1007/s004420000546

Spiteller, D., and G. Spiteller. 2000. Identification of toxic 2,4-decadienal in oxidized, low-density lipoprotein by solid-phase microextraction. Angew. Chem. Int. Ed. **39**: 583–585. doi:10.1002/(SICI)1521-3773(20000204)39:3<583::AID-ANIE583>3.0.CO;2-O

Stumpe, M., and others. 2006. Biosynthesis of C_9-aldehydes in the moss *Physcomitrella patens*. Biochim. Biophys. Acta. **1761**: 301–312. doi:10.1016/j.bbalip.2006.03.008

Taylor, R. L., G. S. Caldwell, H. J. Dunstan, and M. G. Bentley. 2007. Short-term impacts of polyunsaturated aldehyde-producing diatoms on the harpacticoid copepod *Tisbe holothuriae*. J. Exp. Mar. Biol. Ecol. **341**: 60–69. doi:10.1016/j.jembe.2006.10.028

Taylor, R. L., K. Abrahamsson, A. Godhe, and S. A. Wangberg. 2009. Seasonal variability in polyunsaturated aldehyde production potential among strains of *Skeletonema marinoi* (Bacillariophyceae). J. Phycol. **45**: 46–53. doi:10.1111/j.1529-8817.2008.00625.x

Vardi, A., and others. 2006. A stress surveillance system based on calcium and nitric oxide in marine diatoms. PLoS Biol. **4**: 411–419. doi:10.1371/journal.pbio.0040060

Vidoudez, C., and G. Pohnert. 2008. Growth phase-specific release of polyunsaturated aldehydes by the diatom *Skeletonema marinoi*. J. Plankton Res. **30**: 1305–1313. doi:10.1093/plankt/fbn085

Vidoudez, C., R. Casotti, M. Bastianini, and G. Pohnert. 2011. Quantification of dissolved and particulate polyunsaturated aldehydes in the Adriatic Sea. Mar. Drugs **9**: 500–513. doi:10.3390/md9040500

Wendel, T., and F. Jüttner. 1996. Lipoxygenase-mediated formation of hydrocarbons and unsaturated aldehydes in freshwater diatoms. Phytochemistry **41**: 1445–1449. doi:10.1016/0031-9422(95)00828-4

Wichard, T., and others. 2005a. Survey of the chemical defence potential of diatoms: Screening of fifty one species for $\alpha,\beta,\gamma,\delta$-unsaturated aldehydes. J. Chem. Ecol. **31**: 949–958. doi:10.1007/s10886-005-3615-z

Wichard, T., S. A. Poulet, and G. Pohnert. 2005b. Determination and quantification of $\alpha,\beta,\gamma,\delta$-unsaturated aldehydes as pentafluorobenzyl-oxime derivates in diatom cultures and natural phytoplankton populations: Application in marine field studies. J. Chromatogr. B: Anal. Technol. Biomed. Life Sci. **814**: 155–161. doi:10.1007/s10886-005-3615-z

Wichard, T., and G. Pohnert. 2006. Formation of halogenated medium chain hydrocarbons by a lipoxygenase/hydroperoxide halolyase-mediated transformation in planktonic

microalgae. J. Am. Chem. Soc. **128**: 7114–7115. doi: 10.1021/ja057942u

Wichard, T., and others. 2008. Influence of diatoms on copepod reproduction. II. Uncorrelated effects of diatom-derived $\alpha,\beta,\gamma,\delta$-unsaturated aldehydes and polyunsaturated fatty acids on *Calanus helgolandicus* in the field. Prog. Oceanogr. **77**: 30–44. doi:10.1016/j.pocean.2008.03.002

Acknowledgments

We gratefully acknowledge W. Kooistra (Stazione Zoologica Anton Dohrn, Naples, Italy) for providing us the culture of *Chaetoceros didymus* supported by the EC project ASSEMBLE (grant agreement no. 227799). This study was supported by the Jena School of Microbial Communication (C.K., T.W.), the Hans-Böckler-Stiftung (M.D.), and the Deutsche Forschungsgemeinschaft (CRC 1067 "AquaDiva" and CRC 1127 "ChemBioSys"; G.P., N.U.).

Conflict of Interest

None of the authors of this manuscript report any conflicts of interests relevant to this work.

Submitted 25 June 2016
Revised 05 September 2016
Accepted 14 September 2016

Associate editor: Krista Longnecker

4 Discussion

Organisms interact with each other in various ways, mediated by visual, acoustic, mechanical or chemical cues. Whereas we have a good understanding of the first three, which we rely on ourselves, chemically mediated interactions - while being of major importance for single-celled organisms - are far less understood. This evolutionary old chemical language is not just highly matrix-dependent, with different sets of infochemicals in the marine realm compared to the terrestrial. Various methods exist to address research questions in chemical communication and to decipher the molecule-driven communication between organisms, reaching from classical bioassay-guided structure elucidation to newly emerging metabolomics approaches. The prospects of metabolomics approaches for the also still rather new field of chemical ecology of marine phytoplankton are discussed in the following.

4.1 Complementing targeted with untargeted analysis of infochemicals

4.1.1 From targeting PUAs to broad oxylipin profiling

The observation of Miralto et al. (1999), who for the first time linked reduced egg hatching and viability of copepod grazers to diatom-released polyunsaturated aldehydes (PUAs), has motivated a multitude of studies further investigating the ecological role of algal PUAs. Their enzymatic biosynthesis from lipid-derived fatty acids was demonstrated (d'Ippolito et al. 2002b; Pohnert 2002), their biological activity linked to structural properties (Adolph et al. 2003), and their accumulation in the gonads of grazers shown and linked to reduced reproductive success (Ianora et al. 2004; Wolfram et al. 2014). With regard to the differential PUA production within various diatoms (Wichard et al. 2005a), the observation of intra- and interspecific growth inhibition and toxicity (Casotti et al. 2005; Vardi et al. 2006) suggested population-control also on the level of primary producers. In parallel to an increasing number of studies confirming the deleterious effects of PUAs on marine organisms (Ribalet et al. 2007a; Romano et al. 2010), also contradictory observations were reported (Dutz et al. 2008; Jones and Flynn 2005; Wichard et al. 2008). The observation of Fontana et al. (2007), that the production of non-volatile oxylipins in diatoms also results in reduced reproductive success in copepods, lead to an intensified investigation of non-volatile oxylipins in the following years (Barreiro et al. 2011; Ianora et al. 2011; Ianora et al. 2015; Varrella et al. 2016). Separate analytical

platforms for the targeted analysis of diatom-derived PUAs have been introduced to date and since recently also for non-volatile oxylipins. Whereas PUAs are measured after extraction via SP(M)E either directly or subsequent to derivatization using GC-MS (d'Ippolito et al. 2002a; Pohnert 2000; Vidoudez et al. 2011b; Wichard et al. 2005b), non-volatile oxylipins are analysed following derivatization by LC-MS (Cutignano et al. 2011). The developed LC-MS-based protocol (**Manuscript 5**) combines targeted volatile and untargeted non-volatile oxylipin analysis on one analytical platform. It allows to precisely quantify well-known PUAs and, in addition, to screen for e.g. still unknown accompanying lyase products.

4.1.2 Analytical platform for oxylipin profiling

In the following, the developed analytical protocol is discussed focusing on quality control and selected validation key criteria. Sample preparation including all steps from culture filtration to sample injection is fast (ca. 20 min) and easy as no extraction or derivatization is needed. In contrast to the sample preparation for headspace SPME analysis (Pohnert 2000), particulate organic matter has to be removed prior to LC-MS measurement requiring one additional centrifugation step. Cultures are harvested by filtration, which for the small required volume of 40 mL and the investigated cell densities is rapidly and efficiently done. Some optimized protocols allow to centrifuge microalgae without cellular wounding (Bölling and Fiehn 2005). However, other algal species should not be centrifuged (Michels et al. 2016), as diverse hydrodynamic forces act on algal cells during centrifugation leading to cell disruption (Xu et al. 2015). A bottleneck of the developed method for high-throughput analyses is the artificial wounding of algal cells that was achieved by separate ultrasound treatment per sample. Parallel processing of several samples in an ultrasonic bath resulted in decreased analyte intensities (Fig. S 1). Depending on algal cell wall robustness, wounding by ultrasonic baths, freeze-thaw-cycles, exposure to saline or solvent solutions, or bead mill treatment (e.g. for macroalgae, **Manuscript 2**) may help to increase sample throughput (Jüttner 2001; Wichard et al. 2005b). The subsequent UHPLC method was optimized to separate aldehydes in the range of C_6-C_{10} within a chromatography run time of 5 min, which is well below typical GC run times of about 30 min (d'Ippolito et al. 2002a; Wichard et al. 2005b). Taking the polarity of the analytes into account, APCI instead of ESI was chosen to ionize PUAs, resulting in 2-3x higher sensitivity than with the more commonly used ESI (data not shown). When measuring

marine samples with high salt load, the corona discharge needle should be cleaned regularly to ensure robust ionization. APCI has been introduced earlier to analyse e.g. 2,4-dinitrophenylhydrazine-derivatized PUAs (Edwards et al. 2015), the hydroperoxide lyase product 12-oxododeca-5,8,10-trienoic acid (Pohnert 2000), and hydroxy fatty acids as intermediates of oxylipin biosynthetis (Santiago-Vázquez et al. 2004). To further increase the sensitivity of the targeted PUA analysis, positive ionization and targeted SIM mode were applied, resulting in LODs of <1-5×10^{-8} M and LOQs of 1.9-14×10^{-8} M (**Manuscript 5**). Thereby, the instrumental sensitivity was highest for decadienal, followed by heptadienal, hexadienal and octadienal. Recently, an optimized protocol for PUA analysis using SPME with on-fiber derivatization led to a LOD of 0.027 µg L^{-1} for decadienal (Ma et al. 2011b). Previous derivatization methods reported a LOD of 100-200 µg aldehyde per starting sample (d'Ippolito et al. 2002a) and a LOQ of 11 µg L^{-1} per standard (Wichard et al. 2005b). To compare these values, the minimum number of phytoplankton cells in 1 L of seawater was estimated that would be needed for quantitative analyses (Table 1). The achieved LOQ for decadienal of 19 nM, which equals <400 cells of natural phytoplankton with reported 47.7 fmol $cell^{-1}$ (Wichard et al. 2005b), is in the lower range of previous protocols and well suited for the investigation of algal cultures and field samples (d'Ippolito et al. 2002a; Ma et al. 2011b; Wichard et al. 2005b).

Table 1 Limits of detection (LOD) and quantification (LOQ) as reported for several PUA analysis protocols (d'Ippolito et al. 2002a; Ma et al. 2011b; Wichard et al. 2005b) in comparison to the developed method (**Manuscript 5**). For comparison, the minimum amount of PUA-producing algal cells in 1 L of seawater for quantitative studies was estimated. LODs were transferred to LOQs based on S/N and the molar mass of decadienal. Further, a rather high PUA content of 47.7 fmol/cell as reported for natural phytoplankton samples (Wichard et al. 2005b) was considered.

Analyte	LOD	LOQ	Reference	PUA-producing cells/L
Decadienal	0.027 µg/L	-	Ma et al. 2011b	~12
Decadienal	<1×10^{-8} M	1.9×10^{-8} M	Kuhlisch et al. 2017	<400
'Aldehyde'	-	11 µg/L	Wichard et al. 2005b	<2 000
'Aldehyde'	100-200 µg/sample	-	d'Ippolito et al. 2002a	>45 000

Further comparison with alternative protocols is hindered by the poorly documented declaration of descriptors such as selectivity, accuracy, precision, sensitivity, working range, robustness or recovery, which are used to validate analytical methods (van Zoonen et al. 1998). Instrument precision was tested by re-injection of one biological sample at the beginning and end of the measuring sequence, and homoscedasticity was proven (**Manuscript 5**). Relative standard deviation of the peak areas increased

with decreasing analyte concentration in an acceptable range (IS <3%, heptadienal <6.2%, octadienal <8.7%, decadienal <10.4%). Using weighted linear regression analysis, the working range (10^{-8}-10^{-5} M) was extended compared to Wichard et al. (2005b). Sample stability for short periods was similar to Wichard et al. (2005b), which allows to store samples after collection until analysis at 4°C. Prolonged storage for more than 16 weeks at -20°C resulted in recoveries of >84% for dienals and >50% for trienals. With regard to trienal analysis, alternative conditions (e.g. -80°C) should be considered for long-term storage. Furthermore, analyte loss due to covalent binding with matrix components has to be expected when working with biological sample matrices (43-62% recovery, Wichard et al. (2005b)), which will be discussed in the following chapter.

4.1.3 Requirements of oxylipin analyses

The developed method (**Manuscript 5**) provides a snapshot of the current PUA concentrations in the sample matrix, thus representing an integrated view over PUA producing and consuming processes. For accurate quantitative analyses additional aspects should be taken into account. As the enzymatic reactions were not stopped after initiation by sonication, a continuous production of PUAs has to be considered until either the substrate is diminished, enzymatic reactivity is lost due to stability, or substrate encounter rate decreases due to dissolution. Even though enzymes can be active in the sample matrix for up to 20 min (Pohnert 2002), decatrienal formation shows a saturation after already 3 min (Pohnert 2000) in parallel to a decline in polyunsaturated fatty acids (Wichard et al. 2007). The causes for the saturation are not yet known. To control the formation of PUAs, enzymes can be specifically inhibited as shown with phospholipase A2 inhibitors (Pohnert 2002) or by pH regulation (Pohnert 2000). With regard to the fate of PUAs, the inherent reactivity of the α,β-unsaturated structure should result in decreasing concentrations of free PUAs (Wichard et al. 2005b) due to nonspecific reactions with matrix components such as proteins or DNA (Carvalho et al. 1998; Zhu et al. 2010). Supporting this assumption, a moderately specific labelling of proteins involved in energy metabolism was observed, as well as the accumulation of labelled PUAs in copepod gonads (Wolfram et al. 2014; Wolfram et al. 2015). How nonspecific covalent binding and specific accumulation of PUAs are regulated is not yet known. To control the reactivity of PUAs, derivatization protocols can be applied that stabilize PUAs directly upon release, thereby limiting the covalent binding to matrix components (Wichard et al. 2005b).

4.1.4 Ecological relevance of oxylipin formation in microalgae

Applicability of the developed targeted oxylipin protocol was demonstrated by quantitative dienal analysis in exponentially growing diatom cultures. Concentrations ranged from 0.01 fmol cell-1 to 0.48 fmol cell-1 and were well within already reported concentration ranges (**Manuscript 5,** Table S 1). The presence of 2*E*,4*Z*-hexadienal was for the first time demonstrated in a marine diatom. Typically, heptadienal, octadienal and decadienal are monitored and reported in PUA analyses of marine diatoms, which is in part due to the availability of reference standards. Also in a in recent study of marine benthic diatoms hexadienal was found next to several other uncommon mono- and polyunsaturated aldehydes (Pezzolesi et al. 2017). With regard to the known biosynthetic pathways, a LOX and HPL for ω-1 unsaturated fatty acids have to exist, however, such fatty acids have not been reported so far. Thus, unknown mechanisms may be responsible for the generation of 2*E*,4*Z*-hexadienal. This discovery of novel structures highlights the necessity of untargeted methods complementing established targeted PUA analyses in order to discover unexpected compounds and metabolic pathways. Decadienal could only be quantified in the *Thalassiosira rotula* culture even though instrument sensitivity was highest for decadienal (Manuscript 5). Further, it was detected for the first time in traces in *Skeletonema costatum* RCC75. Besides these known PUA producers, *Chaetoceros didymus* was investigated that has not been studied for PUA production before. With low amounts of heptadienal (0.01 fmol cell-1) and only traces of decadienal it is in the lower range of reported PUA concentrations in marine diatoms (**Manuscript 5**, Table S 1), and appears not to be an important PUA producer. The investigated *C. didymus* strain was isolated in the Gulf of Naples, is regularly recorded in temperate to warm ocean areas, and known for its resistance against algicidal bacteria (Paul and Pohnert 2011). Within the cosmopolitan *Chaetoceros* genus, which is among the most abundant and diverse planktonic diatom taxa (Malviya et al. 2016), PUA formation was only observed in a few other species so far namely *C. compressus* and *C. muelleri*, while *C. affinis*, *C. calcitrans*, and *C. socialis* do not produce PUAs at all (Dutz et al. 2008; Fontana et al. 2007; Ma et al. 2011b; Wichard et al. 2005a). In this context it is interesting to note that the diatom genus *Thalassiosira*, which is also among the most abundant and diverse diatom taxa (Malviya et al. 2016), is a well-known PUA producing taxon. The genus *Skeletonema*, which has been investigated intensively with regard to PUA formation, barely contributes to global diatom biomass (Fig. 10, Leblanc et al.

(2012). Thus, despite the wealth of positive effects of PUAs for the releasing algae, there seems to be no relation to their ecological dominance. With the concepts of trait-based phytoplankton ecology in mind (Litchman and Klausmeier 2008), it may be assumed that non-PUA producing diatom taxa exhibit equivalent functional traits based on other chemical molecules as already observed for nonvolatile oxylipins (Ianora et al. 2011). PUA screening of ecologically more relevant microalgae and the recording of HPL gene distributions within algal lineages may assist in the future to determine the actual ecological relevance of PUA formation within the marine plankton.

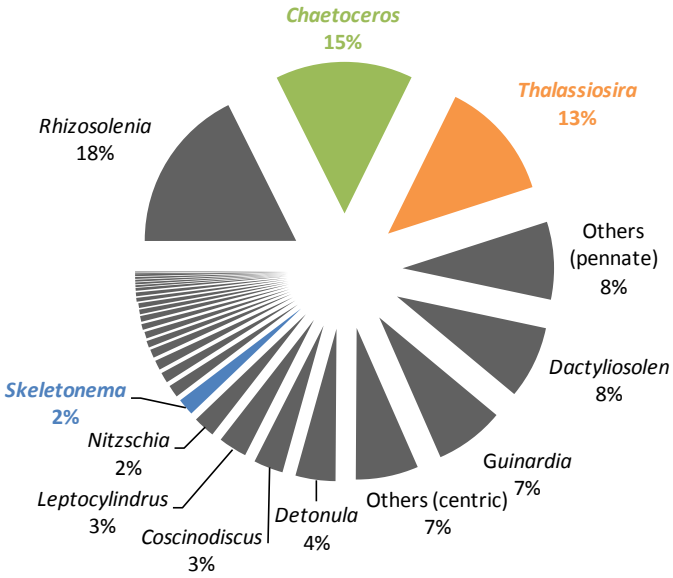

Fig. 10 Proportion of the different diatom genera to the global diatom biomass following Leblanc et al. (2012). The genera highlighted by color exemplary reflect the divergence between relevance in biomass contribution (e.g. *Chaetoceros*, *Thalassiosira*) and in PUA release (e.g. *Thalassiosira*, *Skeletonema*).

Untargeted oxylipin profiling was conducted in addition to the targeted analysis of PUAs. Therefore, full scan mode and targeted SIM mode were run in alternating scans. The high mass resolution (70.000) of the Orbitrap detector allowed to assign chromatographic peaks in full scan mode to known diatom oxylipins, which were further characterized and confirmed by MS/MS measurements as reference standards were not available. Putatively assigned peaks of octa- and decatrienal were integrated and quantified assuming identical response factors as for the respective dienals. Especially in *Thalassiosira rotula* the trienals were present in high concentrations accounting together for 80% of the total quantified aldehyde amount. In many structure-activity studies decadienal is applied (Adolph et al. 2003; Gallina et al. 2014; Pepi et al. 2017; Wolfram et al. 2015), however, with regard to occurrence and concentration of decadienal and decatrienal in so far investigated diatom cultures (**Manuscript 5**, Table

S 1), the contribution of decatrienal may have been underestimated and underrepresented in an ecological context. This again highlights the importance to design ecologically relevant experiments and not base set-ups on available reference standards or techniques. Sampling for untargeted metabolite analyses can control for unexpected or unknown effects. The untargeted oxylipin profiling also enabled to screen for short-chain hydroxylated fatty acids, which are suggested to be the second enzymatic products accompanying PUAs after HPL cleavage in diatoms (Barofsky and Pohnert 2007). Accordingly, 10-hydroxydeca-5*Z*,8*Z*-dienoic acid - the counterpart of decatrienal as most intense observed PUA - could be assigned to a peak in full scan mode. The simultaneous presence of the corresponding ω-oxo-acid with similar intensity may reflect an enzymatic side-reaction as known of plant HPLs (Grechkin and Hamberg 2004).

In conclusion, the developed protocol combines targeted and untargeted oxylipin profiling of diatom extracts by parallel full scan and targeted SIM measurement. Both polar and nonpolar oxylipins are captured using APCI technology. The short analysis time allows experiments with high sample throughput. Nonpolar PUAs can thereby be detected with high sensitivity and without derivatization needs in complex biological sample matrices. After the discovery of PUAs in diatoms and their role for algal defence, the scientific focus was and still is primarily on a few known molecules namely heptadienal, octadienal and decadienal. Still many findings especially with regard to their biosynthesis and mode of action on the molecular level await discovery. However, several studies also showed species-dependent the release of other short chain PUAs and non-volatile oxylipins in even higher amounts than or in the absence of PUAs. The developed method can help to monitor lyase products for a better understanding of the involved enzymatic mechanisms. It allows to screen for new candidates of oxylipin chemistry, thereby broadening our understanding of grazer defence in marine phytoplankton communities. Further, the parallel profiling of polar and nonpolar oxylipins may help to unravel the many contradicting results between oxylipin formation in diatoms and their effect on algal grazers. It may also help to reassess the proposed multifunctional roles of PUAs in plankton ecology that arose in the last years. PUA formation has not only been related to grazer defence, but also to allelopathic effects towards other microalgae, antimicrobial activity, intraspecific cell signalling, and population control. Also to other metabolites in plankton ecology, like DMSP, multiple

roles are assigned that may be re-investigated by combined targeted and untargeted analyses to validate causalities.

4.2 Mapping phenotypic plasticity of microalgae using untargeted metabolite profiling

4.2.1 Stimulating physiological plasticity in laboratory cultures

For a comprehensive understanding of the chemical ecology of marine phytoplankton it is not just necessary to investigate the chemical nature of signal molecules, their biosynthesis and release. It is also important to characterize the responses in perceiving organisms. In general, marine organisms can respond to biotic and abiotic environmental cues with changes in biochemistry, physiology, development, morphology, and behaviour in order to improve their survival, fecundity, and thus fitness. This so called *phenotypic plasticity* is defined as the 'property of individual genotypes to produce different phenotypes when exposed to different environmental conditions' (Pigliucci et al. 2006). *Phenotypic plasticity* can thereby affect the ecology and evolution of chemically-mediated species interactions e.g. by stabilizing populations, structuring food webs, reciprocal plasticity and speciation (Agrawal 2001; Miner et al. 2005). The most rapid organism responses occur on the metabolic level as reflected by fluctuations in transcripts, proteins, and metabolites, and are designated as physiological plasticity. Both primary and secondary metabolism are involved in organism responses resulting in alternating intra- and extracellular metabolite levels. Secondary metabolites seem to be thereby of lower importance for the marine phytoplankton compared to land plants (Metlen et al. 2009; Pohnert et al. 2007). Untargeted metabolite profiling can follow in an unbiased way the physiological organism responses in chemically-mediated interactions. To simulate dynamic, mixed-factorial changes of environmental cues, the physiological plasticity of a marine microalga was mapped for batch culture growth. The physiology of algal cells - as observed e.g. in batch cultures - is hypothesized to have large implications for grazing ecology and thus the marine food web. *Phaeocystis pouchetii* was chosen as study organism to complement available data on *Skeletonema marinoi* (Barofsky et al. 2010; Vidoudez and Pohnert 2012), *Thalassiosira pseudonana* (Barofsky et al. 2009), *Synechococcus elongatus* (Fiore et al. 2015), and *Emiliania huxleyi* (Mausz and Pohnert 2015), and to broaden the knowledge about common and species-specific metabolic marker (**Manuscript 3**).

4.2.2 Constraints of laboratory batch cultures for metabolomics studies

In the following, the implications of monoclonal, non-axenic batch culture set-ups for the quality and interpretation of metabolite profiles will be discussed. Under distinct environmental conditions, a chemical phenotype is not just determined by the environment, but also by the underlying genotype (and its epigenetic transformation, see Schmidt et al. (2016)), and the interaction between both (Falconer 1989). In natural marine phytoplankton populations, a large diversity of genotypes exists due to large population sizes and short generation times that can be further increased by environmental fluctuations (Reusch and Boyd 2013). The occurrence of genotype diversity and phenotypic plasticity was recently shown in monoclonal *Chlamydomonas* cultures by applying untargeted metabolite profiling on the single cell level (Krismer et al. 2017). Single cell metabolite profiling is, however, still the exception for the investigation of chemical phenotypes of unicellular microalgae. Most commonly, bulk analyses of algal cultures are conducted (**Manuscript 2**), assuming low genetic heterogeneity and - as cell metabolism is linked to cell cycle - promoting metabolic homogeneity by cell cycle synchronization using strict light-dark regimes (Krupinska and Humbeck 1994). The putatively diploid flagellates of the monoclonal *Phaeocystis pouchetii* strain AJ01 divide during dark phase, and thus cell cycle synchronization can be assumed (Jacobsen 2002; Jacobsen and Veldhuis 2005). As metabolites were sampled at a fixed time point shortly after the onset of light, a high metabolic synchronization of these algal cultures was supposed (**Manuscript 3**). However, some initial genotype diversity may have been present, as the strain was isolated 1994 (Jacobsen 2002), and subsequently maintained by repeated dilution. Metabolite profiles of the biological replicates diverged with prolonged experimental duration. This, however, did not interfere with the multivariate statistical data analysis (**Manuscript 3**). Batch cultures induce continuous changes in environmental parameters causing physiological plasticity in microalgal cells as described for *Skeletonema marinoi* (Vidoudez and Pohnert 2012), *Emiliania huxleyi* (Mausz and Pohnert 2015), and *Phaeocystis pouchetii* (**Manuscript 3**). Based on population size descriptors as cell abundance, algal growth rates can be calculated, according to which the growth in batch cultures can be divided in different phases (e.g. lag, exponential,

stationary, and declining growth phase, Fig. 11) each with a distinct associated physiology (Bolier and Donze 1989; Monod 1949).

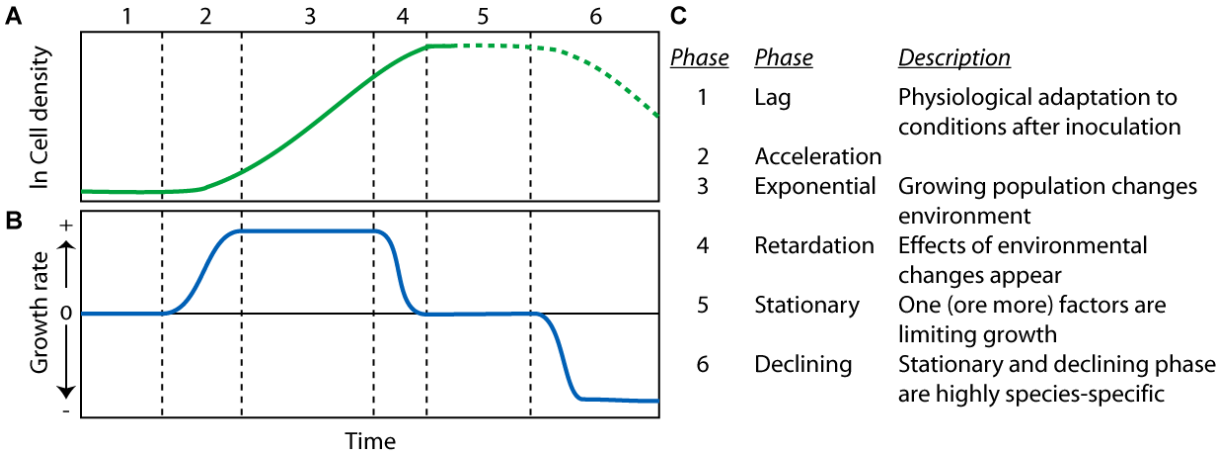

Fig. 11 Phases of algal batch growth as defined by cell density (A) and changes in the growth rate (B). Vertical dotted lines mark the transition between growth phases as described in (C). Figure adapted from Monod (1949).

The cold-water species *Phaeocystis pouchetii* showed a slow growth development taking about 50 days from lag to late stationary phase, which is twice as long as for the previous investigated species. Following 4 days of lag phase, the exponential phase lasted for about 12 days and was sampled for metabolite profiling. Subsequently, algal growth slowly levelled off for about 30 days and thus the last two metabolite samplings were defined as early and late stationary phase. The limiting environmental parameter of the growth-limited phases can vary with different effects on algal physiology and should be characterized based on the accompanying descriptive metadata. Neither nitrate nor phosphate were limiting at the beginning of the stationary phase and based on the elevated nitrite levels a light limitation can be hypothesized (Collos 1998; Lomas and Lipschultz 2006). In the late stationary phase probably additional limitation in phosphate occurred (<1 µM). Co-limitations in phytoplankton are common and complicate data analysis and interpretation (Cloern 1999; Davidson and Gurney 1999). Whereas lag and exponential growth phase can be clearly defined and discriminated, subsequent growth phases show stronger deviations from theoretical models, and were observed in various ways for other investigated algal species (Mausz and Pohnert 2015; Vidoudez and Pohnert 2012) (**Manuscript 3**). Whereas metabolite profiles of exponential growth can be directly compared and interpreted between algal species, this is more complicated for the subsequent growth-limited phases due to the variability in limiting parameters (e.g. nutrients, irradiance or CO_2), and may contribute to the divergence between studies. As final note on the batch culture design, the use of xenic

cultures is discussed. The growth of *Phaeocystis pouchetii* induced the growth of the associated bacterial community but abundances never exceeded 5×10^7 cells mL^{-1} (**Manuscript 3**). Various interactions between algae and bacteria are known (Meyer et al. 2017; Seymour et al. 2008) and may have influenced the growth of *P. pouchetii*. Particularly with regard to the growth-promoting character of algae-bacteria interactions, the investigation of axenic cultures is less representative for natural environments. With regard to the influence of residual bacterial biomass on algal metabolite profiles, the ratio of the average biovolume of 0.2 μm^3 (bacteria) vs. 65 μm^3 (*Phaeocystis*) in combination with 1.2 µm filter pore size should not lead to substantial effects on endometabolomes. The particle size of 80 µm of the SPE cartridges in combination with short solvent contact should limit the effect on algal exometabolomes. However, the potential interference of bacterial biomass has to be considered individually e.g. for small cell sizes of the investigated algal species (Hirth et al. 2017).

4.2.3 Deciphering endometabolic biomarkers of growth physiology

Chemical profiling of endometabolites illustrates the metabolic state of algal cells and can follow the physiological responses of algal cells towards external stimuli such as irradiance, temperature, and grazing. Thereby, especially primary metabolites as direct metabolic intermediates and products but also secondary metabolites are examined as free (not conjugated) intracellular metabolites. Different protocols for metabolite quenching, extraction, and sample processing have been developed in the past with adjustments to various study organisms and aims, including a protocol for the diatom *Skeletonema marinoi* (Vidoudez and Pohnert 2012) (**Manuscript 2**). The most critical parameters for marine microalgae are the filtration, especially for flagellated single-celled cultures, and the metabolic quenching on-filter with a cold mixture of organic solvents to extract a broad polarity range of metabolites. Following sample preparation for GC-MS analysis, spectral processing is conducted with AMDIS, a common software for the deconvolution of GC-MS chromatograms. Subsequent statistical analysis is conducted by canonical analysis of principal coordinates (Anderson and Willis 2003); a supervised multivariate analysis that is less prone to multicollinearity in data matrices, which is common for analyses of derivatized samples. In combination with the NIST and GOLM mass spectral library, a high degree of metabolite coverage and annotation can be achieved for endometabolomes exceeding annotation levels of LC-MS-based profiling studies (Barofsky et al. 2010). This allowed the investigation of growth-associated endometabolic plasticity of different marine microalgal species (Mausz and

Pohnert 2015; Vidoudez and Pohnert 2012) (**Manuscript 3**). In *Phaeocystis pouchetii* batch cultures, more than 80 features were found to be highly growth phase-dependent following this approach. About one third was identified, about half putatively annotated or assigned to compound classes, and one quarter remained unknown. As e.g. the GOLM metabolome database was initiated to collect plant metabolites, a certain percentage of unidentified compounds still has to be expected for marine phytoplankton metabolomes unless databases with broader taxonomic and chemical range are established (e.g. MetaboLights, Haug et al. (2013)). Besides amino acids and fatty acids, primarily carbohydrates such as mono- and disaccharides, sugar alcohols and sugar acids were observed (**Manuscript 3**). Due to their high similarity in mass fragmentation and retention time (Medeiros and Simoneit 2007), many monosaccharides remained unidentified, whereas the identification of amino acids and fatty acids was rather unproblematic. The selected endometabolites mapped the dynamic growth physiology of *Phaeocystis* cells. Induced primary metabolism during active growth and photosynthesis in the exponential phase was manifested in elevated amino acid and carbohydrate levels due to nitrogen- and carbon-acquisition, and increased short-term carbon-storage and oxidative stress metabolites. Growth-limiting conditions in early stationary phase induced lipid metabolism, which was manifested in elevated fatty acid, glycerol, and glyceraldehyde levels, while in the late stationary phase levels of PUFAs and lipid-derived structures such as sterols and antioxidants increased to sustain membrane fluidity and stability. This is in agreement with general lipid metabolism control mechanisms reported for microalgae (Roessler 1990). The synthesis of triacylglycerols with high proportions of saturated and monounsaturated fatty acids is considered as an early cellular response to growth limitation (Roessler 1990), while unsaturated fatty acids, sterols and tocopherols are known to accumulate under stress conditions to scavenge radicals and stabilize membranes (Fryer 1992; Mikami and Murata 2003). During late stationary phase, also the carbohydrate metabolism was induced and manifested in elevated mono- and disaccharide levels (**Manuscript 3**). Under nutrient-limiting conditions, excess energy is stored in form of carbohydrates in *P. pouchetii* as reported earlier (Alderkamp et al. 2007). Whereas these metabolite dynamics reflect general responses of algal primary metabolism during growth, also species-specificity can be observed. Mannitol, which is absent in e.g. diatoms (Dittami et al. 2011), characterised the exponential to early stationary phase of *Phaeocystis pouchetii* (**Manuscript 3**) and *Emiliania huxleyi* (Mausz and

Pohnert 2015; Obata et al. 2013). *Scyllo*-inositol, that characterized the early stationary phase of *Phaeocystis*, is in contrast to *myo*-inositol rarely reported in marine microalgae (Ford and Percival 1965; Kobayashi et al. 2007). Retention time comparison with a reference standard is necessary to discriminate the nine inositol isomers due to their high spectral similarity, which may have hindered more frequent reports of *scyllo*-inositol. Putrescine, as marker for the declining growth phase of diatoms (Vidoudez and Pohnert 2012), has not been detected so far in haptophytes. This observed taxon-specificity should be validated in the future with more taxa and environmental cues to distinguish on different taxonomic levels physiological markers for the analysis of mixed populations in natural plankton communities.

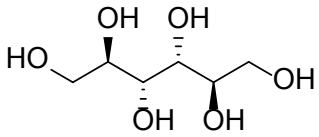

Mannitol

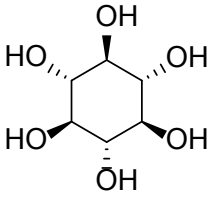

***scyllo*-Inositol**

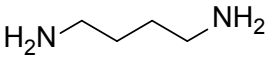

Putrescine

4.2.4 Deciphering exometabolic biomarkers of growth physiology

Chemical profiling of exometabolites illustrates the metabolic state of the algal cells due to e.g. overflow mechanisms during active photosynthesis and growth or metabolite release during cell senescence and death (Thornton 2014). Based on active exudation and passive leakage both primary and secondary metabolites fuel the marine pool of dissolved organic matter (DOM). Also signal molecules for chemical communication within algal populations and between other organisms such as algal species, grazers, or bacteria are transmitted via the aqueous phase (Schwartz et al. 2016). This covers especially secondary metabolites, but also primary metabolites may mediate algal interactions (Segev et al. 2016). Several processes shape the chemical profiles of algal exometabolomes also in laboratory cultures: the passive and active release of primary and secondary metabolites by algal (and bacterial) cells, the transformation of metabolites by abiotic (physically, chemically) and biotic factors (enzymatically), as well as the uptake of metabolites by algal (and bacterial) cells. Few protocols for the extraction of exometabolites have been developed and applied thus far that target the needs of algal cultures or marine samples (**Manuscript 2**). The most pronounced adjustments to mention are the disruption-free separation of cells from the surrounding medium, and the removal of the high salt load that would otherwise

interfere during chemical analysis. Apart from that, extraction of extracellular metabolites is comparable between different liquid phases such as freshwater, culture media, or body fluids, and lessons may be learned from other disciplines. In the current approach, exometabolites are extracted after filtration over glass microfiber filters from the filtrate using hydrophilic, polymeric cartridges with a weak anion exchanger to improve the retention of polar analytes (Fontanals et al. 2005). Based on a recovery assay using glucose, the filtrate was not acidified prior extraction. Subsequent GC-MS analysis, spectral processing, and data analysis followed the endometabolite profiling protocol. Even though less primary metabolites are expected to contribute to exometabolomes, the annotation rate will be higher than for an untargeted profiling based on LC-MS (Barofsky et al. 2009). This approach allowed the first in-depth investigation of growth-associated exometabolic plasticity in marine microalgae revealing potential markers for different growth phases (**Manuscript 3**). More than 80 features were determined that were highly growth phase-specific in *Phaeocystis pouchetii* batch cultures. In comparison to the endometabolome, only a small fraction could be identified (10%), another third was putatively annotated or assigned to compound classes, and more than half the features remained unknown, which will be discussed below. Besides several carboxylic acids, diverse other metabolite classes were observed including saccharides, sugar alcohols, fatty acids, alcohols, and hydrocarbons. The observed exometabolite profiles draw a complex and dynamic picture of the DOM pool that reflects algal physiology as well as putative secondary metabolite-mediated signalling between algae and bacteria. Active photosynthesis in the exponential and early stationary phase was manifested in elevated levels of carboxylic acids and glycerol, whereas cell death in the late stationary phase was manifested in elevated nucleoside levels. The presence of putatively annotated lumichrome and an indole derivative indicate potential algae-bacteria interactions. The observed release of e.g. carboxylic acids may reflect the hypothesis that "*photosynthetic overflow is generally regarded as a consequence of inefficiencies in cell physiology*" (Thornton 2014). Carboxylic acids share like monosaccharides high spectral similarity, and due to the lack of a few standards, this class was not fully annotated. How specific they are as physiological extracellular markers is at the present state difficult to say. Candidates for general growth markers seem to be glycerol indicating active photosynthesis for several algal taxa (Alsufyani et al. 2017; Hellebust 1965) and adenosine indicating cell senescence (Fiore et al. 2015). More

taxon-specific for *Phaeocystis pouchetii* seems to be the release of mono- and disaccharides during late stationary phase as *Phaeocystis* is known for its high accumulation of carbohydrates under growth-limiting conditions (Alderkamp et al. 2006; Alderkamp et al. 2007). Two features that were putatively annotated as lumichrome and as indole derivative (retention time close to indole-3-butanoic acid and tryptophan) are both known to mediate algal-bacterial or bacterial interactions (Amin et al. 2015; Labeeuw et al. 2016; Rajamani et al. 2008). Interestingly, they had opposite occurrence patterns with high levels of the lumichrome-like metabolite at early growth stages and high levels of the indole derivative during later growth stages (**Manuscript 3**). For the related haptophyte *Emiliania huxleyi* lumichrome was putatively annotated in the endometabolome during exponential phase (Mausz and Pohnert 2015) suggesting an intracellular origin. Only a few studies exist so far that link the extracellular occurrence of metabolites with the corresponding endometabolomes (Longnecker et al. 2015b). To provide more evidence for the origin of exometabolites, stable-isotopic labelling experiments should be conducted (Baran et al. 2010; Weber et al. 2013). Thereby, an intracellular formation followed by active or passive metabolite release is assumed excluding chemically transformation processes before, while, or after excretion. The low annotation and identification efficiency for exometabolites will be discussed in the following chapter (see 4.4.3) to highlight the need for further investigations and optimizations. Taken together, exometabolite profiling of marine microalgae reflects the vast diversity of dissolved organic matter that is released by algal cells into the surrounding water effecting not just species interactions and phenotypic plasticity in co-occurring organisms, but also fuelling the microbial loop and thus contributing to the marine food web.

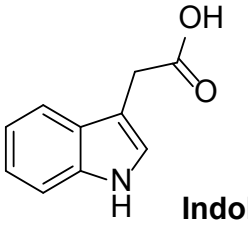

Indole-3-acetic acid

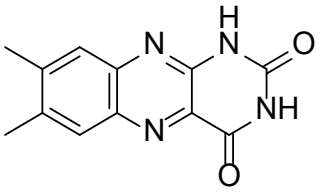

Lumichrome

In conclusion, the untargeted metabolite profiling of endo- and exometabolites allowed to map the physiological plasticity of marine microalgae that accompanies the dynamics of batch culture growth. Algal endo- and exometabolomes were shown to be

growth phase-specific reflecting different cell physiological states. Common and taxon-specific physiological markers could be indicated and were discussed. Based on putative annotation, candidates for further structure elucidation with potentially interesting ecological roles were found, e.g. a lumichrome-like metabolite and an indole derivative. The repeated detection of certain metabolites in several marine microalgae without known function, like pyrrole-2-carboxylic acid or *scyllo*-inositol, suggests the need for further functional characterization within the algal metabolism. This observed physiological plasticity of marine microalgae will allow a dynamic adaption, acclimation, and response to biotic and abiotic environmental factors, which, as a result, will also shape plankton interactions. The physiological plasticity of phytoplankton can also influence the algal nutritional state, and may thus have large implications for the marine food web. Further, algal exometabolites create complex chemical environments that influence associated organisms via the supply of carbon sources and thereby can structure plankton communities.

4.3 Advancing environmental studies

4.3.1 Metabolomics to investigate natural environments

When, within the field of chemical ecology, interactions among organisms are investigated, evidence for the action of chemical mediators is usually adduced in laboratory set-ups. The ecological relevance of laboratory-derived observations has to be confirmed by complementary field investigations. This holds true also for marine plankton ecology (Pohnert 2010). In addition to the direct survey of natural environments, water enclosures such as mesocosms allow to control certain environmental parameters of these semi-natural ecosystems. Experimental set-ups range from mesocosms installed on-land, moored close to the coast, or free-floating off-shore with high resolution in time, to research cruises to the ocean area of interest with high spatial resolution. In contrast to terrestrial systems, marine environmental studies are often more difficult to perform as they depend on research vessels. Stand-alone equipment is primarily available for abiotic parameters and algal toxins so far (Glasgow et al. 2004). However, recent developments such as free-drifting devices analyse nitrogen fixation (Bombar et al. 2015) are promising and may increase spatial and temporal resolution. Also metabolomics approaches such as (comparative) metabolite profiling and metabolic fingerprinting will enhance our understanding of marine environments. Marine plankton communities shape diverse and dynamic chemical landscapes on the extra- and intracellular level based on infochemicals and metabolic markers reflecting ecological interactions. Metabolomics can visualise both, the chemical language and communication that aqueous organisms rely on, as well as their physiology in response to environmental cues. Chemical landscapes were investigated by comparative metabolite profiling, and the suitability of metabolomics approaches for marine environmental studies demonstrated (**Manuscript 3**, **Manuscript 4**). A large physiological plasticity among and between phytoplankton blooms dominated by *Phaeocystis pouchetii* was shown, and linked to growth phase-dependent marker metabolites derived from laboratory experiments (**Manuscript 3**). Exometabolite profiling of natural seawater filtrates showed differential chemical alterations caused by filtration with disturbing effects on subsequent dilution experiments (**Manuscript 4**). Both studies highlight the importance of untargeted chemical analyses in addition to targeted analyses as long as a large part of the organic matter in marine environments remains unidentified.

4.3.2 Mapping endometabolite landscapes during phytoplankton blooms

The physiology of algal cells not just determines their fitness within the abiotic environment, but also influences biotic interactions such as grazing. For a better interpretation of endometabolic patterns during a *Phaeocystis pouchetii* bloom in the field, first growth phase-dependent marker metabolites were identified in controlled laboratory experiments, and then their distribution was monitored in several phytoplankton blooms of the same species (**Manuscript 3**). Growth phases were induced in laboratory batch cultures to simulate dynamic cell growth comparable to natural environments. Comparative untargeted metabolite profiling of small metabolites like amino acids, saccharides, fatty acids, sterols and terpenes using GC-MS allowed to determine several growth phase-dependent metabolites as suitable physiological markers for field experiments. Elevated free amino acid levels during exponential growth reflected active nitrogen assimilation, a feature that is in-line with previous results (Hirth et al. 2017; Kluender et al. 2008; Vidoudez and Pohnert 2012) and thus may be common for the majority of nitrogen-dependent microalgae. In stationary growth phases, the elevated levels in building blocks of carbon-rich macromolecules such as neutral lipids and polysaccharides reflected the need of microalgae to store photosynthetically-acquired carbon under growth-limiting conditions (**Manuscript 3**) (Geider and La Roche 2002). Just a few metabolites show higher taxon-specificity and thus are suited to resolve overlaying physiological patterns within plankton communities. Within those are putrescine as putative diatom senescence marker (Vidoudez and Pohnert 2012), mannitol as short-term storage carbohydrate in haptophytes (Mausz and Pohnert 2015) (**Manuscript 3**), or *scyllo*-inositol (**Manuscript 3**). As for the latter, physiological interpretation is limited for many endometabolites due to lack of knowledge about their specific functions. Laboratory-derived biomarkers for viral infection of the marine microalga *Emiliania huxleyi* are already used for field and mesocosm studies (Hunter et al. 2015; Vardi et al. 2009; Vardi et al. 2012). Similarly, the identified growth phase-dependent endometabolites of *Phaeocystis pouchetii* were investigated for their suitability as physiological growth marker for environmental studies (**Manuscript 3**). About 50 endometabolites of *Phaeocystis* laboratory cultures were detected in natural mixed phytoplankton communities. They showed clear differences between blooms that varied in the dominance of phytoplankton taxa, but also within the *Phaeocystis*-dominated blooms, with diverse patterns of the growth phase-specific metabolites. Nutrient-limitation in the

inner Porsangerfjord lead to highly distinct endometabolite profiles of the present phytoplankton community reflecting their cell physiology. The observed elevated levels in mono- and disaccharides were thereby in accordance with the observations for the late stationary growth phase. Algal physiology can thus imprint endometabolite profiles even stronger than phytoplankton taxonomy. Such an endometabolic landscape shows the great diversity in primary and secondary metabolites within phytoplankton blooms, and thus the large diversity in metabolic states as encountered by zooplankton grazers. In selective feeding experiments of *Calanus* spp. with the diatom *Skeletonema marinoi* and the haptophyte *Phaeocystis pouchetii* it was indicated that phytoplankton bloom phase can be more relevant for food choice than algal abundance (Estep et al. 1990; Ray et al. 2016b), which may be a result of algal physiology (Barofsky et al. 2010; Ray et al. 2016a). However, in the selective feeding experiments with *S. costatum* the identified growth phase-dependent endometabolites were neither annotated nor quantified under copepod grazing (Barofsky et al. 2010). In contrast, the endometabolites of a phytoplankton community under grazing of copepods in a mesocosm study were annotated but not linked to algal physiology (Ray et al. 2016a). Thus, evidence on a metabolic level is still scarce. In parallel to the chemical profiling of phytoplankton blooms (**Manuscript 3**) also grazing experiments were conducted (unpublished results) that may shed light on this in the future.

4.3.3 Mapping exometabolite landscapes during phytoplankton blooms

For the direct interaction with co-occurring organisms, the excreted metabolome (also referred to as 'phycosphere', Seymour et al. (2017)) is even more important than the endometabolome, as it can be directly sensed. Comprehensive analyses of exometabolites in marine environments are still rare, especially with regard to phytoplankton chemical ecology. A detailed study that investigated the growth-dependence of diatom exudates using LC-MS is lacking subsequent feature annotation (Barofsky et al. 2009). Thus, the GC-MS analysis of *Phaeocystis pouchetii* exometabolites in batch cultures allowed for the first time detailed feature annotation and identification of metabolites that may serve as physiological markers in future field experiments (**Manuscript 3**). Carboxylic acids such as glycolic acid or fumaric acid may represent common markers for active growth based on the photosynthetic overflow hypothesis, and nucleosides such as adenosine may in general indicate decaying algal cells (Thornton 2014). Besides such primary metabolites reflecting algal physiology, secondary metabolites as putative infochemicals were present in the

exometabolome of *P. pouchetii*. Several exometabolites are already in the focus of marine chemical ecologists as chemical mediators, e.g. DMSP (Johnson et al. 2016), indole-3-acetic acid (Amin et al. 2015), and lumichrome (Rajamani et al. 2008). Their potential relevance for other phytoplankton taxa and entire communities has been brought forward (**Manuscript 3**). No comprehensive profiling of the exometabolite landscape of marine environments exist to date, and only recently approaches have been developed to search for molecules of interest in available field data (Longnecker et al. 2015a).

During mesocosm experiments and research cruises, many incubation experiments rely on the filtration of seawater such as dilution experiments, which quantify grazing losses of microorganisms like bacteria or phytoplankton (Anderson and Rivkin 2001; Landry and Hassett 1982). In the past, negative or low grazing rates repeatedly indicated that during some phytoplankton bloom situations filtration artifacts may lead to reduced specific growth rates (Calbet et al. 2011; Stoecker et al. 2014). Based on targeted chemical analyses these artifacts were regarded to be induced by the release of DMSP (Wolfe et al. 2000) or PUAs (Stoecker et al. 2015). A release of other molecules is likely, but was so far not addressed. Untargeted exometabolite profiling of filtrates visualised in an unbiased way the impact of filtration on DOM composition (**Manuscript 4**). In these dilution experiments, that aimed on estimating bacterivory during blooms of *Phaeocystis pouchetii*, specific growth rates of the bacteria were altered in the dilutions with filtrated seawater. This is violating one basic assumption of the experimental design (Landry and Hassett 1982). Comparative exometabolite profiling of small molecules demonstrated that filtration alters the chemical composition of the seawater in various ways (**Manuscript 4**). Both, a decrease and an increase in metabolite concentrations was observed after filtration. Reduction in metabolite concentrations may be due to adsorption to the filter material or to organic residues on the filter. Elevated metabolite concentrations may be explained by a metabolite release after cell damage being e.g. filtration-, species-, and cell stage-dependent, or by contamination with artificial compounds due to sample handling and filter residues. Filtration-induced chemical alterations even overlaid the intrinsic phytoplankton bloom-specific exometabolite profiles. However, only a few candidate molecules could be annotated and about two-thirds of the compounds remained unknown. As solid phase extraction discriminates towards metabolites that are retained based on the chemical properties of the selected adsorbent (Minor et al. 2014), occurring allelopathic

metabolite(s) may not have been extracted by the chosen cartridge. Also, the allelochemical(s) might have been too low in concentration to be detected by subsequent analysis. Even though, untargeted exometabolite profiling allowed to visualise on a metabolite level the influence of filtration techniques on subsequent experiments. To test whether the basic assumption of constant specific growth is fulfilled, specific growth rates of the prey organism should be estimated during dilution experiments.

4.3.4 Future developments to improve meta-metabolomics approaches

Selected aspects of metabolomics approaches for environmental studies that need further investigation and improvement in the future are discussed in the following. Metabolomics analyses of natural occurring plankton communities are still scarce and a developing field. In contrast, many laboratory-based metabolomics studies have been already conducted. One might thus aim for combined and comparative data analyses of metabolite profiles that were generated on different analytical platforms as was done for laboratory and field samples in the present environmental study (**Manuscript 3**). However, an automated data analysis was hindered due to difficulties in the alignment of chromatograms. Several data processing tools are available, namely XCMS (Smith et al. 2006), MZmine (Katajamaa et al. 2006), MetAlign (Lommen 2009), MetaboliteDetector (Hiller et al. 2009), the 'metaMS' and 'flagme' packages in R (Robinson 2008; Wehrens et al. 2014), and the Bioinformatics Toolbox™ in MathWorks®. Nevertheless, none of them resulted in acceptable chromatogram alignments (data not shown), and time-consuming manual data evaluation was necessary (**Manuscript 3**). This was due to several differing instrumental properties such as large and non-linear retention time shifts, total scan number, mass resolution, and the presence of a mass calibration standard (Table S 2). With regard to increased data sharing in open repositories like Metabolights (Kale et al. 2016) or Metabolomics Workbench (Sud et al. 2016), the re-usage of data obtained on various analytical platforms should be facilitated in the future. Furthermore, data normalization strategies as developed for laboratory experiments (**Manuscript 2**) have to be reviewed for mixed natural communities that show a large variance in cell size, shape and volume. Biomass estimators like total organic carbon content and wet weight (Longnecker and Kujawinski 2017), peak sum (Hines et al. 2007), cell volume, or more advanced algorithms (Dieterle et al. 2006) may be considered to account for varying particulate and dissolved organic matter content in environmental studies. Additionally,

exometabolite analyses, especially untargeted metabolomics approaches, have to deal with the low natural metabolite concentrations of e.g. ≤0.1 nM for heptadienal and octadienal in the Adriatic Sea (Vidoudez et al. 2011a), with a high background of dissolved organic matter, and contaminations like plasticizers (Kido Soule et al. 2015). These limitations may be overcome by emerging analytical and data processing strategies (Kido Soule et al. 2015; Longnecker et al. 2015a).

To conclude, untargeted metabolite profiling allows to visualise the endo- and exometabolic landscape of marine environments in time and space. On the intracellular level, the physiological state of whole phytoplankton communities can be depicted, which reflects biotic and abiotic interactions. In the highly complex extracellular matrix of phytoplankton cells, chemical cues of diverse plankton taxa and biotic interactions are merged. Emerging metabolomics techniques may allow in the future to go beyond integrated community analyses towards single cell metabolomics in natural environment. Especially for exometabolomics approaches in environmental studies, improvements are needed with regard to metabolite extraction, metabolite identification, and functional characterization.

4.4 Methodological challenges in the field of chemical ecology

Both the field of chemical ecology and metabolomics are rather new disciplines that are jointly developed intensively in recent years (**Manuscript 1**). Thus, it is not of surprise that several open questions remain to be still solved in the near future. In the following, some of these challenges for metabolomics approaches in the field of chemical ecology will be addressed.

4.4.1 Taxonomic diversity in chemical ecology

In contrast to developmental biology (*Drosophila melanogaster*), microbiology (*Escherichia coli*) or plant biology (*Arabidopsis thaliana*), research questions in the field of chemical ecology primarily deal with non-model organisms (**Manuscript 1**). Only a few known model species are also of interest and investigated in the field of chemical ecology e.g. *Caenorhabditis elegans* (Choe et al. 2012; von Reuss et al. 2012). However, several marine phytoplankton species exist of which the whole genome has been recently sequenced, and which thus may serve as potential model organisms in the future e.g. *Phaeodactylum tricornutum*, *Emiliania huxleyi*, and *Ostreococcus tauri* (Tirichine and Bowler 2011). For those, downstream analyses and predictions of metabolites or metabolic pathways are possible. The appropriate transformation methods are, however, still missing for some species like *E. huxleyi*. Many other species that are of interest in chemical ecology have not been sequenced yet such as *Phaeocystis pouchetii*, or are pending such as *P. globosa* and *P. antarctica* for which an annotated standard genome draft is assembled since 2015. Analysis strategies independent of the sequencing and annotation of the whole genome of the study organism would broaden the taxonomic range and applicability for the field of chemical ecology. Instead of large species-specific metabolite databases like ECMDB (Sajed et al. 2016) for *Escherichia coli*, YMDB (Ramirez-Gaona et al. 2017) for yeast, or PlantMetabolomics.org (Bais et al. 2012), species-independent metabolite data bases should be favoured like MetaboLights (Kale et al. 2016) (**Manuscript 3**) to allow an easy deposition and sharing of identified metabolites. This will help to improve increase data usage and knowledge sharing between research groups, or in the identification of cross-kingdom mechanisms.

4.4.2 Standardizing metabolomics protocols in chemical ecology

The same species-specificity exists with regard to the development of protocols for sampling and sample processing (**Manuscript 1**). Instead of a few standardized metabolomics protocols optimized and investigated for just one single species like the model organisms *Arabidopsis thaliana* (Fiehn 2006; Lisec et al. 2006), many protocols will be necessary in the field of chemical ecology, that are robust and flexible enough to be applied on a broader species-range to cope with the large number of interesting species. With regard to sampling for systems biology, this has been already approached (Valledor et al. 2014). Thus, the future aim should be to develop metabolomics protocols that are intended and tested not species- but taxon-specific (**Manuscript 2**). For improved sharing of protocols but also of important observations and conclusions during protocol development, that would otherwise not be public, open data repositories such as MetaboLights (Kale et al. 2016) or MetablomicsWorkbench (Sud et al. 2016) can and should be involved.

4.4.3 Unidentified metabolite diversity in chemical ecology

Usually, a high proportion of unknown, not annotated metabolites remains in untargeted metabolomics studies, especially with regard to non-model organisms in the field of chemical ecology, exometabolomics, and LC-MS-based analyses as reviewed e.g. by Schrimpe-Rutledge et al. (2016) and Allard et al. (2017). Several developments and improvements are already on the way and will be further needed for both, GC- and LC-MS-based metabolomics, to enhance the biological and ecological data interpretation (**Manuscript 5**). These include improvements in analytical chemistry with regard to mass analyser types and mass resolution, but also spatial and temporal resolution for comprehensive metabolite coverage (Dias et al. 2016; Zampieri et al. 2017). Novel bioinformatics solutions such as *in silico* fragmentation (Wolf et al. 2010) or estimators for false discovery rates in metabolite annotation will enhance data analysis (Scheubert et al. 2017). Data repositories with broad taxonomic range, or higher-level data bases that link already existing metabolite data collections from GC-MS, LC-MS^n, NMR etc. with each other for easier access will advance data sharing and data deposition (Vinaixa et al. 2016). An accurate and robust way of annotating mass features has to be defined and applied by following e.g. the recommendations for metabolite annotation of the metabolomics standards initiative (Sumner et al. 2007) to facilitate the link between different experiments and data sets. Following comprehensive functional characterizations, this will allow us to expand our

knowledge from the current small set of multifunctional metabolites including PUAs and DMSP to the existing large metabolite diversity having e.g. additive or subtractive ecological effects. The same increase in complexity has to be reached in terms of organism interaction experiments (Pohnert 2010), going from the usual bi-directional interaction studies in co-culture to tripartite systems, mesocosms and other field experiment set-ups to monitor and entangle chemical interactions in their natural environment.

5 References

Adolf, J. E. and others 2006. Species specificity and potential roles of *Karlodinium micrum* toxin. Afr. J. Mar. Sci. **28**(2): 415-419.

Adolph, S., S. A. Poulet, and G. Pohnert. 2003. Synthesis and biological activity of α,β,γ,δ-unsaturated aldehydes from diatoms. Tetrahedron **59**(17): 3003-3008.

Adolph, S. and others 2004. Cytotoxicity of diatom-derived oxylipins in organisms belonging to different phyla. J. Exp. Biol. **207**(17): 2935-2946.

Agrawal, A. A. 2001. Phenotypic plasticity in the interactions and evolution of species. Science **294**(5541): 321-326.

Akakabe, Y., K. Matsui, and T. Kajiwara. 2003. 2,4-decadienals are produced via (*R*)-11-HPITE from arachidonic acid in marine green alga *Ulva conglobata*. Bioorg. Med. Chem. **11**(17): 3607-3609.

Alderkamp, A. C., J. C. Nejstgaard, P. G. Verity, M. J. Zirbel, A. F. Sazhin, and M. van Rijssel. 2006. Dynamics in carbohydrate composition of *Phaeocystis pouchetii* colonies during spring blooms in mesocosms. Journal of Sea Research **55**(3): 169-181.

Alderkamp, A. C., A. G. J. Buma, and M. van Rijssel. 2007. The carbohydrates of *Phaeocystis* and their degradation in the microbial food web. Biogeochemistry **83**(1-3): 99-118.

Allard, P.-M., G. Genta-Jouve, and J.-L. Wolfender. 2017. Deep metabolome annotation in natural products research: Towards a virtuous cycle in metabolite identification. Curr. Opin. Chem. Biol. **36**: 40-49.

Allen, A. E. and others 2011. Evolution and metabolic significance of the urea cycle in photosynthetic diatoms. Nature **473**(7346): 203-207.

Allen, J. and others 2003. High-throughput classification of yeast mutants for functional genomics using metabolic footprinting. Nat. Biotechnol. **21**(6): 692-696.

Alonso, A., S. Marsal, and A. Julia. 2015. Analytical methods in untargeted metabolomics: State of the art in 2015. Front. Bioeng. Biotechnol. **3**: 23.

Alsufyani, T., A. H. Engelen, O. E. Diekmann, S. Kuegler, and T. Wichard. 2014. Prevalence and mechanism of polyunsaturated aldehydes production in the green tide forming macroalgal genus *Ulva* (Ulvales, Chlorophyta). Chem. Phys. Lipids **183**: 100-109.

Alsufyani, T., A. Weiss, and T. Wichard. 2017. Time course exo-metabolomic profiling in the green marine macroalga *Ulva* (Chlorophyta) for identification of growth phase-dependent biomarkers. Mar. Drugs **15**(1): doi: 10.3390/md15010014.

Amin, R. M., M. Koski, U. Båmstedt, and C. Vidoudez. 2011. Strain-related physiological and behavioral effects of *Skeletonema marinoi* on three common planktonic copepods. Mar. Biol. **158**(9): 1965-1980.

Amin, S. A., D. H. Green, M. C. Hart, F. C. Küpper, W. G. Sunda, and C. J. Carrano. 2009. Photolysis of iron-siderophore chelates promotes bacterial-algal mutualism. Proc. Natl. Acad. Sci. U.S.A. **106**(40): 17071-17076.

Amin, S. A. and others 2015. Interaction and signalling between a cosmopolitan phytoplankton and associated bacteria. Nature **522**(7554): 98-101.

Amo, L., M. A. Rodriguez-Girones, and A. Barbosa. 2013. Olfactory detection of dimethyl sulphide in a krill-eating Antarctic penguin. Mar. Ecol.: Prog. Ser. **474**: 277-285.

Anderson, M. J., and T. J. Willis. 2003. Canonical analysis of principal coordinates: A useful method of constrained ordination for ecology. Ecology **84**(2): 511-525.

Anderson, M. R., and R. B. Rivkin. 2001. Seasonal patterns in grazing mortality of bacterioplankton in polar oceans: A bipolar comparison. Aquat. Microb. Ecol. **25**(2): 195-206.

Andreou, A., F. Brodhun, and I. Feussner. 2009. Biosynthesis of oxylipins in non-mammals. Prog. Lipid Res. **48**(3-4): 148-170.

Armbrust, E. V. and others 2004. The genome of the diatom *Thalassiosira pseudonana*: ecology, evolution, and metabolism. Science **306**(5693): 79-86.

Bais, P., S. M. Moon-Quanbeck, B. J. Nikolau, and J. A. Dickerson. 2012. Plantmetabolomics.org: Mass spectrometry-based *Arabidopsis* metabolomics - database and tools update. Nucleic Acids Res. **40**(Database issue): D1216-1220.

Ban, S. and others 1997. The paradox of diatom-copepod interactions. Mar. Ecol.: Prog. Ser.: 287-293.

Baran, R., B. P. Bowen, N. J. Bouskill, E. L. Brodie, S. M. Yannone, and T. R. Northen. 2010. Metabolite identification in *Synechococcus* sp. PCC 7002 using untargeted stable isotope assisted metabolite profiling. Anal. Chem. **82**(21): 9034-9042.

Barofsky, A., and G. Pohnert. 2007. Biosynthesis of polyunsaturated short chain aldehydes in the diatom *Thalassiosira rotula*. Org. Lett. **9**(6): 1017-1020.

Barofsky, A., C. Vidoudez, and G. Pohnert. 2009. Metabolic profiling reveals growth stage variability in diatom exudates. Limnology and Oceanography-Methods **7**: 382-390.

Barofsky, A. and others 2010. Growth phase of the diatom *Skeletonema marinoi* influences the metabolic profile of the cells and the selective feeding of the copepod *Calanus* spp. J. Plankton Res. **32**(3): 263-272.

Barreiro, A. and others 2011. Diatom induction of reproductive failure in copepods: The effect of PUAs versus non volatile oxylipins. J. Exp. Mar. Biol. Ecol. **401**(1-2): 13-19.

Bergkvist, J., P. Thor, H. H. Jakobsen, S.-Å. Wängberg, and E. Selander. 2012. Grazer-induced chain length plasticity reduces grazing risk in a marine diatom. Limnol. Oceanogr. **57**(1): 318-324.

Blaise, B. J. and others 2016. Power analysis and sample size determination in metabolic phenotyping. Anal. Chem. **88**(10): 5179-5188.

Blossom, H. E., N. Daugbjerg, and P. J. Hansen. 2012. Toxic mucus traps: A novel mechanism that mediates prey uptake in the mixotrophic dinoflagellate *Alexandrium pseudogonyaulax*. Harmful Algae **17**: 40-53.

Blossom, H. E., S. A. Rasmussen, N. G. Andersen, T. O. Larsen, K. F. Nielsen, and P. J. Hansen. 2014. *Prymnesium parvum* revisited: Relationship between allelopathy, ichthyotoxicity, and chemical profiles in 5 strains. Aquat. Toxicol. **157**: 159-166.

Bolch, C. J., T. A. Subramanian, and D. H. Green. 2011. The toxic dinoflagellate *Gymnodinium catenatum* (Dinophyceae) requires marine bacteria for growth. J. Phycol. **47**(5): 1009-1022.

Bolier, G., and M. Donze. 1989. On the accuracy and interpretation of growth-curves of planktonic algae. Hydrobiologia **188**: 175-179.

Bölling, C., and O. Fiehn. 2005. Metabolite profiling of *Chlamydomonas reinhardtii* under nutrient deprivation. Plant Physiol. **139**(4): 1995-2005.

Bolten, C. J., P. Kiefer, F. Letisse, J. C. Portais, and C. Wittmann. 2007. Sampling for metabolome analysis of microorganisms. Anal. Chem. **79**(10): 3843-3849.

Bombar, D. and others 2015. Measurements of nitrogen fixation in the oligotrophic North Pacific Subtropical Gyre using a free-drifting submersible incubation device. J. Plankton Res. **37**(4): 727-739.

Boonprab, K., K. Matsui, Y. Akakabe, N. Yotsukura, and T. Kajiwara. 2003. Hydroperoxy-arachidonic acid mediated *n*-hexanal and (*Z*)-3- and (*E*)-2-nonenal formation in *Laminaria angustata*. Phytochemistry **63**(6): 669-678.

Bowler, C. and others 2008. The *Phaeodactylum* genome reveals the evolutionary history of diatom genomes. Nature **456**(7219): 239-244.

Calbet, A., E. Saiz, R. Almeda, J. I. Movilla, and M. Alcaraz. 2011. Low microzooplankton grazing rates in the Arctic Ocean during a *Phaeocystis pouchetii* bloom (Summer 2007): Fact or artifact of the dilution technique? J. Plankton Res. **33**(5): 687-701.

Caldwell, G. S., P. J. W. Olive, and M. G. Bentley. 2002. Inhibition of embryonic development and fertilization in broadcast spawning marine invertebrates by water soluble diatom extracts and the diatom toxin 2-*trans*,4-*trans* decadienal. Aquat. Toxicol. **60**(1): 123-137.

Carvalho, V. M., P. Di Mascio, I. P. de Arruda Campos, T. Douki, J. Cadet, and M. H. G. Medeiros. 1998. Formation of 1,N^6-Etheno-2‘-deoxyadenosine adducts by *trans*,*trans*-2,4-decadienal. Chem. Res. Toxicol. **11**(9): 1042-1047.

Casotti, R., S. Mazza, C. Brunet, V. Vantrepotte, A. Ianora, and A. Miralto. 2005. Growth inhibition and toxicity of the diatom aldehyde 2-*trans*, 4-*trans*-decadienal on *Thalassiosira weissflogii* (Bacillariophyceae). J. Phycol. **41**(1): 7-20.

Choe, A. and others 2012. Ascaroside signaling is widely conserved among nematodes. Curr. Biol. **22**(9): 772-780.

Cloern, J. E. 1999. The relative importance of light and nutrient limitation of phytoplankton growth: a simple index of coastal ecosystem sensitivity to nutrient enrichment. Aquat. Ecol. **33**(1): 3-15.

Collos, Y. 1998. Nitrate uptake, nitrite release and uptake, and new production estimates. Mar. Ecol.: Prog. Ser. **171**: 293-301.

Cutignano, A. and others 2006. Chloroplastic glycolipids fuel aldehyde biosynthesis in the marine diatom *Thalassiosira rotula*. Chembiochem **7**(3): 450-456.

Cutignano, A., N. Lamari, G. d'Ippolito, E. Manzo, G. Cimino, and A. Fontana. 2011. Lipoxygenase products in marine diatoms: A concise analytical method to explore the functional potential of oxylipins. J. Phycol. **47**(2): 233-243.

Cutignano, A. and others 2015. Development and application of a novel SPE-method for bioassay-guided fractionation of marine extracts. Mar. Drugs **13**(9): 5736-5749.

d'Ippolito, G., I. Iadicicco, G. Romano, and A. Fontana. 2002a. Detection of short-chain aldehydes in marine organisms: The diatom *Thalassiosira rotula*. Tetrahedron Lett. **43**(35): 6137-6140.

d'Ippolito, G. and others 2002b. New birth-control aldehydes from the marine diatom *Skeletonema costatum*: Characterization and biogenesis. Tetrahedron Lett. **43**(35): 6133-6136.

d'Ippolito, G., G. Romano, T. Caruso, A. Spinella, G. Cimino, and A. Fontana. 2003. Production of octadienal in the marine diatom *Skeletonema costatum*. Org. Lett. **5**(6): 885-887.

d'Ippolito, G. and others 2004. The role of complex lipids in the synthesis of bioactive aldehydes of the marine diatom *Skeletonema costatum*. Biochim. Biophys. Acta, Mol. Cell Biol. Lipids **1686**(1-2): 100-107.

d'Ippolito, G., A. Cutignano, S. Tucci, G. Romano, G. Cimino, and A. Fontana. 2006. Biosynthetic intermediates and stereochemical aspects of aldehyde

biosynthesis in the marine diatom *Thalassiosira rotula*. Phytochemistry **67**(3): 314-322.

d'Ippolito, G. and others 2009. 15*S*-lipoxygenase metabolism in the marine diatom *Pseudo-nitzschia delicatissima*. New Phytol. **183**(4): 1064-1071.

Davidson, K., and W. S. C. Gurney. 1999. An investigation of non-steady-state algal growth. II. Mathematical modelling of co-nutrient-limited algal growth. J. Plankton Res. **21**(5): 839-858.

de Alencar, D. B. and others 2017. Chemical composition of volatile compounds in two red seaweeds, *Pterocladiella capillacea* and *Osmundaria obtusiloba*, using static headspace gas chromatography mass spectrometry. J. Appl. Phycol. **29**(3): 1571-1576.

de Vargas, C. and others 2015. Eukaryotic plankton diversity in the sunlit ocean. Science **348.6237**: 1261605.

Derelle, E. and others 2006. Genome analysis of the smallest free-living eukaryote *Ostreococcus tauri* unveils many unique features. Proc. Natl. Acad. Sci. U.S.A. **103**(31): 11647-11652.

Dettmer, K., P. A. Aronov, and B. D. Hammock. 2007. Mass spectrometry-based metabolomics. Mass Spectrom. Rev. **26**(1): 51-78.

Dias, D. and others 2016. Current and future perspectives on the structural identification of small molecules in biological systems. Metabolites **6**(4): 46.

Dicke, M., and M. W. Sabelis. 1988. Infochemical terminology: Based on cost-benefit analysis rather than origin of compounds? Funct. Ecol. **2**(2): 131-139.

Dieterle, F., A. Ross, G. Schlotterbeck, and H. Senn. 2006. Probabilistic quotient normalization as robust method to account for dilution of complex biological mixtures. Application in ^{1}H NMR metabonomics. Anal. Chem. **78**(13): 4281-4290.

Dittami, S. M., T. Wichard, A. M. Malzahn, G. Pohnert, M. Boersma, and K. H. Wiltshire. 2010. Culture conditions affect fatty acid content along with wound-activated production of polyunsaturated aldehydes in *Thalassiosira rotula* (Coscinodiscophyceae). Nova Hedwigia **136**: 231-248.

Dittami, S. M., H. T. N. Aas, B. S. Paulsen, C. Boyen, B. Edvardsen, and T. Tonon. 2011. Mannitol in six autotrophic stramenopiles and *Micromonas*. Plant Signaling Behav. **6**(8): 1237-1239.

Dunn, W. B., N. J. C. Bailey, and H. E. Johnson. 2005. Measuring the metabolome: Current analytical technologies. Analyst **130**(5): 606-625.

Dutz, J., M. Koski, and S. H. Jonasdottir. 2008. Copepod reproduction is unaffected by diatom aldehydes or lipid composition. Limnol. Oceanogr. **53**(1): 225-235.

Edwards, B. R., K. D. Bidle, and B. A. S. van Mooy. 2015. Dose-dependent regulation of microbial activity on sinking particles by polyunsaturated aldehydes: Implications for the carbon cycle. Proc. Natl. Acad. Sci. U.S.A. **112**(19): 5909-5914.

Estep, K. W., J. C. Nejstgaard, H. R. Skjoldal, and F. Rey. 1990. Predation by copepods upon natural populations of *Phaeocystis pouchetii* as a function of the physiological state of the prey. Mar. Ecol.: Prog. Ser. **67**(3): 235-249.

Fabris, M., M. Matthijs, S. Rombauts, W. Vyverman, A. Goossens, and G. J. Baart. 2012. The metabolic blueprint of *Phaeodactylum tricornutum* reveals a eukaryotic Entner-Doudoroff glycolytic pathway. Plant J. **70**(6): 1004-1014.

Falconer, D. S. 1989. Introduction to quantitative genetics, 2nd ed. Longman, Scientific & Technical.

Falkowski, P. G. and others 2004. The evolution of modern eukaryotic phytoplankton. Science **305**(5682): 354-360.

Fernie, A. R., R. N. Trethewey, A. J. Krotzky, and L. Willmitzer. 2004. Metabolite profiling: From diagnostics to systems biology. Nat. Rev. Mol. Cell Biol. **5**(9): 763-769.

Fernie, A. R. and others 2011. Recommendations for reporting metabolite data. Plant Cell **23**(7): 2477-2482.

Fiehn, O. 2001. Combining genomics, metabolome analysis, and biochemical modelling to understand metabolic networks. Comp. Funct. Genomics **2**(3): 155-168.

Fiehn, O. 2006. Metabolite profiling in *Arabidopsis*, p. 439-447. *In* J. Salinas and J. J. Sanchez-Serrano [eds.], Arabidopsis Protocols. Humana Press.

Fiehn, O. and others 2007. The metabolomics standards initiative (MSI). Metabolomics **3**(3): 175-178.

Fiehn, O. and others 2008. Quality control for plant metabolomics: Reporting MSI-compliant studies. Plant J. **53**(4): 691-704.

Field, C. B., M. J. Behrenfeld, J. T. Randerson, and P. Falkowski. 1998. Primary production of the biosphere: Integrating terrestrial and oceanic components. Science **281**(5374): 237-240.

Fiore, C. L., K. Longnecker, M. C. Kido Soule, and E. B. Kujawinski. 2015. Release of ecologically relevant metabolites by the cyanobacterium *Synechococcus elongates* CCMP 1631. Environ. Microbiol. **17**(10): 3949-3963.

Fontana, A. and others 2007. LOX-induced lipid peroxidation mechanism responsible for the detrimental effect of marine diatoms on zooplankton grazers. Chembiochem **8**(15): 1810-1818.

Fontanals, N., R. M. Marce, and F. Borrull. 2005. New hydrophilic materials for solid-phase extraction. TrAC, Trends Anal. Chem. **24**(5): 394-406.

Ford, C. W., and E. Percival. 1965. 1298. The carbohydrates of *Phaeodactylum tricornutum*. Part I. Preliminary examination of the organism, and characterisation of low molecular weight material and of a glucan. J. Chem. Soc. **0**: 7035-7041.

Fryer, M. J. 1992. The antioxidant effects of thylakoid Vitamin E (α-tocopherol). Plant, Cell Environ. **15**(4): 381-392.

Fuchs, C., and G. Spiteller. 1996. Rapid and easy identification of isomers of coumaroyl- and caffeoyl-D-quinic acid by gas chromatography-mass spectrometry. J. Mass Spectrom. **31**(6): 602-608.

Gallina, A. A., C. Brunet, A. Palumbo, and R. Casotti. 2014. The effect of polyunsaturated aldehydes on *Skeletonema marinoi* (Bacillariophyceae): The involvement of reactive oxygen species and nitric oxide. Mar. Drugs **12**(7): 4165-4187.

Garces, E., E. Alacid, A. Rene, K. Petrou, and R. Simo. 2013. Host-released dimethylsulphide activates the dinoflagellate parasitoid *Parvilucifera sinerae*. ISME J. **7**(5): 1065-1068.

Gathungu, R. M. and others 2014. Identification of metabolites from liquid chromatography-coulometric array detection profiling: Gas chromatography-mass spectrometry and refractionation provide essential information orthogonal to LC-MS/microNMR. Anal. Biochem. **454**: 23-32.

Geider, R. J., and J. La Roche. 2002. Redfield revisited: Variability of C:N:P in marine microalgae and its biochemical basis. Eur. J. Phycol. **37**(1): 1-17.

Gerwick, W. H., M. Moghaddam, and M. Hamberg. 1991. Oxylipin metabolism in the red alga *Gracilariopsis lemaneiformis*: Mechanism of formation of vicinal dihydroxy fatty acids. Arch. Biochem. Biophys. **290**(2): 436-444.

Gillard, J. and others 2013. Metabolomics enables the structure elucidation of a diatom sex pheromone. Angew. Chem. Int. Edit. **52**(3): 854-857.

Glasgow, H. B., J. M. Burkholder, R. E. Reed, A. J. Lewitus, and J. E. Kleinman. 2004. Real-time remote monitoring of water quality: A review of current applications, and advancements in sensor, telemetry, and computing technologies. J. Exp. Mar. Biol. Ecol. **300**(1): 409-448.

Goulitquer, S., A. Ritter, F. Thomas , C. Ferec, J. P. Salaün , and P. Potin 2009. Release of volatile aldehydes by the brown algal kelp *Laminaria digitata* in response to both biotic and abiotic stress. Chembiochem **10**(6): 977-982.

Goulitquer, S., P. Potin, and T. Tonon. 2012. Mass spectrometry-based metabolomics to elucidate functions in marine organisms and ecosystems. Mar. Drugs **10**(4): 849-880.

Grechkin, A. N., and M. Hamberg. 2004. The "heterolytic hydroperoxide lyase" is an isomerase producing a short-lived fatty acid hemiacetal. Biochim. Biophys. Acta, Mol. Cell Biol. Lipids **1636**(1): 47-58.

Grice, G. D., and M. R. Reeve. 1982. Marine mesocosms: Biological and chemical research in experimental ecosystems, 1 ed. Springer-Verlag.

Guillarme, D., J. Ruta, S. Rudaz, and J. L. Veuthey. 2010. New trends in fast and high-resolution liquid chromatography: A critical comparison of existing approaches. Anal. Bioanal. Chem. **397**(3): 1069-1082.

Gullberg, J., P. Jonsson, A. Nordström, M. Sjöström, and T. Moritz. 2004. Design of experiments: An efficient strategy to identify factors influencing extraction and derivatization of *Arabidopsis thaliana* samples in metabolomic studies with gas chromatography-mass spectrometry. Anal. Biochem. **331**(2): 283-295.

Halket, J. M., D. Waterman, A. M. Przyborowska, R. K. Patel, P. D. Fraser, and P. M. Bramley. 2005. Chemical derivatization and mass spectral libraries in metabolic profiling by GC-MS and LC-MS/MS. J. Exp. Bot. **56**(410): 219-243.

Hansen, E., A. Ernstsen, and H. C. Eilertsen. 2004. Isolation and characterisation of a cytotoxic polyunsaturated aldehyde from the marine phytoplankter *Phaeocystis pouchetii* (Hariot) Lagerheim. Toxicology **199**(2-3): 207-217.

Hartmann, T. 2008. The lost origin of chemical ecology in the late 19th century. Proc. Natl. Acad. Sci. U.S.A. **105**(12): 4541-4546.

Harvey, E. L., H. J. Jeong, and S. Menden-Deuer. 2013. Avoidance and attraction: Chemical cues influence predator-prey interactions of planktonic protists. Limnol. Oceanogr. **58**(4): 1176-1184.

Haug, K. and others 2013. MetaboLights - an open-access general-purpose repository for metabolomics studies and associated meta-data. Nucleic Acids Res. **41**(D1): D781-D786.

Hellebust, J. A. 1965. Excretion of some organic compounds by marine phytoplankton. Limnol. Oceanogr. **10**(2): 192-206.

Hendriks, M. M. W. B. and others 2011. Data-processing strategies for metabolomics studies. TrAC, Trends Anal. Chem. **30**(10): 1685-1698.

Hiller, K., J. Hangebrauk, C. Jäger, J. Spura, K. Schreiber, and D. Schomburg. 2009. MetaboliteDetector: Comprehensive analysis tool for targeted and nontargeted GC-MS based metabolome analysis. Anal. Chem. **81**(9): 3429-3439.

Hines, A., G. S. Oladiran, J. P. Bignell, G. D. Stentiford, and M. R. Viant. 2007. Direct sampling of organisms from the field and knowledge of their phenotype: Key recommendations for environmental metabolomics. Environ. Sci. Technol. **41**(9): 3375-3381.

Hirth, M., S. Liverani, S. Mahlow, F.-Y. Bouget, G. Pohnert, and S. Sasso. 2017. Metabolic profiling identifies trehalose as an abundant and diurnally fluctuating metabolite in the microalga *Ostreococcus tauri*. Metabolomics **13**(6): 68.

Hunter, J. E., M. J. Frada, H. F. Fredricks, A. Vardi, and B. A. S. van Mooy. 2015. Targeted and untargeted lipidomics of *Emiliania huxleyi* viral infection and life cycle phases highlights molecular biomarkers of infection, susceptibility, and ploidy. Front. Mar. Sci. **2**(81).

Ianora, A., and S. A. Poulet. 1993. Egg viability in the copepod *Temora stylifera*. Limnol. Oceanogr. **38**(8): 1615-1626.

Ianora, A., S. A. Poulet, and A. Miralto. 2003. The effects of diatoms on copepod reproduction: A review. Phycologia **42**(4): 351-363.

Ianora, A. and others 2004. Aldehyde suppression of copepod recruitment in blooms of a ubiquitous planktonic diatom. Nature **429**(6990): 403-407.

Ianora, A., and A. Miralto. 2010. Toxigenic effects of diatoms on grazers, phytoplankton and other microbes: A review. Ecotoxicology **19**(3): 493-511.

Ianora, A. and others 2011. Impact of the diatom oxylipin 15*S*-HEPE on the reproductive success of the copepod *Temora stylifera*. Hydrobiologia **666**(1): 265-275.

Ianora, A. and others 2015. Non-volatile oxylipins can render some diatom blooms more toxic for copepod reproduction. Harmful Algae **44**: 1-7.

Jacobsen, A. 2002. Morphology, relative DNA content and hypothetical life cycle of *Phaeocystis pouchetii* (Prymnesiophyceae); with special emphasis on the flagellated cell type. Sarsia **87**(5): 338-349.

Jacobsen, A., and M. J. W. Veldhuis. 2005. Growth characteristics of flagellated cells of *Phaeocystis pouchetii* revealed by diel changes in cellular DNA content. Harmful Algae **4**(5): 811-821.

Jeong, S.-Y., K. Ishida, Y. Ito, S. Okada, and M. Murakami. 2003. Bacillamide, a novel algicide from the marine bacterium, *Bacillus* sp. SY-1, against the harmful dinoflagellate, *Cochlodinium polykrikoides*. Tetrahedron Lett. **44**(43): 8005-8007.

Jiang, X., D. J. Lonsdale, and C. J. Gobler. 2010. Grazers and vitamins shape chain formation in a bloom-forming dinoflagellate *Cochlodinium polykrikoides*. Oecologia **164**(2): 455-464.

Johnson, W. M., M. C. Kido Soule, and E. B. Kujawinski. 2016. Evidence for quorum sensing and differential metabolite production by a marine bacterium in response to DMSP. ISME J. **10**(9): 2304-2316.

Jones, R. H., and K. J. Flynn. 2005. Nutritional status and diet composition affect the value of diatoms as copepod prey. Science **307**(5714): 1457-1459.

Jüttner, F. 1995. Physiology and biochemistry of odorous compounds from freshwater cyanobacteria and algae. Water Sci. Technol. **31**(11): 69-78.

Jüttner, F. 2001. Liberation of 5,8,11,14,17-eicosapentaenoic acid and other polyunsaturated fatty acids from lipids as a grazer defense reaction in epilithic diatom biofilms. J. Phycol. **37**(5): 744-755.

Jüttner, F., P. Messina, C. Patalano, and V. Zupo. 2010. Odour compounds of the diatom *Cocconeis scutellum*: Effects on benthic herbivores living on *Posidonia oceanica*. Mar. Ecol.: Prog. Ser. **400**: 63-73.

Kajiwara, T., M. Kashibe, K. Matsui, and A. Hatanaka. 1990. Volatile compounds and long-chain aldehydes formation in conchocelis-filaments of a red alga, *Porphyra tenera*. Phytochemistry **29**(7): 2193-2195.

Kale, N. S. and others 2016. MetaboLights: An open-access database repository for metabolomics data. Curr. Protoc. Bioinformatics **53**: 14 13 11-18.

Karsenti, E. and others 2011. A holistic approach to marine eco-systems biology. PLoS Biol. **9**(10): e1001177.

Katajamaa, M., J. Miettinen, and M. Oresic. 2006. MZmine: toolbox for processing and visualization of mass spectrometry based molecular profile data. Bioinformatics **22**(5): 634-636.

Kido Soule, M. C., K. Longnecker, W. M. Johnson, and E. B. Kujawinski. 2015. Environmental metabolomics: Analytical strategies. Mar. Chem. **177**: 374-387.

Kluender, C. and others 2008. A metabolomics approach to assessing phytotoxic effects on the green alga *Scenedesmus vacuolatus*. Metabolomics **5**(1): 59.

Kobayashi, Y., A. Torii, M. Kato, and K. Adachi. 2007. Accumulation of cyclitols functioning as compatible solutes in the haptophyte alga *Pavlova* sp. Phycol. Res. **55**(2): 81-90.

Kolb, A., and S. Strom. 2013. An inducible antipredatory defense in haploid cells of the marine microalga *Emiliania huxleyi* (Prymnesiophyceae). Limnol. Oceanogr. **58**(3): 932-944.

Krismer, J., M. Tamminen, S. Fontana, R. Zenobi, and A. Narwani. 2017. Single-cell mass spectrometry reveals the importance of genetic diversity and plasticity for phenotypic variation in nitrogen-limited *Chlamydomonas*. ISME J. **11**(4): 988-998.

Krupinska, K., and K. Humbeck. 1994. New trends in photobiology: Light-induced synchronous cultures, an excellent tool to study the cell cycle of unicellular green algae. J. Photochem. Photobiol., B **26**(3): 217-231.

Labeeuw, L. and others 2016. Indole-3-acetic acid is produced by *Emiliania huxleyi* coccolith-bearing cells and triggers a physiological response in bald cells. Front. Microbiol. **7**: 828.

Lalli, C. M. 1990. Enclosed experimental marine ecosystems: A review and recommendations, 1 ed. Springer-Verlag.

Landry, M. R., and R. P. Hassett. 1982. Estimating the grazing impact of marine micro-zooplankton. Mar. Biol. **67**(3): 283-288.

Landsberg, J. H. 2002. The effects of harmful algal blooms on aquatic organisms. Rev. Fish. Sci. **10**(2): 113-390.

Leblanc, K. and others 2012. A global diatom database - abundance, biovolume and biomass in the world ocean.

Lim, A. S., H. J. Jeong, T. Y. Jang, S. H. Jang, and P. J. S. Franks. 2014. Inhibition of growth rate and swimming speed of the harmful dinoflagellate *Cochlodinium polykrikoides* by diatoms: Implications for red tide formation. Harmful Algae **37**(Supplement C): 53-61.

Lisec, J., N. Schauer, J. Kopka, L. Willmitzer, and A. R. Fernie. 2006. Gas chromatography mass spectrometry-based metabolite profiling in plants. Nat. Protocols **1**(1): 387-396.

Litchman, E., and C. A. Klausmeier. 2008. Trait-based community ecology of phytoplankton. Annu. Rev. Ecol. Syst. **39**(1): 615-639.

Llewellyn, C. A., U. Sommer, C. L. Dupont, A. E. Allen, and M. R. Viant. 2015. Using community metabolomics as a new approach to discriminate marine microbial particulate organic matter in the western English Channel. Prog. Oceanogr. **137, Part B**: 421-433.

Lomas, M. W., and F. Lipschultz. 2006. Forming the primary nitrite maximum: Nitrifiers or phytoplankton? Limnol. Oceanogr. **51**(5): 2453-2467.

Lommen, A. 2009. MetAlign: Interface-driven, versatile metabolomics tool for hyphenated full-scan mass spectrometry data preprocessing. Anal. Chem. **81**(8): 3079-3086.

Long, J. D., G. W. Smalley, T. Barsby, J. T. Anderson, and M. E. Hay. 2007. Chemical cues induce consumer-specific defenses in a bloom-forming marine phytoplankton. Proc. Natl. Acad. Sci. U.S.A. **104**(25): 10512-10517.

Longnecker, K., J. Futrelle, E. Coburn, M. C. Kido Soule, and E. B. Kujawinski. 2015a. Environmental metabolomics: Databases and tools for data analysis. Mar. Chem. **177, Part 2**: 366-373.

Longnecker, K., M. C. Kido Soule, and E. B. Kujawinski. 2015b. Dissolved organic matter produced by *Thalassiosira pseudonana*. Mar. Chem. **168**: 114-123.

Longnecker, K., and E. B. Kujawinski. 2017. Mining mass spectrometry data: Using new computational tools to find novel organic compounds in complex environmental mixtures. Org. Geochem. **110**: 92-99.

Ma, H. and others 2011a. Isolation of activity and partial characterization of large non-proteinaceous lytic allelochemicals produced by the marine dinoflagellate *Alexandrium tamarense*. Harmful Algae **11**: 65-72.

Ma, J. and others 2011b. Headspace solid-phase microextraction with on-fiber derivatization for the determination of aldehydes in algae by gas chromatography-mass spectrometry. J. Sep. Sci. **34**(12): 1477-1483.

Ma, J., R. Xiao, J. Li, S. Zhu, and L. Lv. 2011c. Determination of aldehydes in diatoms by headspace solid-phase microextraction coupled with GC-MS. J. Chromatogr. Sci. **49**(1): 15-18.

Mahieu, N. G., J. L. Genenbacher, and G. J. Patti. 2016. A roadmap for the XCMS family of software solutions in metabolomics. Curr. Opin. Chem. Biol. **30**: 87-93.

Malviya, S. and others 2016. Insights into global diatom distribution and diversity in the world's ocean. Proc. Natl. Acad. Sci. U.S.A. **113**(11): E1516-E1525.

Martel, C. M. 2009. Conceptual bases for prey biorecognition and feeding selectivity in the microplanktonic marine phagotroph *Oxyrrhis marina*. Microb. Ecol. **57**(4): 589-597.

Mausz, M. A., and G. Pohnert. 2015. Phenotypic diversity of diploid and haploid *Emiliania huxleyi* cells and of cells in different growth phases revealed by comparative metabolomics. J. Plant Physiol. **172**: 137-148.

McGill, B. J., B. J. Enquist, E. Weiher, and M. Westoby. 2006. Rebuilding community ecology from functional traits. Trends Ecol. Evol. **21**(4): 178-185.

Medeiros, P. M., and B. R. Simoneit. 2007. Analysis of sugars in environmental samples by gas chromatography-mass spectrometry. J. Chromatogr. A **1141**(2): 271-278.

Metlen, K. L., E. T. Aschehoug, and R. M. Callaway. 2009. Plant behavioural ecology: Dynamic plasticity in secondary metabolites. Plant, Cell Environ. **32**(6): 641-653.

Meyer, N., A. Bigalke, A. Kaulfuss, and G. Pohnert. 2017. Strategies and ecological roles of algicidal bacteria. FEMS Microbiol. Rev. **41**(6): 880-899.

Michels, M. H. A., A. J. van der Goot, M. H. Vermuë, and R. H. Wijffels. 2016. Cultivation of shear stress sensitive and tolerant microalgal species in a tubular photobioreactor equipped with a centrifugal pump. J. Appl. Phycol. **28**(1): 53-62.

Mikami, K., and N. Murata. 2003. Membrane fluidity and the perception of environmental signals in cyanobacteria and plants. Prog. Lipid Res. **42**(6): 527-543.

Miner, B. G., S. E. Sultan, S. G. Morgan, D. K. Padilla, and R. A. Relyea. 2005. Ecological consequences of phenotypic plasticity. Trends Ecol. Evol. **20**(12): 685-692.

Minor, E. C., M. M. Swenson, B. M. Mattson, and A. R. Oyler. 2014. Structural characterization of dissolved organic matter: A review of current techniques for isolation and analysis. Environmental Science-Processes & Impacts **16**(9): 2064-2079.

Miralto, A. and others 1999. The insidious effect of diatoms on copepod reproduction. Nature **402**(6758): 173-176.

Molnár-Perl, I., A. Vasanits, and K. Horváth. 1998. Simultaneous GC-MS quantitation of phosphoric, aliphatic and aromatic carboxylic acids, proline and hydroxymethylfurfurol as their trimethylsilyl derivatives: In model solutions II. Chromatographia **48**(1-2): 111-119.

Monod, J. 1949. The growth of bacterial cultures. Annu. Rev. Microbiol. **3**: 371-394.

Nanjappa, D., G. d'Ippolito, C. Gallo, A. Zingone, and A. Fontana. 2014. Oxylipin diversity in the diatom family Leptocylindraceae reveals DHA derivatives in marine diatoms. Mar. Drugs **12**(1): 368-384.

Nappo, M. and others 2008. Metabolite profiling of the benthic diatom *Cocconeis scutellum* by GC-MS. J. Appl. Phycol. **21**(3): 295.

Nielsen, J., and S. Oliver. 2005. The next wave in metabolome analysis. Trends Biotechnol. **23**(11): 544-546.

Not, F., R. Siano, W. H. C. F. Kooistra, N. Simon, D. Vaulot, and I. Probert. 2012. Diversity and ecology of eukaryotic marine phytoplankton, p. 1-53. *In* G. Piganeau [ed.], Advances in Botanical Research. Academic Press.

Obata, T., S. Schoenefeld, I. Krahnert, S. Bergmann, A. Scheffel, and A. R. Fernie. 2013. Gas-chromatography mass-spectrometry (GC-MS) based metabolite profiling reveals mannitol as a major storage carbohydrate in the coccolithophorid alga *Emiliania huxleyi*. Metabolites **3**(1): 168-184.

Olli, K., and K. Trunov. 2007. Self-toxicity of *Prymnesium parvum* (Prymnesiophyceae). Phycologia **46**(1): 109-112.

Paffenhöfer, G.-A. 2002. An assessment of the effects of diatoms on planktonic copepods. Mar. Ecol.: Prog. Ser. **227**: 305-310.

Patejko, M., J. Jacyna, and M. J. Markuszewski. 2017. Sample preparation procedures utilized in microbial metabolomics: An overview. J. Chromatogr. B: Anal. Technol. Biomed. Life Sci. **1043**: 150-157.

Paul, C., A. Barofsky, C. Vidoudez, and G. Pohnert. 2009. Diatom exudates influence metabolism and cell growth of co-cultured diatom species. Mar. Ecol.: Prog. Ser. **389**: 61-70.

Paul, C., and G. Pohnert. 2011. Interactions of the algicidal bacterium *Kordia algicida* with diatoms: regulated protease excretion for specific algal lysis. Plos One **6**(6): e21032.

Pepi, M., H. J. Heipieper, C. Balestra, M. Borra, E. Biffali, and R. Casotti. 2017. Toxicity of diatom polyunsaturated aldehydes to marine bacterial isolates reveals their mode of action. Chemosphere **177**: 258-265.

Pezzolesi, L., S. Pichierri, C. Samori, C. Totti, and R. Pistocchi. 2017. PUFAs and PUAs production in three benthic diatoms from the northern Adriatic Sea. Phytochemistry **142**: 85-91.

Pigliucci, M., C. J. Murren, and C. D. Schlichting. 2006. Phenotypic plasticity and evolution by genetic assimilation. J. Exp. Biol. **209**(Pt 12): 2362-2367.

Pinu, F. R., and S. G. Villas-Bôas. 2017. Extracellular microbial metabolomics: The state of the art. Metabolites **7**(3).

Place, A. R., X. Bai, S. Kim, M. R. Sengco, and D. Wayne Coats. 2009. Dinoflagellate host-parasite sterol profiles dictate karlotoxin sensitivity. J. Phycol. **45**(2): 375-385.

Pohnert, G., and W. Boland. 1996. Biosynthesis of the algal pheromone hormosirene by the fresh-water diatom *Gomphonema parvulum* (Bacillariophyceae). Tetrahedron **52**(30): 10073-10082.

Pohnert, G. 2000. Wound-activated chemical defense in unicellular planktonic algae. Angew. Chem. Int. Ed. **39**(23): 4352-4354.

---. 2002. Phospholipase A_2 activity triggers the wound-activated chemical defense in the diatom *Thalassiosira rotula*. Plant Physiol. **129**(1): 103-111.

Pohnert, G. and others 2002. Are volatile unsaturated aldehydes from diatoms the main line of chemical defence against copepods? Mar. Ecol.: Prog. Ser. **245**: 33-45.

Pohnert, G., S. Adolph, and T. Wichard. 2004. Short synthesis of labeled and unlabeled 6*Z*,9*Z*,12*Z*,15-hexadecatetraenoic acid as metabolic probes for biosynthetic studies on diatoms. Chem. Phys. Lipids **131**(2): 159-166.

Pohnert, G., M. Steinke, and R. Tollrian. 2007. Chemical cues, defence metabolites and the shaping of pelagic interspecific interactions. Trends Ecol. Evol. **22**(4): 198-204.

Pohnert, G. 2010. Chemical noise in the silent ocean. J. Plankton Res. **32**(2): 141-144.

Pokrzywinski, K. L., A. R. Place, M. E. Warner, and K. J. Coyne. 2012. Investigation of the algicidal exudate produced by *Shewanella* sp. IRI-160 and its effect on dinoflagellates. Harmful Algae **19**(Supplement C): 23-29.

Poulet, S. A., A. Ianora, A. Miralto, and L. Meijer. 1994. Do diatoms arrest embryonic-development in copepods. Mar. Ecol.: Prog. Ser. **111**(1-2): 79-86.

Poulson, K. L., R. D. Sieg, and J. Kubanek. 2009. Chemical ecology of the marine plankton. Nat. Prod. Rep. **26**(6): 729-745.

Prince, E. K., and G. Pohnert. 2010. Searching for signals in the noise: Metabolomics in chemical ecology. Anal. Bioanal. Chem. **396**(1): 193-197.

Prince, E. K., K. L. Poulson, T. L. Myers, R. D. Sieg, and J. Kubanek. 2010. Characterization of allelopathic compounds from the red tide dinoflagellate *Karenia brevis*. Harmful Algae **10**(1): 39-48.

Prince, E. K., F. Irmer, and G. Pohnert. 2013. Domoic acid improves the competitive ability of *Pseudo-nitzschia delicatissima* against the diatom *Skeletonema marinoi*. Mar. Drugs **11**(7): 2398-2412.

Raes, J., and P. Bork. 2008. Molecular eco-systems biology: Towards an understanding of community function. Nature Reviews Microbiology **6**(9): 693-699.

Rajamani, S. and others 2008. The vitamin riboflavin and its derivative lumichrome activate the LasR bacterial quorum sensing receptor. Molecular plant-microbe interactions : MPMI **21**(9): 10.1094/MPMI-1021-1099-1184.

Ramirez-Gaona, M. and others 2017. YMDB 2.0: A significantly expanded version of the yeast metabolome database. Nucleic Acids Res. **45**(D1): D440-D445.

Rasmussen, S. A., A. J. Andersen, N. G. Andersen, K. F. Nielsen, P. J. Hansen, and T. O. Larsen. 2016. Chemical diversity, origin, and analysis of phycotoxins. J. Nat. Prod. **79**(3): 662-673.

Ray, J. L. and others 2016a. Metabarcoding and metabolome analyses of copepod grazing reveal feeding preference and linkage to metabolite classes in dynamic microbial plankton communities. Mol. Ecol. **25**(21): 5585-5602.

Ray, J. L. and others 2016b. Molecular gut content analysis demonstrates that *Calanus* grazing on *Phaeocystis pouchetii* and *Skeletonema marinoi* is sensitive to bloom phase but not prey density. Mar. Ecol.: Prog. Ser. **542**: 63-77.

Remmel, E. J., and K. D. Hambright. 2012. Toxin-assisted micropredation: Experimental evidence shows that contact micropredation rather than exotoxicity is the role of *Prymnesium* toxins. Ecol. Lett. **15**(2): 126-132.

Reusch, T. B. H., and P. W. Boyd. 2013. Experimental evolution meets marine phytoplankton. Evolution **67**(7): 1849-1859.

Ribalet, F., J. A. Berges, A. Ianora, and R. Casotti. 2007a. Growth inhibition of cultured marine phytoplankton by toxic algal-derived polyunsaturated aldehydes. Aquat. Toxicol. **85**(3): 219-227.

Ribalet, F., T. Wichard, G. Pohnert, A. Ianora, A. Miralto, and R. Casotti. 2007b. Age and nutrient limitation enhance polyunsaturated aldehyde production in marine diatoms. Phytochemistry **68**(15): 2059-2067.

Ribalet, F., L. Intertaglia, P. Lebaron, and R. Casotti. 2008. Differential effect of three polyunsaturated aldehydes on marine bacterial isolates. Aquat. Toxicol. **86**(2): 249-255.

Robinson, M. 2008. Methods for the analysis of gas chromatography - mass spectrometry data. University of Melbourne.

Roessler, P. G. 1990. Environmental control of glyerolipid metabolism in microalgae: Commercial implicatioins and future research directions. J. Phycol. **26**(3): 393-399.

Rokitta, S. D., P. Von Dassow, B. Rost, and U. John. 2014. *Emiliania huxleyi* endures N-limitation with an efficient metabolic budgeting and effective ATP synthesis. BMC Genomics **15**(1): 1051.

Romano, G., A. Miralto, and A. Ianora. 2010. Teratogenic effects of diatom metabolites on sea urchin *Paracentrotus lividus* embryos. Mar. Drugs **8**(4): 950-967.

Rosenwasser, S. and others 2014. Rewiring host lipid metabolism by large viruses determines the fate of *Emiliania huxleyi*, a bloom-forming alga in the ocean. Plant Cell **26**(6): 2689-2707.

Sajed, T. and others 2016. ECMDB 2.0: A richer resource for understanding the biochemistry of *E. coli*. Nucleic Acids Res. **44**(D1): D495-501.

Santiago-Vázquez, L. Z., L. D. Mydlarz, J. G. Pavlovich, and R. S. Jacobs. 2004. Identification of hydroxy fatty acids by liquid chromatography-atmospheric pressure chemical ionization mass spectroscopy in *Euglena gracilis*. J. Chromatogr. B: Biomed. Sci. Appl. **803**(2): 233-236.

Savoca, M. S., and G. A. Nevitt. 2014. Evidence that dimethyl sulfide facilitates a tritrophic mutualism between marine primary producers and top predators. Proc. Natl. Acad. Sci. U.S.A. **111**(11): 4157-4161.

Scheubert, K. and others 2017. Significance estimation for large scale metabolomics annotations by spectral matching. Nat. Commun. **8**(1): 1494.

Schmidt, K., C. van Oosterhout, S. Collins, and T. Mock. 2016. The role of phenotypic plasticity and epigenetics in experimental evolution with phytoplankton. Perspectives in Phycology **3**: 29-36.

Schneider, C., D. A. Pratt, N. A. Porter, and A. R. Brash. 2007. Control of oxygenation in lipoxygenase and cyclooxygenase catalysis. Chemistry & Biology **14**(5): 473-488.

Schrimpe-Rutledge, A. C., S. G. Codreanu, S. D. Sherrod, and J. A. McLean. 2016. Untargeted metabolomics strategies - Challenges and emerging directions. J. Am. Soc. Mass Spectrom. **27**(12): 1897-1905.

Schwartz, E. R., R. X. Poulin, N. Mojib, and J. Kubanek. 2016. Chemical ecology of marine plankton. Nat. Prod. Rep. **33**(7): 843-860.

Segev, E. and others 2016. Dynamic metabolic exchange governs a marine algal-bacterial interaction. eLife **5**: 28.

Selander, E., H. H. Jakobsen, F. Lombard, and T. Kiørboe. 2011. Grazer cues induce stealth behavior in marine dinoflagellates. Proc. Natl. Acad. Sci. U.S.A. **108**(10): 4030-4034.

Selander, E., J. Kubanek, M. Hamberg, M. X. Andersson, G. Cervin, and H. Pavia. 2015. Predator lipids induce paralytic shellfish toxins in bloom-forming algae. Proc. Natl. Acad. Sci. U.S.A. **112**(20): 6395-6400.

Seyedsayamdost, M. R., G. Carr, R. Kolter, and J. Clardy. 2011. Roseobacticides: Small molecule modulators of an algal-bacterial symbiosis. J. Am. Chem. Soc. **133**(45): 18343-18349.

Seymour, J. R., L. Seuront, M. J. Doubell, and J. G. Mitchell. 2008. Mesoscale and microscale spatial variability of bacteria and viruses during a *Phaeocystis globosa* bloom in the Eastern English Channel. Estuarine, Coastal Shelf Sci. **80**(4): 589-597.

Seymour, J. R., S. A. Amin, J. B. Raina, and R. Stocker. 2017. Zooming in on the phycosphere: The ecological interface for phytoplankton-bacteria relationships. Nat. Microbiol. **2**(7): 17065.

Smith, C. A., E. J. Want, G. O'Maille, R. Abagyan, and G. Siuzdak. 2006. XCMS: Processing mass spectrometry data for metabolite profiling using nonlinear peak alignment, matching, and identification. Anal. Chem. **78**(3): 779-787.

Spiteller, D., and G. Spiteller. 2000. Identification of toxic 2,4-decadienal in oxidized, low-density lipoprotein by solid-phase microextraction. Angew. Chem. Int. Ed. **39**(3): 583-585.

Stoecker, D. K., A. Weigel, and J. I. Goes. 2014. Microzooplankton grazing in the Eastern Bering Sea in summer. Deep Sea Res., Part II **109**: 145-156.

Stoecker, D. K. and others 2015. Underestimation of microzooplankton grazing in dilution experiments due to inhibition of phytoplankton growth. Limnol. Oceanogr. **60**(4): 1426-1438.

Sud, M. and others 2016. Metabolomics Workbench: An international repository for metabolomics data and metadata, metabolite standards, protocols, tutorials and training, and analysis tools. Nucleic Acids Res. **44**(D1): D463-470.

Sumner, L. W. and others 2007. Proposed minimum reporting standards for chemical analysis. Metabolomics **3**(3): 211-221.

Tameishi, M., Y. Yamasaki, S. Nagasoe, Y. Shimasaki, Y. Oshima, and T. Honjo. 2009. Allelopathic effects of the dinophyte *Prorocentrum minimum* on the growth of the bacillariophyte *Skeletonema costatum*. Harmful Algae **8**(3): 421-429.

Tang, K. W., W. O. Smith, D. T. Elliott, and A. R. Shields. 2008. Colony size of *Phaeocystis antarctica* (Prymnesiophyceae) as influenced by zooplankton grazers. J. Phycol. **44**(6): 1372-1378.

Thornton, D. C. O. 2014. Dissolved organic matter (DOM) release by phytoplankton in the contemporary and future ocean. Eur. J. Phycol. **49**(1): 20-46.

Tirichine, L., and C. Bowler. 2011. Decoding algal genomes: tracing back the history of photosynthetic life on Earth. Plant J. **66**(1): 45-57.

Tiselius, P., E. Saiz, and T. Kiørboe. 2013. Sensory capabilities and food capture of two small copepods, *Paracalanus parvus* and *Pseudocalanus* sp. Limnol. Oceanogr. **58**(5): 1657-1666.

Turner, J. T., and P. A. Tester. 1997. Toxic marine phytoplankton, zooplankton grazers, and pelagic food webs. Limnol. Oceanogr. **42**(5): 1203-1214.

Uronen, P., P. Kuuppo, C. Legrand, and T. Tamminen. 2007. Allelopathic effects of toxic haptophyte *Prymnesium parvum* lead to release of dissolved organic carbon and increase in bacterial biomass. Microb. Ecol. **54**(1): 183-193.

Valledor, L., M. Escandon, M. Meijon, E. Nukarinen, M. J. Canal, and W. Weckwerth. 2014. A universal protocol for the combined isolation of metabolites, DNA, long RNAs, small RNAs, and proteins from plants and microorganisms. Plant J. **79**(1): 173-180.

van den Berg, R. A., H. C. Hoefsloot, J. A. Westerhuis, A. K. Smilde, and M. J. van der Werf. 2006. Centering, scaling, and transformations: improving the biological information content of metabolomics data. BMC Genomics **7**: 142.

van Gulik, W. M. 2010. Fast sampling for quantitative microbial metabolomics. Curr. Opin. Biotechnol. **21**(1): 27-34.

van Zoonen, P., H. A. van 't Klooster, R. Hoogerbrugge, S. M. Gort, and H. J. van de Wiel. 1998. Validation of analytical methods and laboratory procedures for chemical measurements. Arh. Hig. Rada Toksikol. **49**(4): 355-370.

Vardi, A. and others 2006. A stress surveillance system based on calcium and nitric oxide in marine diatoms. PLoS Biol. **4**(3): 411-419.

Vardi, A. and others 2008. A diatom gene regulating nitric-oxide signaling and susceptibility to diatom-derived aldehydes. Curr. Biol. **18**(12): 895-899.

Vardi, A. and others 2009. Viral glycosphingolipids induce lytic infection and cell death in marine phytoplankton. Science **326**(5954): 861-865.

Vardi, A. and others 2012. Host-virus dynamics and subcellular controls of cell fate in a natural coccolithophore population. Proc. Natl. Acad. Sci. U.S.A. **109**(47): 19327-19332.

Varrella, S., G. Romano, N. Ruocco, A. Ianora, M. G. Bentley, and M. Costantini. 2016. First morphological and molecular evidence of the negative impact of diatom-derived hydroxyacids on the sea urchin *Paracentrotus lividus*. Toxicol. Sci. **151**(2): 419-433.

Veyel, D., A. Erban, I. Fehrle, J. Kopka, and M. Schroda. 2014. Rationales and approaches for studying metabolism in eukaryotic microalgae. Metabolites **4**(2): 184-217.

Vidoudez, C., and G. Pohnert. 2008. Growth phase-specific release of polyunsaturated aldehydes by the diatom *Skeletonema marinoi*. J. Plankton Res. **30**(11): 1305-1313.

Vidoudez, C., R. Casotti, M. Bastianini, and G. Pohnert. 2011a. Quantification of dissolved and particulate polyunsaturated aldehydes in the Adriatic Sea. Mar. Drugs **9**(4): 500-513.

Vidoudez, C., J. C. Nejstgaard, H. H. Jakobsen, and G. Pohnert. 2011b. Dynamics of dissolved and particulate polyunsaturated aldehydes in mesocosms inoculated with different densities of the diatom *Skeletonema marinoi*. Mar. Drugs **9**(3): 345-358.

Vidoudez, C., and G. Pohnert. 2012. Comparative metabolomics of the diatom *Skeletonema marinoi* in different growth phases. Metabolomics **8**(4): 654-669.

Villas-Bôas, S. G., S. Mas, M. Åkesson, J. Smedsgaard, and J. Nielsen. 2005. Mass spectrometry in metabolome analysis. Mass Spectrom. Rev. **24**(5): 613-646.

Vinaixa, M., E. L. Schymanski, S. Neumann, M. Navarro, R. M. Salek, and O. Yanes. 2016. Mass spectral databases for LC-MS- and GC-MS-based metabolomics: State of the field and future prospects. TrAC, Trends Anal. Chem. **78**: 23-35.

von Reuss, S. H. and others 2012. Comparative metabolomics reveals biogenesis of ascarosides, a modular library of small-molecule signals in *C. elegans*. J. Am. Chem. Soc. **134**(3): 1817-1824.

Waggett, R. J., D. R. Hardison, and P. A. Tester. 2012. Toxicity and nutritional inadequacy of *Karenia brevis*: Synergistic mechanisms disrupt top-down grazer control. Mar. Ecol.: Prog. Ser. **444**: 15-30.

Wang, R., and Y. Shimizu. 1990. Bacillariolides I and II, a new type of cyclopentane eicosanoids from the diatom *Nitzschia pungens*. J. Chem. Soc. D **5**: 413-414.

Weber, R. J., E. Selander, U. Sommer, and M. R. Viant. 2013. A stable-isotope mass spectrometry-based metabolic footprinting approach to analyze exudates from phytoplankton. Mar. Drugs **11**(11): 4158-4175.

Wehrens, R., G. Weingart, and F. Mattivi. 2014. metaMS: An open-source pipeline for GC-MS-based untargeted metabolomics. J. Chromatogr. B: Anal. Technol. Biomed. Life Sci. **966**: 109-116.

Weller, M. G. 2012. A unifying review of bioassay-guided fractionation, effect-directed analysis and related techniques. Sensors **12**(7): 9181-9209.

Wendel, T., and F. Jüttner. 1996. Lipoxygenase-mediated formation of hydrocarbons and unsaturated aldehydes in freshwater diatoms. Phytochemistry **41**(6): 1445-1449.

Wichard, T. and others 2005a. Survey of the chemical defence potential of diatoms: Screening of fifty one species for α,β,γ,δ-unsaturated aldehydes. J. Chem. Ecol. **31**(4): 949-958.

Wichard, T., S. A. Poulet, and G. Pohnert. 2005b. Determination and quantification of α,β,γ,δ-unsaturated aldehydes as pentafluorobenzyl-oxime derivates in diatom cultures and natural phytoplankton populations: Application in marine field studies. J. Chromatogr. B: Anal. Technol. Biomed. Life Sci. **814**(1): 155-161.

Wichard, T., and G. Pohnert. 2006. Formation of halogenated medium chain hydrocarbons by a lipoxygenase/hydroperoxide halolyase-mediated transformation in planktonic microalgae. J. Am. Chem. Soc. **128**(22): 7114-7115.

Wichard, T., A. Gerecht, M. Boersma, S. A. Poulet, K. Wiltshire, and G. Pohnert. 2007. Lipid and fatty acid composition of diatoms revisited: rapid wound-activated change of food quality parameters influences herbivorous copepod reproductive success. Chembiochem **8**(10): 1146-1153.

Wichard, T. and others 2008. Influence of diatoms on copepod reproduction. II. Uncorrelated effects of diatom-derived α,β,γ,δ-unsaturated aldehydes and polyunsaturated fatty acids on *Calanus helgolandicus* in the field. Prog. Oceanogr. **77**(1): 30-44.

Williams, T. J., and R. Cavicchioli. 2014. Marine metaproteomics: Deciphering the microbial metabolic food web. Trends Microbiol. **22**(5): 248-260.

Winder, C. L. and others 2008. Global metabolic profiling of *Escherichia coli* cultures: An evaluation of methods for quenching and extraction of intracellular metabolites. Anal. Chem. **80**(8): 2939-2948.

Wohlrab, S., M. H. Iversen, and U. John. 2010. A molecular and co-evolutionary context for grazer induced toxin production in *Alexandrium tamarense*. Plos One **5**(11): e15039.

Wolf, S., S. Schmidt, M. Müller-Hannemann, and S. Neumann. 2010. *In silico* fragmentation for computer assisted identification of metabolite mass spectra. BMC Bioinformatics **11**(1): 148.

Wolfe, G. V., E. B. Sherr, and B. F. Sherr. 1994. Release and consumption of DMSP from *Emiliania huxleyi* during grazing by *Oxyrrhis marina*. Mar. Ecol.: Prog. Ser. **111**(1-2): 111-119.

Wolfe, G. V., M. Levasseur, G. Cantin, and S. Michaud. 2000. DMSP and DMS dynamics and microzooplankton grazing in the Labrador Sea: Application of the dilution technique. Deep-Sea Res., Part I **47**(12): 2243-2264.

Wolfender, J.-L., G. Marti, A. Thomas, and S. Bertrand. 2015. Current approaches and challenges for the metabolite profiling of complex natural extracts. J. Chromatogr. A **1382**: 136-164.

Wolfram, S., J. C. Nejstgaard, and G. Pohnert. 2014. Accumulation of polyunsaturated aldehydes in the gonads of the copepod *Acartia tonsa* revealed by tailored fluorescent probes. Plos One **9**(11): e112522.

Wolfram, S. and others 2015. A metabolic probe-enabled strategy reveals uptake and protein targets of polyunsaturated aldehydes in the diatom *Phaeodactylum tricornutum*. Plos One **10**(10): e0140927.

Wördenweber, R. and others 2017. Phosphorus and nitrogen starvation reveal life-cycle specific responses in the metabolome of *Emiliania huxleyi* (Haptophyta). Limnol. Oceanogr. **63**(1): 203-226.

Xi, B., H. Gu, H. Baniasadi, and D. Raftery. 2014. Statistical analysis and modeling of mass spectrometry-based metabolomics data. Methods Mol. Biol. **1198**: 333-353.

Xia, J., and D. S. Wishart. 2016. Using MetaboAnalyst 3.0 for comprehensive metabolomics data analysis. Curr. Protoc. Bioinformatics **55**: 14. 10. 11-14. 10. 91.

Xu, Y., J. J. Milledge, A. Abubakar, R. Swamy, D. Bailey, and P. Harvey. 2015. Effects of centrifugal stress on cell disruption and glycerol leakage from *Dunaliella salina*. Microalgae Biotechnology **1**(1): 20-27.

Yamasaki, Y. and others 2011. Species-specific allelopathic effects of the diatom *Skeletonema costatum*. Thalassas **27**(1): 21-32.

Zampieri, M., K. Sekar, N. Zamboni, and U. Sauer. 2017. Frontiers of high-throughput metabolomics. Curr. Opin. Chem. Biol. **36**: 15-23.

Zhu, X. C., X. X. Tang, J. Y. Zhang, G. P. Tochtrop, V. E. Anderson, and L. M. Sayre. 2010. Mass spectrometric evidence for the existence of distinct modifications of different proteins by 2(*E*),4(*E*)-decadienal. Chem. Res. Toxicol. **23**(3): 467-473.

Appendix

Fig. S 1 Effect of cell disruption method (ultrasonic homogenizer *vs*. ultrasonic bath) on analyte signal intensity of the short-chained polyunsaturated aldehydes heptadienal (A) and octadienal (B) determined as peak area ratio to the internal standard (IS) vanillin.

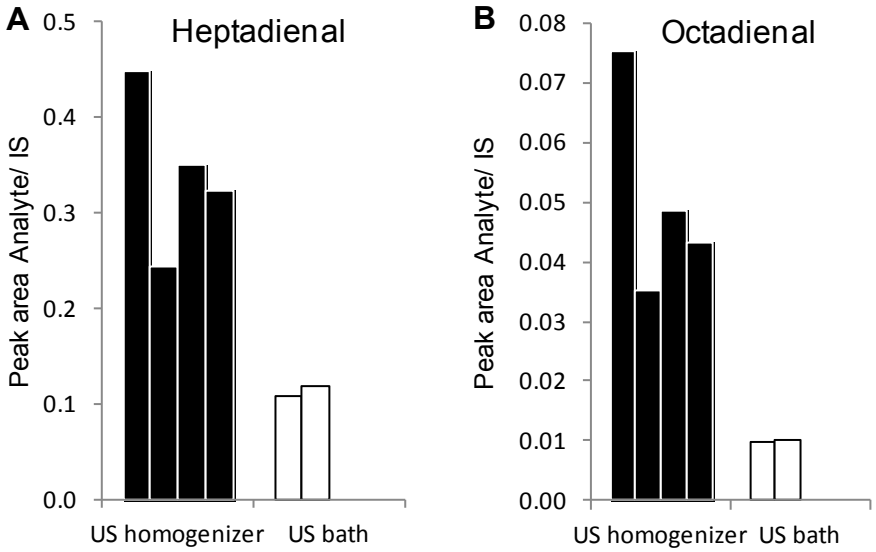

Table S 1 Occurrence of short-chained polyunsaturated aldehydes (PUAs; in fmol/cell) in diatoms as known from previous studies (**Manuscript 5**)(Amin et al. 2011; Dittami et al. 2010; Dutz et al. 2008; Fontana et al. 2007; Jüttner et al. 2010; Ma et al. 2011c; Pezzolesi et al. 2017; Ribalet et al. 2007b; Wichard et al. 2005a).

Genus	Species	Strain	C6:2	C7:2	C8:2	C8:3	C9:2	C10:2	C10:3	Total PUAs	Reference
Asterionellopsis	*glacialis*	-		0.03	0.01	0.002		0	0	0.05	Wichard et al. 2005
Chaetoceros	*affinis*	CCMP 158								0	Dutz et al. 2008
Chaetoceros	*affinis*	-								0	Fontana et al. 2007
Chaetoceros	*calcitrans*	-								0	Wichard et al. 2005
Chaetoceros	*compressus*	-		0.87	0.34	0		0.23	1.38	2.82	Wichard et al. 2005
Chaetoceros	*didymus*	Na20B4	0	0.01	0	0		+	0	0.01	**Manuscript 5**
Chaetoceros	*muelleri*	-		0.01				0.002		0.01	Ma et al. 2011
Chaetoceros	*socialis*	CSFE 17								0	Fontana et al. 2007
Cocconeis	*scutellum parva*	-		0.01			0.003		0.01		Jüttner et al. 2010
Fragilaria	sp.	-		0.07	0.03	0		0.003	0	0.10	Wichard et al. 2005
Guinardia	*delicatula*	-								+	Wichard et al. 2005
Guinardia	*deliculata*	-		0.18	0	0		0	0	0.18	Wichard et al. 2005
Guinardia	*striata*	-								0	Wichard et al. 2005
Leptocylindricus	*danicus*	CCMP 469								0.04	Dutz et al. 2008
Melosira	*nummuloides*	-		0.61	6.25	0		0.17	1.65	8.68	Wichard et al. 2005
Melosira	*sulcata*	-		0	0.01	0		0	0	0.01	Wichard et al. 2005
Navicula	sp.	NAPS 0313	4.16	0	0.40			0			Pezzolesi et al. 2017
Navicula	*sp.*	-								0	Wichard et al. 2005
Nitzschia	*sp.*	-								0	Wichard et al. 2005
Odontella	*regia*	-								traces	Wichard et al. 2005
Proschkinia	*complanatoides*	PCAPS 0313	1.56	0	0	0.16		0			Pezzolesi et al. 2017
Rhizosolenia	*setigera*	-								0	Wichard et al. 2005
Rhodomonas	*sp.*	-								0	Dutz et al. 2008
Scripsiella	*trochoidea*	-		0.001				0		0.00	Ma et al. 2011
Skeletonema	*costatum*	CCMP 1281								0.04	Dutz et al. 2008
Skeletonema	*costatum*	RCC 75		0.08	0.05	0.004		0	0	0.13	Wichard et al. 2005
Skeletonema	*costatum*	RCC 75	0	0.48	0.25	0.08		+	0.02	0.83	**Manuscript 5**
Skeletonema	*costatum*	SAG 19.99		0.01	0.002	0		0	0	0.01	Wichard et al. 2005
Skeletonema	*costatum*			0.01				0.002		0.01	Ma et al. 2011
Skeletonema	*marinoi*	CCMP 2092		4.20	3.30	0.20				7.50	Ribalet et al. 2007

Skeletonema	*marinoi*	CCMP 2092		13.90	14.00	1.00			27.50	Ribalet et al. 2009
Skeletonema	*marinoi*	GF04-1G							0	Amin et al. 2011
Skeletonema	*marinoi*	GF04-7J							0.00	Amin et al. 2011
Skeletonema	*marinoi*	GF04-9B							0.32	Amin et al. 2011
Skeletonema	*marinoi*	-							+	Fontana et al. 2007
Skeletonema	*pseudocostatum*	-		0.19	0.19	0.00	0	0	0.38	Wichard et al. 2005
Skeletonema	*subsalsum*	-		0	0.03	0	0.01	0	0.04	Wichard et al. 2005
Stephanopyxis	*turris*	-							0	Wichard et al. 2005
Tabularia	*affinis*	TAAPS 0313	2.08	0	0	0.41	0			Pezzolesi et al. 2017
Thalassiosira	*aestivalis*	-		1.20	0.25	0.09	0	0	1.54	Wichard et al. 2005
Thalassiosira	*anguste-lineata*	-		1.06	0.26	0.21	0	0	1.53	Wichard et al. 2005
Thalassiosira	*minima*	-		0.01	0.01	0	0	0.03	0.05	Wichard et al. 2005
Thalassiosira	*nordenskioeldii*	-		0	0.01	0	0	0	0.01	Wichard et al. 2005
Thalassiosira	*pacifica*	-		6.86	1.86	1.08	0	0	9.80	Wichard et al. 2005
Thalassiosira	*pseudonana*	CCMP 1335							0	Wichard et al. 2005
Thalassiosira	*rotula*	-		0.30	0.10	0.52	0	0.34	1.27	Wichard et al. 2005
Thalassiosira	*rotula*	-		0.40	0.91	1.02	0	3.30	5.69	Wichard et al. 2005
Thalassiosira	*rotula*	CCMP 1018							0	Dutz et al. 2008
Thalassiosira	*rotula*	CCMP 1018		0.07	0.10	0.05	0	0	0.22	Wichard et al. 2005
Thalassiosira	*rotula*	CCMP 1018		9.00	9.00	4.00		7.00		Dittami et al. 2010
Thalassiosira	*rotula*	CCMP 1647							2.27	Dutz et al. 2008
Thalassiosira	*rotula*	CCMP 1647		1.80	0.50	0.70		1.00	4.60	Dittami et al. 2010
Thalassiosira	*rotula*	CCMP 1647		0.32	2.03	0.70	0.13	3.18	6.35	Wichard et al. 2005
Thalassiosira	*rotula*	CCMP 1647		1.00	3.00	1.00	1.50	4.00		Wichard et al. 2005
Thalassiosira	*rotula*	CCMP 1812		0.25	0.29	0.24	0	0.25	1.04	Wichard et al. 2005
Thalassiosira	*rotula*	RCC 776	+	0.18	0.17	0.42	0.03	1.08	1.88	**Manuscript 5**
Thalassiosira	*weissflogii*	-							0	Dutz et al. 2008

Table S 2 Instrument properties of analytical platforms as used in **Manuscript 3** that made an automated chromatogram alignment difficult. Ribitol was used as internal standard (IS). Both instruments were operated at a scan rate of 5 scans/sec, however, the use of the DRE mode (dynamic range extension) for the GCT Premier™ resulted in a reduced total scan number.

Instrument parameter	**Phytoplankton bloom samples**	**Growth phase experiment samples**
Instrument	WATERS Micromass GCT Premier™	THERMOSCIENTIFIC™ ISQ™ LT
t_R (min) of IS	10.75-10.79	11.84
Total scan number	3544	6862
Mass resolution	6129 at *m*/*z* 501.97	866 at *m*/*z* 502.20
Mass calibration solution	yes (perfluorotributylamine)	no

Supporting information of Publication P3:

For full scale images and tables the reader is referred to the electronic version of this thesis and the embedded compact disc.

Supplementary information

Metabolomics-derived marker metabolites to characterize *Phaeocystis pouchetii* in natural plankton communities

Constanze Kuhlisch[a], Julia Althammer[a,1], Andrey F. Sazhin[b], Hans H. Jakobsen[c], Jens C. Nejstgaard[d,2], Georg Pohnert[a *]

[a] Institute for Inorganic and Analytical Chemistry, Friedrich Schiller University Jena, Lessingstraße 8, 07743 Jena, Germany; constanze.kuhlisch@uni-jena.de

[b] P.P. Shirshov Institute of Oceanology, Russian Academy of Sciences, Nakhimovsky Prospect 36, Moscow, Russia; andreysazhin@yandex.ru

[c] Department of Bioscience, Aarhus University, Frederiksborgvej 399, 4000 Roskilde, Denmark; hhja@bios.au.dk

[d] Uni Research Environment, Uni Research AS, Postboks 7810, 5020 Bergen, Norway

[1] Present address: JenaBios GmbH, Löbstedter Straße 80, 07749 Jena, Germany; j.althammer@jenabios.de

[2] Present address: Leibniz-Institute of Freshwater Ecology and Inland Fisheries, Dep. 3, Alte Fischerhütte 2, 16775 Stechlin, Germany; nejstgaard@igb-berlin.de

* corresponding author, e-mail: georg.pohnert@uni-jena.de, Institute for Inorganic and Analytical Chemistry, Friedrich Schiller University Jena, Lessingstraße 8, 07743 Jena, Germany

Table 1 MetaboliteDetector 2.0: 'RI Calibration Wizard' advanced parameters.

Calibration compound	Ribitol (5TMS)
Required score	0.7

Table 2 MetaboliteDetector 2.0: Deconvolution settings.

Baseline adjustment	yes
Peak threshold	10
Minimal peak height	10
Bins/scan	10
Deconvolution width	1

Table 3 MetaboliteDetector 2.0: 'Batch quantification' parameters.

Non-targeted analysis	
Compound matching:	
ΔRI	15
Pure/Impure	0.7
scoring method	RI + Spec
req. score	0.5
Identification:	
ΔRI	15
Pure/Impure	0.7
Scoring Method	RI + Spec
Ref. library	
Compound filter:	
Compound reproducibility	0.3
Max. peak disc. index	100
Req. S/N	0
Min # ions	10

Table 4 Spearman rank correlation coefficients for selected Phaeocystis pouchetii endometabolites and environmental parameters for PHAEONIGMA cruise samples. MC estimated p-values and 95%-CI limits are given.

		Spearman rank correlation		
Environm. parameter	Endometabolite	Coefficient	p-value	95%-CI
Irradiance	Hexose	0.552	0.010	(0.251,0.853)
Nitrate	Maltose	-0.512	0.030	(-0.893, -0.131)
	Ribose	-0.459	0.056	(-0.943,0.026)
Diatom biomass	C20:5n-3	0.544	0.011	(0.220,0.869)
Phaeocystis biomass	Mannitol	0.552	0.010	(0.223,0.881)
	Scyllo-Inositol	0.644	0.002	(0.396,0.893)

Table 5 Intracellular metabolites that are highly correlated (x ≥0.8) with the exponential (A), early stationary (B) or late stationary (C) growth phase of *Phaeocystis pouchetii* AJ01 (n = 4). # - Metabolites are shown as tabulated in Fig. 3B. Vector - correlation coefficient. Factor - phase median maximum/minimum, Phase - correlated growth phase, Ion - model ion used for peak integration, t_R - retention time (min), R.Match - parameter for spectral database comparison (MS Search), I_L - linear retention index, Level - identification level according to Sumner et al. (2007).

#	Ion	t_R	Vector	A1	A2	A3	A4	B1	B2	B3	B4	C1	C2	C3	C4	Factor	Phase	Class	Substance name	R.Match	I_L	r I_L	Level
22	114.9	5.454	0.8232	0.0004	0.0002	0.0005	0.0004	0.0000	0.0000	0.0002	0.0000	0.0002	0.0000	0.0000	0.0003	10	A	Unknown		<700	1007		L4
24	117	5.534	0.9144	0.0003	0.0002	0.0003	0.0002	0.0011	0.0010	0.0003	0.0008	0.0013	0.0009	0.0011	0.0005	3	C	Unknown		<700	1015		L4
27	160	5.715	0.8538	0.0004	0.0002	0.0004	0.0003	0.0000	0.0000	0.0003	0.0000	0.0001	0.0000	0.0000	0.0000	8	A	Unknown		<700	1034		L4
34	151	5.953	0.8759	0.0039	0.0044	0.0040	0.0037	0.0076	0.0048	0.0045	0.0114	0.0128	0.0150	0.0568	0.0148	6	C	Others	Phenol (1TMS)	918	1059		L2
36	242.3	6.034	0.8756	0.0000	0.0001	0.0000	0.0000	0.0000	0.0000	0.0000	0.0000	0.0000	0.0000	0.0000	0.0000	24	A	Unknown		<700	1067		L4
38	173.1	6.122	0.9313	0.0009	0.0007	0.0008	0.0006	0.0010	0.0004	0.0010	0.0007	0.0015	0.0029	0.0057	0.0028	3	C	Fatty acid	Hexanoic acid (1TMS)	719	1076	1075	L3
42	145.9	6.315	0.9374	0.0001	0.0001	0.0001	0.0002	0.0000	0.0000	0.0001	0.0000	0.0000	0.0000	0.0000	0.0001	6	A	Amino acid	Valine (1TMS)	798	1096	1093	L1
47	116	6.408	0.9098	0.0034	0.0041	0.0044	0.0033	0.0001	0.0001	0.0026	0.0000	0.0001	0.0001	0.0000	0.0002	62	A	Amino acid	Alanine (2TMS)	841	1106	1103	L1
83	103.1	7.561	0.8763	0.0003	0.0003	0.0005	0.0003	0.0021	0.0012	0.0009	0.0014	0.0019	0.0008	0.0024	0.0004	5	B/C	Saccharide	Glyceraldehyde (Meox 2TMS)	819	1226	1224	L1
86	110	7.787	0.8198	0.0145	0.0102	0.0206	0.0115	0.0026	0.0050	0.0058	0.0031	0.0020	0.0007	0.0000	0.0009	17	A	Others	1-Methyl-6-pyrimidinone	749	1249		L3
95	132	7.968	0.8287	0.0008	0.0008	0.0007	0.0005	0.0000	0.0000	0.0002	0.0000	0.0001	0.0000	0.0001	0.0000	50	A	Amino acid	Serine (2TMS)	777	1268	1265	L1
96	153.1	7.985	0.8102	0.0010	0.0004	0.0006	0.0005	0.0001	0.0000	0.0005	0.0001	0.0001	0.0000	0.0000	0.0001	11	A	Unknown		<700	1270		L4
98	117	8.063	0.8306	0.0293	0.0157	0.0159	0.0195	0.0342	0.0230	0.0281	0.0258	0.0151	0.0141	0.0113	0.0139	2	B	Sugar alcohol	Glycerol (3TMS)	915	1278	1277	L1
105	117	8.314	0.8415	0.0014	0.0010	0.0009	0.0012	0.0003	0.0001	0.0004	0.0002	0.0001	0.0001	0.0001	0.0002	8	A	Amino acid	Threonine (2TMS)	821	1304	1300	L1
109	174	8.434	0.8116	0.0004	0.0012	0.0009	0.0003	0.0000	0.0000	0.0003	0.0000	0.0000	0.0001	0.0000	0.0001	38	A	Amino acid	Glycine (3TMS)	819	1316	1313	L1
118	166	8.855	0.8510	0.0001	0.0001	0.0001	0.0001	0.0000	0.0000	0.0000	0.0000	0.0001	0.0000	0.0000	0.0000	8	A	Others	Pyrrole-2-carboxylic acid (2TMS)	818	1360	1357	L1
121	162	8.927	0.8454	0.0004	0.0003	0.0005	0.0005	0.0001	0.0001	0.0004	0.0000	0.0001	0.0000	0.0000	0.0000	17	A	Unknown		<700	1368		L4
122	188.1	8.939	0.8704	0.0027	0.0043	0.0053	0.0054	0.0032	0.0035	0.0048	0.0044	0.0028	0.0020	0.0000	0.0025	2	A	Amino acid	Alanine (3TMS)	905	1369	1366	L1
123	110	8.994	0.8037	0.0074	0.0031	0.0079	0.0045	0.0005	0.0004	0.0029	0.0002	0.0002	0.0001	0.0000	0.0000	108	A	Unknown		<700	1375		L4
130	143	9.175	0.8111	0.0005	0.0005	0.0003	0.0004	0.0002	0.0001	0.0005	0.0001	0.0002	0.0004	0.0000	0.0003	2	A	Unknown		<700	1393		L4
150	232.2	9.882	0.8658	0.0002	0.0001	0.0002	0.0002	0.0000	0.0000	0.0000	0.0000	0.0000	0.0000	0.0000	0.0000	36	A	Unknown	Pyruvic acid oxime (2TMS) or Aspartic acid (3TMS)	747	1467		L4
155	109.1	10.018	0.8887	0.0002	0.0001	0.0001	0.0001	0.0001	0.0001	0.0001	0.0001	0.0003	0.0003	0.0004	0.0002	4	C	Alcohols	Pentadecanal or Decanediol or Dodecenol	758	1481		L3
159	228.1	10.101	0.8764	0.0003	0.0003	0.0002	0.0003	0.0001	0.0001	0.0002	0.0000	0.0000	0.0000	0.0000	0.0000	14	A	Unknown		<700	1490		L4
165	241.9	10.191	0.8355	0.0001	0.0001	0.0002	0.0001	0.0000	0.0000	0.0001	0.0000	0.0000	0.0000	0.0000	0.0000	114	A	Unknown		<700	1499		L4

The full list is also provided as excel sheet in a separate file.

Table 6 Extracellular metabolites that are correlated (x ≥0.735) with the exponential (A), early stationary (B) or late stationary (C) growth phase of *Phaeocystis pouchetii* AJ01 (n = 4). # - Metabolites are shown as tabulated in Fig. 4B. Vector - correlation coefficient. Factor - phase median maximum/minimum, Phase - correlated growth phase, Ion - model ion used for peak integration, t_R - retention time (min), R.Match - parameter for spectral database comparison (MS Search), I_L - linear retention index, Level - identification level according to Sumner et al. (2007).

#	Ion	t_R	Vector	A1	A2	A3	B1	B2	B3	B4	C1	C2	C3	C4	Factor	Phase	Class	Substance name	R.Match	I_L	r I_L	Level
33	160.0	5.716	0.804	0.0043	0.0015	0.0033	0.0008	0.0003	0.0016	0.0025	0.0000	0.0000	0.0004	0.0000		A	Unknown		<700	**1011**		L4
34	103.1	5.725	0.865	0.0019	0.0034	0.0034	0.0034	0.0039	0.0069	0.0346	0.0000	0.0000	0.0008	0.0000		B	Unknown		<700	**1012**		L4
46	150.2	5.878	0.939	0.0000	0.0000	0.0000	0.0000	0.0000	0.0000	0.0000	0.0003	0.0003	0.0002	0.0002	19	C	Unknown		<700	**1029**		L4
48	152.1	5.928	0.838	0.0473	0.0293	0.0286	0.0000	0.0000	0.0147	0.0000	0.0000	0.0000	0.0239	0.0052		A	Contamination	Hydroxypyridine 1TMS	875	**1034**		L2
54	224.2	6.028	0.809	0.0000	0.0001	0.0000	0.0000	0.0000	0.0000	0.0001	0.0002	0.0001	0.0001	0.0002	30	C	Unknown		<700	**1045**		L4
59	151.2	6.114	0.898	0.0206	0.0361	0.0264	0.0209	0.0267	0.0137	0.0119	0.0000	0.0000	0.0124	0.0000		A	Others	Phenol 1TMS	934	**1054**		L2
61	143.2	6.159	0.825	0.0001	0.0002	0.0002	0.0002	0.0001	0.0003	0.0005	0.0005	0.0004	0.0004	0.0004	3	C	Unknown		<700	**1059**		L4
63	260.2	6.201	0.822	0.0000	0.0000	0.0000	0.0000	0.0001	0.0000	0.0000	0.0002	0.0003	0.0000	0.0002		C	Unknown		<700	**1064**		L4
64	148.1	6.219	0.899	0.0000	0.0013	0.0002	0.0013	0.0016	0.0033	0.0037	0.0000	0.0010	0.0000	0.0000		B	Carboxylic acid	Glycolic acid 2TMS	907	**1066**	1072	L1
71	148.1	6.331	0.974	0.0005	0.0003	0.0006	0.0006	0.0005	0.0008	0.0013	0.0000	0.0000	0.0001	0.0000		A/B	Carboxylic acid	Pyruvic acid 2TMS	826	**1078**	1086	L1
74	134.2	6.373	0.790	0.0023	0.0001	0.0004	0.0011	0.0000	0.0000	0.0022	0.0044	0.0029	0.0028	0.0049	9	C	Unknown		<700	**1083**		L4
80	101.1	6.481	0.864	0.0267	0.0407	0.0293	0.0166	0.0188	0.0000	0.0000	0.0001	0.0196	0.0313	0.0100	4	A	Saccharide	Glyceraldehyde Meox 2TMS	723	**1094**		L3
82	142.1	6.524	0.809	0.0157	0.0245	0.0157	0.0093	0.0114	0.0000	0.0015	0.0047	0.0153	0.0237	0.0106	3	A	Saccharide	Glyceraldehyde Meox 2TMS	725	**1099**		L3
83	140.0	6.556	0.916	0.0014	0.0005	0.0000	0.0000	0.0001	0.0000	0.0000	0.0064	0.0051	0.0020	0.0064		C	Unknown		<700	**1102**		L4
87	110.0	6.602	0.829	0.0001	0.0001	0.0001	0.0001	0.0001	0.0000	0.0004	0.0000	0.0000	0.0000	0.0000		B	Unknown		<700	**1107**		L4
95	100.1	6.695	0.807	0.0016	0.0016	0.0013	0.0012	0.0000	0.0000	0.0000	0.0006	0.0001	0.0006	0.0007	68	A	Unknown		<700	**1118**		L4
98	168.2	6.756	0.771	0.0000	0.0000	0.0000	0.0000	0.0001	0.0000	0.0009	0.0005	0.0005	0.0002	0.0006		C	Unknown		<700	**1124**		L4
101	156.1	6.814	0.788	0.0020	0.0007	0.0037	0.0023	0.0010	0.0025	0.0023	0.0000	0.0000	0.0007	0.0000		A/B	Carboxylic acid	Alpha-Ketoglutaric acid Meox 2TMS	722	**1131**		L3
102	133.0	6.832	0.859	0.0007	0.0059	0.0030	0.0000	0.0006	0.0018	0.0000	0.0066	0.0060	0.0048	0.0073	23	C	Carboxylic acid	Oxalic acid 2TMS	748	**1133**		L3
104	116.0	6.846	0.835	0.0017	0.0007	0.0012	0.0001	0.0000	0.0000	0.0004	0.0000	0.0000	0.0000	0.0000		A	Unknown		<700	**1134**		L4

The full list is also provided as excel sheet in a separate file.

Table 7 Normalized abundance (peak area/peak sum) of intracellular metabolites of *Phaeocystis pouchetii* laboratory cultures (n = 4) in natural plankton communities sampled at station 1-6 during the PHAEONIGMA cruise (3 depths with n = 3). # - Metabolites are shown as tabulated in Fig. 3B and 4B (n.e. - not extracted). Phase - correlated growth phase (exponential phase (A), early stationary phase (B), late stationary phase (C), not regulated (-), unknown (?)). Cluster - respective cluster according to Supplementary Figure 3. Substance name - Metabolite name indicating MS Search match via "?" and modification of functional groups (TMS - trimethylsilyl, Meox - methoxyamine, Me - methyl). Level - identification level according to Sumner et al. (2007).

Lab data		Field data		Metabolite identification			Station 1								Station 2							
#	Phase	#	Cluster	Class	Substance name	Level	1a	1b	1c	2a	2b	2c	3a	3b	1a	1b	2a	2b	2c	3a	3b	3c
n.e.	?	286	1b	Alcohol	1-Octadecanol (1TMS)	L1	0.000505	0.000333	0.004448	0.000692	0.000722	0.001178	0.003155	0.000000	0.000460	0.002750	0.000327	0.000000	0.002313	0.012974	0.001577	0.000531
286	B	240	1b	Fatty acid	C16:0 (Me)	L1	0.000711	0.000462	0.002043	0.000497	0.000395	0.001473	0.003162	0.000023	0.000090	0.001502	0.000297	0.003973	0.003402	0.007533	0.000617	0.000172
n.e.	?	281	1b	Fatty acid	C18:0 (Me)	L1	0.000121	0.000018	0.000120	0.000037	0.000036	0.000041	0.000415	0.000000	0.000007	0.000154	0.000046	0.000746	0.000654	0.001395	0.000071	0.000049
333	-	279	1b	Fatty acid	C18:1 (Me)	L1	0.000011	0.000004	0.000112	0.000011	0.000009	0.000000	0.000111	0.000000	0.000004	0.000049	0.000013	0.000131	0.000094	0.000192	0.000023	0.000009
327	B/C	274	1a	Fatty acid	C18:4n-3 (Me)	L1	0.000504	0.000186	0.001930	0.000314	0.000343	0.001639	0.002167	0.000088	0.000018	0.001082	0.000163	0.001490	0.001584	0.002454	0.000393	0.000036
395	B/C	339	1a	Fatty acid	C22:6n-3 (Me)	L1	0.000190	0.000030	0.000316	0.000148	0.000193	0.000840	0.001287	0.000051	0.000000	0.000452	0.000089	0.000579	0.000597	0.000953	0.000213	0.000000
n.e.	?	386	1a	FA derivative	1-C18:0-glycerol (2TMS)	L1	0.000359	0.000000	0.001088	0.000381	0.000356	0.001845	0.001256	0.000000	0.000051	0.001425	0.000123	0.000727	0.000460	0.001288	0.000600	0.000000
473	C	416	1a	Sterol	24-Methylcholesta-5,22-dien-3beta-ol (1TMS)	L1	0.000263	0.000051	0.001248	0.000751	0.001013	0.003087	0.003836	0.000006	0.000191	0.003444	0.000199	0.001271	0.001519	0.002346	0.000810	0.000004
284	A/B	239	1a	Sugar alcohol	Mannitol (6TMS)	L1	0.000606	0.002192	0.000000	0.001289	0.001558	0.003310	0.002578	0.000000	0.000899	0.005292	0.000546	0.000000	0.003534	0.000000	0.001715	0.000000
311	B	262/3	1a	Sugar alcohol	Scyllo-Inositol (6TMS)	L1	0.000288	0.001364	0.000000	0.001667	0.001769	0.004872	0.005703	0.000000	0.000952	0.005263	0.000347	0.002599	0.000000	0.007715	0.001710	0.000000
n.e.	?	72	1b	Unknown	-	L4	0.000000	0.000000	0.000000	0.000005	0.000005	0.000000	0.000000	0.000000	0.000007	0.000046	0.000000	0.000000	0.000000	0.000000	0.000000	0.000000
172/173	-	147	1b	Unknown	-	L4	0.000628	0.001118	0.000901	0.000685	0.000717	0.001991	0.001860	0.000129	0.000302	0.003868	0.000164	0.000985	0.001475	0.001327	0.000882	0.000201
n.e.	?	338	1b	Unknown	-	L4	0.000080	0.000000	0.000111	0.000059	0.000056	0.000221	0.000194	0.000000	0.000025	0.000514	0.000024	0.000284	0.000401	0.000280	0.000115	0.000009
253	-	215	1a	Unknown	? Skel_Media_C168/205	L4	0.000910	0.001304	0.001893	0.001593	0.001608	0.003566	0.004956	0.000000	0.000581	0.008078	0.000476	0.000000	0.002332	0.002969	0.002369	0.000300
n.e.	?	97	1b	Unknown	?? Skel_Media_C086	L4	0.000762	0.001254	0.002352	0.001210	0.001257	0.001776	0.003494	0.000001	0.000002	0.005586	0.000402	0.001718	0.002768	0.004111	0.001403	0.000004
314	-	261	2a	Fatty acid	C16:1 (1TMS)	L1	0.000000	0.000000	0.000000	0.000434	0.000811	0.000000	0.002842	0.000000	0.001298	0.002348	0.000455	0.000000	0.000000	0.001613	0.002083	0.000202
332	-	278	2a	Fatty acid	? C18:1/C18:3 (Me)	L2	0.000000	0.000000	0.000000	0.000082	0.000087	0.000000	0.000299	0.000000	0.000059	0.000112	0.000037	0.000000	0.000000	0.000058	0.000105	0.000000
383	-	330	2a	FA derivative	1-C14:0-glycerol (2TMS)	L1	0.000318	0.000510	0.002677	0.001450	0.001080	0.003698	0.003832	0.000000	0.000200	0.001281	0.000182	0.000480	0.000185	0.001297	0.000725	0.000057
410	B/C	358	2a	FA derivative	1-C16:0-glycerol (2TMS)	L1	0.000707	0.000213	0.003053	0.001625	0.001302	0.006616	0.004368	0.000000	0.000230	0.002733	0.000285	0.000697	0.000287	0.002285	0.001125	0.000005
403	A	351	2a	Saccharide	? Galactosylglycerol (6TMS)/Glucopyranose (5TMS)	L3	0.000213	0.000021	0.002079	0.000241	0.000456	0.005191	0.000462	0.000002	0.000038	0.000952	0.000049	0.000269	0.000104	0.000298	0.000190	0.000000
281	-	235	2a	Saccharide	Hexose: ? Glucose/Galactose (Meox 5TMS)	L3	0.016893	0.019588	0.053802	0.011080	0.013960	0.033822	0.012287	0.000000	0.000016	0.028379	0.003813	0.000000	0.000000	0.000034	0.008306	0.000000
413	B/C	367/8	2a	Saccharide	?? Disaccharide	L3	0.000124	0.000017	0.000581	0.000242	0.000387	0.002652	0.000642	0.000002	0.000031	0.000905	0.000041	0.000228	0.000129	0.000462	0.000161	0.000000
180	-	162	2a	Saccharide	?? Monosaccharide	L3	0.000417	0.001326	0.011196	0.001536	0.001975	0.000000	0.002418	0.000000	0.001507	0.000000	0.001074	0.000000	0.000000	0.000512	0.001789	0.000177
429	C	381	2a	Saccharide	Maltose (Meox TMS)	L1	0.000089	0.000000	0.001595	0.000171	0.000379	0.003112	0.000254	0.000000	0.000026	0.000502	0.000020	0.000070	0.000050	0.000155	0.000074	0.000000
205	B/C	188	2a	Saccharide	Ribose (Meox 4TMS)	L1	0.000249	0.000423	0.000095	0.000335	0.000336	0.000000	0.000653	0.000000	0.000067	0.000000	0.000140	0.000000	0.000000	0.000000	0.000236	0.000000
341	C	288	2a	Terpene	Phytol (1TMS)	L1	0.001412	0.000825	0.007134	0.003608	0.003183	0.006151	0.014572	0.000000	0.001335	0.008525	0.001575	0.003081	0.003726	0.009563	0.003543	0.000486
n.e.	?	151	2a	Unknown	-	L4	0.000058	0.000092	0.000307	0.000138	0.000118	0.000154	0.000173	0.000016	0.000031	0.000385	0.000032	0.000000	0.000120	0.000042	0.000071	0.000007

The full list is also provided as excel sheet in a separate file.

Figure 1 Concentrations of nitrite (A), nitrate (B) and phosphate (C) during logistic growth of *Phaeocystis pouchetii* AJ01. Average ± SD concentrations within the algal cultures (n = 4) and one medium control (open circles) as measured by spectrophotometry (black filled circles) or ICPMS (grey filled circles) are shown. Arrows indicate metabolite sampling.

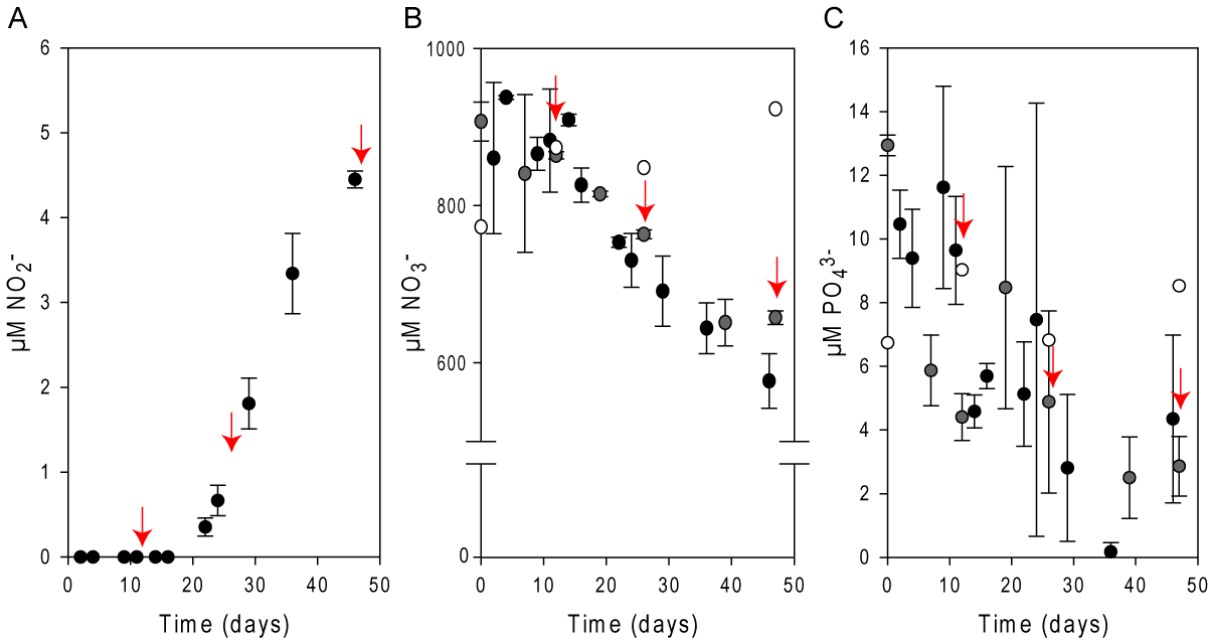

Figure 2 Mass spectral and retention time characterization of unknown quinic acid derivative detected in the endometabolome of *Phaeocystis pouchetii* AJ correlating with the exponential growth phase. A) Mass spectra of quinic acid reference standard and the unknown derivative. Insert shows schematic formation of the typical indole fragment with *m*/*z* = 202. as well as of representative algal extract (EIC, *m*/*z* = 202). Characteristic fragments are indicated as reported by [1] (Molnár-Perl et al. 1998) and [2] (Fuchs and Spiteller 1996). B) Extracted ion chromatograms (EICs) of quinic acid reference standard and representative algal extract (*m*/*z* = 345) scaled to retention time indices.

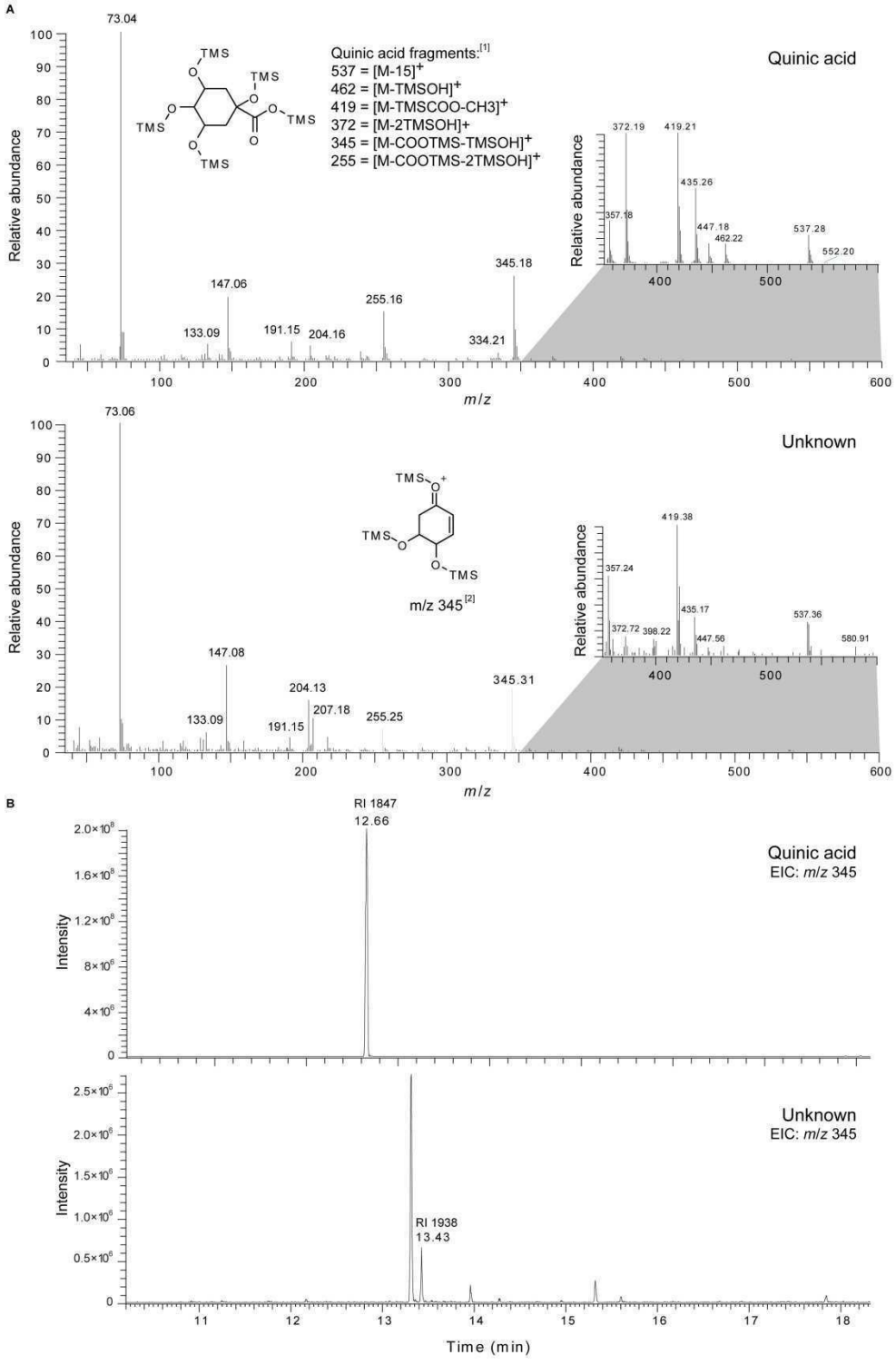

Figure 3 Mass spectral and retention time characterization of unknown indole derivative detected in the exometabolome of *Phaeocystis pouchetii* AJ correlating with late stationary growth phase. A) Composite chromatogram of five measurements including reference standards of indole-3-ethanol, -acetic acid, -propanoic acid and -butanoic acid each depicted with its chemical structure, as well as of representative algal extract (EIC, *m*/*z* = 202). B) Extracted mass spectrum of unknown indole derivative. Insert shows schematic formation of the typical indole fragment with *m*/*z* = 202. [1] Gathungu et al. (2014).

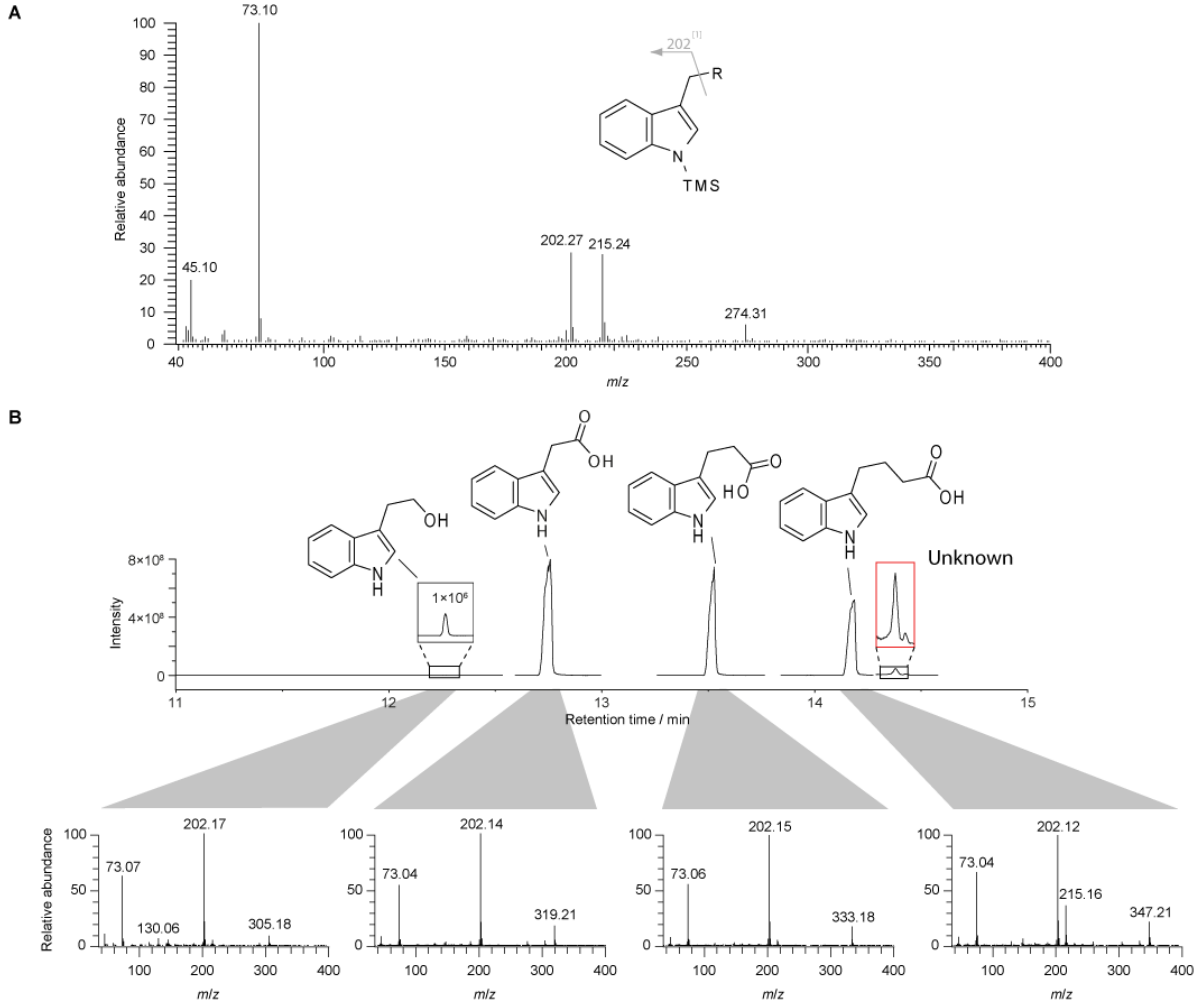

Figure 4 Heat map of endometabolites (peak area/peak sum) averaged per cruise station (class 1-7) and sorted by hierarchical cluster analysis using Pearson distance measure and Ward cluster algorithm.

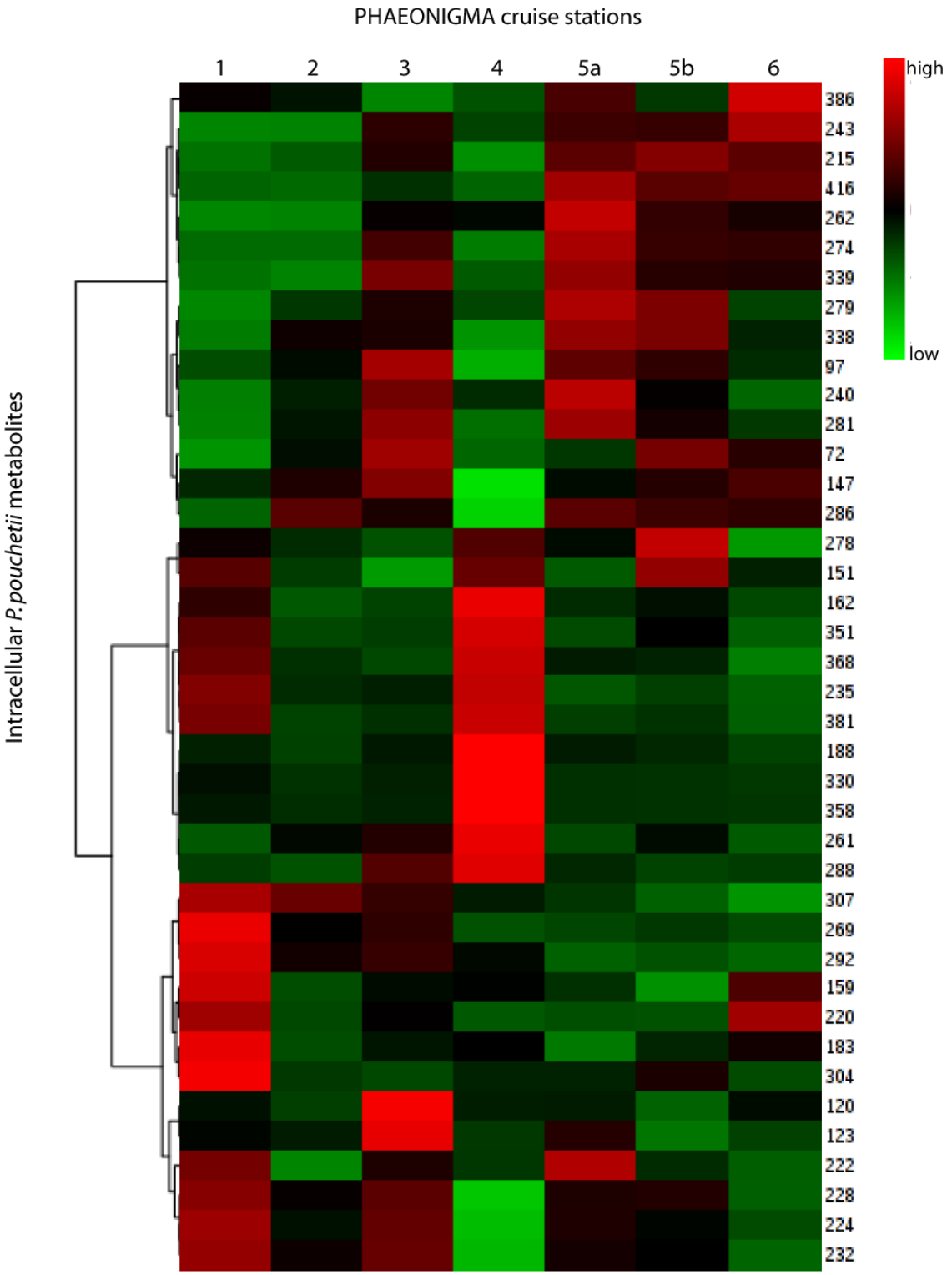

References

Fuchs, C., and G. Spiteller. 1996. Rapid and easy identification of isomers of coumaroyl- and caffeoyl-D-quinic acid by gas chromatography/mass spectrometry. Journal of Mass Spectrometry 31: 602-608.

Gathungu, R. M. and others 2014. Identification of metabolites from liquid chromatography-coulometric array detection profiling: gas chromatography-mass spectrometry and refractionation provide essential information orthogonal to LC-MS/microNMR. Anal Biochem 454: 23-32.

Molnár-Perl, I., A. Vasanits, and K. Horváth. 1998. Simultaneous GC-MS quantitation of phosphoric, aliphatic and aromatic carboxylic acids, proline and hydroxymethylfurfurol as their trimethylsilyl derivatives: in model solutions II. Chromatographia 48: 111-119.

Sumner, L. W. and others 2007. Proposed minimum reporting standards for chemical analysis. Metabolomics 3: 211-221.

Supporting information of Publication P4:

SI 1a

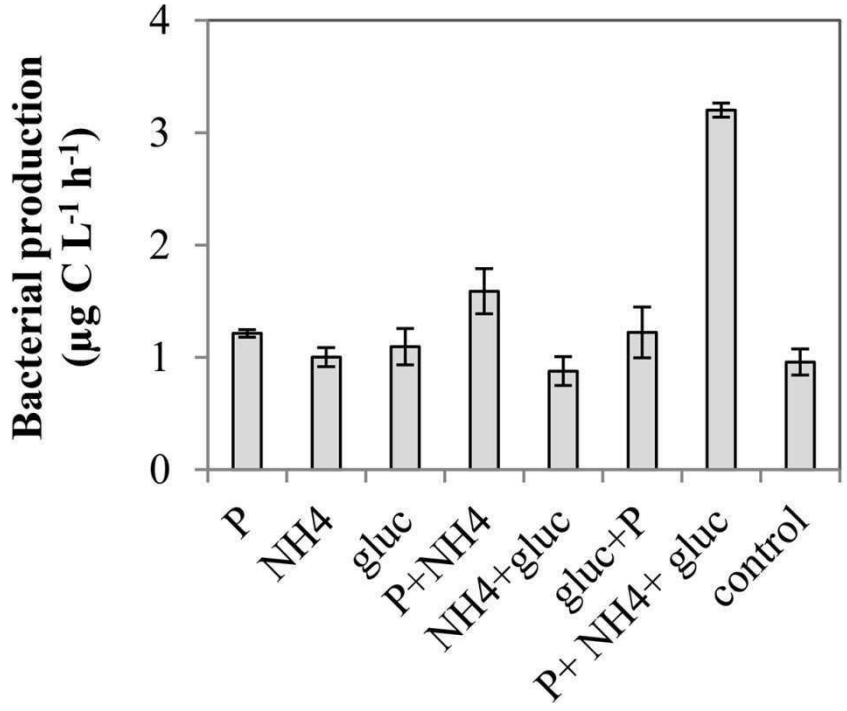

SI 1b

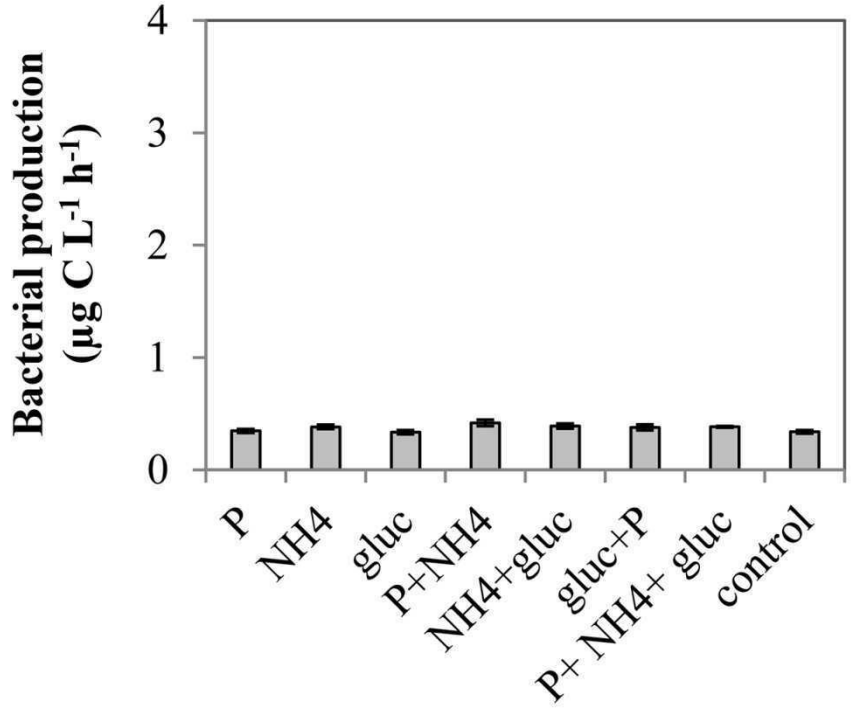

SI Fig. 2a

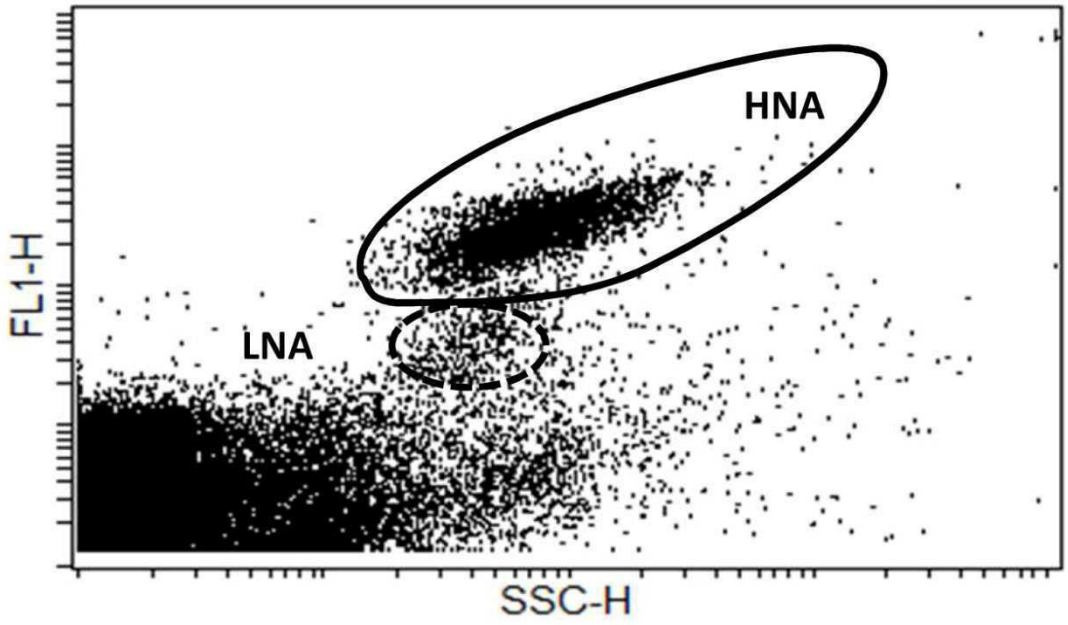

SI Fig. 2b

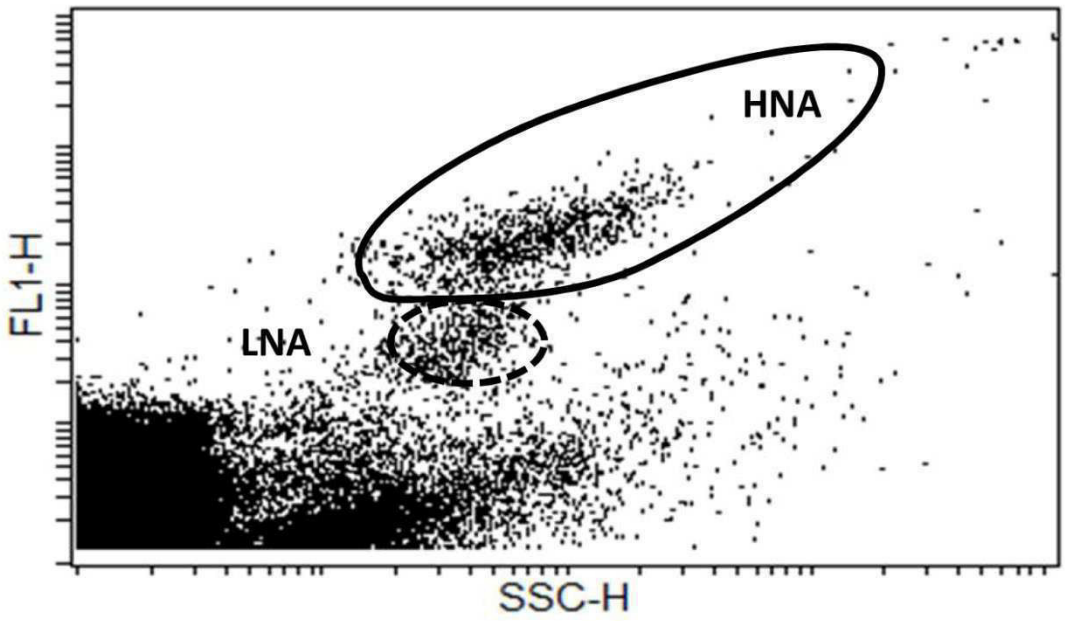

SI 3

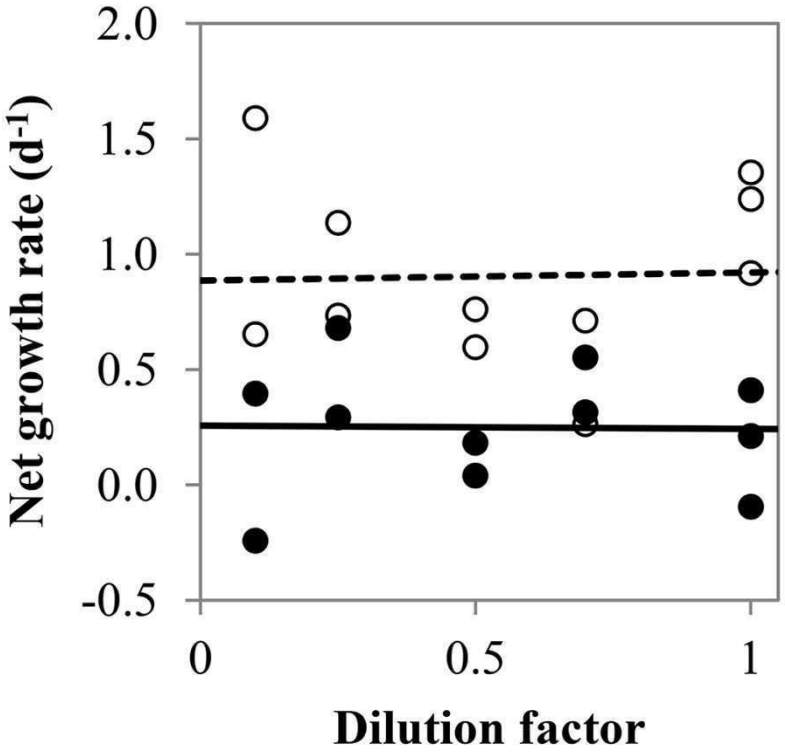

Supporting information of Publication P5:

For full scale images the reader is referred to the electronic version of this publication or thesis.

Supplementary Information

A fast and direct liquid chromatography - mass spectrometry method to detect and quantify polyunsaturated aldehydes and polar oxylipins in diatoms

Constanze Kuhlisch[1], Michael Deicke[1], Nico Ueberschaar[1], Thomas Wichard[1], Georg Pohnert[1]

[1] Institute for Inorganic and Analytical Chemistry, Friedrich Schiller University Jena, Lessingstraße 8, 07743 Jena, Germany

* corresponding author, e-mail: georg.pohnert@uni-jena.de

S1. UHPLC-HRMS spectrum of A) 2,4,7-octatrienal (**5**, *m*/*z* = 123.08044, t_R = 1.35 min) and B) 2,4,7-decatrienal (**6**, *m*/*z* = 151.11174, t_R = 2.70 min) as obtained in full scan mode of a *Thalassiosira rotula* RCC776 extract. $[M + H]^+$ labelled with the according *m*/*z* value.

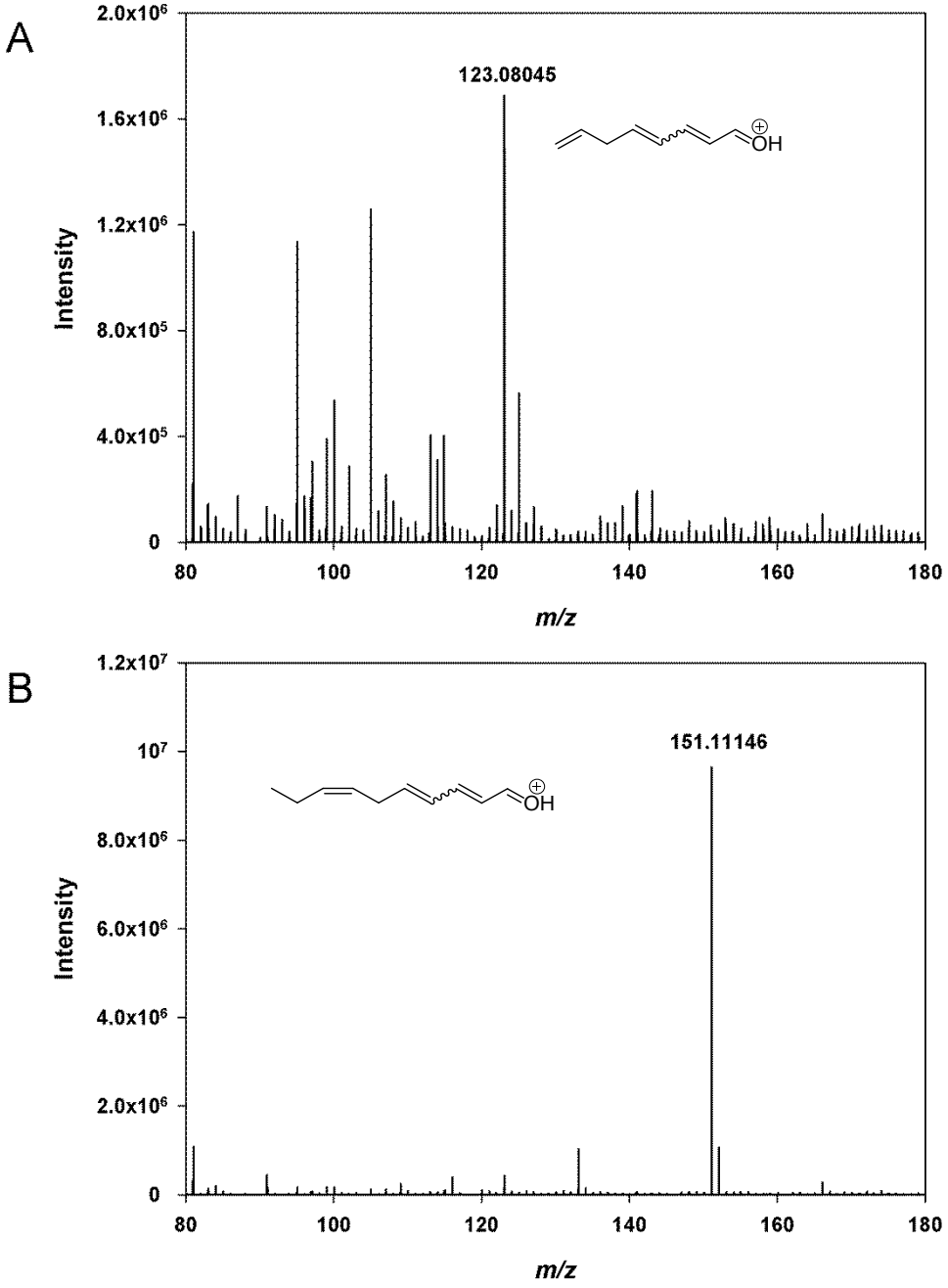

S2. MS/MS fragmentation of 2*E*,4*Z*,7*Z*-decatrienal (**6**).

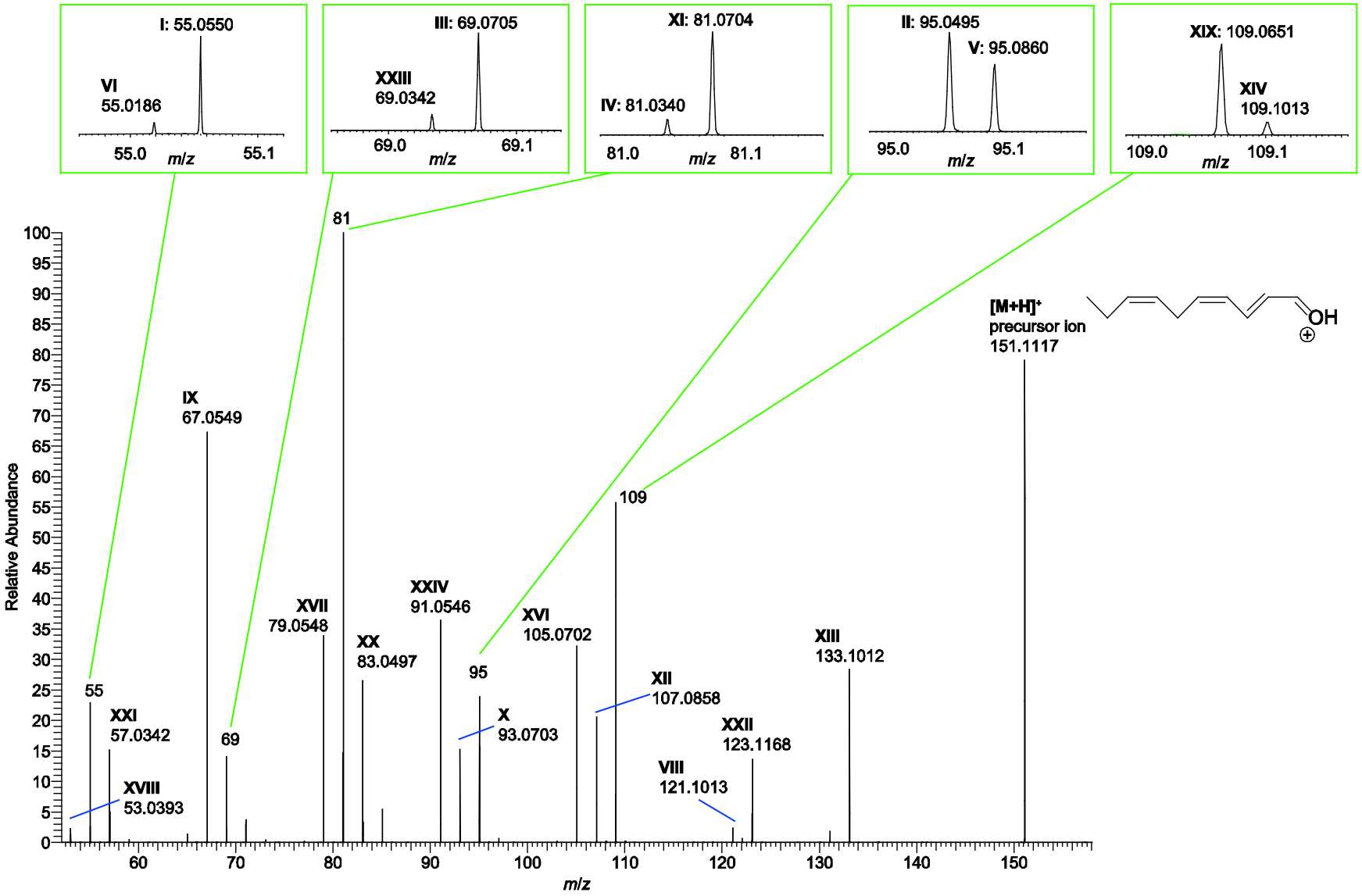

S3. Fragmentation tree of 2*E*,4*Z*,7*Z*-decatrienal (**6**) according to the spectrum **S2**.

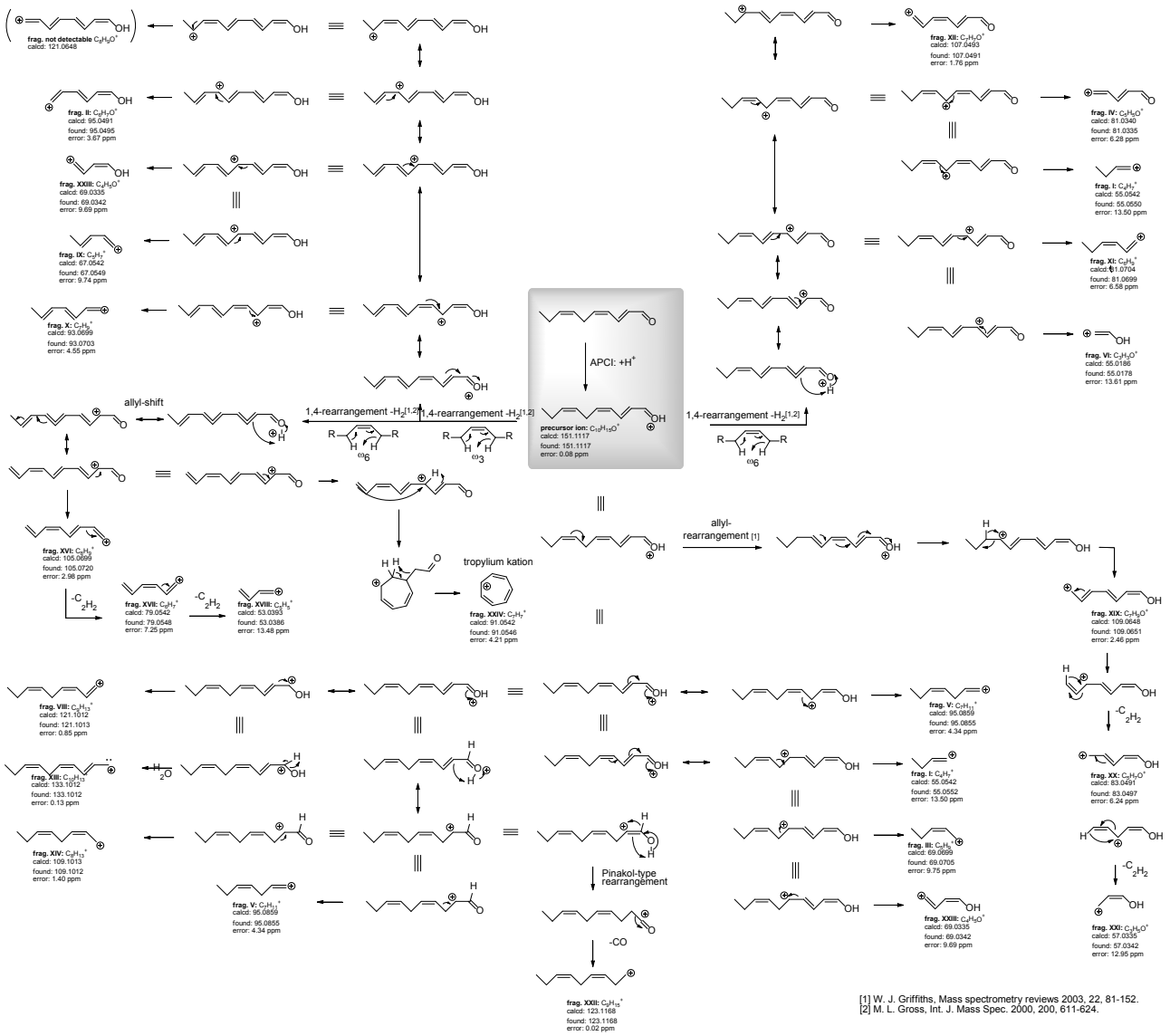

[1] W. J. Griffiths, Mass spectrometry reviews 2003, 22, 81-152.
[2] M. L. Gross, Int. J. Mass Spec. 2000, 200, 611-624.

S4. Fragmentation of (5*Z*,8*Z*)-10-hydroxydeca-5,8-dienoic acid (**7**).

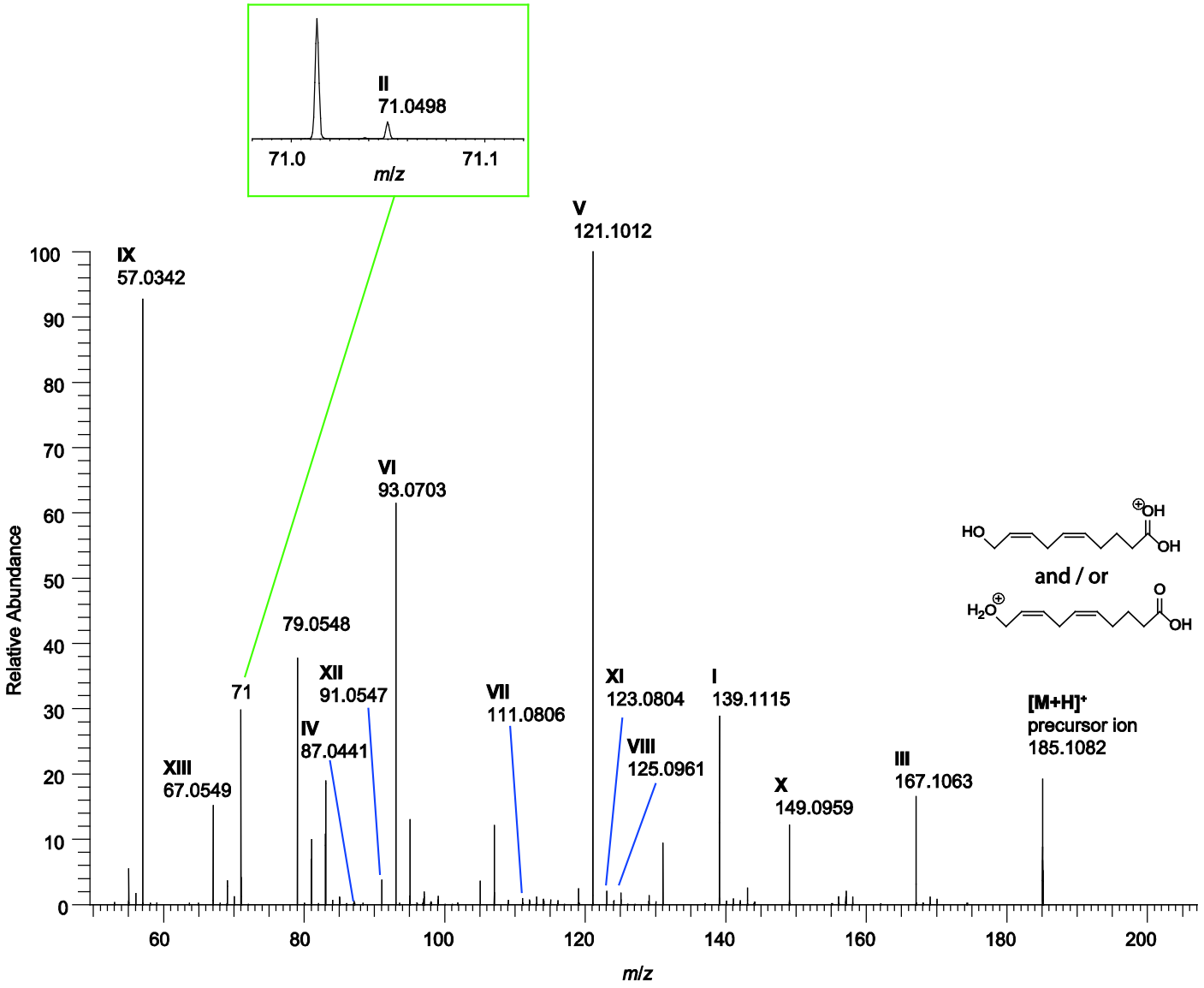

S5. Fragmentation tree of (5*Z*,8*Z*)-10-hydroxydeca-5,8-dienoic acid (**7**) according to the spectrum **S4**.

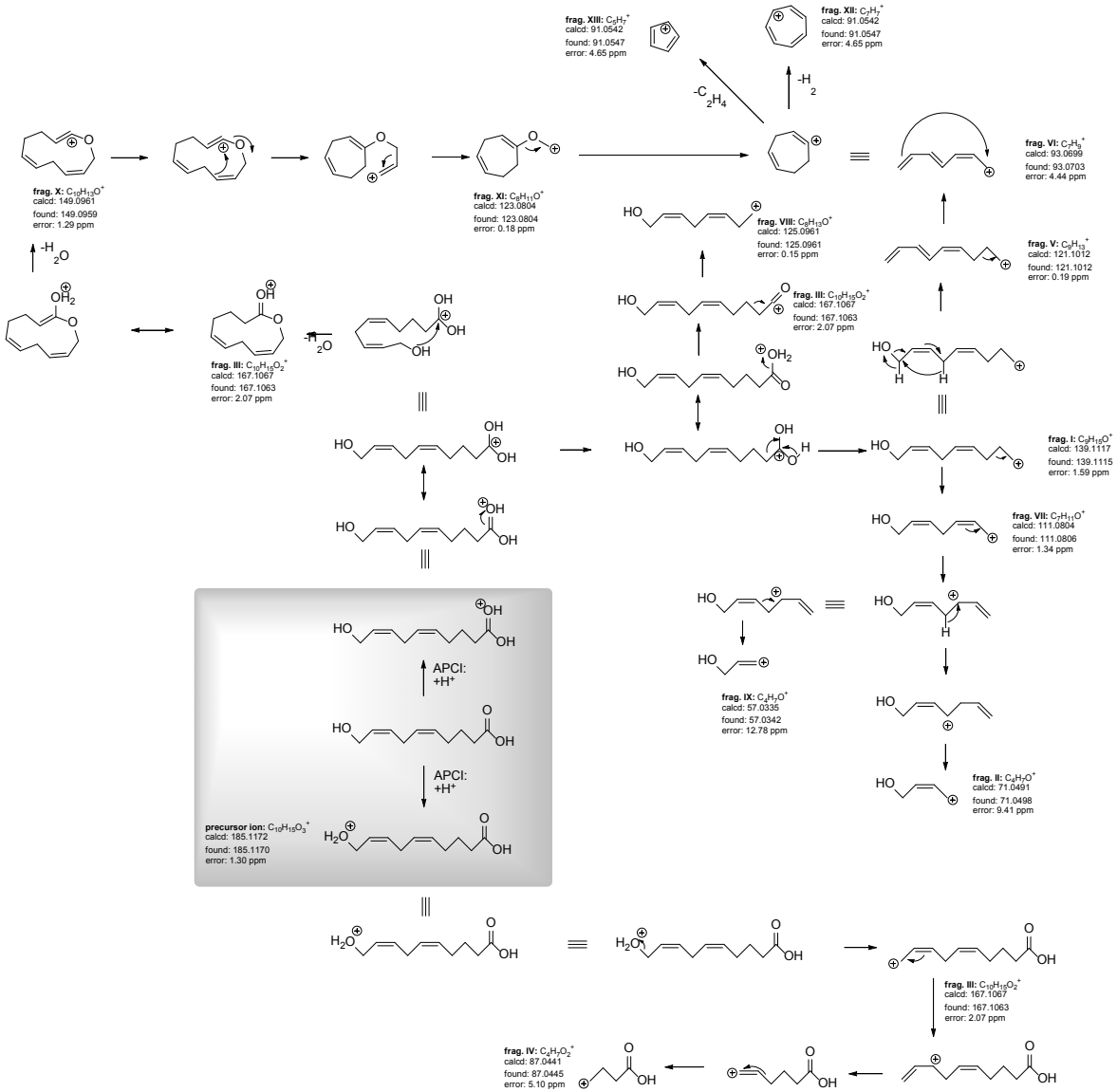

S6. Fragmentation of (5*Z*,8*Z*)-10-oxodeca-5,8-dienoic acid (**8**).

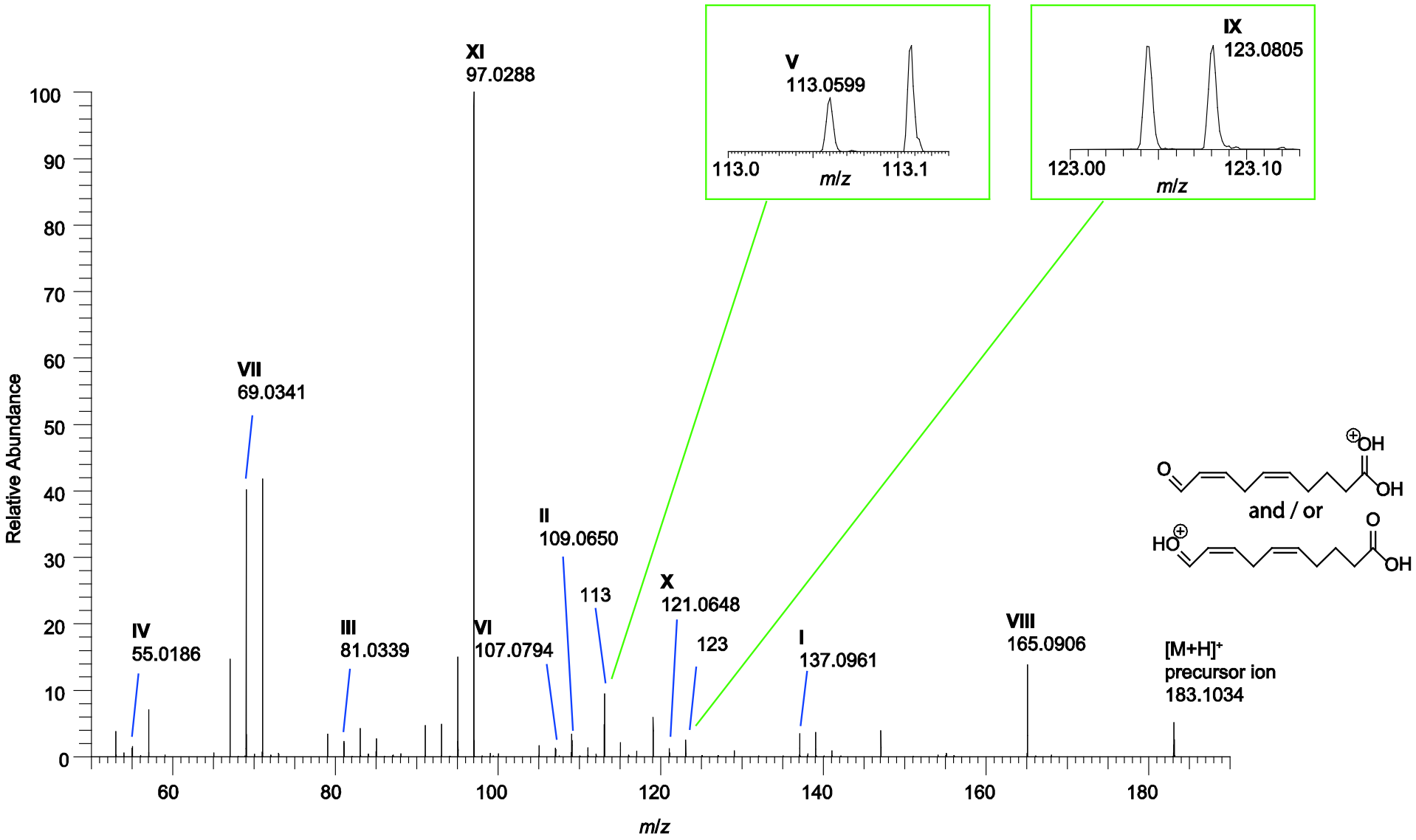

S7. Fragmentation tree of (5*Z*,8*Z*)-10-oxodeca-5,8-dienoic acid (**8**) according to the spectrum **S6**.

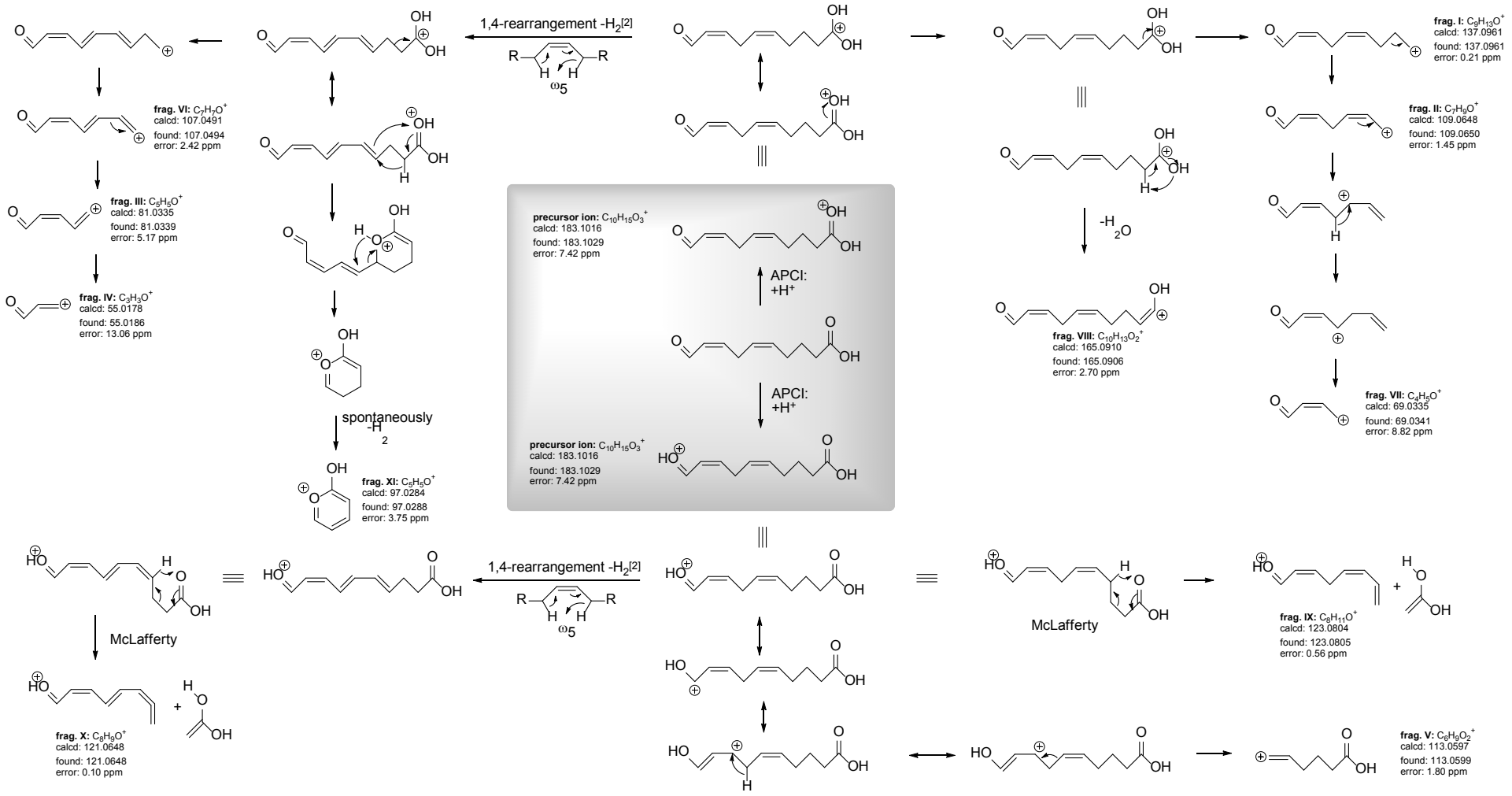

[2] M. L. Gross, *Int. J. Mass Spec.* **2000**, *200*, 611-624.

S8. Re-measurement of PUAs in algal extracts (MeOH:H_2O, 1:2; *v*:*v*) after 113 days of storage at -20 °C. Extracts were derived from *Thalassiosira rotula* RCC776 (n = 3). Peak areas were obtained in full scan mode using *m*/*z* values as listed in **Table 3**. Average (± S.D.) peak area ratios of analyte to internal standard (IS; vanillin) are depicted.

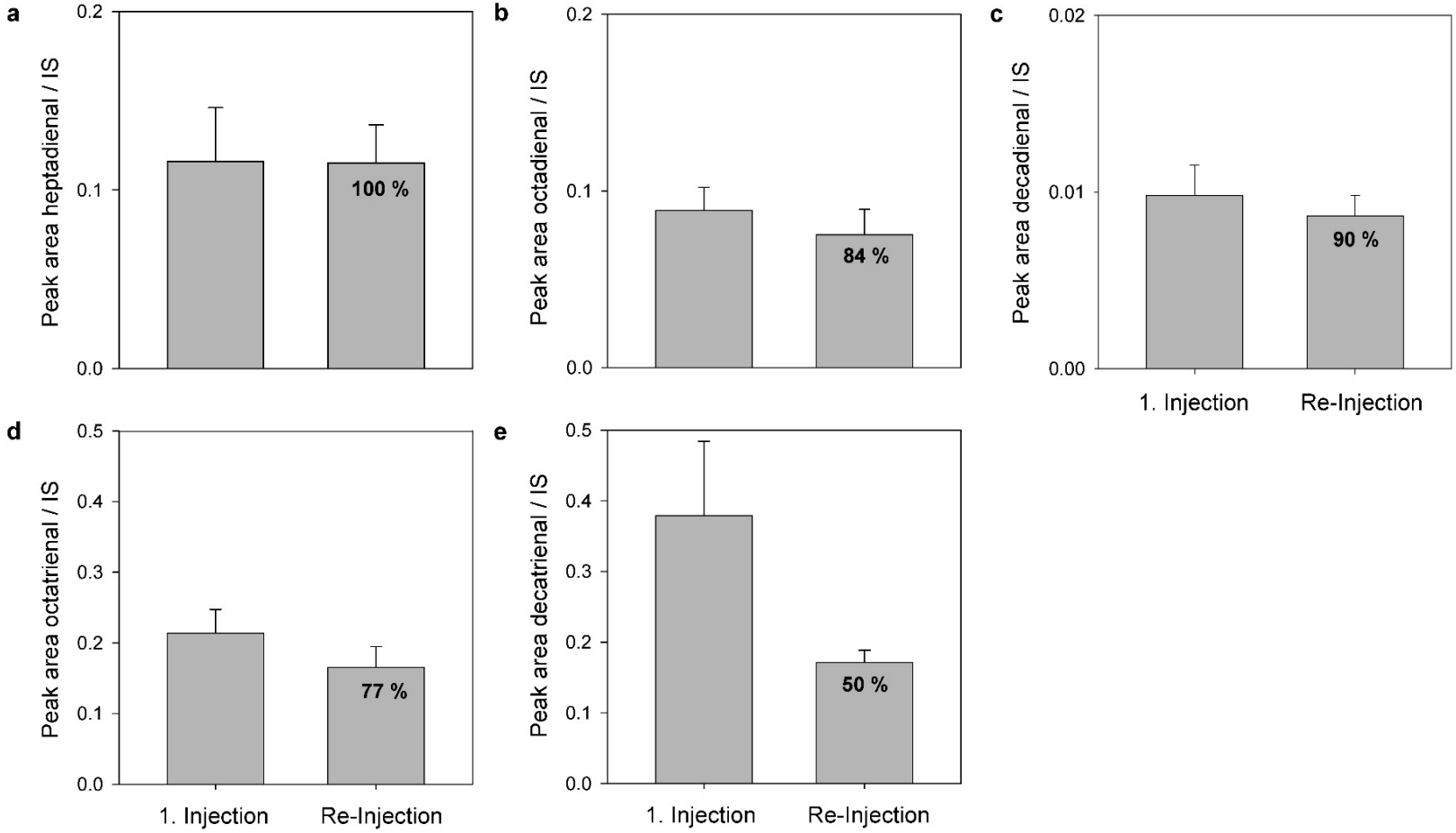

Acknowledgements

An erster Stelle möchte ich mich bei Dir, Georg, dafür bedanken, dass Du mich 2013 in Deiner Gruppe aufgenommen hast, und mir den Freiraum, die instrumentellen Möglichkeiten, und die fachliche Betreuung gegeben hast, um diese Dissertation zu erstellen. Die Entscheidung, als Meeresbiologin in die instrumentelle Analytik gegangen zu sein, werde ich nie bereuen, und das liegt nicht zuletzt an Deiner Begeisterung für die chemische Ökologie, die Natur und Deinen fesselnden Vorträgen! Dir, Severin, möchte ich dafür danken, dass Du mit Interesse den Verlauf meiner Arbeit in den letzten Jahre verfolgt, begutachtet, und kommentiert hast. Und Dir, Thomas, möchte ich für die vielen Gespräche, Dispute und Diskussionen im Flur oder Pausenraum danken, welche sich über wissenschaftliche Streitfragen hinweg auch auf die ein oder andere Lebensfrage erstreckten.

Further, I would like to thank all co-operation partners for the shared time and work. It was a pleasure to see how fruitful it is to combine different knowledge and experience to get the bigger picture. Dir, Jule, möchte ich für die gemeinsame Zeit im großen Labor danken, für all die langen Abende vor Filtrationsanlagen, Abzügen und der Diva, sei es im TO oder auf einem Schiff, dafür, mit dir über die Ökologie von *Phaeocystis* philosophieren zu können, fürs Anpacken, für die Kaffeepausen, und unsere Hütten-Ski-Tour! Ob bei GC-FID, GC-Quadrupole, GCT oder meinem Fahrrad - wenn geschraubt und repariert werden musste, warst Du nicht weit, und hast mir mit Rat und Tat zur Seite gestanden - danke Micha! Auch für Deine vielen, vielen Fragen zu Arbeit, Zukunft, Leben oder dem Gebrauch von Doppelbettdecken! Dir, Nico, möchte ich dafür danken, dass Du der Herzblutchemiker "gegenüber" warst, für die Inspiration, was Glasgeräte(konstruktionen) und den lockeren Umgang mit Strukturformeln und Fragmentierungsbäume angeht, sowie für die Eppi-Geschenke im Papierkorb und jeden einzelnen schlechten Witz. I would like to thank all the people from the PHAEONIGMA-Cruise and especially Jens Nejstgaard, Aud Larsen, and Bernadette Pree for their warm incorporation into the research team. Further, I would like to thank Hans Christian Eilertsen for hosting me in his group in spring 2014 and facilitating the cruise to Porsangerfjorden, as well as Gunilla Eriksen, Richard Ingebrigtsen and Martina Uradnikova for answering patient all my questions and giving me a warm welcome in the cold north. Besonderen Einen großen Dank möchte ich an Steffi Gäbler-Schwarz richten! Durch dich und mit dir war die Zeit am AWI eine der intensivsten, bereicherndsten, und erfüllendsten Phasen meiner Doktorandenzeit, nicht zu vergessen, dass Du mir währen der Zeit in Bremerhaven auch Freundin und Familie warst. I would like to thank Anya Waite for hosting me, Helga Mehl und Erika

Allhusen für die Lösung der vielen kleinen Probleme im Laboralltag, und Ulf Karsten für den entscheidenden Hinweis in Stralsund.

Was wäre diese Arbeit ohne die Arbeitsgruppe gewesen? Ihr ward Kollegen, Lehrer, und Freunde, die fehlende Hand, ehrliche Kritiker, tägliche Inspiration und Motivation. Hannes - dir danke ich neben all der Unterstützung im Labor vor allem für die stete Stählung meiner Nerven! Björn - dir danke ich für meine erste chemische Synthese, morgendliche Abgangsgruppen und die gedanklichen Exkurse. Euch - Andrea, Caro, Anett, Michi, Stefanie, Tini und Katha G. - möchte ich dafür danken, dass ich euch ein Stück in eurem Leben begleiten durfte, mit all seinen Hochs und Tiefs, Grill-, Polter- und Pullerparties, und ich hoffe sehr, dass davon noch einige folgen werden. Danke Kathleen, dass Du so flexibel, belastbar, kreativ, innovativ, begeisterungsfähig, teamfähig und… äh… kreativ bist, und mit Deiner Geselligkeit zur Verbesserung des Betriebsklimas beigetragen hast! Emilio - dir danke ich für die gemeinsame Hinterfragung von Metabolomics, Sprache und Motorik, und dir, Nils, für diese wunderbare Kombination aus Präzision und Ironie. Danke Raphael für Dein unbändiges Interesse, die tiefgründigen Gespräche, und Deinen Wortwitz, and you, Karen, for flying late at night together to the ocean. Thanks Gianmaria for asking the right questions and spreading happiness and relaxation, dank dir, Tim, für jeden einzelnen fachlichen Schlagabtausch, dir, Frieder, dafür, dass Du auch ein Faible für Pfeifen hast, und dir, Marino, für unser kleines Syntheseprojekt. Mein Dank geht auch an JJ für all die wertvollen Lebensweisheiten, an Michel für seine soziale Ader, und an Tino für seine Einführung in die Welt der Diva. Der Kontroll-Lese-Task Force Kathleen und Nils sei dafür gedankt, alles außer diesen zwei Seiten gegengelesen zu haben. KuK danke ich für zwei Seiten weniger Wochenende! And finally I thank every single person that supported the transcontinental printing und submission process.

Zu allerletzt gilt mein Dank all denen, welche mich in den letzten Jahren auf meinem Weg über kurz oder lang begleitet haben, und mit dazu beigetragen haben, dass es wunderbar aufregende, erlebnisreiche und reichhaltige Jahre waren, allen voran meinen Eltern für all die Freiheit, meinem Bruder für seine Liebe zur Natur, und Herrn Sperfeld für den entscheidenden Hinweis vor 5 Jahren und seine Gelassenheit!

Der JSMC danke ich für die finanzielle Unterstützung, all the other fellows for the inspiration during symposia, retreats and collogues, the MiCom team 2014 for organizing together this event, und Katja Präfcke für ihr Engagement.

Curriculum vitae

The *curriculum vitae* is available in the printed version of this thesis.

Declarations

Einverständniserklärung des Betreuers

Ich bin mit der Abfassung der Dissertation als publikationsbasiert, d.h. kumulativ, einverstanden und bestätige die vorstehenden Angaben. Eine entsprechend begründete Befürwortung mit Angabe des wissenschaftlichen Anteils des Doktoranden/ der Doktorandin an den verwendeten Publikationen werde ich parallel an den Rat der Fakultät der Chemisch-Geowissenschaftlichen Fakultät richten.

Prof. Dr. Georg Pohnert, Jena, den _____ _____

Selbstständigkeitserklärung

Hiermit erkläre ich, dass ich die vorliegende Arbeit selbstständig und unter Verwendung der angegebenen Hilfsmittel, persönlichen Mitteilungen, und Quellen angefertigt habe.

Constanze Kuhlisch, Jena, den _____ _____

Erklärung zu den Eigenanteilen der Promovendin sowie der weiteren Doktoranden/Doktorandinnen als Koautoren an den Publikationen und Zweitpublikationsrechten bei einer kumulativen Dissertation

Für alle in dieser kumulativen Dissertation verwendeten Manuskripte liegen die notwendigen Genehmigungen der Verlage ("Reprint permissions") für die Zweitpublikation vor.

Die Koautoren der in dieser kumulativen Dissertation verwendeten Manuskripte sind sowohl über die Nutzung, als auch über die unten angegebenen Eigenanteile informiert und stimmen dem zu.

Constanze Kuhlisch, Jena, den _____ _____

The following section contains a list of the individual authors' contributions to the publications reprinted in this thesis. Publication equivalents of contributing PhD students as coauthors are given according to the implementing provision of the doctoral regulations of the Faculty of Chemistry and Earth Sciences of the Friedrich Schiller University Jena.

Publication 1

Constanze Kuhlisch[1], Georg Pohnert[2], "Metabolomics in chemical ecology", *Nat. Prod. Rep.*, **2015**, 32, 937-955.

Author	1	2
Development of concept	x	x
Literature research	x	-
Preparation of the manuscript	x	x
Correction of the manuscript	-	x
Proposed publication equivalent	0.5	-

Publication 2

Constanze Kuhlisch[1], Gianmaria Califano[2], Thomas Wichard[3], Georg Pohnert[4], "Metabolomics of intra- and extracellular metabolites from micro- and macroalgae using GC-MS and LC-MS", in *Protocol book on macroalgae* (Eds.: C.R.K. Reddy, T. Wichard, B. Charrier), Taylor & Francis Group, *submitted.*

Author	1	2	3	4
Development of concept	x	x	x	x
Preparation of the manuscript	x	x	-	-
Correction of the manuscript	-	-	x	x
Proposed publication equivalent	0.5	0.5	-	-

Publication 3

Constanze Kuhlisch[1], Julia Althammer[2], Andrey F. Sazhin[3], Hans H. Jakobsen[4], J.C. Nejstgaard[5], Georg Pohnert[6], "Metabolomics-derived marker metabolites to characterize *Phaeocystis pouchetii* in natural plankton communities", *submitted.*

Author	1	2	3	4	5	6
Development of concept	x	-	-	-	x	x
Metabolomics analysis	x	x	-	-	-	-
Lab: Nutrient analysis	x	x	-	-	-	-
Cruise: microscopy	-	-	x	-	-	-
Cruise: nutrient analysis	-	-	-	x	-	-
Cruise: Flow Cam analysis	-	-	-	x	-	-
Data analysis	x	-	-	-	-	-
Preparation of the manuscript	x	-	-	-	-	x
Correction of the manuscript	-	x	x	x	x	x
Proposed publication equivalent	1.0	0.5	-	-	-	-

Publication 4

Bernadette Pree[1], Constanze Kuhlisch[2], Georg Pohnert[3], Andrey F. Sazhin[4], Hans H. Jakobsen[5], Maria Lund Paulsen[5], Marc E. Frischer[7], Diane Stoecker[8], Jens C. Nejtgaard[9], Aud Larsen[10], "A simple adjustment to test reliability of bacterivory rates derived from the dilution method", *Limnol. Oceanogr.: Methods*, **2016**, 14, 114-123.

Author	1	2	3	4	5	6	7	8	9	10
Development of concept	x	-	-	-	-	-	-	-	-	x
Dilution experiment	x	-	-	-	-	-	-	-	-	-
Exometabolome analysis	-	x	-	-	-	-	-	-	-	-
Preparation of the manuscript	x	x	-	-	-	-	-	-	-	-
Correction of the manuscript	-	x	x	x	x	x	x	x	x	x
Proposed publication equivalent	-	0.5	-	-	-	-	-	-	-	-

Publication 5

Constanze Kuhlisch[1], Michael Deicke[2], Nico Ueberschaar[3], Thomas Wichard[4], Georg Pohnert[5], "A fast and direct liquid chromatography-mass spectrometry method to detect and quantify polyunsaturated aldehydes and polar oxylipins in diatoms", *Limnol. Oceanogr.: Methods*, **2017**, 15, 70-79.

Author	1	2	3	4	5
Development of concept	x	x	x	-	x
Sample processing & analysis	x	x	x	-	-
Data analysis & interpretation	x	x	x	-	-
Preparation of the manuscript	x	-	-	-	-
Correction of the manuscript	-	x	x	x	x
Proposed publication equivalent	1.0	0.75	-	-	-